DISSECTING MECHANISMS OF CELL FATE SPECIFICATION IN C. ELEGANS MESODERM DEVELOPMENT

A Dissertation

Presented to the Faculty of the Graduate School

of Cornell University

In Partial Fulfillment of the Requirements for the Degree of

Doctor of Philosophy

by

Nirav Mahesh Amin

January 2009

DISSECTING MECHANISMS OF CELL FATE SPECIFICATION IN C. ELEGANS MESODERM DEVELOPMENT

Nirav Mahesh Amin, Ph.D.

Cornell University 2009

The fundamental question of developmental biology is how a single cell can generate a multicellular organism with a diverse set of cell types with specialized functions. A classic example of this paradigm is how the mesodermal germ layer of metazoan species can give rise to a range of cell types, including cells that form muscle, bone, blood, kidneys and the heart in vertebrate organisms. In my dissertation, I have used the *C. elegans* postembryonic mesoderm as a model to study the mechanisms of how various cell fates can be specified from the mesoderm.

The *C. elegans* postembryonic mesoderm, or the M lineage, gives rise to a small, but diverse, set of cell types that include striated body wall muscles (BWMs), non-muscle cells of a scavanger-like function known as coelomocytes (CCs), and sex myoblasts (SMs), which further divide and generate the non-striated sex muscles used for egg-laying. My project began with the characterization of the gene *fozi-1*, which was identified in a screen for M lineage mutant phenotypes. *fozi-1* encodes a unique transcription factor that functions autonomously in the M lineage for the proper specification of BWMs and CCs. Moreover, *fozi-1* functions redundantly with the MyoD homolog *hlh-1* and the Hox gene *mab-5* to specify the myogenic BWM fate.

In an RNAi screen to search for additional factors required for M lineage development, I identified 37 transcription factors that are required for proper M lineage development. I have focused my studies on one of these genes, *ceh-34*, which

encodes a homeodomain protein that is conserved among metazoans. I found that CEH-34 and its cofactor EYA-1 are individually required for the CC fate and together can induce the specification of CC fates from cells that will normally become BWMs. I present evidence for the regulation of *ceh-34* and *eya-1* by the transcription factors *fozi-1, hlh-1* and *mab-5*, along with well-conserved signaling mechanisms that regulate dorsal-ventral (TGFβ and Notch) and anterior-posterior (Wnt) asymmetry within the M lineage to specify non-muscle fates. Many of the components functioning in the M lineage are conserved in metazoans, and similar paradigms have also been found in Drosophila mesodermal fate specification, suggesting that the mechanism for distinguishing non-myogenic and myogenic fates in the mesoderm is conserved in other animals.

BIOGRAPHICAL SKETCH

Nirav was born on July 14, 1981 in Mount Laurel, a small town in southern New Jersey, son of Mahesh and Daksha Amin. Originally expected to be a girl, Nirav was named by his parents as Nilam, only to disappoint older brother Parag.

Nirav was a hyperactive child, often frustrating his parents with his constant fussiness and by instigating his brother Parag and getting into fights. Byproducts of his hyper behavior was his inability to stay focused on anything for too long and the desire to break things apart and see how they worked. Unfortunately, this led to him breaking a lot of his toys, and his brother's toys, leading to more fighting.

Nirav soon found a hobby to channel his energy when he began to play sports. He loved to play baseball and follow the New York Mets and vowed to one day become a professional baseball player. However, he did not physically develop enough to compete with trained athletes and make playing sports his profession and had to choose another one.

Throughout his early schooling, Nirav excelled in Mathematics and Science courses. He would often get into trouble in these courses because he would finish his assignments in class too early and then let his hyperness get the best of him. It was not until high school when he took an advanced placement Biology course with Ms. Tidswell that he began to seriously consider pursuing science for some sort of career. In this course, Ms. Tidswell challenged Nirav not only to learn some of the more complex biology covered in the course, but forced him to help teach what he learned to any of his classmates that needed help. Nirav found this to be both a challenging and rewarding way of spending his time. He especially enjoyed drawing Punnett squares and learning about Hardy-Weinberg equilibrium because it made him use his mathematical and scientific skills.

Nirav went on to Rutgers University for his undergraduate education, where he majored in Genetics and Microbiology. While enrolled at Rutgers, Nirav performed research under the supervision of Dr. Amrik Sahota, first at Robert Wood Johnson University Hospital and then at the Rutgers University Cell and DNA Repository. His research at the hospital was in a pathology lab developing a method to detect Bcr-Abl translocations in leukemia using RT-PCR. In the DNA Repository, he helped develop a procedure to amplify whole genomic DNA from small quantities of starting sample. While he learned a lot while working in these labs, Nirav was most excited by a research course he took in which students were introduced to *C. elegans* research and performed RNAi to examine the effects on nematode survival and growth, most likely because it appealed most to his childhood tendencies to take things apart and see how they work.

Nirav decided to go to graduate school, where he could further enhance his knowledge in genetics and molecular biology. He chose to go to Cornell University and because of his supposed mathematical skills planned to study population genetics under the tutelage of some of the brightest minds in this field and enjoy the beauty of Ithaca while we was there. However, he appeared to have a late epiphany. Once he started his coursework as a first year student in the Field of Genetics and Development, he quickly learned that population genetics was not for him. Instead he was rather fascinated by the course taught by Dr. Ken Kemphues, Developmental Genetics. It was there that he was really excited to be able to take multiple approaches to perturb development and understand the mechanisms of how organisms develop. He rotated in Dr. David Lin's lab and realized that he really enjoyed developmental biology and he finally found his true calling. Needing to set up a second rotation and soon, he contacted Dr. Jun "Kelly" Liu, who was shocked and probably dismayed that Nirav waited until the last second to set up his rotation with her. It turned out Nirav

enjoyed the research and the environment of the Liu lab and his interactions with Kelly and joined her lab, where he studied the mechanisms involved in mesoderm patterning. While in Kelly's lab, Nirav began to appreciate more and more the wonders of developmental biology and has decided to pursue research in mesoderm development, specifically the mechanisms in which cell fates are specified within the developing vertebrate heart.

To my friends and family that have supported me along the way…

ACKNOWLEDGMENTS

I would like to thank all the people that inspired and supported me along the way to becoming the person and scientist that I have become. I would especially like to thank Kelly Liu for everything she has done for me during my time here at Cornell. Kelly has been an inspiration to me with her wonderful work ethic and dedication to her family and very instrumental in me reaching this point in my career. I cannot express how much she has framed my approach to science and very grateful for the opportunities within the lab and the overall advice that she continues to give me today. I was very blessed to have a focused project and stay on task over these last few years to have a very productive graduate career and a dissertation that I am genuinely proud of, and that is a direct reflection of the influence of Kelly.

I would also like to thank my committee members Ken Kemphues and Lee Kraus for all of their wonderful advice and critiques during my committee meetings. I especially thank Ken for the knowledge and interest he instilled in me while I took his two courses, Developmental Genetics and Introduction to Developmental Biology. He taught these classes with such enthusiasm that it rubbed off on all of his students as well, including me of course. I have had the honor to have Ken as pretty much a second mentor, as he is very knowledgeable about my project and has given me a lot of advice to enhance my project as well as my presentation skills. Though he has been quite busy as the chair of the department, he has made the time to be there for so many students, as evidenced by when he stepped in and came to my practice talk when Kelly had to leave for a family emergency as well as taken the time to give critical comments on my manuscripts.

I would like to thank all the past and present members of the Liu lab for all of their help in the lab and enjoyment outside of the lab. I would especially like to thank

Marisa Foehr, a former graduate student in the lab, who has remained a close friend of mine even after she left the lab. When I started in the lab, Marisa was my mentor during my rotation, which she constantly reminds me of, jokingly. But in all seriousness, she has been very helpful in teaching me many of the things I learned in the lab and has remained an honorary member of the lab to whom I can still go for help and comments on my manuscripts and presentations. I would also like to thank Yuan Jiang, who also taught me a lot of things and kept things fun in the lab. After Marisa and Yuan left the lab, another graduate student Chenxi Tian has provided me with entertainment, taught me some Chinese words and has been a good lab member. Thank you to the technicians and undergraduates who poured the many plates I used to culture worms and bacteria, including Herong Shi, Erin Haithcock, Christine Gallati and Amanda Lindy. A special thanks to Herong for her hard work and efficiency in keeping the lab up to date with all the supplies and plates needed and for doing a lot of my cloning for me over my last year or so. She has really helped me be more efficient in the lab with her help. Christie Lim was a very special undergraduate who did a lot of work to establish that the Wnt signaling pathway is involved in generating asymmetry within the M lineage. Zach Via was a wonderful rotation student in the lab who helped me in performing the RNAi screen. I have also had the pleasure of teaching/mentoring quite a few rotation students and undergraduates who have worked in the lab and it was for the most part a wonderful experience in improving my teaching skills.

I would like to thank a lot of people who have helped me scientifically via collaborations, providing reagents, providing comments on my research or simply helping with administrative things. Dave Pruyne and Tony Bretscher were a great resource when I wanted to look at the potential of FOZI-1 to bind actin and Dave collaborated with me and performed the actin-based assays described in Chapter 2.

Dave has also been a great person to have in the Cornell Worm Group and has given me a lot of feedback on my projects. Tony also served as an additional committee member on my A exam and gave me nice feedback on the FOZI-1 project. I would also like to thank David Lin and Sylvia Lee, with whom I rotated in my first year and really enjoyed their enthusiasm for research and their overall sense of humor. Within the Cornell community, I have just been generally impressed with the overall friendliness within the department and campus and willingness to collaborate or even share equipment. I would like to thank Jim Smith for this help with cell sorting and Wei Wang for discussing microarray analysis and RNA quality with me. I thank Amanda Larracuente for answering all of my annoying statistic questions, and Karen Osorio for her advice in setting up cell sorting experiments. I appreciate the use of the Nanodrop (Lis lab), spectrophotometer (Wolfner lab) and electroporator (Goldberg lab), along with any other shared equipment that I am likely forgetting. I would like to thank Diane Colf for her assistance in my grad school needs and Cathy Ervay for assistance with accounting for conferences I attended and purchases I made for the lab.

I would like to thank all of the friends I have made at Cornell that made life very fun and interesting, providing distraction from research when things when needed (and sometimes not needed). In general, I appreciate the good times I have had with everyone here and their tolerance of my booming voice and overall goofiness. My first friend at Cornell was Amanda Larracuente, who I met during my interview weekend at Cornell. Amanda and I shared an apartment our first year here with another first year student, Fairuz Zein. We had a lot of good times our first year in grad school and every year since, and I am glad that she was able to put up with my off-tune singing at home and other wacky ways. I think one reason that helps is that she is just as wacky as I am. Amanda and I have remained very good friends and I have enjoyed spending

time with her and her husband Mark, especially when Amanda is busy with work and she pawns Mark off onto me. Some of my other close friends that I met my first year here are Marisa and her husband Leo Guelpa, Ryan Lewis, Marie Bechler, Nick Fuda, Leighton Core, Abbie Saunders, Vanessa Horner and her husband Kevin, and Amy Lyndaker and her husband Aaron. Thanks especially to Ryan and Marie for all the wonderful gourmet meals they have cooked. I also want to thank Donato Aceto, who advised me to be able to laugh at things when they go wrong, rather than dwell on the negatives. That piece of advice has gotten me through a lot of trying times when experiments were not working properly and other overall drama in and out of the lab. I have had the pleasure of meeting and getting to know a lot of incoming students and friends after my first year, including Chelsea McLean, Nick Brideau, Karen Osorio, Sarah Denial, Will Walker, Katherine Kieckhafer, Jay Phillips and his wife Jen, and Matt McCoy. I will take with me the many memories I have shared with everyone, whether it be weekly bowling with the guys, ultimate frisbee games, summer softball, skiing, golfing and any of the various parties and outings that we had that may have included some to a lot of alcohol. I will miss going to and yelling at the Cornell hockey games with Marisa, Leo, Vanessa, Becky Bean, Ryan, Marie and others. As the saying goes, times goes by fast when you are having fun, and the time really has gone by pretty fast.

Last but not least, I would like to thank my family for supporting me over my entire lifetime, but especially for the last few years where I have been further away from home. Though they may not fully understand what it is I was actually doing in grad school and why I would work strange hours to do things to worms, they were supportive of me every step of the way and I will always remember that.

TABLE OF CONTENTS

LIST OF FIGURES

LIST OF TABLES

CHAPTER 1

TRACKING THE CONSERVED AND DIVERGENT MECHANISMS OF MESODERM SPECIFICATION AND DIVERSIFICATION DURING METAZOAN DEVELOPMENT

Introduction

An interesting question in developmental biology is how a pool of multipotent progenitor cells can generate a diverse number of organs consisting of multiple specialized cell types. The process of organ formation relies on a number of cell-cell interactions and asymmetric distribution of cytoplasmic determinants that lead to the gradual specification of these progenitor cells. During metazoan development, these events have been observed in the specification of the three germ layers, the ectoderm, mesoderm and endoderm, and throughout the diversification of these germ layers. In vertebrates, ectoderm forms the epidermis, neural crest cells and the neural tube, while the endoderm forms the digestive tube, pharynx and respiratory tube. Meanwhile, the mesoderm contributes to a large variety of the internal organs and cell types, including the heart, kidneys, bone, cartilage, tendons, skeletal muscle, bone and blood. A number of model organisms have been used to study the mechanisms by which these cell fates are specified within the mesodermal germ layer, and in this dissertation, I describe my use of *C. elegans* as a model to study these mechanims. In this chapter, I will discuss in detail the advances made in *Drosophila* and vertebrates towards understanding the mechanisms of how the mesoderm is specified and how it is regulated to give rise to its diverse cell population. I will then highlight what is known about mesoderm development in *C. elegans* and discuss its conserved and divergent

mechanisms of cell fate specification and patterning compared to *Drosophila* and vertebrates.

Drosophila mesoderm

The establishment of the mesoderm layer in Drosophila has been well-studied. The mesoderm germ layer forms on the ventral side of the developing embryo. The graded morphogen DORSAL (DL) is broadly expressed in the precellular Drosophila embryo with peak nuclear levels in the ventral region (Roth et al., 1989; Rushlow et al., 1989; Steward, 1989). This gradient is responsible for the formation of three embryonic layers: mesoderm, neuroectoderm and dorsal ectoderm. A key target of DORSAL in establishing the mesoderm layer is the bHLH transcription factor TWIST, or TWI (Jiang et al., 1991; Thisse et al., 1991). TWI, together with DL, leads to the activation of another key factor SNAIL (SNA), a zinc finger protein (Ip et al., 1992). SNA is a transcriptional repressor that is required for the repression of neuroectoderm and ectoderm regulatory genes in ventral regions, thereby establishing a boundary between the ventral mesoderm and the lateral neuroectoderm (Leptin, 1991). Gastrulation initiates at the ventral side via cell invagination. *sna* is sufficient to initiate the invagination at the ventral furrow, while *twi* is further required to activate mesoderm-specific genes in the invaginating cells (Ip et al., 1994). These invaginating cells then require the function of the FGF receptor HEARTLESS (HTL) to migrate and spread over the ectoderm, a critical step in patterning of the dorsal mesoderm (Beiman et al., 1996; Gisselbrecht et al., 1996; Shishido et al., 1997). *twi* is required in this process to activate the expression of *htl* (Shishido et al., 1997).

The differentiation of the newly formed mesoderm layer occurs in a multi-step process of gradual specification of clusters of cells prior to differentiation into the multiple cell types. A number of signaling pathways help pattern the mesoderm along

the dorsal-ventral and anterior-posterior axes, while various transcription factors also contribute to pattern various segments of the mesoderm. A key event in this patterning process is the dynamic regulation of *twi*, and its restriction from or enrichment in specific mesodermal cell types (Dunin-Borkowski and Brown, 1995; Riechmann et al., 1997; Tapanes-Castillo and Baylies, 2004). Another target of TWI in the early mesoderm is the NK homeobox gene *tinman (tin)* (Yin et al., 1997). Later, both *tin* and *twi* expression patterns are tightly regulated to control pattern asymmetry in the developing mesoderm.

During germ band extension of the Drosophila embryo, the level of *twi* is reduced in anterior regions of parasegments and enriched in posterior regions of parasegments along the anterior-posterior axis (Thisse et al., 1991; Dunin-Borkowski and Brown, 1995). This regulation of *twi* expression influences the formation of the various somatic, visceral and cardiac mesoderm and other minor cell types. In this section, I describe some of the inductive events and transcriptional networks that are required for proper specification of these different layers.

Visceral mesoderm

The visceral mesoderm layer is derived from the dorsal-most cells of the mesoderm and primarily consists of the musculature of the digestive tract. This musculature is composed of two types, an inner layer of circular muscles and an outer layer of longitudinal muscles (Goldstein and Burdette, 1971). A key factor that is required for the specification of visceral muscles is *bagpipe (bap),* which encodes an NK homeodomain transcription factor (Azpiazu and Frasch, 1993). Mutations in *bap* lead to a severe disruption in visceral mesoderm formation and a transformation of some cells into body wall musculature (Azpiazu and Frasch, 1993). Two factors are important for the expression of *bap* in the dorsal mesoderm, *decapentaplegic (dpp)*

and *tin*. DPP belongs to the BMP/TGFβ superfamily of proteins and transduces the signal via Smads to affect transcription. While *dpp* is required for the specification of dorsal mesoderm progenitors, it is not sufficient on its own to induce these progenitors (Staehling-Hampton et al., 1994; Frasch, 1995). Instead, *dpp* acts in concert with mesoderm competence factors that are required to potentiate the activity of *dpp*. A key intrinsic factor of the dorsal mesoderm is *tin*, which together with DPP inputs can lead to the expression of dorsal mesoderm regulatory genes (Yin et al., 1997; Lee and Frasch, 2005). *tin* expression is maintained in the dorsal mesoderm by DPP-activated Smads and mesoderm intrinsic levels of TIN proteins, and is required for many dorsal mesoderm fates as described below (Bodmer, 1993; Lee and Frasch, 2005). Both Dpp-activated Smads and TIN can bind directly to the *bap* promoter to positively regulate its transcription in the dorsal mesoderm (Lee and Frasch, 2005). The transcriptional effects of TIN and DPP in the dorsal mesoderm are further modulated along the anterior-posterior axis by WINGLESS (WG) signaling. As reviewed in (Lawrence and Sampedro, 1993), the anterior-posterior axis of the Drosophila embryo is organized in parasegments. WG exerts regulatory roles in the mesoderm in anterior-posterior segments along the length of the embryo. In the anterior compartments of parasegments, WG signals from the segmented ectoderm abolish the repressive activity of the dTCF/Lef-1 protein PANGOLIN (Lee and Frasch, 2000). PANGOLIN directly binds to the enhancers of the forkhead domain encoding genes *sloppy-paired*, *slp1* and *slp2*, to activate their expression (Lee and Frasch, 2000). These forkhead domain proteins directly bind to the *bap* promoter to restrict *bap* expression in posterior segments of the dorsal mesoderm (Lee and Frasch, 2005). Hence, the combined action of DPP, WG and TIN leads to the segmented expression pattern of *bap* in the dorsal mesoderm in only posterior parasegments (Lee and Frasch, 2005). These general patterning events are depicted in Figure 1.1.

Figure 1.1. Summary of patterning events in the Drosophila embryonic mesoderm. DPP and WG pattern each parasegment along the dorsal-ventral and anterior-posterior axis, respectively. TIN and SIX-4/EYA are expessed in a mutually opposite manner, with TIN expressed in the dorsal domain (pink) and SIX-4/EYA in the ventral domain (blue). These patterning events and mesoderm-intrinsic factors lead to the expression of cell-type determining factors and to the indicated cell fates.

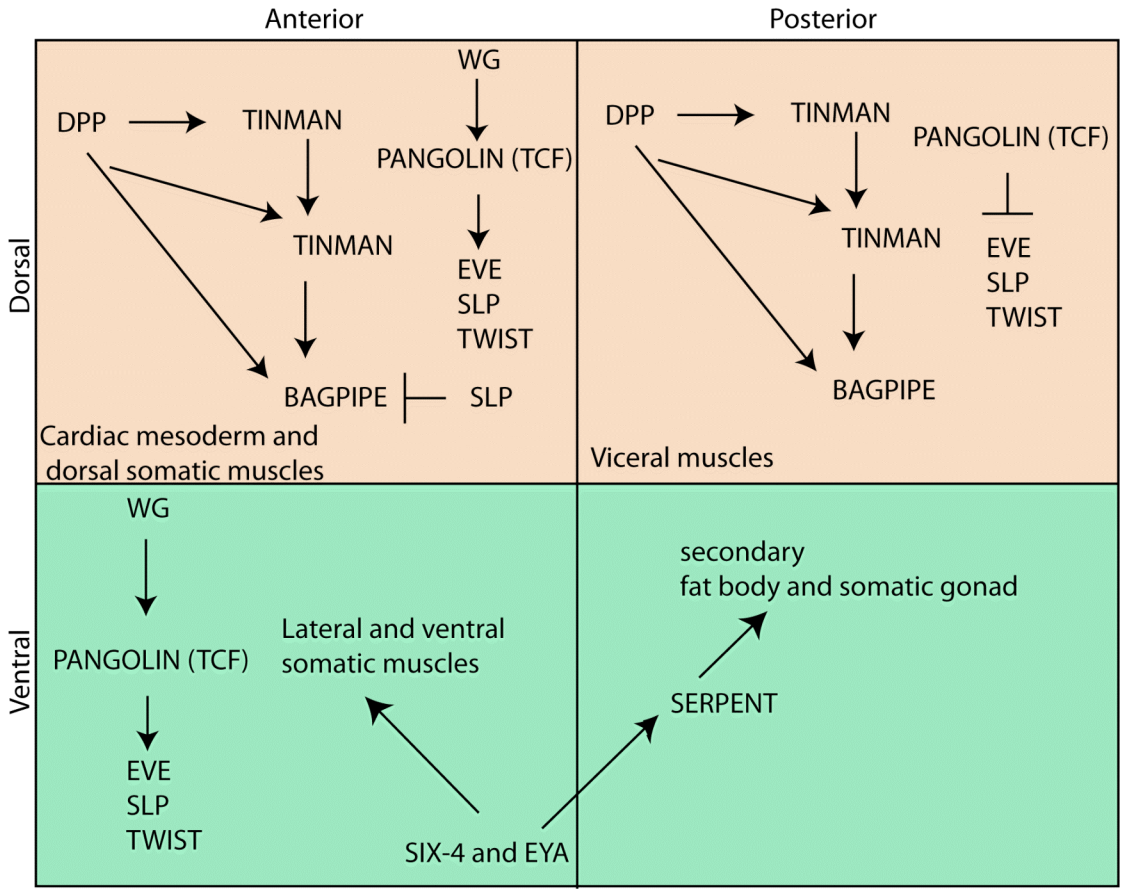
Anterior
Posterior
Dorsal
Ventral
WG
DPP
TINMAN
PANGOLIN (TCF)
TINMAN
EVE
SLP
TWIST
BAGPIPE
SLP
Cardiac mesoderm and
dorsal somatic muscles
DPP
TINMAN
PANGOLIN (TCF)
TINMAN
EVE
SLP
TWIST
BAGPIPE
Visceral muscles
WG
PANGOLIN (TCF)
EVE
SLP
TWIST
Lateral and ventral
somatic muscles
SIX-4 and EYA
SERPENT
secondary
fat body and somatic gonad

One of the major targets of BAP in the visceral mesoderm is the FoxF forkhead transcription factor encoding gene, *biniou (bin). bin* expression relies on direct regulation by BAP and DPP-activated Smads and its activity is required for most of the functions of BAP (Zaffran et al., 2001). *bin* mutants display similar phenotypes to *bap* mutants, while forced expression of *bin* in a *bap* mutant can rescue many of the visceral mesoderm defects of *bap*. Interestingly, *bin* is also required to positively regulate and perhaps maintain *bap* expression in the visceral mesoderm (Zaffran et al., 2001). Additionally, *bin* and *bap* play a key role in activating differentiation genes of the visceral mesoderm such as β-3tubulin (Zaffran and Frasch, 2002). Recently, a temporal ChIP-on-chip experiment has revealed that BIN, unlike BAP, may have a regulatory role through all stages of visceral muscle development (Jakobsen et al., 2007). In this study, 146 direct target genes were found to have at least one BIN-bound enhancer element (Jakobsen et al., 2007). Further characterization of these targets may help elucidate the differentiation of the visceral mesoderm.

Cardiac mesoderm

The cardiac mesoderm gives rise to the Drosophila heart, or dorsal vessel. The Drosophila heart is comprised of a number of cell types. These include cardiomyocytes, or cardioblasts, which are arranged in two rows and surround the lumen of the heart. These cardioblasts are surrounded by various types of pericardial cells. Finally, segmentally arranged alary muscles anchor the dorsal vessel to the epidermis (Tao and Schulz, 2007).

Like the visceral mesoderm, the early specification of the cardiac mesoderm has been well studied. The cardiac mesoderm arises from cells of the posterior parasegments of the dorsal mesoderm. As described above, the posterior parasegments are subjected to WG signals that activate Pangolin. This in turn leads to the expression

of *slp1* and *slp2*, which repress the expression of *bap* (Lee and Frasch, 2000). The intersection of WG and DPP signaling domains, along with TIN and TWI expression in the dorsal anterior, defines the origin of cardiac and somatic mesoderm, and is necessary for the development of both (Carmena et al., 1998a). The further specification of cell-types within this broad competence domain created by the combined actions of WG, DPP, TIN and TWI is dependent on other signaling cues and mesoderm intrinsic factors. Within the region of high TWI expression in the anterior compartments of parasegments, further subdivision is observed and marked by the sequential expression of the proneural gene *lethal of scute (l'sc)* in 19 clusters of cells in each high *twi* expression domain (Carmena et al., 1995). Within these 19 clusters, most often one and sometimes two cells (P1-19) retain high expression of *l'sc* as well as putative identity genes (Carmena et al., 1995).

One of the well studied genes involved in cardiac specification is the homeobox gene *even skipped* (*eve*). *eve* null mutants lack visceral and cardiac mesoderm altogether, suggesting an early role for this gene (Azpiazu et al., 1996). Temperature sensitive mutants of *eve* reveal a later role in the cardiac mesoderm, and the development of pericardial cell fates (Su et al., 1999). Specifically, *eve* is expressed in the P2 muscle progenitor cell, which undergoes an asymmetric division to give rise to a founder of Eve^+ pericardial cell and a sibling that loses expression of *eve*. This founder of Eve^+ pericardial cell divides to form two *eve* pericardial cells, or EPCs (Carmena et al., 1998b; Carmena et al., 2002). Meanwhile the sibling becomes the progenitor of the somatic muscle dorsal oblique muscle 2, DO2 (Carmena et al., 2002). The asymmetric cell division is dependent on the activity of the cortically localized proteins NUMB and INSCUTEABLE during division (Carmena et al., 1998b). During cell division, these proteins are located at opposite poles, leading to the asymmetric inheritance of NUMB to the daughter cell (Carmena et al., 1998b).

This asymmetric segregation of NUMB into one of the daughter cells results in the antagonism of NOTCH signaling in the cell receiving NUMB and formation of the EPC founder (Carmena et al., 1998b). Therefore NUMB is the major factor involved in specifying the lineage of *eve*-expressing progenitor cells.

So what are the factors that control the expression of *eve* in the specific cardiac and somatic muscle progenitors? It appears there are quite a few factors involved in controlling the expression of *eve*. *eve* is expressed within a subset of the WG, DPP, TWI and TIN-expressing domains of the mesoderm. In fact, the WG-activated PANGOLIN, DPP-activated Smads, TIN and TWI directly bind to the enhancer of the homeobox gene *eve* and positively regulate its expression in the posterior parasegments (Knirr and Frasch, 2001). Within the intersecting domains of DPP and WG signaling, the transcription of *eve* requires the integration of one more signal, via Ras/MAPK activation. Two receptor tyrosine kinases (RTKs), HTL and the Drosophila epidermal growth factor (DER), generate the Ras/MAPK inductive signal and ultimately activate the Ets domain transcription factor PointedP2 (PNT), which can bind the *eve* promoter and function synergistically with TIN, TWI, DPP-activated Smads and PANGOLIN to achieve *eve* expression (Halfon et al., 2000; Knirr and Frasch, 2001). In addition to TIN and TWI, the zinc finger and homeobox-containing gene *zfh-1*, is expressed in the forming heart and required for formation of EPCs. *zfh-1* is required to maintain *eve* expression in forming EPCs and ZFH-1 has been shown to bind the *eve* promoter *in vitro*, suggesting ZFH-1 acts as yet another direct regulator of *eve* (Fortini et al., 1991; Su et al., 1999).

In addition to its role in specification of the dorsal mesoderm, including the cardiac mesoderm, tinman plays a role in multiple stages of cardiac development. After the early expression of tinman to specify cardioblasts, it is required for the diversification of developing cardioblasts (Zaffran et al., 2006). At least three pairs of

diverse cardioblast cell identities are found, based on the expression of (1) *tin*, (2) *tin* and *ladybird* or (3) *sevenup* (*svp*) and *dorsocross* (*doc*) within each segment of the dorsal vessel (Lo and Frasch, 2003). *tin* is negatively regulated by the COUP-TF transcription factor *seven-up* in the pair of cells expressing the Dorsocross T-box gene family (Lo and Frasch, 2001). Conversely, TIN is required to repress the expression of *doc* in the other cardioblast progenitors, leading to a mutual repression of *tin* and *doc* to achieve cardioblast specificity (Zaffran et al., 2006). These relationships in which cells express or do not express *tin* likely affect functional properties of the carbioblasts, as the presence or absence of *tin* is thought to affect physiological properties (Zaffran et al., 2006). Also consistent with a role of *tin* throughout the life of the developing heart, when later stage developing hearts lack *tin* expression, there is abnormal ultrastructure, remodeling and function of the larval and adult hearts (Zaffran et al., 2006).

Another transcription factor that is crucial to heart development in Drosophila is the bHLH transcription factor HAND. HAND plays an essential role in Drosophila heart development as mutations in *hand* result in a number of cardiac defects in embryos and during larval growth (Han et al., 2006). *hand* is expressed broadly in the dorsal mesoderm within the circular gut muscles and in all cell types of the developing heart (Kolsch and Paululat, 2002). Though *hand* is expressed within the visceral mesoderm, it does not appear to affect differentiation of visceral muscle fates (Popichenko et al., 2007). Much like the case for the regulation of *eve* expression, a number of factors coordinate to regulate the expression of *hand* in the dorsal mesoderm. In cardioblasts and pericardial nephrocytes, TIN and the GATA factor PANNIER directly regulate the expression of *hand* (Han and Olson, 2005). Meanwhile, *hand* expression in the visceral mesoderm is directly regulated by the visceral mesoderm-specific gene *biniou* (Popichenko et al., 2007). Recently, it has

been shown that the expression of *hand* specifically in *svp*/*doc* cardioblasts and pericardial cells is further regulated by the LIM homeodomain transcription factor TAILUP (Tao et al., 2007).

As seen above with specific examples of how the cardiac mesoderm is patterned and individual cell fates specified, a common theme that has emerged is the use of a combination of a number of signaling pathways, cell competence factors and asymmetric lineage decisions at multiple temporal and spatial manners that lead to specification of individual cell types with unique identities to form a functional heart.

Somatic mesoderm

The somatic mesoderm generates the somatic or skeletal musculature of Drosophila, which consists of single mononucleate fibers that attach to the cuticular exoskeleton of the Drosophila larva (Frasch, 1999). These muscles are arranged in pattern of about 30 fibers per hemisegment, with each fiber defined by its size, position, attachment sites and innervation (Bate, 1990). These muscle fibers are generated by the fusion of two types of cells, founder cells (FCs) and fusion-competent myoblasts (FCMs). The FCs contain all the information required to properly specify the identity of muscle fibers, whereas the FCMs appear to belong to a more generic type of myoblasts whose function is to fuse to specified FCs. This is apparent by mutations in the gene *myoblast city*, in which fusion of myoblasts into multinucleate muscles is virtually abolished, yet a subset of cells (FCs) develop specific muscle-like characteristics (Rushton et al., 1995). In this section I will describe the specification of the somatic mesoderm and the mechanisms of how individual founder cells are singled out from the somatic mesoderm.

The somatic mesoderm arises from the areas of the mesoderm that have high WG and SLP activity. In the absence of either, somatic muscle formation is almost

completely missing. As described above, the cardiac mesoderm arises from these same regions of WG activity that also receive inputs from DPP signaling. These regions can also give rise to dorsal somatic mesoderm, while the regions of WG activity lacking DPP comprise the ventral somatic mesoderm. One of the major targets of WG activity in specification of the somatic mesoderm is the bHLH TWI. As described above, *twi* expression is first detected in all cells of the presumptive mesoderm before it is segmentally restricted. *twi* expression is segmented in response to *slp* at high levels in the regions of high WG activity (Riechmann et al., 1997). Meanwhile, *twi* expression is inhibited directly and indirectly by activation of the Notch signaling pathway (Tapanes-Castillo and Baylies, 2004). *twi* is required for the formation of most body wall muscles, consistent with a role in the somatic mesoderm. The spatial regulation of *twi* expression in the anterior domains of parasegments is thought to make cells in the somatic mesoderm competent to generate somatic muscles.

Within these competence domains, cells are singled out by the same process described for EPCs in the cardiac mesoderm. Specifically, groups of cells within the high TWI domain are specified by WG signaling into groups of equivalent myoblasts which express the bHLH gene *lethal of scute*, or *l'sc* (Carmena et al., 1995; Brennan et al., 1999). Within these 19 clusters of cells that express *l'sc*, individual progenitors are singled out by the influences of Ras activity and Notch signaling (Figure 1.2). Briefly, the EGF signal SPITZ or FGF signals PYR and THS (Schweitzer et al., 1995b; Stathopoulos et al., 2004) lead to the localized activation of FGF (Heartless) and EGF (Drosophila EGF receptor, DER) pathways within the equivalence groups (Michelson et al., 1998). The downstream Ras effector leads to MAP kinase (MAPK) activation within these cells (Carmena et al., 1998a). This leads to the expression of ARGOS

Figure 1.2. A model for the specification of muscle progenitor cells. A combination of WG and/or DPP signals pattern the regions of the parasegments to be competent to generate muscle progenitors. Localized EGF or FGF signals activate the MAPK/Ras pathway and specify promuscular clusters which express *l'sc*. Within these clusters, lateral inhibition occurs in which the muscle progenitor is singled out and Notch signaling inhibits neighboring cells from becoming muscle progenitors. Ras signals also activates the expression of muscle identity genes, such as EVE in this example, lending to the specific identity of the muscle progenitor. This figure is adapted from the work published by Carmena et al. (Carmena et al., 1998a).

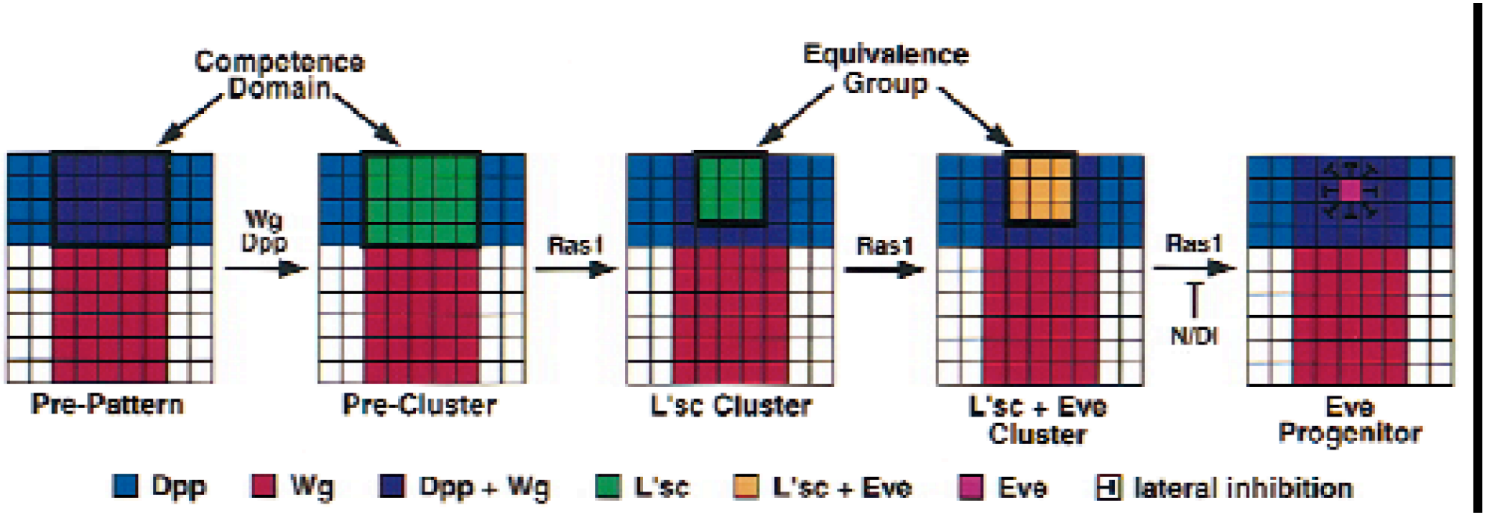
Competence Domain
Equivalence Group
Wg
Dpp
Ras1
Ras1
Ras1
N/Dl
Pre-Pattern
Pre-Cluster
L'sc Cluster
L'sc + Eve Cluster
Eve Progenitor
Dpp
Wg
Dpp + Wg
L'sc
L'sc + Eve
Eve
lateral inhibition

(AOS), the DER antagonist and DELTA (DL), the ligand for Notch signaling (Schweitzer et al., 1995a; Carmena et al., 2002). These two proteins are involved in lateral inhibition, in which they non-autonomously inhibit Ras signaling and elevate Notch activity to maintain non-progenitor identity (Carmena et al., 2002). Notch activity in turn inhibits Ras activity and further activates Notch activity. What initiates this imbalance where Ras signaling is high in the presumptive progenitor and Notch activity is high in nonprogenitor cells is not yet known.

The presence of *l'sc* in all the promusclular equivalence groups suggests a role in the selection of muscle progenitors. However, loss of *l'sc* results in a weak muscle phenotype, suggesting that *l'sc* is not essential for this process or that other genes may function redundantly with *l'sc* in progenitor selection (Carmena et al., 1995). Indeed, the gene *Pox meso (Poxm)* was recently shown to be partially redundant with *l'sc* within the somatic mesoderm, but still does not completely abolish muscle progenitors (Duan et al., 2007). An alternative hypothesis to the role of *l'sc* as a promuscular gene is that TWI and its bHLH binding partner daughterless function as the promuscular factors that regulate the competence domain and muscle identity genes to specify muscle progenitors (Duan et al., 2007). Recently, a number of direct targets of TWI were identified via ChIP-on-chip technology (Sandmann et al., 2007). Further analysis of TWI targets identified in this study may aid in the elucidation of this conundrum.

Within the progenitor cells, MAPK activates the expression of muscle identity genes, such as *eve* in the P2 cell described above, via its effector PNT (Halfon et al., 2000). Each progenitor then divides asymmetrically to form sibling founder cells that express various muscle identity genes. For example, the ventral acute muscles 26 and 27 develop from a common progenitor called p26/27 that expresses *Krüppel* and *slouch*. Asymmetric division of this cell marked by the asymmetric distribution of NUMB to muscle 27 leads to inhibition of Notch while Notch remains active in

muscle 26. When Notch is active in the founder of muscle 26, *Krüppel* and *slouch* expression is inhibited, while they are still expressed in muscle 27 (Baker and Schubiger, 1996; Knirr et al., 1999). In embryos lacking *Krüppel* activity, muscle 27 is often transformed to muscle 26 (Ruiz-Gomez et al., 1997). Overexpression of *Krüppel* is sufficient to transform the fate of muscle 26 to muscle 27. These experiments demonstrate the importance of asymmetric division of progenitors and of muscle identity genes such as *Krüppel* in specification of individual muscle fibers. A number of muscle identity genes have been identified, including *Krüppel*, *slouch*, *apterous*, *ladybird*, *muscle segment homeobox*, *collier*, the MyoD homolog *nautilus* and *pox meso* (Bourgouin et al., 1992; Ruiz-Gomez et al., 1997; Jagla et al., 1998; Nose et al., 1998; Crozatier and Vincent, 1999; Knirr et al., 1999; Balagopalan et al., 2001; Duan et al., 2007). These genes all encode transcription factors and are expressed in distinct muscle progenitors and founders and often in an overlapping manner, suggesting individual muscles are specified by defined combinations of these genes (Frasch, 1999).

Once these FCs are specified by the muscle identity genes, differentiation of the muscles, attachment to proper epidermal location and specific innervation must take place. Differentiation of muscles requires the action of the factors MEF2 and MUSCLEBLIND (Lilly et al., 1994; Bour et al., 1995; Artero et al., 1998). Studies of the *mef2* enhancer suggest that individual muscle identity genes can control its expression to directly regulate differentiation. The muscle identity genes may also control cell surface proteins that are essential for proper axon guidance leading to innervation as shown for *Krüppel* (Abrell and Jackle, 2001). Thus it seems founder cells require muscle identity genes to directly control proper differentiation within the somatic mesoderm.

Recently, the muscle identity gene *collier* has been shown to be required for its activation in the FCMs that fuse to the DA3 FC which also expresses *collier*, suggesting another function of muscle identity genes in regulating fusion of FCMs during myogenesis (Dubois et al., 2007). In addition to the regulation of fusion of FCMs by FC genes, the Gli family member LAME DUCK has an essential role in FCMS for proper differentiation, including regulating the expression of the differentiation and fusion genes *mef2* and *sticks-and-stones*, respectively (Duan et al., 2001)

non-muscle forming mesoderm (fat body)

In addition to giving rise to somatic muscles, the non-dorsal (lateral and ventral) mesoderm gives rise to non-muscles cells, namely the somatic cells of the gonad and the fat body. These regions are defined by the absence of dpp and tinman activity. As shown in Figure 1.1, the Six homeodomain protein SIX-4 and its cofactor EYES ABSENT (EYA) are expressed in this domain in a pattern complementary to TIN (Clark et al., 2006). Moreover, SIX-4 and EYA are required for the proper development of the fat body and somatic gonad, as well as somatic muscles in the non-dorsal mesoderm (Clark et al., 2006). The GATA-like transcription factor *serpent* is necessary and sufficient for fat-cell development (Hayes et al., 2001). The function of SIX-4 and EYA is required for the expression of *serpent* in the developing fat cell. On the other hand, ectopic expression of SIX-4 and EYA in the mesoderm leads to ectopic expression of *serpent* and production of fat-cell clusters and somatic gonad (Clark et al., 2006). These studies suggest that *six-4* and *eya* function in the non-dorsal mesoderm in a manner similar to the function of *tinman* in the dorsal mesoderm.

Vertebrate mesoderm

The mesoderm is induced in vertebrates by the expression of two types of signals. One type is the Nodal and Nodal-related genes of the TGFβ superfamily and their targets (Zhou et al., 1993; Conlon et al., 1994; Feldman et al., 1998; Nomura and Li, 1998; Rebagliati et al., 1998; Song et al., 1999; Agius et al., 2000). The production of these signals in Xenopus is controlled by maternal VegT transcription factors and produced in the endoderm (Kofron et al., 1999; Agius et al., 2000). In addition to Nodal related proteins, FGF signaling is also required to induce mesoderm formation (Slack et al., 1987; Slack et al., 1988; Amaya et al., 1993). The inductive effects of Nodal and FGF signaling lead to the expression of Brachyury, a T-box transcription factor that is expressed in and required for proper mesoderm development (Herrmann et al., 1990; Wilkinson et al., 1990; Smith et al., 1991; Umbhauer et al., 1995; Miya and Nishida, 2003). Moreover, ectopic expression of Brachyury can lead to the ectopic production of mesoderm (Cunliffe and Smith, 1992). In Xenopus, Nodal has been shown to act in a gradient in which high levels of Nodal specify dorsal mesoderm and low levels specify ventral mesoderm (Agius et al., 2000). One consequence of these levels in the dorsal mesoderm is the production of BMP inhibitors, such as Noggin and Chordin. These BMP inhibitors subsequently inhibit ventralizing BMP signals allowing for the formation of dorsal mesoderm structures, as well as neural tube and dorsal endoderm formation (Smith et al., 1993; Sasai et al., 1994).

Once the mesoderm has been specified in vertebrates, it will migrate interior to the embryo in a characteristic manner, in which the first group of cells to migrate will populate the head. Subsequently, cells will migrate and give rise to four regions (from medial to lateral): (1) the notochord, a transient structure that serves an important inductive role in neural tube formation and other mesodermal structures, (2) the paraxial mesoderm, which gives rise to the somites and their derivatives, (3) the

intermediate mesoderm, which forms the urogenital system and (4) the lateral plate mesoderm, which gives rise to heart, blood vessels, blood cells, lining of body cavities, limb mesoderm (except muscle) and some extraembryonic tissues. The origins of the vertebrate mesoderm are depicted in Figure 1.3. The formation of these regions appears to be dependent on BMP4 gradients (Pourquie et al., 1996; Tonegawa et al., 1997). This BMP4-dependent regionalization, at least in part, functions through the regulation of forkhead transcription factors that are specific to each region (El-Hodiri et al., 2001; Wilm et al., 2004). In this chapter, I will examine the factors and mechanisms by which mesodermal derivatives are defined and patterned within these regions, focusing on the paraxial and lateral plate mesoderm regions.

Notochord

As mentioned above, the notochord is a transient mesodermal rod that forms during embryonic development. The main purpose of the notochord is to serve as a signaling center. During neural tube formation of the overlying ectoderm, the notochord produces Sonic hedgehog protein (Shh), which signals to the medial hinge cells of the overlying neural tube to induce the floor plate. This floor plate is then induced to produce a gradient of high Shh along in the ventral portion of the neural tube to low Shh in the dorsal portion. Conversely, dorsalizing signals of the TGFβ family, BMPs, are produced in the epidermal layer located above the neural tube and induce the dorsal-most cells of the neural tube to form the roof plate. This produces an opposite gradient to that of Shh. The gradients of Shh and BMP pattern the neural tube and lead to the proper specification of neuronal identities along the dorsal-ventral axis. The role of the notochord in this process is primarily the secretion of Shh, as replacing notochord with cultured cells secreting Shh can induce a floor plate in the neural tube.

Figure 1.3. The derivatives of the vertebrate mesoderm. The cartoon depicts a schematic of the mesoderm and the cell types to which each component contributes. The neural tube and overlying ectoderm are shown in blue and are important sources of patterning cues for the developing mesoderm. The notochord forms ventral to the neural tube, while the remaining mesodermal compartments form more laterally. This figure was adapted from Gilbert (Gilbert, 2006).

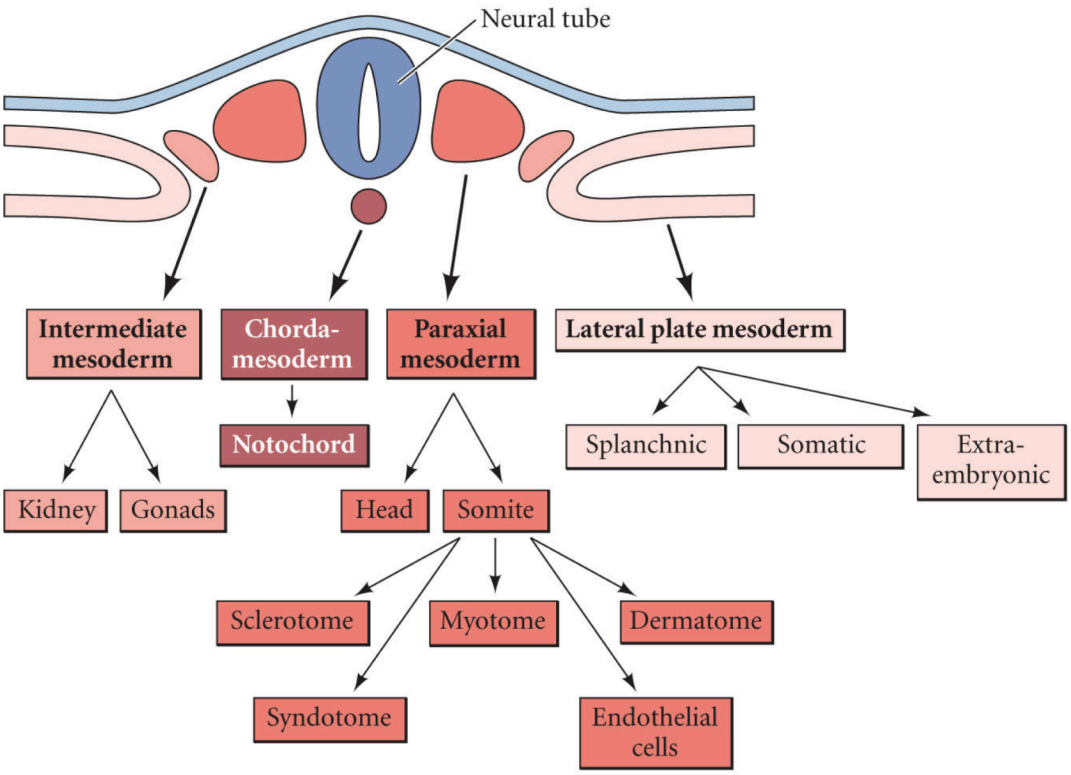
Neural tube
Intermediate mesoderm
Chorda-mesoderm
Paraxial mesoderm
Lateral plate mesoderm
Notochord
Splanchnic
Somatic
Extra-embryonic
Kidney
Gonads
Head
Somite
Sclerotome
Myotome
Dermatome
Syndotome
Endothelial cells

Paraxial (somitic) mesoderm

The paraxial mesoderm forms on either side of the developing neural tube and separates into blocks of cells known as somites. The specification of the paraxial mesoderm requires the antagonism of BMP signaling by the inhibitor Noggin. Placing Noggin-expressing beads within the lateral plate mesoderm can induce ectopic somite formation (Tonegawa and Takahashi, 1998). Once the somites are specified they arrange in a metameric pattern along the anterior-posterior axis during embryonic development to determine the arrangement of segmental structures such as the vertebral column, ribs, dorsal root ganglia, peripheral nerves and blood vessels (Christ et al 2007). The somitic epithelium is marked by N-Cadherin and Paraxis (Marcelle et al., 2002). The differentiation of the somites into these multiple cell types is influenced by structures surrounding the somites. Ventral signals from the notochord and ventral neural tube, Shh and Noggin, are necessary for the induction and maintenance of the ventral portion of somites to de-epithelialize and form the mesenchymal sclerotome. As the mesenchymal scleretome is formed, it is marked by the absence of N-Cadherin and Paraxis (Marcelle et al., 2002). In the absence of notochord, the N-Cadherin expression spreads into the ventral scleretome, while transplanted notochord or implanted Shh to other regions of somites can lead to a reduction of N-Cadherin (Brand-Saberi et al., 1996a; Brand-Saberi et al., 1996b). Two paired domain transcription factors, Pax1 and Pax9 are expressed in the newly formed scleretome (Koseki et al., 1993; Peters et al., 1995). These two genes are under the control of the ventralizing Shh and Noggin signals emenating from the notochord. The scleretome will further give rise to the vertebral column, meninges, connective tissue and ribs.

Meanwhile, the dorsal-lateral portion of the somite will become the epithelial dermomyotome, which gives rise to muscle, endothelia, cartilage, connective tissue

and dermis. The medial half of the somite is specified by Wnt1 and Wnt3a from the dorsal neural tube, while Wnt4, Wnt6 and Wnt7a from the ectoderm influences the specification of the lateral half of the dermomyotome. Much like the scleretome, the dermomyotome is marked by the expression of paired domain transcription factors, Pax3 and Pax7 (Stockdale et al., 2000). Soon after the dermomyotome is established, the medial portion of the somite bends underneath the dermomyotome and forms a third layer known as the myotome. This myotome layer has been hypothesized to arise from muscle pioneers that serve as a substrate for the addition of subsequent myotomal cells derived from the dermamyotome, with the pioneers analogous to the founder cells described in Drosophila myogenesis (Kahane et al., 1998; Yusuf and Brand-Saberi, 2006). The formation of this layer is achieved by the synergistic activities of dorsal Wnt signals and ventral Shh signals through the Gli2 and Gli3 zinc finger transcription factors during early myotome development and maintained by the dorsal Wnt signals later during development. These Wnt signals also promote myogenesis via the expression of MyoD and Myf5 in the myotome. BMP signals also negatively regulate myogenesis and therefore formation of the myotome is accompanied by the production of the BMP-antagonist Noggin (Reshef et al., 1998).

As the dermomyotome develops, it undergoes a high rate of proliferation and provides a niche for a wide variety of progenitor cells. Some cells within the central dermomyotome undergo symmetric divisions to help in the growth of the dermomyotome. Meanwhile, other cells divide along the apical-basal axis to push one daughter ventrally into the myotome and the other daughter dorsally to form the dermis (Ben-Yair and Kalcheim, 2005). Much like as has been shown in asymmetric divisions of the Drosophila cardiac and somatic mesoderm, Numb has been shown to be unequally distributed to the asymmetrically dividing cells of the central dermomyotome (Venters and Ordahl, 2005).

Somites give rise to two types of muscle, epaxial and hypaxial. Epaxial muscles form the muscles of the back and arise from the myotome, while hypaxial muscles form the limb and body wall muscles and arise from the lateral edges of the dermomyotome. Myotome cells express members of a family of bHLH transcription factors that are known as myogenic regulatory factors, or MRFs. These factors are both necessary and sufficient for the specification and differentiation of myogenic fates. In the mouse, there are four members of the MRF family, MyoD, Myf5, myogenin and MRF4. Both MyoD and Myf5 are expressed in the early myotome when it is specified and double mutants for both results in a loss of all skeletal muscles (Rudnicki et al., 1993). Meanwhile, the hypaxial muscle progenitors migrate ventrolaterally from the dermomyotome to populate their target structures. This requires deepithelialization of the muscle precursors which is induced by Scatter factor, or SF/HGF, that is secreted by the lateral plate mesoderm (Brand-Saberi et al., 1996b). These cells that migrate away from the dermomyotome retain expression of Pax3, Lbx1, Six1/Six4, Eya1/Eya2/Eya4 and Dach2. Once these cells migrate to their position, these genes can turn on the expression of the MRFs, MyoD and myogenin (Heanue et al., 1999). It has recently been shown that Pax3/7 and the FOXO forkhead transcription factor can both directly bind the MyoD promoter and activate its expression (Hu et al., 2008). The expression of the MRFs in both epaxial and hypaxial muscle progenitors leads to further positive regulation of MRFs such as MRF4 and myogenin as well as muscle specific genes, such as Myosin Heavy Chain, or MHC (Arnold and Braun, 2000).

The role of the MRF family in vertebrates appears to be in sharp contrast to what happens in Drosophila. In Drosophila, the lone homolog of the MRF family, *nautilus*, does not appear to be required for the overall specification of muscle fates and has been proposed to play the role of a muscle identity gene instead. However,

nautilus is capable of inducing widespread myogenesis in culture, much like its homologs in vertebrates. The role of *nautilus* in specification of founder cells remains controversial. Recent mutations identified in *nautilus* reflect a greater role in *nautilus* in a larger number of founder cells than previously reported, but it is not required for all muscle development as has been shown for its vertebrate homologs (Wei et al., 2007). Meanwhile, in Drosophila, the bHLH transcription factor *twist* marks the developing myogenic precursors and is required for myogenic fates. In vertebrates, Twist is also expressed in the developing somites that give rise to myogenic cell populations. However, during the separation of somitic layers, Twist expression is confined to that of the dermamyotome and sclerotome, but not the myotome (O'Rourke and Tam, 2002). These observations have led to the hypothesis that Twist activity is required for the suppression of myogenic differentiation by counteracting the activity of the MRFs. Therefore, though Twist activity in Drosophila and vertebrates appears to compartmentalize the mesoderm, it appears its mode of action is quite different between the two.

Intermediate mesoderm

The intermediate mesoderm gives rise to the urogenital system, which includes the kidneys, the gonads and their duct systems. As mentioned earlier, this mesodermal layer is in part specified by a gradient of BMP. In addition to this gradient, signaling from the paraxial mesoderm likely contributes to the proper patterning of the intermediate mesoderm. These interactions lead to the expression of Pax2, Pax8 and Lim1, transcription factors required for kidney fates. Pax2 is sufficient to convert the paraxial mesoderm to intermediate mesoderm and lead to the expression of Lim1 and kidney formation. Meanwhile, Pax2 and Pax8 are necessary for proper kidney

development. For a review of the mechanisms of kidney development, see (Dressler, 2006).

Lateral plate mesoderm

The lateral plate mesoderm of vertebrates gives rise to a variety of organs and cell types, including the heart, blood vessels, blood, body cavity lining and cells of the limb (except muscle). The specification of this layer and its derivatives requires signaling from the adjacent endoderm as well as the notochord and neural tube. BMP signals from the endoderm promote both heart and blood development. Meanwhile in the anterior endoderm, BMP induces the synthesis of FGF8, which is critical for heart-specific genes. This process is blocked in the center of the embryo by signals from the notochord, Noggin and Chordin, which block BMP signaling. In addition, Wnt signals from the neural tube prevent heart formation and promote blood formation. These signals are antagonized by Wnt inhibitors, such as Cerberus and Dickkopf, which are produced by the anterior endoderm. Together these signaling mechanisms promote the formation of cardiac progenitors in the mesoderm adjacent to the anterior endoderm (Dunwoodie, 2007).

The cardiac mesoderm is different and much more complex compared to the Drosophila dorsal vessel. The vertebrate heart requires the movement of two sets of cardiac precursors towards the midline, followed by fusion and looping. In addition, research in the past few years has revealed there are two origins of myocardial cells, the primary and secondary heart fields, which contribute to the various compartments of the developing heart. The primary heart field arises during the early stages of gastrulation of the mesoderm. Meanwhile, the secondary heart field, also known as the anterior heart field, was found to arise from the pharyngeal mesoderm (Buckingham et al., 2005). A number of studies have focused on the contributions of the lineages of

these two heart fields to the various compartments of the heart (Buckingham et al., 2005). β-galactosidose lineage tracing of primary heart field cells shows that these cells contribute to both ventricles, both atria and the atrioventicular canal (Meilhac et al., 2004). Meanwhile, the secondary heart field contributes to the outflow tract and all other heart regions, except for the left ventricle, and there is considerable overlap of primary and secondary heart fields contributions to the heart (Meilhac et al., 2004). Here, I will describe some of the important factors required within the primary and/or secondary heart fields for proper cardiac growth and differentiation.

The bHLH transcription factor Mesp1 is one of the earliest markers of cardiovascular cells (Saga et al., 1999). Lineage-tracing in which Cre-recombinase is knocked into the Mesp1 locus, reveals that most cardiac cells at one point expressed Mesp1. Meanwhile, Mesp1 null mice exhibit severe heart morphogenesis defects and failure of fusion of the heart tube at the midline (Saga et al., 1999). Recent work in mouse ES cells has shown that Mesp1 can directly activate many of the genes in the core cardiac transcriptional machinery (Bondue et al., 2008; Lindsley et al., 2008).

Another gene required early in cardiogenesis is the transcription factor GATA4. GATA4 is required for heart tube formation and the ventral heart morphogenesis and mutations lead to the failure of primary heart field cells to migrate to the midline and fuse to form the primary heart tube, resulting in cardiac bifida (Kuo et al., 1997; Molkentin et al., 1997). The forkhead transcription factor Foxp4 plays a similar role in primary heart tube formation, and mutants also result in cardiac bifida. Interestingly, when unfused hearts are allowed to mature further, they still get populated by cells from the secondary heart field, suggesting cardiac fusion is not a prerequisite for secondary field and progenitor migration (Li et al., 2004; Wang et al., 2004). The differentiation of cardiomyocytes in vertebrates requires combinations of different transcription factors. Null mutations of individual transcription factors

involved in cardiac differentiation have unique phenotypes within the context of the heart. Since the primary and secondary heart lineages overlap in the contributions of progenitors to individual compartments of the heart, this may also reflect perturbations of just one of the two lineages in individual mutations.

Among the transcription factors identified in vertebrate heart development are homologs of the Drosophila Tinman (Nkx2-5) and Hand (Hand1 and Hand2). Mutations in Nkx2-5 lead to the loss of ventricular tissue. Nkx2-5 function likely is most important in the primary heart field as these cells are still present, but now fail to express Hand1 and form the left ventricle which is composed of only primary heart field progenitors (Yamagishi et al., 2001; Meilhac et al., 2004). More recent studies have shown that Nkx2-5 can regulate the proliferation of the secondary heart field and outflow tract morphology (Prall et al., 2007). Moreover, much like the regulation of Tinman in Drosophila is dependent on Dpp-activated Smads, Nkx2-5 gene induction is also regulated by a Smad-binding region (Liberatore et al., 2002; Lien et al., 2002). In turn, Nkx2-5 expression in cardiac progenitors leads to negative regulation of BMP2/Smad1 signaling (Prall et al., 2007). One role of Nkx2-5 that was identified is the facilitation of serum response factor (SRF) binding to the cardiac α-actin promoter (Chen et al., 1996). SRF encodes a MADS box transcription factor that uses Myocardin as a cofactor to regulate the differentiation of most cardiac and smooth muscles found in the heart (Kim et al., 1997; Wang et al., 2001; Wang et al., 2002; Wang et al., 2003; Miano et al., 2004; Wang et al., 2004). In Xenopus, Myocardin is necessary and sufficient to promote smooth muscle differentiation, similar to the roles of the MRFs in skeletal muscle differentiation (Wang et al., 2001; Wang et al., 2003). These observations suggest the presence of different cassettes used during metazoan development to initiate the differentiation of skeletal versus smooth muscle.

Another transcription factor used in primary heart field development is the T box transcription factor Tbx5, which contributes to the proper specification of primary heart field progenitors in the left ventricle, likely by negatively regulating the expansion of other regions of the heart (Bruneau et al., 1999; Bruneau et al., 2001).

While the primary heart field cells provide the majority of the left ventricle, secondary field cells similarly are the only cells that contribute to the outflow tract of the heart. Mutations affecting this structure along with lineage-tracing experiments have identified genes affecting derivatives of the secondary field (Buckingham et al., 2005). Another T box transcription factor, Tbx1, plays a major role in the secondary heart field, as targeted deletion leads to reduced proliferation of the secondary field and diminished contribution of these cells to the heart. On the other hand, overexpression of Tbx1 leads to an increase in the outflow tract myocardium and the upregulation of Fgf8 and Fgf10. Work in the chick embryo has shown that Fgf8 is required for growth of the secondary heart field and development of the outflow region. Tbx1 requires regulation of the Foxa2 transcription factor and has been shown to directly regulate Fgf8 expression in the cardiac outflow tract (Hu et al., 2004). These genes of the secondary heart field are negatively regulated by the functions of retinoic acid (RA), as deficiencies in Raldh2 lead to an expansion of the domains expressing Tbx1 and Fgf8, while exogenous RA can lead to reductions in Fgf8 (Ryckebusch et al., 2008).

Other transcription factors required for proper secondary heart field differentiation include the LIM homeodomain Isl1, the forkead Foxh1, the serum response factor related protein Mef2c, the bHLH Hand2 and the T-box Tbx20 (Srivastava et al., 1995; Srivastava et al., 1997; Cai et al., 2003; Dodou et al., 2004; von Both et al., 2004; Takeuchi et al., 2005). Identification of these factors in the primary and secondary heart field will continue to aid in our understanding of

congenital heart defects. For example, Tbx1 is often associated with DiGeorge syndrome, which has pleiotropic phenotypes, including cardiac defects (Chieffo et al., 1997). Nkx2-5 is the most commonly mutated single gene in congenital heart defects.

Much like the developing heart, where vertebrates and Drosophila have homologs such as Nkx2-5/Tinman, Hand1/Hand, Fgf8/Heartless which serve critical functions in the developing heart, similarities are seen with visceral or gut muscle specification among these species. For example, vertebrate homologs of *bagpipe*, a critical transcription factor required for visceral mesoderm in Drosophila, also has roles in patterning the vertebrate gut mesoderm (Lettice et al., 2001). Similarly, the vertebrate homologs of the forkhead transcription factor biniou, FoxF1 and FoxF2, are expessed in the mesodermal tissues that will line the digestive tract. Moreover, FoxF1 is required for proper development of the lateral plate mesoderm, and mutations lead to the expression of the somatic mesoderm marker Irx1. Together, these studies suggest that there are indeed conserved elements in the development of visceral mesoderm in Drosophila and vertebrates.

C. elegans mesoderm

Compared to Drosophila and vertebrates, the mesoderm of *C. elegans* is much simpler and does not result in the production of as many cell types. Because of its relative simplicity, the *C. elegans* mesoderm has become a useful model to study the mechanisms of cell fate specification that occurs during the course of metazoan development. The invariant lineage of the nematode, ease of culture and powerful genetic approaches allow for the study of these mechanisms at single cell resolution. The *C. elegans* mesoderm gives rise to a number of muscles, including (1) pharyngeal muscles used for pumping food from the head to the posterior of the animal (2) enteric muscles, used for defecation, (3) striated body wall muscles, used for locomotion and

(4) non-striated uterine and vulval muscles, or sex muscles, used for egg-laying. In addition to these muscles, the *C. elegans* mesoderm gives rise to six non-muscle coelomocytes of unknown function. The majority of these mesodermal cells are derived during embryogenesis, while the sex muscles and a subset of striated body wall muscles and coelomocytes are generated during postembryonic development. Here I will discuss the mechanisms identified for cell fate specification of the embryonic and postembryonic mesodermal lineages in *C. elegans*.

Embryonic mesoderm

Studies of cell fate specification in the embryonic mesoderm have focused on factors required for pharyngeal, enteric and body wall muscles from the MS, AB, C and D blastomeres. Genetic analyses have identified individual transcription factors required for these different cell fates. Of these blastomeres, MS gives rise to the majority of the embryonic mesoderm (Sulston et al., 1983). The MS cell results from a division of EMS, the ventral-most cell of 4-cell stage embryos, and requires cell-cell interactions and maternally loaded determinants to be properly specified. While MS gives rise to mostly mesoderm, its posterior sister, E, gives rise to endodermal tissues. The specification of EMS requires the maternally contributed transcription factor SKN-1 as most *skn-1* mutants lack the endoderm and mesoderm derivatives of E and MS (Bowerman et al., 1992; Bowerman et al., 1993). SKN-1 directly regulates the expression of two GATA factors, MED-1 and MED-2, which specify the mesendoderm (Maduro et al., 2001; Maduro et al., 2007). The E and MS fates are distinguished by the activity of Wnt signaling, in which the EMS cell receives a Wnt signal, MOM-2, from the P2 blastomere which binds to the Frizzled receptor MOM-5 (Rocheleau et al., 1997). This results in the downregulation of the TCF/Lef homolog POP-1 in the posterior E cell (Lin et al., 1998; Huang et al., 2007). The divergent β-

catenin SYS-1 has been shown to bind to POP-1 and convert it from a repressor to an activator in a dose-dependent manner in this posterior daughter of EMS, analogous to regulation of Pangolin in Drosophila development (Kidd et al., 2005; Huang et al., 2007). In the anterior MS cell, POP-1 nuclear levels exceed SYS-1 levels, and it acts as a constitutive repressor, likely bound by co-repressors. This in turn leads to the repression of the E-specific genes, *end-1* and *end-3* in MS and allows for expression of mesoderm specification (Lin et al., 1995; Maduro et al., 2001).

In the pharynx, the homolog of the Tinman and Nkx2-5 genes, CEH-22, is a key factor in pharyngeal muscle development. CEH-22 is specifically expressed within pharyngeal muscles and was found to directly bind to enhancers of pharyngeal muscle-specific genes and lead to their activation (Okkema and Fire, 1994; Okkema et al., 1997). *ceh-22* is also required for pharyngeal muscle development as mutants display weak muscle contractions (Okkema et al., 1997). Though there is no heart formation in *C. elegans* development, a parallel may be drawn between the pumping of the pharyngeal bulb and the pumping of the heart. Moreover, *ceh-22* mutants can be rescued by Nkx2-5, suggesting a conservation of this family of transcription factors in developing these pumping organs (Haun et al., 1998). While *ceh-22* appears to regulate the expression of a subset of pharyngeal muscle genes, the forkhead transcription factor PHA-4 appears to be required for all pharyngeal muscles and for expression of pharyngeal muscle specific genes, including *ceh-22* (Mango et al., 1994; Horner et al., 1998; Kalb et al., 1998; Gaudet and Mango, 2002). These functions of PHA-4 closely resemble the functions of *bagpipe* and the forkhead transcription factor *biniou* in visceral mesoderm development in Drosophila. As is the case with *biniou*, microarray analysis has identified a number of downstream targets of PHA-4 (Gaudet and Mango, 2002). Further characterization of these targets and their relationship with targets of *biniou* will prove useful in dissecting mechanisms of how these transcription

factors function in these muscle types and how individual fates are specified. One such target is the T-box transcription factor *tbx-2*, which has been shown to required for anterior pharyngeal fates (Smith and Mango, 2007).

Less is known about the specification of the four enteric muscles that are involved in defecation. One factor that is expressed in the enteric muscles and required for the proper specification of three of the four muscles is the *twist* homolog, *hlh-8* (Harfe et al., 1998b; Corsi et al., 2000). Interestingly, *hlh-8* expression is not detected in the remainder of the embryonic mesoderm and is not required for overall embryonic mesoderm development (Harfe et al., 1998b; Corsi et al., 2000). Thus the function of Twist in *C. elegans* differs from its *Drosophila* homolog and mimics more closely its function in vertebrates, where Twist also is not required for overall mesoderm development and specification. These observations reiterate the divergent mechanisms of Twist function in metazoans. More functions of the *C. elegans* Twist homolog in postembryonic development will be discussed later.

There are 81 embryonically-derived striated body wall muscles (BWMs) in *C. elegans*. These muscles are derived from 4 founder blastomeres, AB, MS, C and D. The lone *C. elegans* homolog of the MRF/MyoD family member described above, *hlh-1*, is expressed within each of the BWMs (Krause et al., 1990). Much like what is seen in *Drosophila* for *nautilus*, null mutations of *hlh-1* have body wall muscles form. However, mutations also lead to embryonic lethality and reduced contractility of the muscles that do form (Chen et al., 1992; Chen et al., 1994). These observations showed that though *hlh-1* may not be the sole factor required for muscle specification, it plays a key role in differentiation of embryonic muscles. Recently, in vivo studies showed that HLH-1 can act like the MRF family and induce widespread myogenesis in *C. elegans* embryos when ectopically expressed (Fukushige and Krause, 2005). Interestingly, two other factors, the Hand1 homolog *hnd-1* and the SRF homolog *unc-*

120, possess similar myogenic potential to *hlh-1* in the early embryo. The expression of all three of these genes depends on the caudal related factor PAL-1 (Fukushige et al., 2006). Moreover, double and triple mutant analyses of *hlh-1*, *hnd-1* and *unc-120* revealed that these three factors function redundantly and together are both necessary and sufficient to induce BWM fates (Fukushige et al., 2006). This mechanism of striated muscle fate specification, termed the "muscle module," has a striking relationship to the specification of a more diverse set of muscle types in higher organisms. As mentioned above in the discussion of vertebrate mesoderm development, Hand1 and SRF are involved in cardiac and smooth muscle specification, respectively. These studies in *C. elegans* suggest that skeletal, cardiac and smooth muscles at one point shared a common ancestral muscle type (Figure 1.4) and the factors identified may have evolved different roles to allow for the diversification of cell types and generation of additional organs throughout evolution (Fukushige et al., 2006).

Postembryonic mesoderm

The postembryonic mesoderm of *C. elegans* gives rise to the somatic gonad and a small subset of diverse cell types (Sulston and Horvitz, 1977). The non-gonadal postembryonic mesoderm of *C. elegans* arises from the M mesoblast, is born during embryogenesis and remains quiescent until the larva hatches (Sulston and Horvitz, 1977). During larval growth, the M lineage gives rise to 14 BWMs, 2 non-muscle coelomocytes (CCs) and 2 sex myoblasts (SMs) (Figure 1.5A). The 2 sex myoblasts migrate to the presumptive vulva, proliferate and give rise to 4 type I and 4 type II vulval muscles and 4 type I and 4 type II uterine muscles (Sulston and Horvitz, 1977).

Figure 1.4. Evolutionary origins of muscle specification. In vertebrates, there are cadiac, smooth and skeletal muscles that are specified by the transcription factors indicated. C. elegans striated muscle development requires the function of some of the genes that serve to differentiate among the three types of muscles in vertebrates as shown here. This figure was adapted from work published by Fukushige et al. (Fukushige et al., 2006).

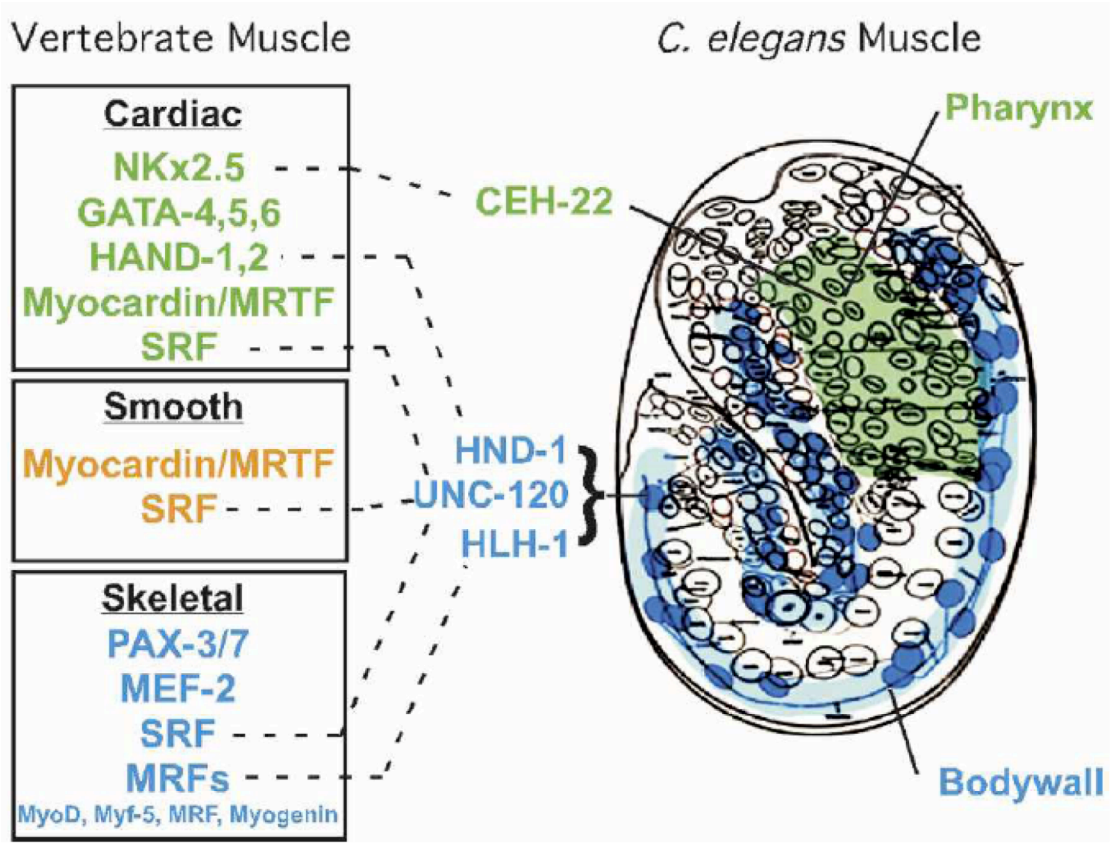
Vertebrate Muscle
C. elegans Muscle
Cardiac
NKx2.5
GATA-4,5,6
HAND-1,2
Myocardin/MRTF
SRF
Smooth
Myocardin/MRTF
SRF
Skeletal
PAX-3/7
MEF-2
SRF
MRFs
MyoD, Myf-5, MRF, Myogenin
CEH-22
HND-1
UNC-120
HLH-1
Pharynx
Bodywall

Figure 1.5. Transcriptional networks regulating the C. elegans postermbyonic mesodermal lineage. (A) Schematic of the M lineage showing the divisions of the M mesoblast and the cell types that arise (Sulston et al., 1983). (B) Transcription factors (with classification underneath) are shown with determined interactions required for specific cell fates. M, M mesoblast; d, dorsal; v, ventral; l, left; r, right; a, anterior, p, posterior.

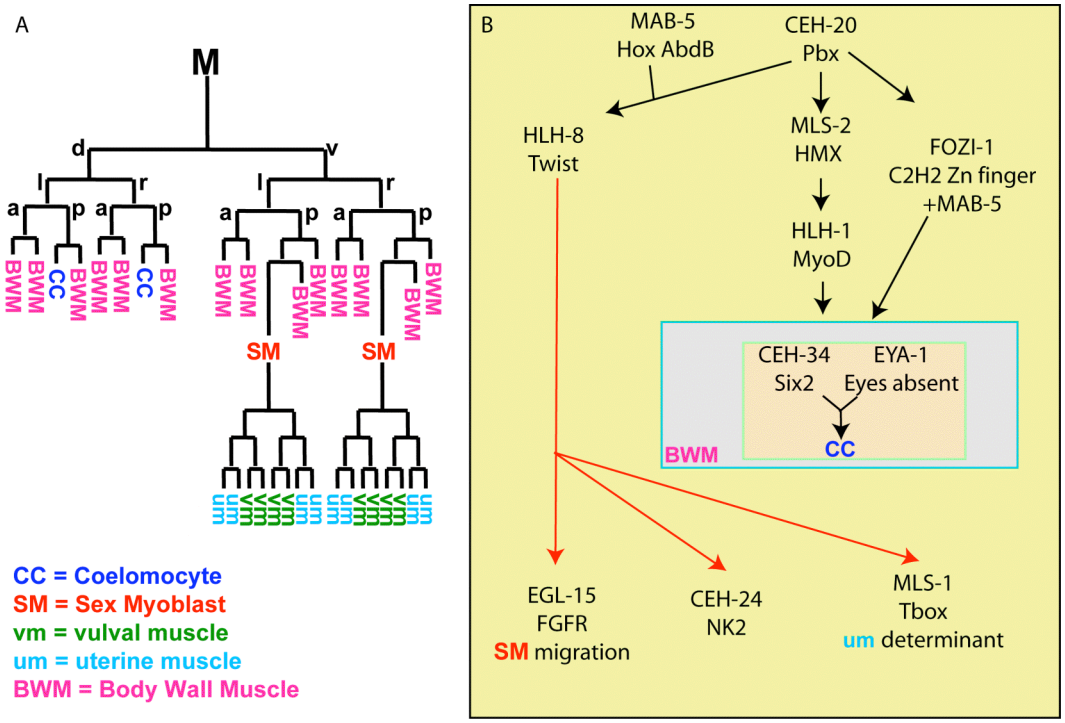
A
M
d
v
l
r
a
p
BWM
CC
SM
CC = Coelomocyte
SM = Sex Myoblast
vm = vulval muscle
um = uterine muscle
BWM = Body Wall Muscle
B
MAB-5
Hox AbdB
CEH-20
Pbx
HLH-8
Twist
MLS-2
HMX
FOZI-1
C2H2 Zn finger
+MAB-5
HLH-1
MyoD
CEH-34
Six2
EYA-1
Eyes absent
CC
BWM
EGL-15
FGFR
SM migration
CEH-24
NK2
MLS-1
Tbox
um determinant

The Hox genes *mab-5* and *lin-39* and their Pbx cofactor *ceh-20* are required for the proliferation and patterning of the M lineage (Liu and Fire, 2000). These genes also are required for the expression of the Twist homolog *hlh-8*, which is expressed in all undifferentiated cells of the M lineage and required for proper patterning (Harfe et al., 1998b; Corsi et al., 2000; Liu and Fire, 2000). Another factor that functions downstream of CEH-20 that is required for proliferation and proper cleavage orientations within the M lineage is the HMX homeodomain protein MLS-2 (Jiang et al., 2005; Jiang et al., 2008). MLS-2 also regulates the specification of the non-muscle CCs and striated BWMs by positively regulating the expression of HLH-1.

Much like during embryogenesis, *hlh-1* is expressed in all the BWMs that are derived from the M mesoblast. *hlh-1* is also expressed within the non-muscle CC and is required for its proper specification (Harfe et al., 1998a). These observations are quite surprising considering the role of *hlh-1* as a putative myogenic factor and suggest that *hlh-1* may have an additional role in specification of non-muscle cell fates. Recent work in which the fates of cells expressing the MRF family gene Myf5 were followed revealed that some cells do not become muscle, rather they adopt a brown adipose tissue fate (Seale et al., 2008). It remains to be seen if Myf5 itself is required for this non-muscle fate, and it will be interesting to see if this is the case. *hlh-1* loss of function in the M lineage leads to a transformation of some BWM fates to the SM fate, but most BWMs are specified correctly (Harfe et al., 1998a). Two genes that are also expressed in all the M-derived BWM and CC precursors and display similar M lineage phenotypes to *hlh-1* mutants are *mab-5* and the C2H2 zinc finger encoding gene *fozi-1* (Liu and Fire, 2000; Amin et al., 2007). Double mutants of *hlh-1* and *fozi-1* or *hlh-1* and *mab-5* result in the transformation of most, if not all, BWMs in the M lineage to SMs (Amin et al., 2007). These observations suggest that HLH-1 functions redundantly with FOZI-1 and MAB-5 in specification of BWM fates

in the M lineage. The presence of a small number of M-derived BWMs in some of the double and triple mutants of these factors suggests even more factors may function in this process. Thus, although *C. elegans* anatomically is quite simple, it has quite a complex and redundant set of mechanisms to specify a single striated muscle fate in both embryonic and postembryonic lineages.

While *hlh-1*, *mab-5* and *fozi-1* represent transcription factors that function intrinsically within the M lineage to specify BWM and CC fates, a number of asymmetric events help pattern the M lineage and specify cell fates. Two signaling pathways are involved in regulating dorsal-ventral asymmetry in the M lineage. LIN-12, a *C. elegans* Notch receptor, is required for the ventral SM fates, and loss of function results in a duplication of the dorsal CC fates (Greenwald et al., 1983). On the other hand, *sma-9*, the *C. elegans* homolog of the Drosophila zinc finger protein Schnurri, functions to antagonize the Sma/Mab TGFβ pathway to specify dorsal CC fates. Loss of *sma-9* function results in a duplication of the ventral SM fates and loss of the dorsal CCs (Foehr et al., 2006). Both pathways appear to act independently to specify dorsal and ventral fates (Foehr and Liu, 2008).

Recently, through work described in Chapter 3 of this dissertation, I discovered a role of Wnt signaling in anterior-posterior patterning of the M lineage. Specifically, the TCF/LEF homolog POP-1 is enriched in anterior daughters of the M lineage and likely functions as a repressor, while the divergent β-catenin SYS-1 is enriched in the posterior daughters of the M lineage and likely converts POP-1 to a transcriptional activator (Chapter 3, this dissertation). One consequence of this is the differential regulation of the Six homeodomain protein CEH-34 and its cofactor EYA-1, which are required for CC fates. Thus Wnt signaling appears to regulate the decisions between non-muscle CCs and the striated BWMs. Consistent with the role of Wnt signaling in Drosophila, there appears to be a requirement of other cell competence factors within

the M lineage that are required for the regulation of CEH-34 and EYA-1, as not all cells respond to POP-1 repressive activity in the same way (Chapter 3, this dissertation).

The proper diversification of the SM and its descendants requires the function of the twist homolog *hlh-8*. *hlh-8* mutant animals are egg-laying defective and lack functional vulval muscles (Corsi et al., 2000). HLH-8 directly regulates the expression of a number of genes required for the different sex muscle types, including *egl-15*, *ceh-24* and *mls-1* (Harfe et al., 1998b; Corsi et al., 2000; Kostas and Fire, 2002). *egl-15* encodes a homolog of the FGF receptor/Heartless and is expressed in the SM and the type I vulval muscles. Much like Heartless is required for the migration of the mesoderm in the early Drosophila embryo, EGL-15 is required for the migration of the SM to the presumptive vulva (DeVore et al., 1995). *ceh-24* encodes an NK-2 homeodomain protein, similar to *tinman* in Drosophila, which is similarly regulated by *twist*, providing yet another example of conservation of gene regulation in the mesoderm among metazoan species. *mls-1* encodes a T-box transcription factor that acts as a determinant of uterine muscles fates (Kostas and Fire, 2002). Genetic networks for cell fate specification and in the M lineage are summarized in Figure 1.5B. Additional targets of *hlh-8* have recently been identified in microarray studies and will likely help in identification of additional factors that may be involved in sex muscle or enteric muscle specification (Wang et al., 2006).

Summary

In this chapter, I have reviewed the mechanisms of mesoderm specification and diversification in Drosophila, vertebrates and *C. elegans*. As these mechanisms continue to be elucidated, it is becoming apparent that many of the mechanisms employed in one aspect of mesoderm development are conserved within species and

throughout evolution. Signaling pathways, such as TGFβ, Notch and Wnt and many of the mesoderm-intrinsic factors, such as Twist, MyoD, Nkx2-5, SRF, Forkhead, Six and Eya are employed by all animal models. Studies in simpler model organisms such as Drosophila and *C. elegans* will continue to provide useful methods with which to understand basic development and the progression of congenital defects associated with mesodermal subtypes. In this dissertation, I describe my efforts to dissect the mechanisms by which cell fates are specified in the *C. elegans* postembryonic mesoderm, the M lineage. These studies provide examples of potentially conserved and divergent mechanisms of cell fate specification in metazoan development.

Dissertation outline

This dissertation describes genetic and molecular studies to identify the mechanisms by which cell fates are specified in the C. elegans postermbyronic mesoderm, the M lineage.

Chapter 2 describes the characterization of the gene *fozi-1*, which encodes a unique protein that likely functions as a transcription factor. Double and triple mutant analysis of *fozi*-1 with the CeMyoD homolog *hlh-1* and the Hox factor *mab-5* demonstrate that these three transcription factors function redundantly to specify striated muscle fates in the M lineage.

Chapter 3 demonstrates the role of the Six2 homeodomain factor CEH-34 and its putative cofactor, the eyes absent homolog EYA-1, in specification of non-myogenic versus myogenic fates. Genetic and molecular epistasis analysis places these two genes downstream of the myogenic fate specification factors described in Chapter 2, along with dorsal-ventral (TGFβ and Notch) and anterior-posterior (Wnt) patterning mechanisms.

Chapter 4 describes an RNAi screen to identify transcription factors involved in M lineage patterning. Further characterization of one of the genes identified, *let-381*, shows that it is involved in dorsal-ventral patterning within the M lineage.

Chapter 5 is an overall summary and provides a synopsis of future work that will be needed to build upon the information provided in this dissertation.

Appendix 1 summarizes the mapping of suppressors of the *sma-9* mutation. The results from this work contributed to the finding that *sma-9* antagonizes the Sma/Mab TGFβ signaling pathway for proper specification of dorsal fates in the M lineage.

Appendix 2 summarizes attempts to purify mRNA from enriched populations of M lineage cells. Results from this study provide a foundation to perform large-scale gene expression profiling experiments in the future.

Appendix 3 describes characterization of the *ceh-34* promoter by mutational analysis. The elements of the *ceh-34* promoter identified to be required for its expression provides a starting point to identify direct *trans*-regulatory factors for *ceh-34* expression.

Appendix 4 describes characterization of the *fozi-1* promoter and suggests that the M lineage expression and function of *fozi-1* is dependent on longe range *cis*-regulatory elements.

CHAPTER 2[1]

A ZN-FINGER/FH2-DOMAIN CONTAINING PROTEIN, FOZI-1, ACTS REDUNDANTLY WITH CeMYOD TO SPECIFY STRIATED BODY WALL MUSCLE FATES IN THE CAENORHABDITIS ELEGANS POSTEMBRYONIC MESODERM

Introduction

Mesodermal development is a complex multistep process in which the pluripotent precursor cells become increasingly specialized to form specific cell types. This process requires a coordination of multiple transcriptional pathways and cellular signaling mechanisms. The *C. elegans* postembryonic mesodermal lineage, the M lineage, allows us to study these mechanisms at single cell resolution. The M lineage arises from a single blast cell, the M mesoblast, which is born during embryogenesis and remains dormant until the larva hatches (Sulston and Horvitz, 1977; Sulston et al., 1983). During larval development this pluripotent blast cell undergoes a series of reproducible divisions to give rise to all of the postembryonically-derived, non-gonadal mesodermal cells in the animal (Sulston and Horvitz, 1977). In hermaphrodites, the M mesoblast undergoes a series of divisions to give rise to a total of 18 cells. Fourteen of these cells become striated body wall muscles (BWMs) and two become non-muscle coelomocytes (CCs) (Figure 2.1; Sulston and Horvitz, 1977). The remaining two cells become sex myoblasts (SMs) that migrate to the presumptive

[1] Part of this chapter has been published in *Development* (Amin N.M., Hu, K. Pruyne, D., Terzic D., Bretscher and Liu J., 2007. Development 134: 19-29) and is reprinted with permission. Mapping was performed by Jun Liu, Kejin Hu and Dino Terzic, actin assays presented in Figure 2.4 were performed by David Pruyne and rescue of *fozi-1(cc609)* was performed by Jun Liu.

Figure 2.1. The *C. elegans* hermaphrodite postembryonic M lineage.

Times are indicated post-hatching at 25˚C. (A) The M lineage showing all differentiated cell types that arise from M (modified from Sulston and Horvitz, 1977). (B) A schematic lateral view of the M lineage through larval development. D, dorsal; V, ventral; L, left; R, right; A, anterior; P, posterior.

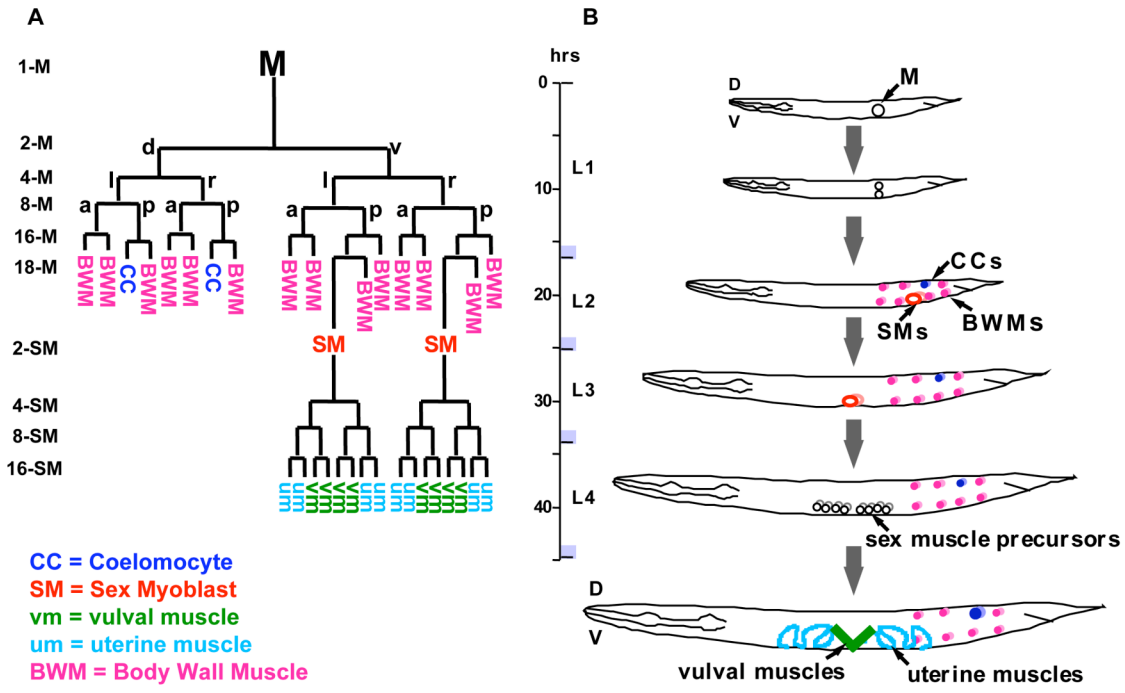
A
1-M
2-M
4-M
8-M
16-M
18-M
2-SM
4-SM
8-SM
16-SM
M
d
v
l
r
a
p
BWM
CC
SM
CC = Coelomocyte
SM = Sex Myoblast
vm = vulval muscle
um = uterine muscle
BWM = Body Wall Muscle
B
hrs
0
10
20
30
40
L1
L2
L3
L4
D
V
M
CCs
SMs
BWMs
sex muscle precursors
vulval muscles
uterine muscles

vulval region and further proliferate to give rise to eight vulval muscles and eight uterine muscles (Sulston and Horvitz, 1977). Previous studies have identified a number of transcriptional regulators that are required for proper CC and BWM fate specification in the M lineage. These factors include the Hox factor MAB-5 and its cofactor CEH-20 (Liu and Fire, 2000), the HMX homeodomain protein MLS-2 (Jiang et al., 2005), the MyoD homolog HLH-1 (Harfe et al., 1998a) and the Twist ortholog HLH-8 (Harfe et al., 1998b). MAB-5 and CEH-20 directly activate expression of HLH-8 (Liu and Fire, 2000), while MLS-2 regulates the expression of CeMyoD/HLH-1 in the M lineage (Jiang et al., 2005). Among these transcriptional regulators, HLH-1 is required specifically for BWM and CC fate specification in the M lineage (Harfe et al., 1998a). Lack of HLH-1 in the M lineage does not cause any early defects within the lineage. Instead, it causes stochastic cell fate transformations of several BWMs and the two CCs to SMs (Harfe et al., 1998a). HLH-1 is the only member of the myogenic bHLH family in *C. elegans* (Krause et al., 1990). Its requirement for BWM fate specification in the M lineage suggests a functional similarity between HLH-1 and the vertebrate myogenic bHLH proteins (Pownall et al., 2002). However, since only a subset of the BWM cells are transformed in mutant animals completely lacking HLH-1 in the M lineage, additional factors must exist for the proper specification of BWM fates.

To identify these additional factors, we screened for mutants with defects in the M lineage (*mesodermal lineage specification* mutants, or *mls* mutants). In this chapter, I describe one gene, *fozi-1 (formin zinc finger protein-1)*, that was identified through these screens. *fozi-1* encodes a novel nuclear protein with motifs characteristic of transcription factors and actin-binding proteins. Like *hlh-1*, *fozi-1* is expressed in the M lineage and functions within the M lineage for proper CC and BWM cell fate

specification. I show that FOZI-1 and the Hox factor MAB-5 function redundantly with HLH-1 to specify BWM fates in the M lineage.

Materials and Methods

C. elegans strains

Strains were maintained and manipulated using standard conditions (Brenner, 1974). Analyses were performed at 20˚C, unless otherwise noted. The following strain was generated to visualize the M lineage in *fozi-1(cc609)* mutant animals throughout postembryonic development: LW0679 [*fozi-1*(*cc609*) *ccIs4438*(*intrinsic CC::gfp*) III; *ayIs2*(*egl-15::gfp*) IV; *ayIs6*(*hlh-8::gfp*) X]. The strain LW0081 [*ccIs4438*(*intrinsic CC::gfp*) III; *ayIs2*(*egl-15::gfp*) IV; *ayIs6*(*hlh-8::gfp*) X] was used in parallel as a wild-type control. The strain LW0064 [*cup-5(ar465) fozi-1(cc609)* III; *jjIs64(arg-1::gfp)* V; *arIs39(secreted CC::gfp)* X] was used to generate transgenic lines for rescue. *Intrinsic CC::gfp* is a twist-derived coelomocyte marker (Harfe et al., 1998b). *Secreted CC::gfp* is another coelomocyte marker using a *myo-3::secreted GFP* construct (Harfe et al., 1998a). Additional M lineage specific reporters were as described in Kostas and Fire (Kostas and Fire, 2002). The M lineage was followed in live animals under a fluorescence stereomicroscope and confirmed using a compound microscope. Other strains used in this work are:

LG II: *hlh-1(cc561ts)*, *hlh-1(cc450)/mIn1[dpy-10(e128) mIs14]* II (Harfe et al., 1998a)

LG III: *mab-5(e1239)* (Kenyon, 1986), *fozi-1(tm0563)* (gift from Shohei Mitani, Tokyo Women's Medical University School of Medicine, Japan), *ceh-20(n2513)* (Liu and Fire, 2000), WM31: *dpy-17(e164) vab-7(e1562)***.**

LG V: *him-5(e1467)* (Hodgkin et al., 1979)

LG X: *mls-2(cc615)* (Jiang et al., 2005), *hlh-8(nr2061)* (Corsi et al., 2000)

The CB4856 strain (Hodgkin and Doniach, 1997) was used for snip-SNP mapping of *fozi-1* (Wicks et al., 2001).

Mutagenesis screens and analysis of *fozi-1*

In screens for mutants with M lineage defects (Jiang et al., 2005; Foehr et al., 2006), four recessive mutations (*cc607, cc608, cc609 and cc610*) were isolated that failed to complement one another. These alleles define the *fozi-1* locus. Mapping and complementation analysis of *fozi-1* was carried out using standard methods by monitoring the number of CCs using the *CC::gfp* markers described above. Three-factor mapping using *dpy-17* and *vab-7* and snip-SNP mapping (Wicks et al., 2001) placed *fozi-1* between cosmids K04H4 and F54G8 on chromosome III. The molecular lesions of *fozi-1* mutant alleles were identified through sequencing PCR products of genomic fragments spanning the entire coding region of K01B6.1.

Plasmid constructs and transgenic lines

A full-length *fozi-1* cDNA was generated by piecing together two cDNA clones, *yk288g3* and *yk779b02* (gifts from Yuji Kohara, National Institute of Genetics, Japan). A 5 kb fragment spanning the entire coding region and 3' UTR of *fozi-1* was PCR amplified from N2 genomic DNA using the iProof™ High-Fidelity DNA Polymerase (Bio-Rad). The cDNA and PCR product were used to generate the following constructs:

Forced expression constructs:

pNMA37, *hlh-8p::fozi-1::fozi-1 3'UTR*

pNMA36, *hsp-16p::fozi-1::fozi-1 3'UTR*

Recombinant fusion constructs for protein expression in bacteria:

pNMA04, GST-*fozi-1* cDNA (amino acids 1-171)

pNMA27, GST-*fozi-1 c*DNA (full length)

pNMA28, GST-*fozi-1* cDNA (amino acids 366-732)

pGEX-6P-3-*cyk-1* cDNA (amino acids 681-1435 of *cyk-1*)

All constructs were confirmed by sequencing. Transgenic lines were generated using the plasmid pRF4 (Mello et al., 1991) as a marker.

RNAi

Plasmids *yk288g3* and *yk779b02* were used as templates for synthesizing dsRNA against *fozi*-1 as described by Fire and colleagues (Fire et al., 1998). Plasmid *yk116b7* was used for synthesizing dsRNA against M01A8.2. All yk clones are from Yuji Kohara (National Institute of Genetics, Japan). dsRNAs for *hlh-1, mab-5* and *ceh-20* were synthesized using plasmids pVZ1200 (gift from Mike Krause, NIDDK, NIH, USA), pJKL718.2, and pJKL422.1 (Liu and Fire, 2000), respectively. *fozi-1, M01A8.2* or *ceh-20* dsRNA was injected into gravid adults of our wild-type reference strain LW0081. Progeny from the injected animals were scored for M lineage phenotypes and, in the case of *ceh-20*, for FOZI-1 expression via immunostaining.

For *hlh-1(RNAi)* and *mab-5(RNAi),* synchronized L1 animals expressing various M lineage GFP markers were soaked in *hlh-1* dsRNA, *mab-5* dsRNA, or both, for 24-48 hours following the protocol of Maeda and colleagues (Maeda et al., 2001). Animals were allowed to recover at 20˚C and scored for M lineage phenotypes. Water was used as a soaking control.

Heat-shock experiments

The following strains were generated and used in the heat-shock experiments: *ccIs4251(myo-3::gfp)*; *jjEx[hsp::hlh-1(pPD50.63) + rol-6(d)]*

ccIs4251(myo-3::gfp); *jjEx[hsp::fozi-1(pNMA36) + rol-6(d)]*

ccIs4438(*intrinsic CC::gfp*); *ayIs2*(*egl-15::gfp*); *ayIs6*(*hlh-8::gfp*); *jjEx[hsp::hlh-1 + rol-6(d)]*

ccIs4438(*intrinsic CC::gfp*); *ayIs2*(*egl-15::gfp*); *ayIs6*(*hlh-8::gfp*); *jjEx[hsp::fozi-1 + rol-6(d)]*

ccIs4438(*intrinsic CC::gfp*); *ayIs2*(*egl-15::gfp*); *ayIs6*(*hlh-8::gfp*); *jjEx[hsp::hlh-1 + hsp::fozi-1 + rol-6(d)]*

Two different heat-shock protocols were used to test the myogenic potential of FOZI-1. In each case, global ectopic expression of FOZI-1 was confirmed by anti-FOZI-1 antibody staining four hours after heat-shock. The first protocol was the same as described in Fukushige and Krause (Fukushige and Krause, 2005). One- to two-cell embryos were harvested and incubated at 20˚C for 30 minutes. Embryos were then heat-shocked for 30 minutes at 37˚C and allowed to recover at 20˚C. Embryos were observed periodically over a 20 hour window for ectopic *myo-3::gfp* expression and an arrested development phenotype. For the second protocol, transgenic animals were given multiple heat-shock pulses (5-7 pulses) starting from mid-embryo/early L1 stage through adulthood. Heat-shock pulses were performed for 30 minutes at 37˚C followed by 3 to 4 hours at 20˚C prior to subsequent heat-shock treatments. Heat-shocked animals were scored for their M lineage phenotypes. In both experiments, heat-shocked non-transgenic animals were used as negative controls.

in vitro actin-binding assays

Plasmids pNMA27, pNMA28 and pGEX-6P-3-*cyk-1*^{FH1FH2COOH} were used to generate GST-fusion proteins in BL21(DE3) cells for FOZI-1, FOZI-1 FH2 domain and CYK-1 FH1FH2 domains plus COOH-terminal residues, respectively. All GST-fusion proteins were bound to glutathione sepharose 4B beads (Amersham

Biosciences) and cleaved from GST by GST-3CPro precision protease (Amersham Biosciences) and soluble FOZI-1, FOZI-1^{FH2}, or CYK-1^{FH1FH2COOH} were extracted. GST-Bni1p^{FH1FH2COOH} was purified as previously described (Pruyne et al., 2002). Samples were analyzed by SDS-PAGE.

The effects of FOZI-1 on rates of actin polymerization and barbed end capping of actin filaments were examined using pyrene-actin assays (Pollard, 1983) with the above-purified recombinant proteins. Recombinant FOZI-1 proteins were incubated with F-actin in co-sedimentation assays to test whether FOZI-1 binds filamentous actin (Bretscher, 1981).

Antibody production and immunofluorescence staining

The N terminus of FOZI-1 (amino acids 1-171) was cloned into pGEX-4T-1 (Smith and Johnson, 1988). The resulting plasmid pNMA04 was transformed into BL21(DE3)pLysS cells. Fusion proteins were purified from Glutathione sepharose 4B beads (Amersham Biosciences) and further purified by SDS-PAGE. Gel slices containing purified FOZI-1 protein were used to immunize guinea pigs (Cocalico Biologicals, PA). Resulting antiserum was tested by Western blot analysis using bacterially expressed GST-FOZI-1 fusion proteins. Antibodies were affinity purified against GST-FOZI-1 bound to a nitrocellulose membrane (Olmsted, 1981; Smith and Fisher, 1984).

Animal fixation and immunostaining were performed following the protocol of Hurd and Kemphues (Hurd and Kemphues, 2003). For immunostaining with HLH-1 antibodies, animals were fixed and stained following the protocol of Harfe and colleagues (Harfe et al., 1998a). The following antibodies were used: affinity purified anti-FOZI-1 (CUMC-GP19; 1:50), goat anti-GFP (Rockland Immunochemicals; 1:5000), rat anti-MLS-2 (Jiang et al., 2005) and rabbit anti-HLH-1 (Harfe et al.,

1998a). All secondary antibodies were from Jackson ImmunoResearch Laboratories and used in a dilution of 1:100 to 1:200. Differential interference contrast and epifluorescence microscopy were performed using a Leica DMRA2 compound microscope. Images were captured with a Hamamatsu Orca-ER Camera using the Openlab software (Improvision). Subsequent image analysis was performed using Adobe Photoshop 7.0 and Adobe Illustrator CS.

Results

fozi-1 mutants display cell fate specification defects in the M lineage

In screens to identify mutants affecting M lineage development (see Materials and Methods), four recessive mutations were isolated that failed to complement one another, *cc607*, *cc608*, *cc609* and *cc610*. These mutations define the *fozi-1* locus (see below). Animals homozygous for these mutations lack M-derived CCs, with 100% penetrance in *cc607, cc608 and cc609* and 81% penetrance in *cc610* (Table 2.1, Figure 2.2).

To determine the basis for the missing CCs in these mutants, I followed the M lineage in *cc609* mutant animals using a combination of cell-type specific markers. Using the *hlh-8::gfp* reporter as a marker for undifferentiated cells of the M lineage (Harfe et al., 1998b), I found that the M mesoblast in *cc609* mutant animals gives rise to a total of 18 descendants (Figure 2.2J-L, data not shown), like wild-type (Figure 2.2I). However, the fates of these 18 cells in *cc609* mutants were not specified correctly. Of the 18 cells that arise from M in wild-type animals, 14 become body wall muscles (BWMs), 2 become (CCs), and 2 become sex myoblasts (SMs; Figure 2.1). In *cc609* mutants, however, both M-derived CCs (Harfe et al., 1998a) were missing, fewer than 14 M-derived BWMs (Fire et al., 1998) were present (Table 2.1, Figure

Table 2.1. M lineage defects of *fozi-1* mutant alleles.

Genotype	Number of M-derived CCs (*intrinsic CC:gfp*)	Number of M-derived BWMs (*myo-3::gfp*)	Number of SM-like cells (*hlh-8::gfp*)	Number of vm1-like cells (*egl-15::gfp*)
wild-type	2 (n>100)	14 (n=5)	2 (n>100)	4 (n>100)
cc607	0 (n>100)	nd	4.11 ± 0.88 (n=55)	8.26 ± 1.39 (n=31)
cc608	0 (n>100)	nd	nd	Nd
cc609	0 (n>100)	12.5 ± 0.85 (n=10)	4.10 ± 0.86 (n=58)	8.41 ± 1.54 (n=37)
cc610	0.58 ± 0.78 (n=161)[†]	nd	3.17 ± 0.97 (n=88)	6.45 ± 1.41 (n=64)
tm0563	0 (n>100)	nd	4.01 ± 0.85 (n=61)	8.81 ± 1.37 (n=42)

Data indicated are average counts plus or minus standard deviation where applicable.
nd. not determined.
[†] 60% of animals scored had 0 M-derived CCs, 21% had 1, and 19% had 2.

Figure 2.2. The M lineage phenotypes of *cc609* mutants.

All images are ventral/lateral views with anterior to the left.

(A-H): Wild-type (A, B, E, F) and *cc609* mutant (C, D, G, H) animals at the late L2 stage (A-D) and adult stage (E-H), respectively. SMs are visualized using *hlh-8::gfp* and labeled with red arrows. CCs are visualized using *intrinsic CC::gfp*; embryonic CCs are labeled with white arrowheads and M-derived CCs with blue arrows. Type I vulval muscles are visualized using *egl-15::gfp* and labeled with green arrows. Note the presence of two SMs in the wild-type larva (A, B) and four SM-like cells in the *cc609* larva (C, D). (B) and (D) show the SM-like cells at higher magnification. Also note the lack of M-derived CCs in *cc609* larva (C, G) as compared to wild-type animals (A, E). *cc609* adults have extra type I vulval muscles (vm1-like cells) (G, H) compared to wild-type (E, F). (F) and (H) show the vulval muscles in higher magnification.

(I-L): Representations of the hermaphrodite M lineage in wild-type (I) and different *cc609* mutant (J-L) animals. Unmarked cells refer to BWMs. (I) Wild-type animals always give rise to 2 CCs, 2 SMs and 14 BWMs. (J-L) *cc609* mutant animals consistently have a loss of M-derived CCs and some BWMs, with the concomitant gain of SM-like cells.

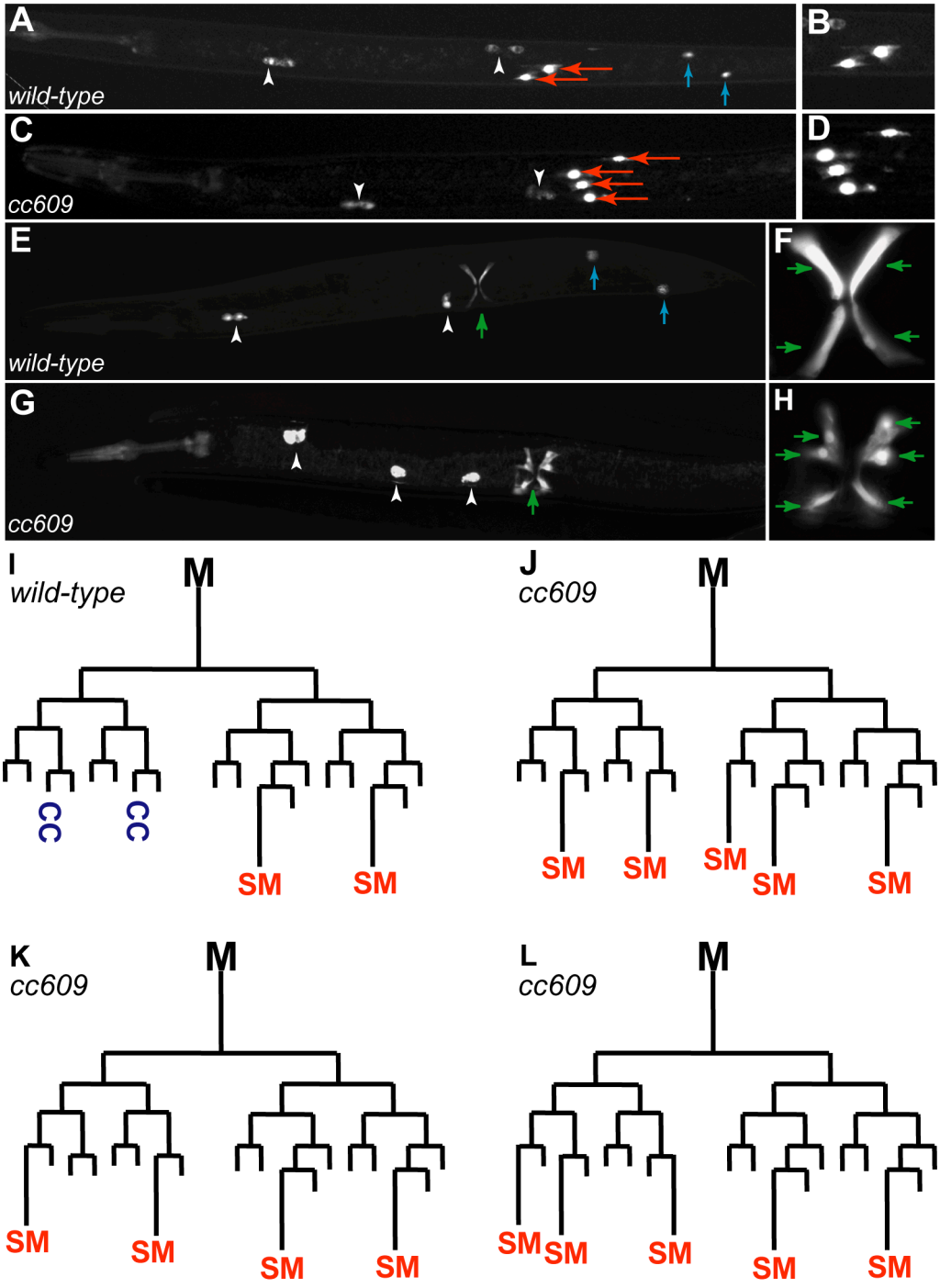
A
wild-type
B
C
cc609
D
E
wild-type
F
G
cc609
H
I
wild-type
M
CC
CC
SM
SM
J
cc609
M
SM
SM
SM
SM
SM
K
cc609
M
SM
SM
SM
SM
L
cc609
M
SM
SM
SM
SM
SM

2.2J-L), and more than two of the 18 M-derived cells displayed SM-like characteristics (*hlh-8::gfp* expression, SM shape, enlarged size and potential to migrate to the presumptive vulval region; Table 2.1, Figure 2.2A-D**)**. Two of the SM-like cells in *cc609* mutants always migrated to the ventral side near the presumptive vulval region and generated the correct number of sex muscles that attached properly, as visualized by *egl-15::gfp*, *arg-1::gfp*, *myo-3::gfp* and polarized light microscopy. The remaining SM-like cells divided one to three times and gave rise to extra sex muscles either around the vulva or in the posterior region of the animal (Table 2.1, Figure 2.2G-H, data not shown). Thus *cc609* mutants exhibit cell fate transformations from M-derived CCs and BWMs to SMs (Figure 2.2J-L). Similar M lineage defects were also observed in *cc607, cc608* and *cc610* mutant animals (Table 2.1).

fozi-1 encodes a novel formin with two C_2H_2 Zn fingers and an FH2 formin homology domain

cc609 mapped to an interval between cosmids K04H4 and F54G8 in the middle of chromosome III. Two overlapping cosmids in this region, M01A8 and K01B6, rescued the M lineage defects of *cc609* mutants. RNAi was performed for each of the two genes located at the junction between M01A8 and K01B6, M01A8.2 and K01B6.1 (see Materials and Methods). RNAi of M01A8.2 gave no M lineage defects. However, RNAi of K01B6.1 in wild-type animals resulted in similar M lineage defects to those seen in *cc609* mutant animals. Sequencing the coding regions of K01B6.1 in *cc607*, *cc608*, *cc609* and *cc610* mutant animals showed that they all contain molecular lesions in the K01B6.1 coding region (Figure 2.3A). *cc607* and *cc608* contain the same nonsense mutation at residue 112 (CAG to TAG, Gln to amber stop). The *cc609* mutant contains a deletion that spans residues 160 to 260 of K01B6.1 and causes a frameshift in the remaining coding sequence (Figure 2.3A). In *cc610*

Figure 2.3. *fozi-1* encodes a novel protein.

(A) *fozi-1* gene structure (not drawn to scale) showing molecular lesions of *fozi-1* mutants. The first intron of *fozi-1* spans 7 kb upstream of the translation start site. (B) The structural motifs of FOZI-1 include a Q rich region (aa 88-133), two C_2H_2 zinc finger motifs (aa 177-201) and an FH2 formin homology domain (aa 369-732). (C) pNMA04, pNMA27 and pNMA28 are *fozi-1* fusion constructs used to purify recombinant FOZI-1 fragments. pNMA36 and pNMA37 were used in transgenic assays.

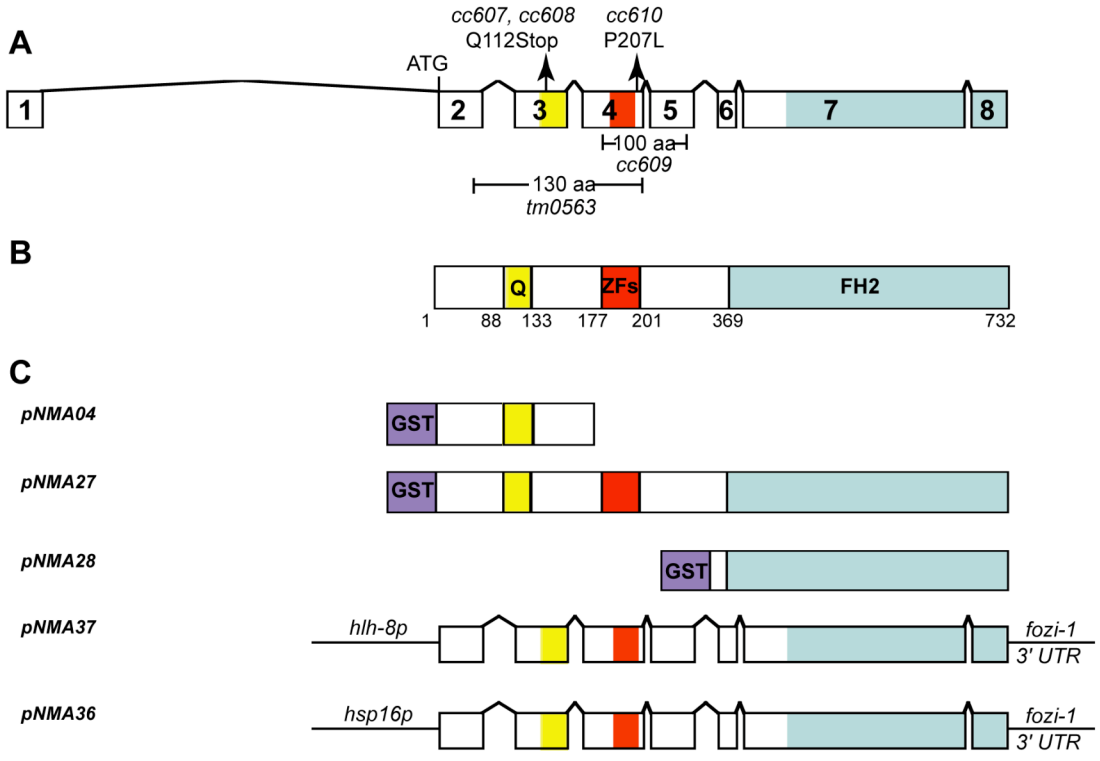
A
cc607, cc608
Q112Stop
cc610
P207L
ATG
1
2
3
4
5
6
7
8
100 aa
cc609
130 aa
tm0563
B
Q
ZFs
FH2
1
88
133
177
201
369
732
C
pNMA04
GST
pNMA27
GST
pNMA28
GST
pNMA37
hlh-8p
fozi-1
3' UTR
pNMA36
hsp16p
fozi-1
3' UTR

mutants, there is a missense mutation at residue 207 (CGA to TGA, Pro to Leu) (Figure 2.3A). During the course of my studies, the National Bioresource Project for the Experimental Animal Nematode *C. elegans* generated another deletion allele of K01B6.1, *tm0563*, which deletes a larger region than *cc609* and also results in a frameshift (Figure 2.3A). *tm0563* mutant animals displayed similar M lineage phenotypes to *cc609* animals (Table 2.1). Since *cc607*, *cc608, cc609* and *tm0563* all exhibit 100% penetrance in their M lineage defects (Table 2.1) and they contain either early termination codons or deletions in K01B6.1 (Figure 2.3A), all four alleles are likely null alleles. Additional evidence supporting this is provided by the immunostaining results discussed below.

The predicted protein encoded by K01B6.1 is FOZI-1 (FOrmin homology ZInc finger protein-1), a 732 amino acid-protein with three distinct motifs (Figure 2.3B): a glutamine-rich region (residues 88-133), two C_2H_2 zinc finger motifs (residues 177-201), and a FH2 formin homology domain (residues 369-732). The glutamine-rich region and the zinc finger motifs are characteristics of transcription factors (Matsuzaki et al., 1995; Iuchi, 2001; Stepchenko and Nirenberg, 2004). The FH2 domain is conserved among a large family of proteins called formins that are present from yeast to humans (Higgs and Peterson, 2005). Formins have been shown to use their FH2 domains to form dimers that bind actin and play critical roles in multiple processes of actin dynamics, such as nucleation, capping, severing and bundling of actin filaments (Pruyne et al., 2002; Sagot et al., 2002; Kovar et al., 2003; Zigmond et al., 2003; Harris et al., 2004; Xu et al., 2004; Michelot et al., 2005; Moseley and Goode, 2005). The FH2 domain of FOZI-1 is unique in that it contains many of the conserved residues involved in dimerization, but lacks the key residues critical for actin-binding (Figure 2.4A). The ability of the FH2 domain of FOZI-1 or the full length FOZI-1 protein could bind filamentous actin, induce actin polymerization, or cap the barbed-

ends of actin filaments in vitro was tested. FOZI-1 was unable to polymerize actin filaments, while the *C. elegans* CYK1 FH1FH2 protein domains were fully active in this process (Figure 2.4B). Furthermore, FOZI-1 was unable to bind actin or show capping activity in vitro (data not shown). Since residues critical for dimerization in the FH2 domain of FOZI-1 are conserved, the FOZI-1 FH2 domain likely functions as a dimerization domain, consistent with in vitro data obtained by Johnston and colleagues (Johnston et al., 2006).

FOZI-1 is a nuclear protein expressed in the M-derived CC and BWM precursors

As described above, *fozi-1* mutant animals exhibit cell fate transformations from M-derived CCs and BWMs to SMs. To begin to understand how FOZI-1 functions in regulating fate specification in the M lineage, I examined the expression pattern of FOZI-1 during development. I generated antibodies to FOZI-1 and performed immunostaining to detect the endogenous FOZI-1 protein (see Materials and Methods). The antibodies specifically recognized a protein of the predicted size for FOZI-1 (~80 kD) on Western blots using worm extracts (data not shown), and failed to detect any signal in *cc609* mutant embryos and larvae (Figure 2.5C,D,T).

Using these antibodies, I found that FOZI-1 protein is localized in nuclei of a distinct set of cells in wild-type animals. Expression of FOZI-1 was first detectable in a small subset of nuclei (likely neuroblasts) in embryos at the 2-fold stage (Figure 2.5A-B**)**. During larval development, FOZI-1 expression is restricted to a subset of unidentified neurons in the head (7 to 12 cells) and along the ventral nerve cord (5 to 7 cells) (Figure 2.5E-F). FOZI-1 is also present transiently during the L1 larval stage in cells derived from the M lineage (see below).

Figure 2.4. The FH2 domain of FOZI-1 is divergent from other eukaryotic formins.

(A) An alignment report from Megalign (DNAStar, Inc.) of the FH2 domain of FOZI-1 with the FH2 domains of the *S. cerevisiae* formins Bni1p (Jansen et al., 1996; Kohno et al., 1996) and Bnr1p (Imamura et al., 1997), the *M. muscularis* formin mDia1 (Watanabe et al., 1997), *C. elegans* CYK-1 (Swan et al., 1998) and *C. briggsae* (CbFOZI-1) and *C. remanei* FOZI-1 (CrFOZI-1) homologs (Wormbase). The FH2 domain was defined as the minimal portion of the *S. cerevisiae* formin Bni1p (residues 1348 to 1750) able to nucleate actin filaments (Moseley and Goode, 2005), plus 9 additional residues that were resolved in the Bni1p FH2 domain crystal structure (Xu et al., 2004). Numbering of residues begins with the first residue of each FH2 domain. Color scheme is as follows: yellow = lasso residues, red = actin-interacting residues, blue = post residues, purple = dual post/actin-interacting residues. Criteria for conserved residues are as previously described (Shimada et al., 2004; Xu et al., 2004; Otomo et al., 2005). Asterisks denote conserved residues in the lasso domain that are found at the hydrophobic pocket of the post domain in Bni1p FH2 dimers (Xu et al., 2004). Arrowheads denote actin binding residues from Bni1p crystal structure (Xu et al., 2004).

(B) The FH2 domain of FOZI-1 does not nucleate actin filaments *in vitro*. Actin polymerization is represented as a measure of pyrene fluorescence over time. CYK-$1^{FH1FH2COOH}$ and GST-$Bni1p^{FH1FH2COOH}$ (used as positive controls) show a robust amount of actin polymerization over 10 minutes. Varying concentrations of FOZI-1 (not shown) and FOZI-1^{FH2} are unable to promote actin polymerization to levels significantly higher than buffer alone or GST controls.

A

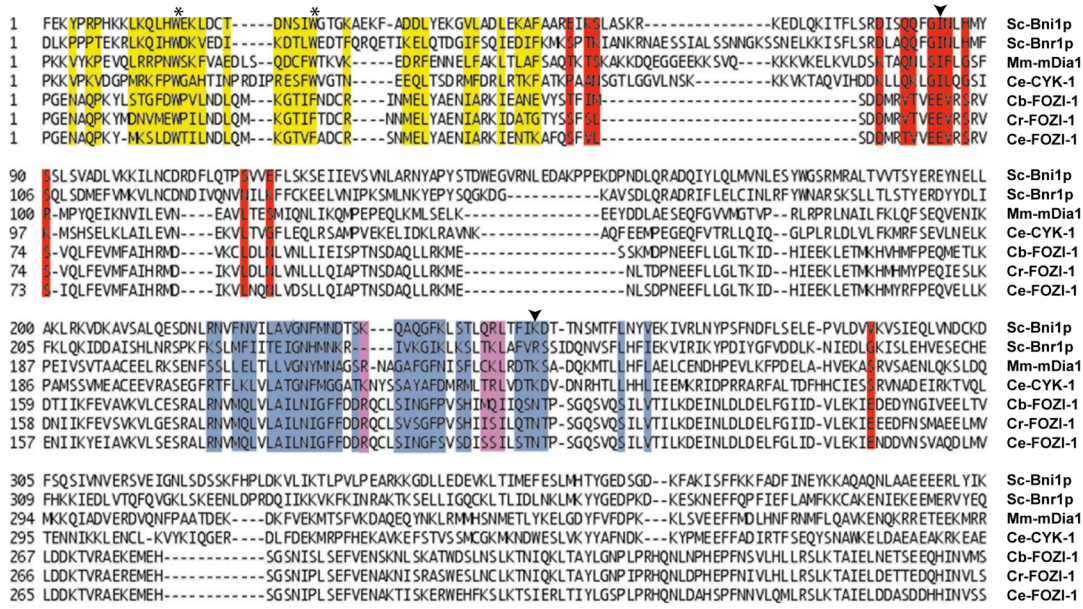
Sc-Bni1p
Sc-Bnr1p
Mm-mDia1
Ce-CYK-1
Cb-FOZI-1
Cr-FOZI-1
Ce-FOZI-1

B

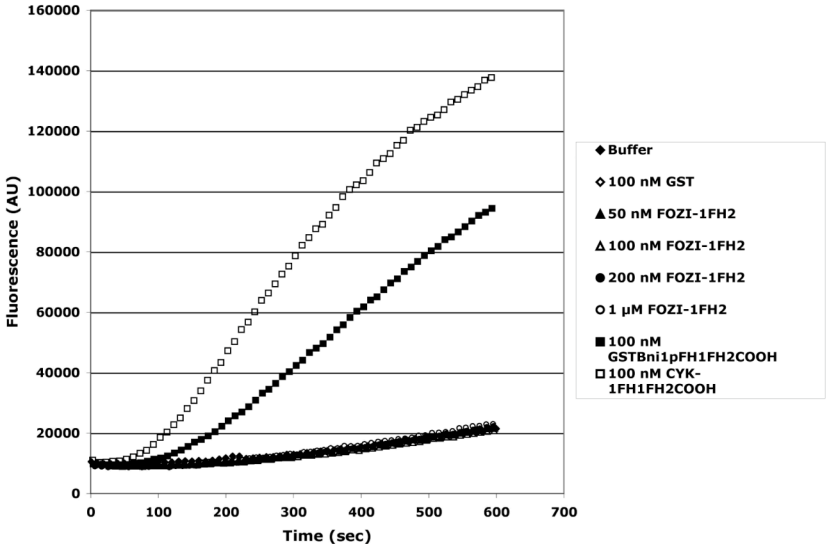
Fluorescence (AU)
Time (sec)
Buffer
100 nM GST
50 nM FOZI-1FH2
100 nM FOZI-1FH2
200 nM FOZI-1FH2
1 μM FOZI-1FH2
100 nM GSTBni1pFH1FH2COOH
100 nM CYK-1FH1FH2COOH

Figure 2.5. Expression pattern of FOZI-1 in wild-type, *cc609* and *cc610* hermaphrodites and embryos.

All images are lateral views with anterior to the left and dorsal up (unless otherwise noted).

(A-D): Wild-type (A, B) and *cc609* (C, D) embryos stained with anti-FOZI-1 antibody (A, C) and DAPI (B, D). Nuclear FOZI-1 is seen in a subset of cells at the 2-fold stage of embryogenesis in wild-type (A) but not in *cc609* (C) embryos.

(E,F) FOZI-1 staining in a wild-type L1 larva on two different focal planes. FOZI-1 was observed in the nuclei of 7-12 head neurons (arrow, E) and 5-7 cells along the ventral nerve cord (arrowheads, E,F) and in cells derived from the M lineage (red box, E,F).

(G-R) Double labeling with anti-FOZI-1 antibody and *hlh-8::gfp* at the 2-M (G-I), 16-M (J-L), 18-M (M-O) and 2-SM (P-R) stages in wild-type animals. Anti-FOZI-1 antibody staining is shown in panels G, J, M and P; *hlh-8::gfp* is shown in panels H, K, N and Q; the corresponding merged images are shown in panels I, L, O and R. FOZI-1 staining was first detected at the 2-M stage (G-I) and persisted through the 16-M (J-L) stages. At the 18-M stage (M-O) FOZI-1 is still present in all undifferentiated CC and BWM precursors but is absent in the SMs. Arrowheads in panel M denote cells in the ventral nerve cord. (P-R) FOZI-1 is not present in the 2-SM cells and the subsequent SM-lineage (data not shown). (S) Summary of FOZI-1 expression in the M lineage. The wild-type M lineage is shown with overlay of FOZI-1 expression highlighted in red.

(T,U) Staining of *cc609* (T) and *cc610* (U) animals at mid-L1 stage using anti-FOZI-1 antibodies. (T) No FOZI-1 was detected in *cc609* animals. (U) Wild-type level and localization pattern of FOZI-1 are detected in *cc610* mutant animals in head neurons (arrow), ventral nerve cord (arrowheads) and the M lineage (red box).

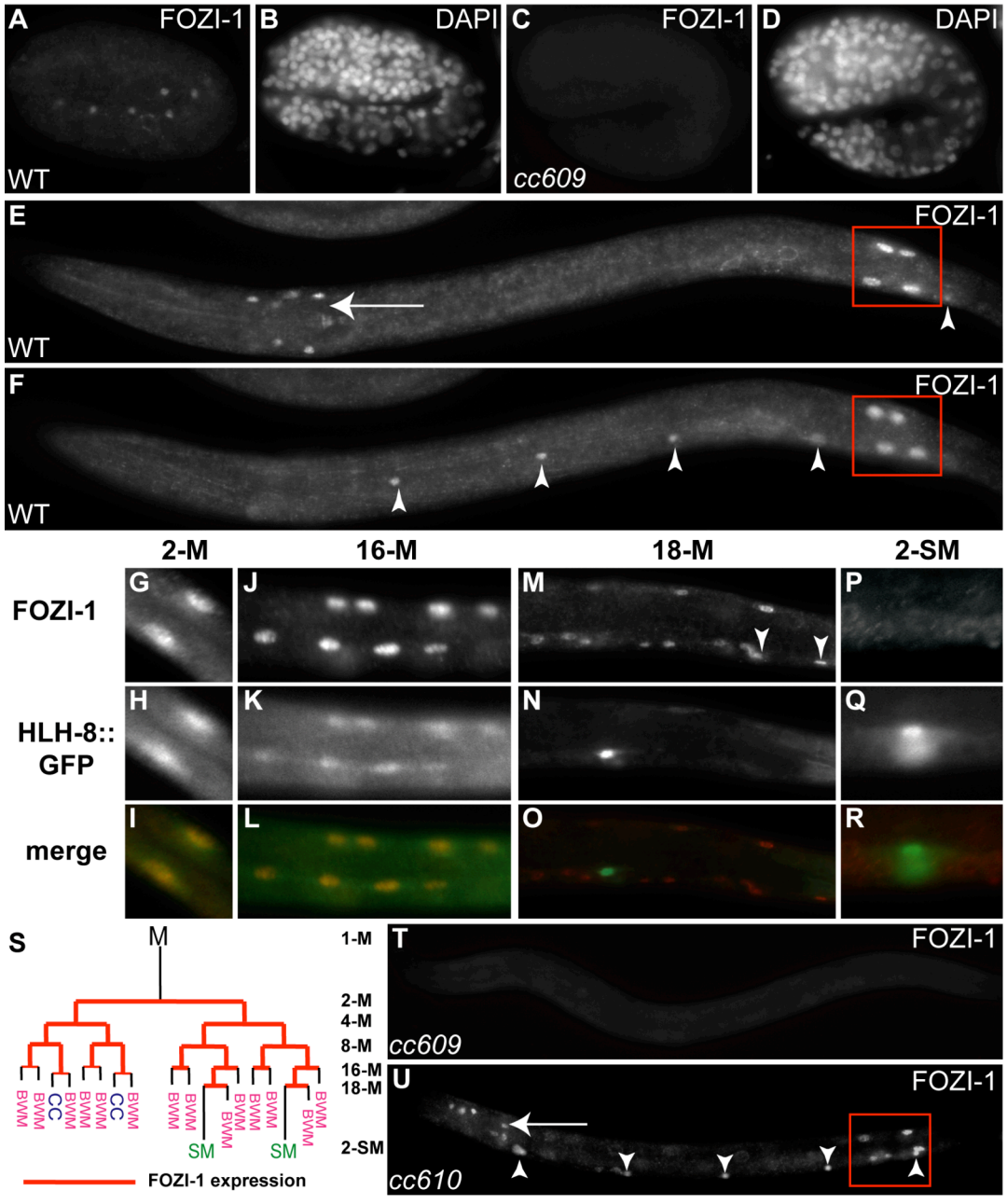
A
FOZI-1
WT
B
DAPI
C
FOZI-1
cc609
D
DAPI
E
FOZI-1
WT
F
FOZI-1
WT
2-M
16-M
18-M
2-SM
FOZI-1
HLH-8::
GFP
merge
G
J
M
P
H
K
N
Q
I
L
O
R
S
M
BWM
CC
SM
FOZI-1 expression
1-M
2-M
4-M
8-M
16-M
18-M
2-SM
T
FOZI-1
cc609
U
FOZI-1
cc610

To examine the M lineage expression pattern of FOZI-1, I performed double-labeling experiments using anti-FOZI-1 antibodies and the M lineage specific *hlh-8::gfp* marker (Harfe et al., 1998b). FOZI-1 expression in the M lineage was first detectable in the nuclei of M.d and M.v at the 2-M stage (in 43% of the animals stained, n=21, Figure 2.5G-I**)**. This expression persisted through the next three rounds of cell divisions, such that all animals (n>50) at the 4-M through the 16-M stage showed FOZI-1 expression in the M lineage (Figure 2.5J-L). At the 16-M stage, two cells on the ventral side (M.vlpa and M.vrpa) divide one more time to produce two SMs and two BWM precursors and reach the 18-M stage (Figure 2.1). At the 18-M stage, FOZI-1 was still detectable in the undifferentiated BWMs and CCs, but not in the SMs (n=22, Figure 2.5M-O). This expression of FOZI-1 at the 18-M stage appeared transiently and quickly became undetectable in the differentiated BWMs and CCs. FOZI-1 expression was not detected in the SM lineage (n>50, Figure 2.5P-R, data not shown). The expression pattern of FOZI-1 in the M lineage is summarized in Figure 2.5S. Thus, expression of FOZI-1 is tightly regulated within the M lineage at the time when BWM and CC cell fate specification occurs.

Residues proximal to the C_2H_2 zinc fingers are required for FOZI-1 function in the M lineage

To determine whether FOZI-1 expression and subcellular localization were lost in *fozi-1* mutants, we performed FOZI-1 staining in all of the *fozi-1* mutants at all developmental stages. As discussed above, *cc609* animals have no detectable levels of FOZI-1 at any stage during development (Figure 2.5C-D, T). *cc607* and *tm0563* also show no FOZI-1 immunostaining at any stage (data not shown; I did not examine *cc608* animals since *cc607* and *cc608* contain the same molecular lesion). These results are consistent with the hypothesis that *cc607*, *cc609* and *tm0563* are null

alleles. Animals mutant for *cc610*, however, showed nuclear anti-FOZI-1 staining in a pattern identical to wild-type animals in the head neurons, ventral nerve cord and the M lineage (Figure 2.5U, n>50). Since *cc610* mutants exhibit M lineage defects (Table 2.1) and the missense mutation in *cc610* is located six residues downstream of the second histidine residue of the second zinc finger (Figure 2.3A), I conclude that the residues surrounding the C_2H_2 zinc fingers are required for proper FOZI-1 function in the M lineage.

FOZI-1 functions within the M lineage for proper CC and BWM cell fate specification

The expression pattern of *fozi-1* and the M lineage defects of *fozi-1* mutants suggest that FOZI-1 functions within the M lineage to specify the fates of the CCs and BWMs. To directly test this hypothesis, I expressed *fozi-1* specifically in the M lineage in *cc609* mutants using the *hlh-8* promoter (Harfe et al., 1998b). Transgenic animals carrying an *hlh-8p::fozi-1* transgene (Figure 2.3C) in the *cc609* mutant background showed M lineage specific expression of *fozi-1* (data not shown). This M lineage specific expression is sufficient to restore M-derived CCs in *cc609* mutant animals (23.2%, n=56). The low level of rescue may be attributed to the difference between endogenous *hlh-8* and *fozi-1* expression patterns: *fozi-1* persists slightly longer than *hlh-8* in the BWM and CC precursors (Harfe et al., 1998b). Thus, FOZI-1 appears to function cell-autonomously within the M lineage for proper mesodermal cell fate specification.

FOZI-1 functions redundantly with CeMyoD/HLH-1 to specify BWM fates in the M lineage

Previous studies (Harfe et al., 1998a) have shown that the *C. elegans* MyoD ortholog, Ce-MyoD/HLH-1, is expressed in the M lineage in a pattern like that of FOZI-1 (except that HLH-1 persists in all differentiated M-derived BWMs while FOZI-1 does not) and that *hlh-1* mutants showed similar CC and BWM to SM fate transformation as *fozi-1* mutants. To examine the functional relationship between FOZI-1 and HLH-1, I examined the expression and nuclear localization of HLH-1 in *fozi-1(cc609)* mutants and of FOZI-1 in temperature-sensitive *hlh-1(cc561ts)* mutants at the non-permissive temperature (25˚C). As shown in Figure 2.6A-D, expression and nuclear localization of FOZI-1 in *hlh-1(cc561ts)* and HLH-1 in *fozi-1(cc609*) were normal. Thus, HLH-1 and FOZI-1 do not regulate each other's expression or sub-cellular distribution.

Since both *hlh-1* and *fozi-1* mutant animals exhibit loss of some, but not all, body wall muscles (BWMs) derived from the M lineage (Harfe et al., 1998a), I investigated the possibility that *hlh-1* and *fozi-1* act redundantly. Because *hlh-1* null mutants are embryonic/L1 lethal due to the essential functions of HLH-1 in proper differentiation of the embryonically-derived BWMs (Chen et al., 1992; Chen et al., 1994), I used two approaches to assess the possible redundancy of HLH-1 and FOZI-1 in the M lineage. I first soaked *fozi-1(cc609)* L1 larvae with *hlh-1* dsRNA to deplete levels of HLH-1 in *fozi-1(cc609)* worms (referred to as *hlh-1(RNAi); fozi-1(cc609*), see Materials and Methods). I also generated *hlh-1(cc561ts); fozi-1(cc609)* double mutants and examined them at the restrictive temperature (25°C) for *cc561ts*. Both approaches gave almost identical results. The *hlh-1(cc561); fozi-1(cc609)* or *hlh-1(RNAi); fozi-1(cc609)* animals had a significant increase in the number of SM-like cells (Figure 2.7A) and a concomitant decrease in the number of M-derived BWMs

Figure 2.6. Expression of FOZI-1 in different M lineage mutants.

(A-C): A *fozi-1(cc609); ayIs6(hlh-8::gfp)* mutant animal at the 8-M stage stained with anti-HLH-1 antibody (red in A,B) and DAPI (C). White arrows represent M lineage as marked by *hlh-8::gfp*. Embryonically-derived BWMs are denoted by open arrowheads. (D-F) Anti-FOZI-1 staining in *hlh-1(cc561ts)* (D), *mab-5(e1239)* (E) and *mls-2(cc615)* (F) animals. FOZI-1 is present in the M lineage of all three mutants. Arrowhead denotes a cell from the ventral nerve cord (F). (G) A *ceh-20(n2513)* animal stained with anti-FOZI-1 antibody. FOZI-1 is detected in the head neurons (arrow) and the ventral nerve cord (arrowheads), but not in the M lineage (red box).

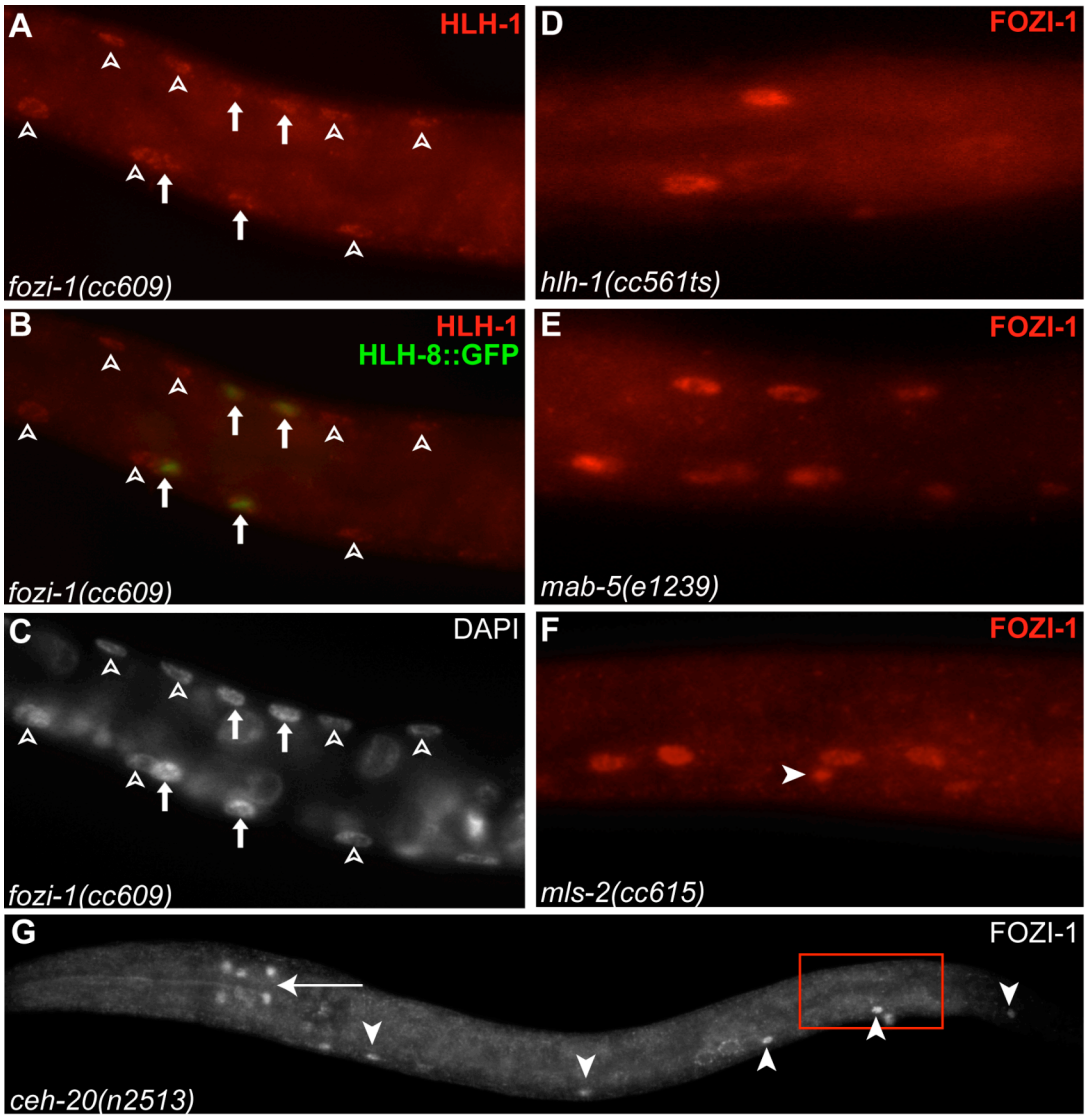
A
HLH-1
fozi-1(cc609)
B
HLH-1
HLH-8::GFP
fozi-1(cc609)
C
DAPI
fozi-1(cc609)
D
FOZI-1
hlh-1(cc561ts)
E
FOZI-1
mab-5(e1239)
F
FOZI-1
mls-2(cc615)
G
FOZI-1
ceh-20(n2513)

Figure 2.7. HLH-1 functions redundantly with FOZI-1 and MAB-5 to specify M-derived BWMs. (A,B) Quantification of the number of SM-like cells (expressing *hlh-8::gfp*) (A) and M-derived BWMs (expressing *myo-3::gfp*) (B). *n* values are given for each genotype scored. Mean values are shown with error bars representing standard deviation for each sample set. All animals showed normal proliferation in the early M lineage up to the 16-M stage. The number of SM-like cells and M-derived BWMs were also scored in the following animals: *mab-5(RNAi)*, *hlh-1(RNAi)*, *hlh-1(RNAi); mab-5(e1239)*, *hlh-1(RNAi); fozi-1(cc609)*, *hlh-1(RNAi); fozi-1(cc609) mab-5(RNAi)* and *hlh-1(cc561ts+RNAi); fozi-1(cc609) mab-5(e1239)*. For each genotype, more than 50 animals were scored for the number of SMs and more than 10 animals were scored for the number of M-derived BWMs. * A small percentage of these animals lacked all M-derived BWMs and had a total of 16-18 SM-like cells.

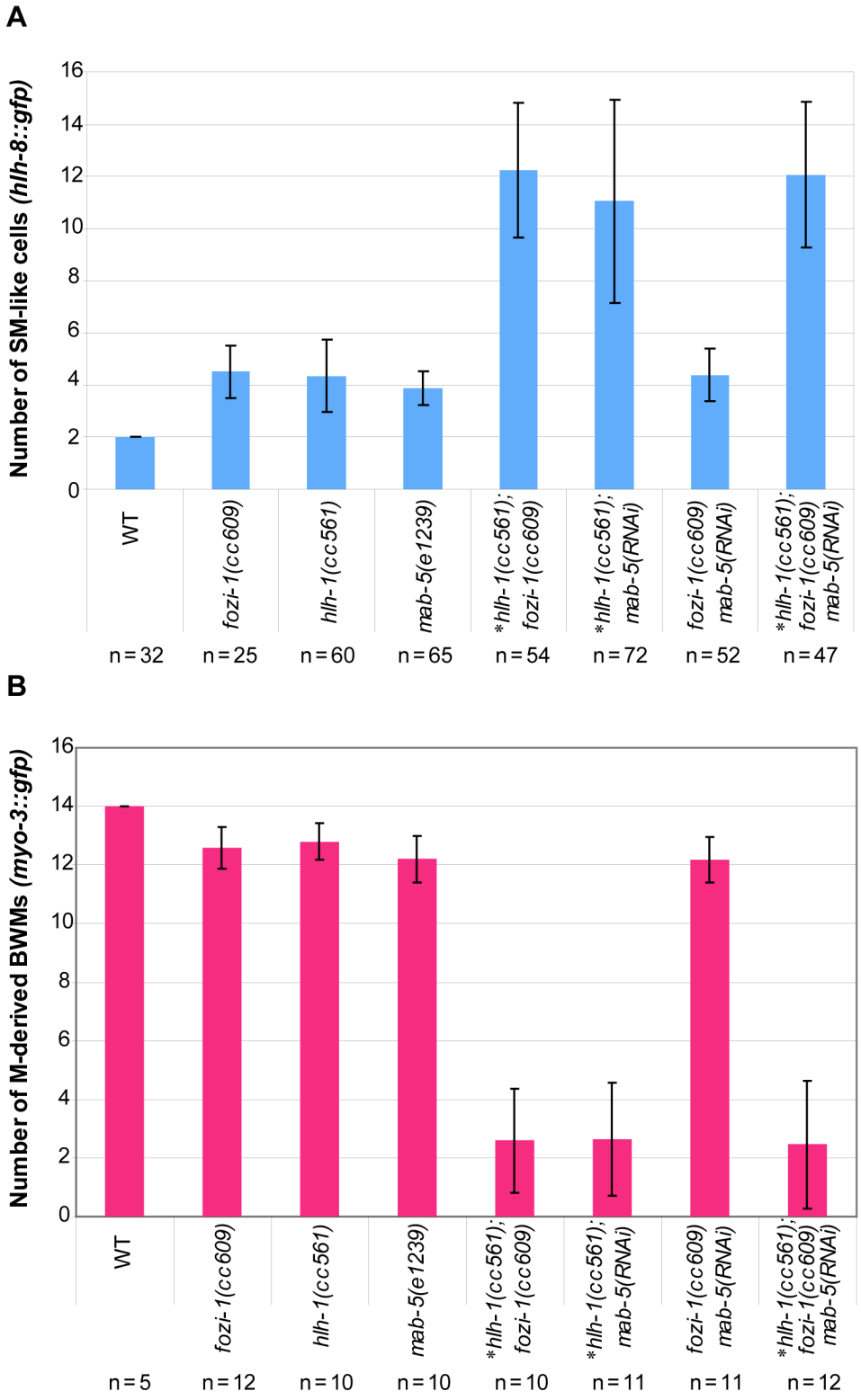
A
Number of SM-like cells (hlh-8::gfp)
16
14
12
10
8
6
4
2
0
WT
fozi-1(cc609)
hlh-1(cc561)
mab-5(e1239)
*hlh-1(cc561); fozi-1(cc609)
*hlh-1(cc561); mab-5(RNAi)
fozi-1(cc609) mab-5(RNAi)
*hlh-1(cc561); fozi-1(cc609) mab-5(RNAi)
n = 32
n = 25
n = 60
n = 65
n = 54
n = 72
n = 52
n = 47
B
Number of M-derived BWMs (myo-3::gfp)
16
14
12
10
8
6
4
2
0
WT
fozi-1(cc609)
hlh-1(cc561)
mab-5(e1239)
*hlh-1(cc561); fozi-1(cc609)
*hlh-1(cc561); mab-5(RNAi)
fozi-1(cc609) mab-5(RNAi)
*hlh-1(cc561); fozi-1(cc609) mab-5(RNAi)
n = 5
n = 12
n = 10
n = 10
n = 10
n = 11
n = 11
n = 12

(Figure 2.7B) when compared to *fozi-1*(*cc609), hlh-1(cc561)* or *hlh-1(RNAi)* single mutants. The increased number of SM-like cells in *hlh-1(cc609); fozi-1(cc609)* or *hlh-1(RNAi); fozi-1(cc609)* animals was correlated with the significantly higher number of type I vulval muscle-like cells that express *egl-15::gfp* (vm1-like cells, data not shown). To distinguish whether these changes in the numbers of SMs and BWMs arose from cell fate transformations or cell proliferation defects, I followed the M lineage closely in three *hlh-1(RNAi); fozi-1(cc609)* mutant animals using a combination of *hlh-8::gfp* and DIC optics. I did not observe any proliferation defects in the first four rounds of cell divisions of the M mesoblast in these animals. Instead, all three animals exhibited a fate transformation from M-derived BWMs and CCs to SMs. There were 8 SM-like cells and 1 M-derived BWM on the right side of animal #1, and 9 SM-like cells and 0 M-derived BWM on the right side of animal #2. Animal #3 was monitored on both the right and the left sides. There were a total of 12 SM-like cells and 4 M-derived BWMs in this animal. All three animals had the correct number of embryonically-derived BWMs (data not shown). These observations indicate that FOZI-1 and HLH-1 function redundantly to specify striated body wall muscle fate in the postembryonic mesoderm.

FOZI-1 functions in the same process as the Hox factor MAB-5 in specifying M-derived BWMs

In addition to HLH-1 and FOZI-1, mutations in the Hox gene *mab-5* also result in the fate transformation of both M-derived CCs and some, but not all, M-derived BWMs to SMs (Harfe et al., 1998a). I therefore examined the relationship among MAB-5, FOZI-1 and HLH-1 in M-derived BWM fate specification. Because *mab-5* and *fozi-1* map very close to each other on chromosome III, I used RNAi to knock down the expression of *mab-5* in *hlh-1(cc561ts), fozi-1(cc609)* or *hlh-1(cc561ts); fozi-*

1(cc609) mutants (see Materials and Methods). I first established that *mab-5(RNAi)* caused similar M lineage phenotypes as the null *mab-5(e1239)* mutant (Figure 2.7, data not shown). I then followed the M lineage and counted the number of M-derived BWMs and SMs in various mutants soaked with *mab-5* dsRNA. All mutant animals exhibited normal proliferation in the early M lineage (data not shown). However, their terminal M lineage phenotypes differed from each other. As shown in Figure 2.7A,B, *fozi-1(cc609) mab-5(RNAi)* animals behaved just like *fozi-1(cc609)* or *mab-5(RNAi)* single mutant animals with only a few M-derived BWMs transformed to SMs, whereas *hlh-1(cc561ts); mab-5(RNAi)* animals behaved just like *hlh-1(cc561ts); fozi-1(cc609)* animals in that most, if not all, M-derived BWMs were transformed to SMs (Figure 2.7A,B). *hlh-1(cc561ts); fozi-1(cc609) mab-5(RNAi)* animals were indistinguishable from *hlh-1(cc561ts); fozi-1(cc609)* animals or *hlh-1(cc561ts); mab-5(RNAi)* animals in their BWM/SM phenotype (Figure 2.7A,B). Collectively, these results suggest that both MAB-5 and FOZI-1 function redundantly with HLH-1 to properly specify striated BWM fates in the M lineage and that MAB-5 and FOZI-1 act in the same process.

mab-5 is expressed in the M mesoblast and its expression persists throughout the M lineage . Since *mab-5* expression precedes *fozi-1* expression in the M lineage, I asked if *mab-5* is required for *fozi-1* expression. I stained *mab-5(e1239)* null mutant animals with anti-FOZI-1 antibodies and found a wild-type FOZI-1 expression and sub-cellular localization pattern (Figure 2.6E), indicating that *mab-5* is not required for the proper expression and localization of FOZI-1. It is unlikely that *fozi-1* is required for *mab-5* expression, as *fozi-1(cc609)* mutants do not display cleavage orientation defects or loss of *hlh-8* expression in the M lineage (Figure 2.2 and data not shown), phenotypes exhibited by *mab-5(e1239)* single mutants (Harfe et al., 1998b). Thus, FOZI-1 and MAB-5 do not regulate each other's expression in the M lineage.

The homeodomain protein CEH-20 is required for *fozi-1* expression in the M lineage

In addition to MAB-5, three other transcription factors critical for proper M lineage development, CEH-20, MLS-2 and HLH-8, are expressed in the M lineage beginning at the 1-M (or the M mesoblast) stage (Harfe et al., 1998b;Jiang et al., 2005;Yang et al., 2005). I asked whether these factors are required for *fozi-1* expression in the M lineage. I stained animals mutant for the presumed null alleles *mls-2(cc615)* and *hlh-8(nr2061)* using anti-FOZI-1 antibodies and found that *fozi-1* expression level and pattern were not altered (Figure 2.6F, data not shown). Similarly, expression of *mls-2* and *hlh-8* in the M lineage does not depend on FOZI-1 (data not shown).

In contrast, when I stained animals from the strong loss-of-function allele *ceh-20(n2513)*, we found that close to 90% of the animals (n=205) lacked *fozi-1* expression in the M lineage (Figure 2.6G). M lineage expression of *fozi-1* was also lost in progeny of animals injected with *ceh-20* dsRNA (data not shown). In both *ceh-20(n2513)* and *ceh-20(RNAi)* animals, *fozi-1* expression was still detectable in the head neurons and the ventral nerve cord (Figure 2.6G and data not shown), indicating that CEH-20 is specifically required for M lineage expression of *fozi-1*.

Discussion

I have identified a gene, *fozi-1*, encoding a unique zinc finger-FH2 domain containing protein that is required for proper fate specification in the *C. elegans* postembryonic mesoderm. I have shown that the FH2 domain of the FOZI-1 protein does not bind actin (Figure 2.4) and that FOZI-1 is localized to the nucleus (Figure 2.5). As FOZI-1 contains a Q rich region and two C2H2 zinc finger motifs that are

characteristic of transcription factors (Matsuzaki et al., 1995; Iuchi, 2001; Stepchenko and Nirenberg, 2004), I propose that FOZI-1 acts as a transcription factor required for proper fate specification in the M lineage.

In animals lacking FOZI-1, some M lineage-derived BWMs and non-muscle CCs are transformed to SM-like cells (Figure 2.2). Since M-lineage specific expression of *fozi-1* rescued these M lineage defects of *fozi-1(cc609)* mutants, I conclude that FOZI-1 functions cell autonomously within the M lineage to specify both BWM and CC fates. FOZI-1 is present in the early M lineage as well as in all M-derived BWM and CC precursors, but not SMs (Figure 2.6). It is not clear at present whether FOZI-1 functions early in the M lineage in the multipotent precursors or in the early cell cycle of the terminal BWM/CC/SM cells.

FOZI-1 and CeMyoD function redundantly to specify the striated BWM fate in the M lineage

The stochastic loss of a fraction of M-derived BWMs in *fozi-1(cc609)* mutants is very similar to phenotypes exhibited by animals lacking CeMyoD/HLH-1 in the M lineage (Harfe et al., 1998a). I have shown that *hlh-1(cc561ts); fozi-1(cc609)* and *hlh-1(RNAi); fozi-1(cc609)* animals exhibit normal proliferation in the early M lineage, yet most, if not all, of their M-derived BWMs are transformed to SM-like cells. These results demonstrate that FOZI-1 and CeMyoD/HLH-1 function redundantly to specify M-derived BWM fates. While the presence of a few M-derived BWMs in some *hlh-1(cc561ts); fozi-1(cc609)* or *hlh-1(RNAi); fozi-1(cc609)* animals could be due to the partial loss-of-function nature of the *hlh-1(cc561ts)* mutation or the inefficiency of *hlh-1(RNAi),* I cannot rule out the possibility that other factor(s) may also contribute to the specification of BWM fate in the M lineage.

The synergistic loss of M-derived BWMs in *hlh-1(RNAi); fozi-1(cc609)* animals suggests functional overlap between FOZI-1 and HLH-1 in specifying BWM fate. However, each factor alone is clearly required for proper BWM fate specification as *fozi-1* or *hlh-1* single mutants lack a small fraction of M-derived BWMs (Harfe et al., 1998a). Both *fozi-1* and *hlh-1* are expressed in the early M lineage as well as in the BWM and CC precursors at the time when these cell fates are specified (Harfe et al., 1998a). While FOZI-1 is no longer detectable after these cells differentiate, HLH-1 continues to be expressed in differentiated BWM cells (Harfe et al., 1998a). I have shown that *fozi-1* and *hlh-1* do not regulate each other's expression and subcellular localization in the M lineage (Figure 2.6). It is possible that in the M lineage, FOZI-1 and HLH-1 together contribute to process(es) required to specify BWM and CC fates that compete with an opposing process leading to SM fate specification. A slight shift in the balance between these two processes, as in *fozi-1* or *hlh-1* single mutants, can lead to transformation of the CC fate and loss of a fraction of M-derived BWMs. Loss of both FOZI-1 and HLH-1, however, shifts the balance strongly in favor of SMs. This interpretation requires that the M-derived CC fate is more sensitive than the BWM fate to the imbalance of these two opposing processes.

HLH-1 is a myogenic factor and has been shown to be capable of inducing widespread myogenesis when ectopically expressed during early embryogenesis (Fukushige and Krause, 2005). FOZI-1, however, does not appear to be a myogenic factor. Forced global expression of FOZI-1 did not lead to precocious myogenesis during embryogenesis, nor did it cause a SM to BWM fate transformation within the M lineage (data not shown, see Methods and Materials for heat-shock conditions). The failure of FOZI-1 to induce myogenesis is not unexpected as FOZI-1 is also expressed in a subset of head neurons and along the ventral nerve cord (Figure 2.5E,F), and FOZI-1 has been shown to function in the specification of left/right asymmetric fates

of the ASE neurons (Johnston et al., 2006). Thus FOZI-1 is required not only for the specification of striated BWM fates, but also for the specification of non-muscle cells such as CCs and ASE neurons. It is likely that different cofactors are required for FOZI-1 to exert its different functions in different cell types.

I believe that the Hox factor MAB-5 is one of the factors that function together with FOZI-1 in specifying the striated BWM fate in the M lineage. MAB-5 is present throughout the M lineage. *mab-5(0)* mutation results in multiple defects in the M lineage, including abnormal cleavage orientations, loss of expression of the Ce-Twist homolog HLH-8 in the early M lineage, and BWM and CC to SM fate transformations (Salser, 1995;Harfe et al., 1998b). I have shown that *fozi-1(cc609) mab-5(RNAi)* animals behaved similarly to *fozi-1(cc609)* or *mab-5(0)* animals regarding BWM fate specification, whereas *hlh-1(cc561ts); mab-5(RNAi)*, like *hlh-1(cc561ts); fozi-1(cc609)* animals, exhibited synergistic loss of M-derived BWMs (Figure 2.7A,B). As MAB-5 and FOZI-1 do not appear to regulate each other's expression (Figure 2.6E), the results suggest that MAB-5 and FOZI-1 function either together or in parallel in specifying M-derived BWM fate and that they do this by affecting a common downstream target that functions redundantly with HLH-1.

CEH-20 functions upstream of postembryonic myogenic pathways

Previous studies have shown that the homeodomain protein MLS-2 is required to activate the expression of HLH-1 in the M lineage and that *mls-2(0)* mutants have defects in BWM and CC fate specification (Jiang et al., 2005). I found that MLS-2 is not required for M lineage expression of FOZI-1, indicating that HLH-1 and FOZI-1 are regulated by different sets of transcription factors in the M lineage. I found that the Pbx/Exd homolog CEH-20 is required for the M lineage expression of FOZI-1 and that this regulation is independent of the Hox factor MAB-5 (Figure 2.6).

Interestingly, CEH-20 is also required for the expression of MLS-2 in the M lineage (Jiang et al., 2008). These observations place CEH-20 upstream of both HLH-1 and FOZI-1. As *ceh-20* mutant animals lack all M-derived BWMs (Liu and Fire, 2000), it is likely that any additional factors required for specifying M-derived BWM fate would also be downstream targets of CEH-20.

Based on all my results, I propose a model for how M-derived BWMs are specified, as depicted in Figure 2.8. In this model, at least two redundant mechanisms are involved in specifying myogenic fates in the M lineage. First, MLS-2 regulates the expression of HLH-1, a myogenic factor. Second, FOZI-1 and MAB-5 regulate an unknown myogenic factor X that functions redundantly with HLH-1. At present, it is not clear whether MAB-5 functions together or in parallel with FOZI-1 in regulating factor X. The data do not exclude the possibility of a third factor (Y) in addition to HLH-1 and factor X to promote myogenic fate specification. The Pbx/Exd homolog CEH-20 appears to act upstream of all of these myogenic pathways in the M lineage.

C. elegans embryonic and postembryonic myogenesis involve distinct mechanisms in addition to CeMyoD

The *C. elegans* striated musculature consists of 81 embryonically-derived and 14 M lineage-derived BWMs (Sulston and Horvitz, 1977; Sulston et al., 1983). Despite their different lineage history, all 95 BWMs appear morphologically and functionally equivalent. It has been previously shown that although HLH-1 is sufficient to induce striated BWM fate (Fukushige and Krause, 2005), *hlh-1(0)* mutants still make all 81 embryonically-derived BWMs (Chen et al., 1992; Chen et al., 1994). These studies suggest that other factors share redundant functions with HLH-1 in specifying these 81 BWMs. Neither FOZI-1 nor MAB-5 appears to be one of these factors, as FOZI-1 and MAB-5 are not expressed in the 81 embryonically-derived

Figure 2.8. A model for muscle fate specification in the postembryonic mesoderm. At least two redundant mechanisms functioning downstream of the Pbx/Exd homolog CEH-20 are involved in specifying myogenic fates in the postembryonic mesoderm (see Discussion). Solid lines in this model do not necessarily represent direct regulation. Dashed lines represent a hypothetical situation.

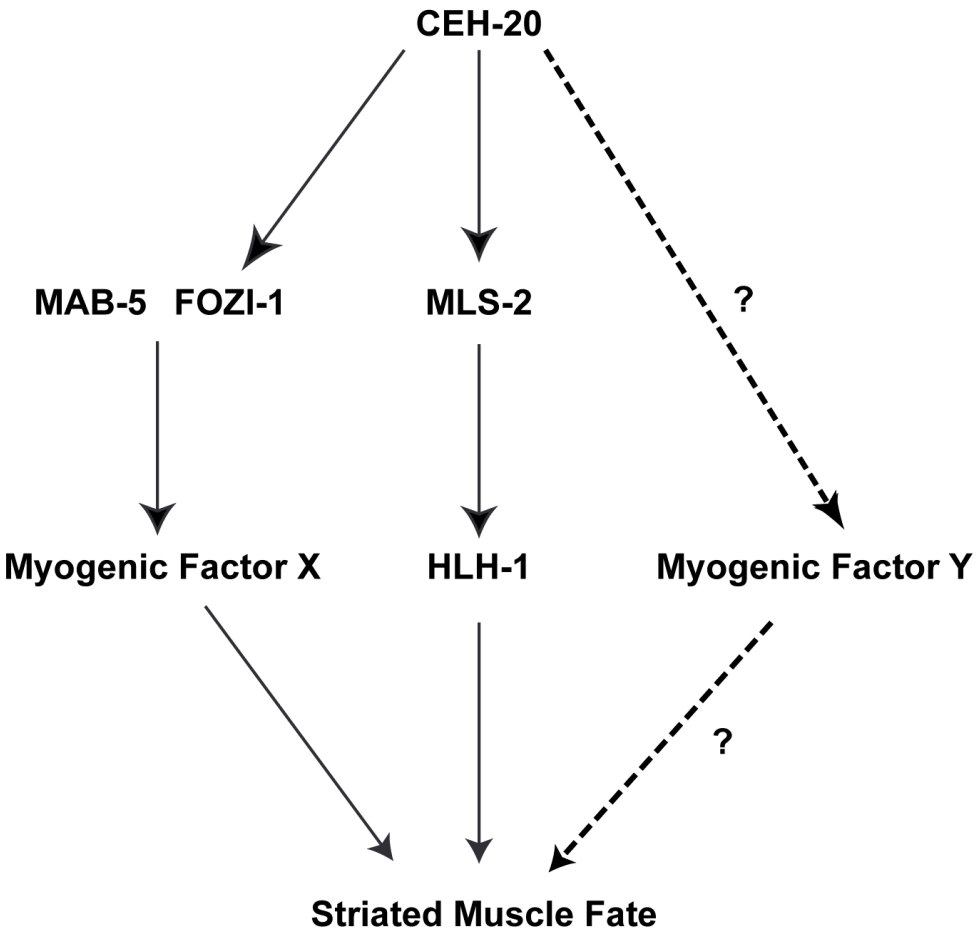
CEH-20
MAB-5
FOZI-1
MLS-2
?
Myogenic Factor X
HLH-1
Myogenic Factor Y
?
Striated Muscle Fate

BWMs or their precursors, and *fozi-1(0), mab-5(0)*, *hlh-1(cc561ts); fozi-1(0)*, *hlh-1(cc561ts); mab-5(RNAi)* and *hlh-1(cc561ts); fozi-1(cc609); mab-5(RNAi)* double and triple mutant animals do not have any defect in the specification of these 81 BWMs. Thus, although HLH-1 functions in the development of all BWMs, embryonic and post-embryonic BWMs require distinct sets of transcription factors that function redundantly with HLH-1. Therefore there is a remarkable level of complexity for the production of a simple striated musculature in *C. elegans*.

Functional redundancy in myogenic fate specification in vertebrates and invertebrates

Functional redundancy in specification of striated muscle fates has been observed in both vertebrates and invertebrates. In vertebrates, the redundancy is limited to proteins in the MyoD family. There are multiple members of the MyoD family of myogenic regulatory factors (MRFs) in vertebrates, including MyoD, Myf-5, myogenin and MRF4 (Buckingham, 2001; Pownall et al., 2002; Buckingham et al., 2003). Each of these factors is capable of inducing the transcription of muscle-specific genes when overexpressed, but they also share functional redundancy in striated muscle development (Pownall et al., 2002). For example, mice lacking either Myf-5 or MyoD are viable and fertile (Braun et al., 1992; Rudnicki et al., 1992; Kaul et al., 2000). However, double mutants lacking both Myf-5 and MyoD do not form any skeletal muscles (Rudnicki et al., 1993).

Different from vertebrates, many invertebrate organisms have only one MyoD homolog, including ascidians (Araki et al., 1994), sea urchins (Venuti et al., 1991) and *Drosophila* (Michelson et al., 1990). In Drosophila, *nautilus* is present in a subset of muscle precursors and differentiated muscle fibers (Michelson et al., 1990; Paterson et al., 1991). *nautilus* loss-of-function mutants only have defects in a distinct subset of

cells normally expressing *nautilus*, and the defects appear to be a combination of abnormal differentiation of some muscle fibers and inappropriate fate specification (Keller et al., 1998; Balagopalan et al., 2001). These observations indicate that there are factor(s) functioning redundantly with *nautilus* in muscle fate specification and differentiation. The identity of these factors is currently unknown. It is possible that some of the muscle identity genes such as *slouch, apterous, muscle segment homeobox, ladybird and Krüppel* (Baylies et al., 1998; Frasch, 1999) could share redundant functions with *nautilus* in specifying the fate of certain muscle fibers.

This work shows that the combinatorial functions of HLH-1 with FOZI-1 and MAB-5 are required to specify the M-derived BWM fate. This is similar to the situation in *Drosophila* where unique combinations of different muscle identity genes specify distinct muscle fiber fates, and loss-of-function mutations in these genes cause fate transformation from one type of muscle fiber to another (Bourgouin et al., 1992; Ruiz-Gomez et al., 1997; Jagla et al., 1998; Nose et al., 1998; Knirr et al., 1999). Notably, both MAB-5 and FOZI-1 are expressed in other cell types outside of the M lineage in *C. elegans* (Salser et al., 1995; this work). The expression pattern of muscle identity genes in *Drosophila* is also not restricted to only muscle cells (Bourgouin et al., 1992; Ruiz-Gomez et al., 1997; Jagla et al., 1998; Nose et al., 1998; Knirr et al., 1999). What is unique in this study is that *hlh-1(cc561ts); mab-5(RNAi)* and *hlh-1(cc561ts); fozi-1(cc609)* animals show clear fate transformations from M-derived BWMs to non-muscle sex myoblasts (SMs)-like cells, which not only display the morphology of SMs, but also go on to proliferate and produce differentiated non-striated sex muscles. This muscle to non-muscle fate transformation may be due to these cells adopting a developmental ground state represented by the SMs when myogenic factors are missing from the M lineage.

ACKNOWLEDGEMENTS

We thank Marisa Foehr for repeating the RNAi experiments to confirm the identity of *fozi-1*; Mike Krause, Yuji Kohara, Shohei Mitani and the Sanger Center for *C. elegans* strains, cosmids, cDNA clones and antibodies; Marisa Foehr, Yuan Jiang, Ken Kemphues, Siu Sylvia Lee and Diane Morton for helpful discussions, suggestions and valuable comments on the manuscript. J. L. appreciates the advice and support of Andy Fire, in whose lab the *fozi-1* mutants were isolated. Some strains used in this study were obtained from the *C. elegans* Genetics Center (CGC), which is supported by a grant from the NIH National Center for Research Resources. This work was supported by NIH R01 GM066953 (to J. L.) and GM39066 (to D. P. and A. B.). During part of this work, N.M.A. was supported by NIH T32 GM07617 and a GAANN fellowship sponsored by the U.S. Department of Education. D. T. was supported by the Summer Research Fellowship from Weill Cornell Medical College in Qatar.

CHAPTER 3[2]

A CONSERVED SIX-EYA CASSETTE ACTS DOWNSTREAM OF WNT SIGNALING TO DIRECT NON-MYOGENIC VERSUS MYOGENIC FATES IN THE C. ELEGANS POSTEMBRYONIC MESODERM

Introduction

How distinct cell fates are acquired from multipotent progenitor cells is a fundamental question in developmental biology. I am interested in the mechanisms involved in distinguishing myogenic and non-myogenic cell fates in the mesoderm. The Six family of homeodomain proteins has been found to regulate cell fate specification in multiple tissue types, including in the mesoderm (Kawakami et al., 2000). The founding member of the Six family of genes is the Drosophila sine oculis (*so*) gene (Cheyette et al., 1994; Serikaku and O'Tousa, 1994). The role of *so* is best characterized in the Drosophila eye, where it functions downstream of the Pax6 gene eyeless (*ey*) for proper eye development (Halder et al., 1998). *so* and its cofactor eyes absent (*eya*) function upstream of the transcription factor dachshund (*dac*) to regulate the expression of eye specification genes (Chen et al., 1997; Pignoni et al., 1997; Shen and Mardon, 1997; Halder et al., 1998). This Pax-Six-Eya-Dac network of regulation is also required for proper eye development in vertebrates (Hanson, 2001). In addition, members of this network also function in other developmental processes such as mesodermal development in Drosophila and vertebrates, and sensory organ

[2] POP-1::GFP and SYS-1::GFP localization studies in this chapter were performed by Sung-Eun Lim, yeast-two hybrid studies were done by Tiffany L. Chan and cloning of some *ceh-34* constructs was performed by Herong Shi. *ceh-34(RNAi)* was identified to play a role in the M lineage in an RNAi screen described in Chapter 4 with the assistance of Zach Via.

development in mammals (Heanue et al., 1999; Xu et al., 1999; Hanson, 2001; Clark et al., 2006)

C. elegans has four homologs of the Six family (CEH-32, CEH-33, CEH-34 and CEH-35/UNC-39) (Hobert and Ruvkun, 1999; Dozier et al., 2001; Colosimo et al., 2004; Furuya et al., 2005). We have observed that knockdown of *ceh-34* during postembryonic development results specifically in the loss of non-muscle cell types in the mesoderm. In this study we investigate how *ceh-34* functions in the M lineage, which gives rise to all of the postembryonically-derived non-gonadal mesodermal cells in the animal (Sulston and Horvitz, 1977). The M lineage arises from a single blast cell, the M mesoblast, which is born during embryogenesis and remains dormant until the larva hatches (Sulston and Horvitz, 1977; Sulston et al., 1983). During hermaphrodite larval development this pluripotent blast cell first undergoes a series of reproducible divisions to produce 18 cells that are specified into three cell types: 2 non-muscle coelomocytes (CCs), 14 striated bodywall muscles (BWMs) and 2 sex myoblasts (SMs), which subsequently give rise to the non-striated egg-laying muscles (Sulston and Horvitz, 1977). Within the M lineage, cell fate specification occurs in an asymmetric manner, as CCs are born dorsally and SMs are born ventrally (Figure 3.1A). In addition, there appear to be asymmetries along the anterior-posterior axis on both the dorsal and ventral sides, in which cell-fate decisions are made between posterior BWMs and anterior CCs or SMs at the 16- and 18-M stages (Figure 3.1A).

The process in which multiple cell types are derived from the M mesoblast depends on the coordination of symmetry breaking events and transcriptional outputs. Previous studies have implicated the LIN-12/Notch and TGFβ signaling pathways in generating proper asymmetry of the M lineage along the dorsal-ventral axis: the LIN-12/Notch pathway promotes ventral SM fates, while the *C. elegans* Schnurri homolog

Figure 3.1. *ceh-34* is required for CC fates.

All images are ventral/lateral views with anterior to the left.

(A,B) Early M lineage in wild-type (A) and *ceh-34(RNAi-P)* (B) animals. Stages of the early M lineage (1-M to 18-M) are indicated in (A). (C,D) L4440 empty vector RNAi treated control (C) and *ceh-34(RNAi-P)* (D) adults. CCs are visualized using *intrinsic CC::gfp*, with embryonic CCs labeled with arrowheads and M-derived CCs with arrows. Type I vulval muscles are visualized using *egl-15::gfp*, denoted by asterisks. M-derived CCs are missing in *ceh-34(RNAi)* animals (D). (E-F) L1 larva of water-injected (E) or *ceh-34* dsRNA (F) injected animals. The M mesoblast is indicated by expression of *hlh-8::gfp* (open arrow). Note the abnormal anterior morphology of the *ceh-34(RNAi-E)* animal. (G) *ceh-34(RNAi-E)* adult with only one pair of embryonic CCs (arrowhead). M, M mesoblast; d, dorsal; v, ventral; l, left; r, right; a, anterior; p, posterior; CC, coelomocyte; BWM, body wall muscle; SM, sex myoblast.

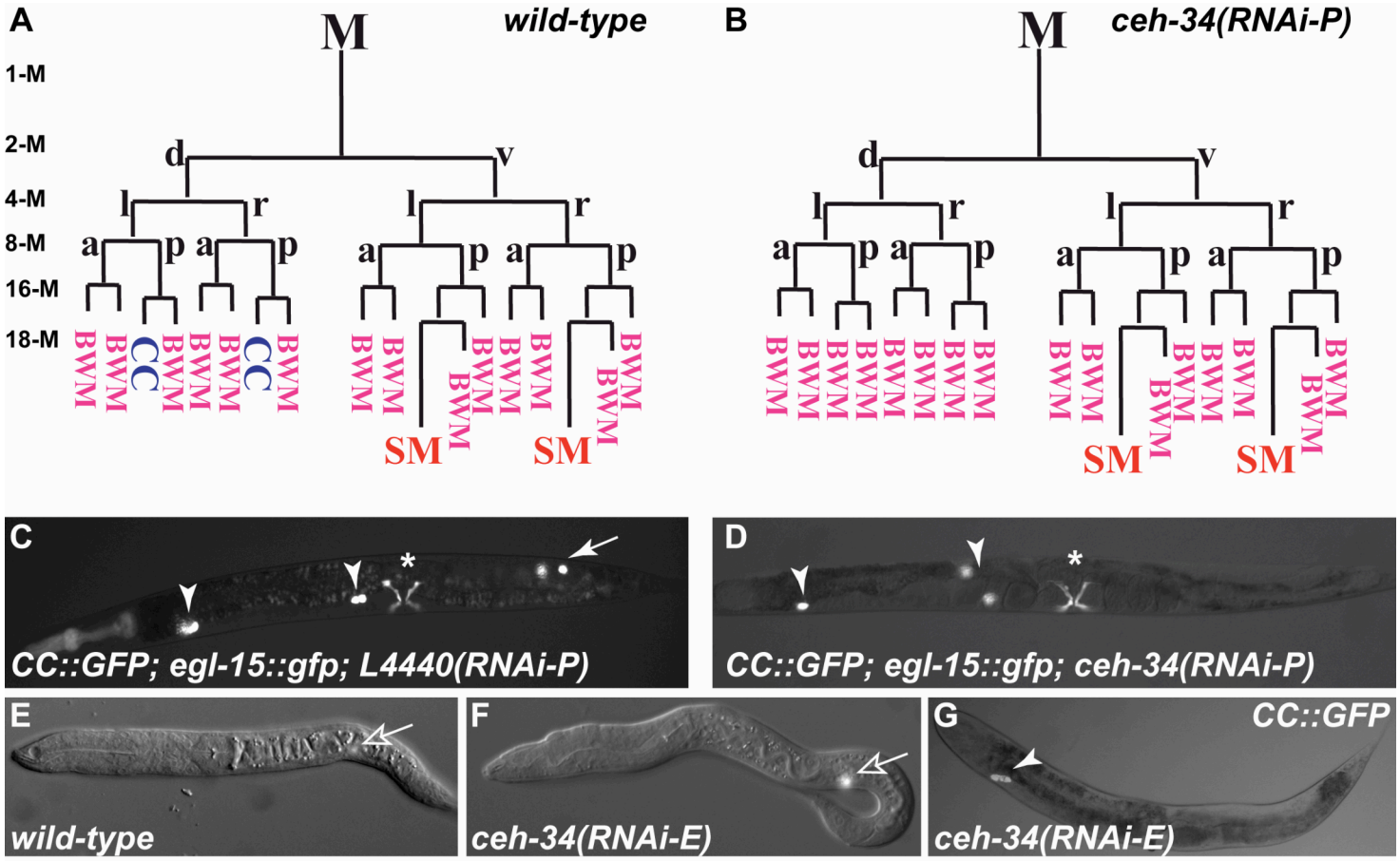
A
wild-type
B
ceh-34(RNAi-P)
1-M
2-M
4-M
8-M
16-M
18-M
M
d
v
l
r
a
p
BWM
CC
SM
C
CC::GFP; egl-15::gfp; L4440(RNAi-P)
D
CC::GFP; egl-15::gfp; ceh-34(RNAi-P)
E
wild-type
F
ceh-34(RNAi-E)
G
CC::GFP
ceh-34(RNAi-E)

SMA-9 antagonizes the Sma/Mab TGFβ pathway to promote dorsal CC fates (Greenwald et al., 1983; Foehr et al., 2006; Foehr and Liu, 2008). The target genes of these pathways in the M lineage have not been identified.

The conserved Wnt/β-catenin asymmetry pathway also plays a role in multiple asymmetric fate specification events in *C. elegans* (Mizumoto and Sawa, 2007). Specifically, the β-catenin homolog SYS-1 and the TCF transcription factor POP-1 show reciprocal asymmetric anterior-posterior or proximal-distal nuclear distribution in multiple cell divisions during *C. elegans* development, with SYS-1 being enriched in the posterior or distal nuclei and POP-1 enriched in the anterior or proximal nuclei (Lin et al., 1995; Lin et al., 1998; Herman, 2001; Siegfried and Kimble, 2002; Kidd et al., 2005; Huang et al., 2007; Phillips et al., 2007; Liu et al., 2008). POP-1 nuclear localization is further regulated by the LIT-1 kinase and another β-catenin WRM-1, which facilitate the nuclear export of POP-1 in an asymmetric manner (Lo et al., 2004; Takeshita and Sawa, 2005). Recently it has been shown that in the M lineage, WRM-1 localizes to the anterior cortex during anterior-posterior cell divisions but to the nuclei of posterior daughters afterwards (Takeshita and Sawa, 2005). However, a role of the Wnt/β-catenin asymmetry pathway in the M lineage has yet to be described.

In addition to the signaling pathways regulating dorsal-ventral asymmetry in the M lineage, a number of mesoderm-intrinsic transcription factors are involved in the specification of both muscle (BWM) and non-muscle (CC) fates derived from the M mesoblast. The single *C. elegans* MyoD family member HLH-1 has been shown to function redundantly with the Hox protein MAB-5 and another transcription factor, FOZI-1, to specify the M-derived BWMs (Harfe et al., 1998a; Liu and Fire, 2000; Amin et al., 2007). Curiously, all of these factors are also expressed in and required for the specification of the M-derived non-muscle CCs (Harfe et al., 1998a; Liu and

Fire, 2000; Amin et al., 2007). These observations suggest that other factor(s) must be required to differentiate between M-derived muscle and non-muscle fates.

In this chapter, I describe the role of the Six2 family homolog CEH-34 and its cofactor EYA-1 in proper specification of non-muscle CC fates in the M lineage. I propose a model in which *ceh-34* and *eya*-1 expression and the subsequent specification of non-muscle cell fates from myogenic precursor cells are regulated in a combinatorial manner by the mesoderm-intrinsic factors HLH-1, FOZI-1 and MAB-5, by SMA-9 and LIN-12 along the dorsal-ventral axis, and by SYS-1 and POP-1 along the anterior-posterior axis.

Materials and Methods

C. elegans strains

Strains were maintained and manipulated using standard conditions (Brenner, 1974). Analyses were performed at 20˚C, unless otherwise noted. The following strains were used:

LG I: *eya-1(ok654)* (Furuya et al., 2005), *sys-1(q544)* (Miskowski et al., 2001), *pop-1(q645)*, *pop-1(q624)* (Siegfried and Kimble, 2002)

LG II: *hlh-1(cc561ts)* (Harfe et al., 1998a); *rrf-3(pk1426)* (Sijen et al., 2001)

LG III: *dac-1(gk213)*, *dac-1(gk211)* (Colosimo et al., 2004)*; lin-12(n676n930ts)* (Sundaram and Greenwald, 1993)

LG V: *ceh-34(tm3330)* (gift from Shohei Mitani, Tokyo Women's Medical College, Tokyo, Japan), *him-5(e1467)* (Hodgkin et al., 1979)

LG X: *sma-9(cc604)* (Foehr et al., 2006)

Integrated transgenic lines:

JK3930: *qIs95[sys-1p::venus::sys-1+pttx-3::dsRED]* (Phillips et al., 2007)

LW0755: *jjIs755[hlh-8p::pop-1::gfp+dpy-20(+)]; dpy-20(e1282ts)* (Siegfried et al., 2004)

JK3437: *him-5(e1490) V; qIs74(pop-1p::pop-1::gfp)* (Siegfried et al., 2004)

LW1066: *jjIs1066[pJKL705.1(hlh-8p::mRFP+unc-119(+))]; unc-119(ed4)* (Jiang et al., 2008)

LW1475: *jjIs1475[pJKL758.1(myo-3::nls::rfp::lacZ+unc-119(+)] I; unc-119(ed4)*

WM75: *wrm-1(tm514); neIs2[WRM-1::GFP + pRF4(rol-6)]* (Takeshita and Sawa, 2005)

WM79: *rol-6(n1270) II; neEx1[LIT-1::GFP + pRF4(rol-6)]* (Takeshita and Sawa, 2005)

The strains LW0683 *[rrf-3(pk1426) II; ccIs4438 (intrinsic CC:::gfp)III; ayIs2(egl-15::gfp) IV; ayIs6(hlh-8::gfp) X]* and LW1734 *[jjIs1475(myo-3::rfp) I; rrf-3(pk1426) II; ccIs4438(intrinsic CC:::gfp) III; ayIs2(egl-15::gfp) IV; ayIs6(hlh-8::gfp) X]* were used to visualize M lineage cells in RNAi experiments. *Intrinsic CC::gfp* is a twist-derived coelomocyte marker (Harfe et al., 1998b). *Secreted CC::gfp* is another coelomocyte marker using a *myo-3::secreted GFP* that is secreted from the body wall muscles and taken up by differentiated CCs (Harfe et al., 1998a). Additional M lineage specific reporters were as described in Kostas and Fire (Kostas and Fire, 2002). The M lineage was followed in live animals under a fluorescence stereomicroscope and confirmed using a compound microscope.

Plasmid constructs and transgenic lines

Two plasmids were generated to examine the expression pattern of *ceh-34*. Fragments spanning 3.9 kb of the *ceh-34* promoter and the entire coding region or the promoter alone were PCR amplified from N2 genomic DNA using iProof™ High-

Fidelity DNA Polymerase (Bio-Rad). I obtained a cDNA clone, *yk209b2*, which spans the entire ORF and the 3'UTR of *ceh*-34 (gift from Yuji Kohara, National Institute of Genetics, Japan). These PCR fragments and cDNA were used to generate the following reporter constructs: pNMA90: *ceh-34p::ceh-34 genomic ORF::gfp::unc-54 3'UTR*; pNMA94: *ceh-34p::gfp::ceh-34 cDNA::ceh-34 3'UTR*. Forced expression constructs: pNMA107: *hlh-8p::gfp::ceh-34 cDNA::ceh-34 3' UTR*; pNMA109: *hlh-8p::eya-1 genomic ORF::unc-54 3' UTR*; pNMA88: *hsp-16p::ceh-34 cDNA::ceh-34 3'UTR*; pNMA110: *hsp-16p::eya-1 cDNA::unc-54 3'UTR*; Other reporter constructs: pJKL758: *myo-3p::NLS::mRFP::lacZ::unc-54 3'UTR*; pJKL601: *hlh-8p::pop-1::gfp::unc-54 3' UTR*. Transgenic lines were generated using the plasmid pRF4 (Mello et al., 1991), LiuFD61 (*mec-7p::mRFP*, gift from Sylvia Lee, Cornell University) or pJKL815 (*myo-2p::mRFP*) as markers.

Plasmids used for RNAi: ceh-34(11068@D5), *eya-1*(11020@D3), *dac-1*(11007@F3), *ceh-35*(11062@A7), *pax-3*(11038@B3), *ceh-33*(11058@H10) *and egl-38*(10018@H7) were retrieved from the ORFeome-RNAi v1.1 library (Rual et al., 2004). *sys-1*(T23D8.9) and *ceh-32*(W05E10.3) RNAi plasmids were obtained from the RNAi library generated by Dr. Julie Ahringer and provided by Geneservice Ltd. The identities of all RNAi clones obtained from the libraries were confirmed by sequencing. The *eya-1* RNAi clone was subsequently used for additional cloning. The constructs pNMA49 (*fozi-1* RNAi), pNMA50 (*mab-5* RNAi), pJKL528 (*lit-1* RNAi) were made by sub-cloning full-length cDNAs for each gene from the plasmids pNMA24 (Amin et al., 2007) and p198 (Liu and Fire, 2000) and *yk457d2* (gift from Yuji Kohara, National Institute of Genetics, Japan) respectively, into the L4440 vector (Timmons and Fire, 1998). pJKL833 (*vab-3* RNAi), pJKL834 (*pax-3* RNAi) and pJKL835 (*pax-2* RNAi), were generated by subcloning into L4440 a PCR fragment corresponding to a genomic region for each gene. RNAi constructs pSP28 (*pop-1*

RNAi) and LiuFD31 (*wrm-1* RNAi) were gifts from David Eisenmann and Brian Harfe respectively.

Heat-shock experiments

Transgenic animals harboring pNMA88 (*hsp-16p::ceh-34*) and/or pNMA110 (*hsp-16p::eya-1*) were subjected to periodic heat-shock at 37˚C for 30 minutes followed by recovery for 3-4 hours at 20˚C beginning at the 1-M stage of development until after M-derived CCs were visible using *intrinsic CC::gfp*. Alternatively, animals were subjected to continuous heat-shock at 30˚C from embryogenesis until the 16-M stage of the M lineage. Both periodic and continuous heat-shock conditions yielded the same results. Non-transgenic heat-shocked animals were used as controls for heat-shock conditions.

RNAi

RNAi by injection (RNAi-E): ceh-34 dsRNA was synthesized with the T7 RiboMax RNA Production System (Promega) using the *ceh-34* RNAi plasmid (above) as a template. To observe the effects of RNAi during embryonic development, dsRNA was further purified and injected into wild-type hermaphrodites of the reference strain LW0683, with water as an injection control. The progeny of injected animals were scored for phenotypes.

RNAi by ingestion (RNAi-P): To observe the effects of RNAi during postembryonic development, I performed RNAi by ingestion with a synchronous population of L1 larvae. L1 animals synchronized by standard methods (Kamath and Ahringer, 2003) were plated in triplicate on HT115(DE3) bacteria expressing dsRNA for genes of interest. Bacteria for ingestion were prepared as described by Kamath and Ahringer (Kamath and Ahringer, 2003), using 4 mM IPTG to induce dsRNA

production. RNAi-P was performed at 25˚C and animals were scored for M lineage phenotypes or used for immunostaining 24-48 hours after plating.

Yeast two-hybrid assays

Two hybrid analysis was performed using the protocol described by James et al. (James et al., 1996). The plasmids pJKL822 and pTLC6 were generated by cloning full length *ceh-34* and *eya-1* cDNAs in frame with the GAL4 binding domain (pGBD-C1) and the GAL4 activation domain (pGAD-C1), respectively (James et al., 1996).

Immunofluorescence staining

Animal fixation, immunostaining, microscopy and image analysis were performed as described previously (Amin et al., 2007). Guinea pig anti-FOZI-1 (Amin et al., 2007) and goat anti-GFP (Rockland Immunochemicals; 1:5000) antibodies were used. All secondary antibodies were from Jackson ImmunoResearch Laboratories and used in a dilution of 1:50 to 1:200.

Results

***ceh-34* is required for specifying the non-muscle CC fates in the M lineage**

In an RNAi screen to identify transcription factors important for M lineage development (Chapter 4), I found that RNAi knockdown of *ceh-34* during postembryonic development (see Materials and Methods, referred to as RNAi-P) resulted in a loss of M-derived CCs (Table 3.1, Figure 3.1B, D). To determine the basis for the missing M-derived CCs, I followed the development of the M lineage in *ceh-34(RNAi-P)* animals using a combination of cell-type specific markers. Compared to wild-type animals, *ceh-34(RNAi-P)* animals exhibit normal cleavage orientations

Table 3.1. M lineage phenotypes of *C. elegans* Pax-Six-Eya-Dac mutants

Gene family	Genotype	Number of Embryonic CCs	Number of M-derived CCs
	wild-type	4 (n>200)	2 (n>200)
Six1/2	*ceh-34(RNAi-P)*	4 (n>200)	0 (98.3%); 2 (1.7%) (n=362)
	ceh-34(RNAi-E)	11.3% with 1st pair missing 16.7% with 2nd pair missing 14.1% with both pairs missing (n=538)	0 (98.6%) 1-2 (1.4%) (n=425)
Six3/6	*ceh-32(RNAi-P)*	4 (n>200)	2 (n>200)
Six1/2	*ceh-33(RNAi-P)*	4 (n>200)	2 (n>200)
Six4/5	*ceh-35(RNAi-P)*	4 (n>200)	2 (n>200)
Eyes absent	*eya-1(ok654)*	9.5% with 1st or 2nd pair missing 87.7% with both pairs missing (n=203)	0 (84.7%);1 (1.0%); 2 (14.3%) (n=203)
Pax6	*vab-3(RNAi-P)*	4 (n>200)	2 (n>200)
Pax3	*pax-3(RNAi-P)*	4 (n>200)	2 (n>200)
Pax1/9	*pax-1(RNAi-P)*	4 (n>200)	2 (n>200)
Pax2/5/8	*pax-2(RNAi-P)*	4 (n>200)	2 (n>200)
	egl-38(RNAi-P)	4 (n>200)	2 (n>200)
	egl-38(n578)	4 (n>200)	2 (n>200)
Dachshund	*dac-1(gk211)*	4 (n>200)	2 (n>200)
	dac-1(gk213)	4 (n>200)	2 (n>200)

and proliferation in the M lineage to give rise to 18 descendents at the end of L1 larval growth, observed by the *hlh-8::gfp* reporter and αFOZI-1 immunostaining (Harfe et al., 1998b; Amin et al., 2007). In wild-type animals, two of these 18 cells, M.drpa and M.dlpa, differentiate into CCs (Figure 3.1A). In 10 of 11 *ceh-34(RNAi-P)* animals examined, these two cells failed to become CCs (Figure 3.1B). Instead, they adopted the fate of their sister cells (M.drpp and M.dlpp) and became BWMs (visualized using *myo-3::rfp*). The remaining animal had a CC to BWM fate transformation in only one side of the body, resulting in the loss of 1 M-derived CC (data not shown). Fate specification of SMs (visualized using *hlh-8::gfp*) and their derivatives (visualized using *egl-15::gfp;* Figure 3.1D) was unaffected in *ceh-34(RNAi-P)* animals, suggesting that *ceh-34* is specifically required for the proper specification of M-derived CC fates.

I obtained a deletion allele of *ceh-34*, *tm3330*, from the National Bioresource Project of Japan in which 235 bp of the second intron are deleted (Figure 3.2A). I saw no M lineage defect in *tm3330* mutants (Table 3.1), suggesting that this allele does not compromise the function of *ceh-34*. Postembryonic RNAi knockdown of the three other Six family members in *C. elegans*, *ceh-32, ceh-33* and *unc-39*/*ceh-35* had no effect on the M lineage (Table 3.1). Thus *ceh-34* is the only Six family gene required for the specification of M-derived CC fate.

ceh-34 **is essential for embryonic CC fates and larval viability**

To assess the role of *ceh-34* during embryonic development, we knocked down *ceh-34* during embryogenesis by injecting *ceh-34* dsRNA into wild-type animals (referred to as RNAi-E). I then examined the progeny of the injected animals for phenotypes. Among 2210 embryos laid by *ceh-34(RNAi-E)*-injected hermaphrodites, 17% arrested at the three-fold stage of embryogenesis and 82%

Figure 3.2. *ceh-34* is expressed in the M-derived CC precursors.

All images in Figures 2-5 are lateral views with anterior to the left and dorsal up (unless otherwise noted).

(A) Schematic representations of the *ceh-34* translational reporter constructs: pNMA90 *[ceh-34p*::*ceh-34 genomic ORF::gfp::unc-54 3'UTR]* and pNMA94 *[ceh-34p::gfp::ceh-34 cDNA::ceh-34 3'UTR].* (B-G): Representative images of live animals expressing *ceh-34::gfp* at different developmental stages. (B,C) Two focal planes of a bean stage embryo. (D,E) Two focal planes of a three fold state embryo. (F) A L1 larva and (G) an adult. Arrows in G denote BWMs. (H-J) The left side of an L1 larva double labeled with CEH-34::GFP (H) and anti-FOZI-1 antibody (I) at the 16-M stage. (J) A merged image of H and I. CEH-34::GFP was detected in M.dlpa (I) and M.drpa (not shown), both M-derived CC precursors. (K) Summary of *ceh-34::gfp* expression in the M lineage, with *ceh-34::gfp*-positive cells in green circles.

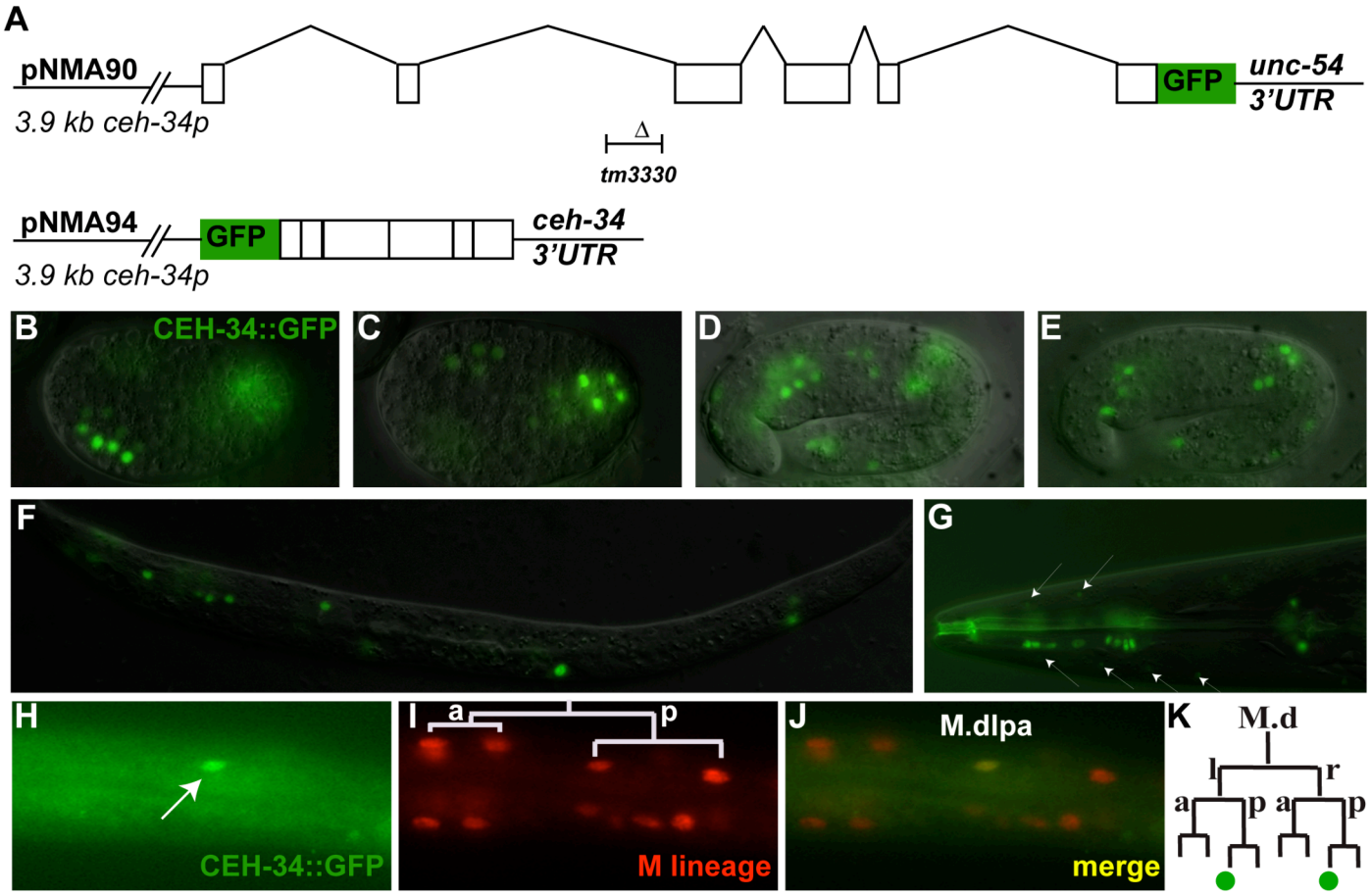
A
pNMA90
3.9 kb ceh-34p
GFP
unc-54
3'UTR
Δ
tm3330
pNMA94
GFP
ceh-34
3'UTR
3.9 kb ceh-34p
B
CEH-34::GFP
C
D
E
F
G
H
CEH-34::GFP
I
a
p
M lineage
J
M.dlpa
merge
K
M.d
l
r
a
p
a
p

arrested at the L1 larval stage with abnormal anterior morphology (Figure 3.1E). Among the 24 animals that survived to adulthood, 8 had fewer than 6 CCs, varying from missing M-derived CCs to missing some or all of the four embryonically-derived CCs (Figure 3.1F). These results suggest that *ceh-34* is an essential gene required for embryonic and early larval development. Furthermore, *ceh-34* might be required for embryonic CC development.

To further assess the role of *ceh-34* in embryonic CC development, I repeated the *ceh-34(RNAi-E)* experiment and scored a larger number of animals that escaped the embryonic arrest for their phenotypes regarding the embryonic CCs using two independent reporters of the CC fate (see Materials and Methods). As shown in Table 3.1, 42% (n=538) of these animals had a reduced number of embryonically derived CCs. The missing CCs included the pair located in the head (the 1st pair), the pair located near the vulva (the 2nd pair) or both pairs. Thus, in addition to its role in specifying the M-derived CCs, *ceh-34* is also required for the proper development of the four embryonically derived CCs.

ceh-34 is expressed in the CC precursor cells in the M lineage

To understand how *ceh-34* functions during development, especially in the proper specification of M-derived CCs, I generated two translational *ceh-34::gfp* fusion constructs as diagrammed in Figure 3.2A: pNMA90 and pNMA94. Transgenic animals carrying either construct showed identical patterns of GFP expression and localization. Consistent with the role of CEH-34 as a transcription factor, these two GFP fusion proteins are localized to the nucleus (Figure 3.2). I found that *ceh-34::gfp* expression begins late during embryogenesis and in a few anterior BWM cells and other unidentified cells in the head and persists through post-embryonic development (Figure 3.2B-G).

To determine the expression pattern of *ceh-34* in the M lineage, I performed double-labeling experiments using the *ceh-34::gfp* fusions and *hlh-8p::rfp* or αFOZI-1 immunofluorescence staining to label M lineage cells (Harfe et al., 1998b;Amin et al., 2007). I found that *ceh-34::gfp* is transiently expressed in the M lineage, specifically in M.dlpa and M.drpa, the two M-derived CC precursors, before they terminally differentiate (Figure 3.2H-K). *ceh-34::gfp* expression is no longer detectable in the CCs after they differentiate.

ceh-34 alone is not sufficient to specify CC fates

Because *ceh-34* is expressed in the M-derived CC precursors and is required for specifying the M-derived CCs, I next asked whether forced expression of *ceh-34* in other cell types is sufficient to direct the CC fate. I first generated transgenic lines expressing *ceh-34* under the control of the heat shock promoter *hsp-16p* (pNMA88). Heat-shocking (see Materials and Methods) mixed staged animals carrying pNMA88 had no effect on the number of cells expressing the *intrinsic CC::gfp* marker. To more specifically test whether *ceh-34* is sufficient to specify the CC fate in the M lineage, I generated transgenic animals expressing *ceh-34* under the control of the *hlh-8* promoter (pNMA107), which is active in all undifferentiated cells of the M lineage (Harfe et al., 1998b). None of the transgenic lines produced any extra M-derived CCs (Figure 3.3H). Thus, although *ceh-34* is required for specifying the CC fate, it is not sufficient on its own to induce other cells to adopt the CC fate, either within or outside of the M lineage.

EYA-1 is required for CC fate specification

In both Drosophila and vertebrates, Six homeodomain proteins have been shown to function together with other proteins, including Pax, Eya and Dac

(Kawakami et al., 2000). *C. elegans* contains five Pax homologs, *pax-1, pax-2, egl-38, pax-3,* and *vab-3*/*pax-6*, and one homolog each for Eya and Dac, *eya-1* and *dac-1* (Hobert and Ruvkun, 1999; Dozier et al., 2001; Colosimo et al., 2004; Furuya et al., 2005). To determine whether any of these factors participate in proper fate specification in the M lineage, I used mutant alleles or RNAi-P or both to systematically knock down the function of each of these factors and then analyzed the resulting M lineage phenotypes. RNAi knockdown during postembryonic development or mutants of the Pax and Dac homologs did not show any M lineage defects (Table 3.1), suggesting that none of the Pax genes on their own, nor the single Dachshund homolog are essential in the M lineage. However, I found that the strong loss-of-function allele of *eya-1*, *ok654* (Furuya et al., 2005), displayed M lineage phenotypes similar to *ceh-34(RNAi-P)*. Like *ceh-34(RNAi-P)*, *eya-1(ok654)* animals displayed a loss of M-derived CCs (Table 3.1, Figure 3.3A). In addition, *eya-1(ok654)* animals also exhibited a variable loss of the embryonic CCs (Table 3.1, Figure 3.3A). Thus, both *ceh-34* and *eya-1* are required for specifying the embryonic and M-derived CCs.

EYA-1 acts as a cofactor for CEH-34 in CC fate specification

Six family proteins have been shown in the fruit fly and the mouse to use Eya as a cofactor to regulate gene expression (Pignoni et al., 1997; Ohto et al., 1999; Li et al., 2003). Because loss of function of *ceh-34* and *eya-1* exhibited similar phenotypes, I tested whether EYA-1 can act as a cofactor for CEH-34 in *C. elegans*. I found that *eya-1::gfp* (Furuya et al., 2005) is expressed in a similar pattern to *ceh-34::gfp* both within and outside of the M lineage. However, *eya-1::gfp* expression differs slightly from that of *ceh-34::gfp,* which is transiently expressed in M-derived CC precursors;

Figure 3.3. EYA-1 acts as a cofactor for CEH-34 in CC fate specification.
(A) An *eya-1(ok654)* L4 larva missing one pair of embryonic CCs and both M-derived CCs (using *intrinsic CC::gfp*). Arrowhead denotes the anterior pair of embryonically-derived CCs. GFP positive cells in the middle of the worm (near the asterisk) are SM descendants labeled by *hlh-8::gfp*. (B,C) A wild-type adult expressing *eya-1::gfp* (B). GFP was detected in the four embryonically-derived CCs (arrowheads). Magnified DIC view of the anterior pair of CCs (C) corresponds to box in (B). (D-F) The left side of an L1 larva double labeled with EYA-1::GFP (D), anti-FOZI-1 antibody (E) at the 16-M stage. (F) A merged image of D and E. EYA-1::GFP was detected in M.dlpa (F) and M.drpa (not shown). (G) Summary of *eya-1::gfp* expression in the M lineage, with *eya-1::gfp*-positive cells in green circles. (H) CEH-34 binds EYA-1 via the yeast two-hybrid assay. (I,J) Forced expression of both *ceh-34* and *eya-1* in the M lineage leads to ectopic CC fates. Panel I shows an example of such a worm. Arrowheads point to embryonically-derived CCs while arrows point to M-derived CCs.

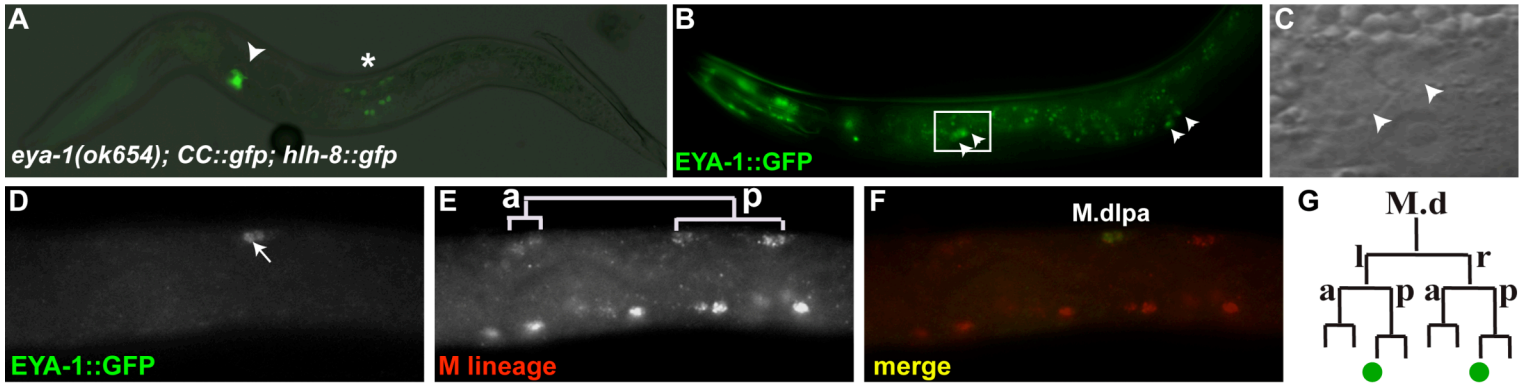

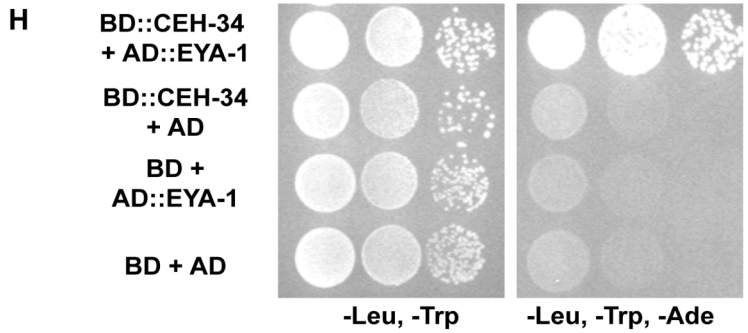

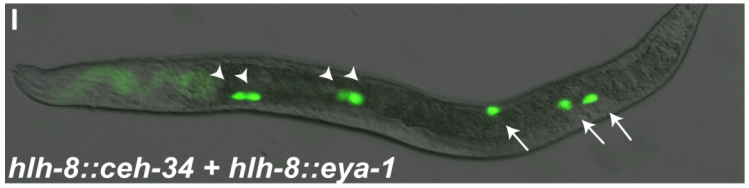

J

Genotype	Number of M-derived CCs
wild-type	2 (n>200)
hlh-8::ceh-34	2 (n>200)
hlh-8::eya-1	2 (n>200)
hlh-8::ceh-34 + hlh-8::eya-1	1 (1.0%); 2 (83.0%); 3-4 (16.0%) line 1 (n=106)
hlh-8::ceh-34 + hlh-8::eya-1	2 (81.82%); 3-4 (18.18%) line 2 (n=66)

in contrast, *eya-1::gfp* expression is detected in all six differentiated CCs throughout development (Figures 3.3B-F).

I next tested whether CEH-34 and EYA-1 can interact in a yeast two-hybrid assay, and found that CEH-34 fused to the GAL-4 DNA binding domain (BD::CEH-34) can bind to EYA-1 fused to the GAL-4 activation domain (AD::EYA-1) (Figure 3.3G). Reciprocal interaction between AD::CEH-34 and BD::EYA-1 could not be tested because BD::EYA-1 can auto-activate reporter gene expression on its own. The colocalization and interaction of CEH-34 and EYA-1, along with their similar mutant phenotypes, suggest the interaction between Six and Eya is conserved in *C. elegans* and that EYA-1 may serve as a cofactor for CEH-34 in CC fate specification.

To test whether CEH-34 and EYA-1 together can promote the CC fate, I forced the expression of each gene or both genes together using the *hlh-8* promoter (Harfe et al., 1998b). Forced expression of either *ceh-34* or *eya-1* alone did not result in any ectopic CCs in the M lineage (Figure 3.3J). However, when both genes were simultaneously expressed in the M lineage, we observed an increase in the number of M-derived CCs (Figure 3.3I, J). Thus CEH-34 and EYA-1 can act together to specify ectopic CC fates. The low frequency of induction (Figure 3.3J) prevented detailed lineage analysis to determine the source of the extra CCs. The infrequency of induction and low numbers of induced cells could be due to the low level of ectopic expression of one or both genes or could indicate that not all cells in the M lineage are competent to respond to elevated levels of the two proteins. Taken together, our data are consistent with the role of EYA-1 as a cofactor for CEH-34 in non-muscle CC-specific transcription.

CEH-34 and EYA-1 act downstream of mesoderm-intrinsic transcription factors necessary for muscle and non-muscle fates

The expression of CEH-34 and EYA-1 in the M lineage is preceded by expression of a number of transcription factors that are required for both BWM and CC fates. MAB-5, HLH-1 and FOZI-1 are expressed in the early descendants of the M mesoblast, including the CC and BWM precursor cells and are required for the specification of these M lineage fates (Harfe et al., 1998a; Liu and Fire, 2000; Amin et al., 2007). To test whether these factors are required for *ceh-34* and *eya-1* function, I examined the consequences of knockdown of these genes on the expression pattern of both *ceh-34* and *eya-1*. I found that *mab-5(RNAi)* and *fozi-1(RNAi)* animals lost expression of *ceh-34::gfp* and *eya-1::gfp* in the presumptive CCs (Figure 3.4A). Similarly, *ceh-34::gfp* and *eya-1::gfp* were not detected in the M lineage of the temperature sensitive *hlh-1*(*cc561ts)* mutants at the restrictive temperature (Figure 3.4A). Thus *mab-5, hlh-1* and *fozi-1* are required for the expression of *ceh-34* and *eya-1*.

CEH-34 and EYA-1 act downstream of the LIN-12/Notch and SMA-9/TGFβ pathways

As shown above, both *ceh-34* and *eya-1* are expressed in and act in the dorsal M lineage descendants. Dorsal-ventral asymmetry in the M lineage is regulated by both the LIN-12/Notch signaling pathway and the Sma/Mab TGFβ signaling pathway, which is antagonized by SMA-9 (Greenwald et al., 1983; Foehr et al., 2006; Foehr and Liu, 2008). Thus, I expected that *ceh-34* and *eya-1* expression in the dorsal CC precursors is under the control of these two patterning pathways. Indeed, as expected, I found that *ceh-34* activity is required for the ectopic CC fates that appear

Figure 3.4. *ceh-34* acts downstream of M lineage CC competence factors as well as dorsal-ventral patterning systems.

(A) *ceh-34::gfp* and *eya-1::gfp* are not expressed in the M lineage of *mab-5*, *fozi-1*, *hlh-1* and *sma-9* mutants. (B) *ceh-34* is required for the ectopic CC fates in *lin-12(n941)* null mutants. (C-E) *ceh-34* M lineage expression in *sma-9* mutants. *ceh-34::gfp* is detected in the head (not shown), but not in M.dlpa or M.drpa in *sma-9(cc604)* animals (C). Anti-FOZI staining marks the M lineage cells (D). (E) A merged image of C and D.

A

Genotype	*ceh-34::gfp* expression in M.d(l/r)pa	*eya-1::gfp* expression in M.d(l/r)pa
wild-type	96.19% (n=105)	100% (n=53)
mab-5(RNAi-P)	5.08% (n=59)	14.71% (n=34)
fozi-1(RNAi-P)	0% (n=57)	0% (n=48)
hlh-1(cc561)	0% (n=59)	0% (n=50)
sma-9(cc604)	0.94% (n=106)	0% (n=126)

B

Genotype	Number of M-derived CCs *(secreted CC::gfp)*
lin-12(n941)	4 (n=26)
lin-12(n941); ceh-34(RNAi-P)	0 (n=44)

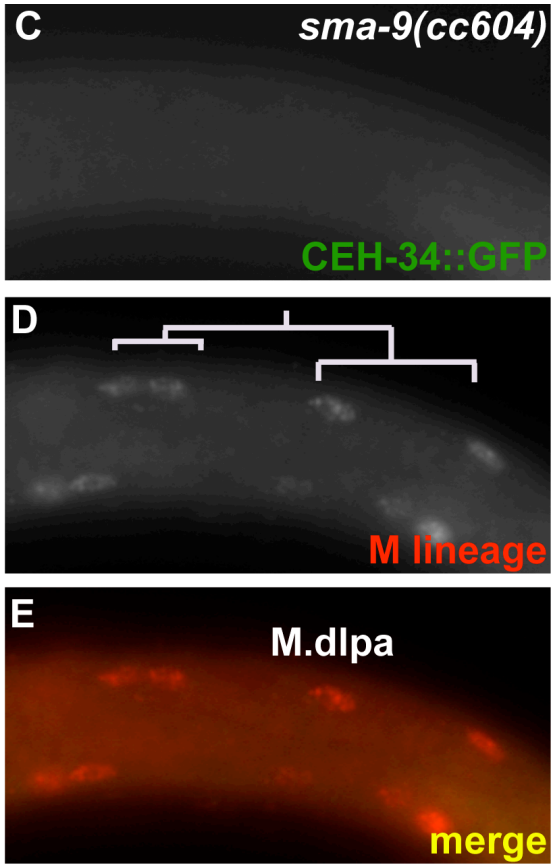

in *lin-12(n941)* mutants (Figure 3.4B), and that SMA-9 is required to activate the expression of *ceh-34* and *eya-1* in the M-derived CC precursors (Figure 3.4A,C-E).

CEH-34 and EYA-1 act downstream of POP-1 and SYS-1, components of the Wnt/β-catenin asymmetry pathway

SYS-1 and POP-1 are asymmetrically distributed along the anterior-posterior axis in the M lineage

Since CEH-34 expression is limited to the anterior daughters of M.dlp and M.drp, I wanted to identify factors regulating this anterior expression. The Wnt/β-catenin asymmetry pathway is involved in multiple anterior-posterior fate decisions in *C. elegans* (Mizumoto and Sawa, 2007). In particular, the TCF/LEF homolog POP-1 is enriched in the anterior daughter, while the β-catenin homolog SYS-1 is enriched in the posterior daughter of an A-P cell division (Lin et al., 1995; Lin et al., 1998; Huang et al., 2007; Phillips et al., 2007). Could *pop-1* and *sys-1* play any role in regulating *ceh-34* expression or M lineage fate specification?

The expression patterns of *sys-1* and *pop-1* in the anterior-posterior divisions within the early M lineage were examined using functional *sys-1::gfp* and *pop-1::gfp* reporters (see Materials and Methods). Both *sys-1::gfp* and *pop-1::gfp* are present in the early M lineage starting from the 1-M stage, and are evenly distributed through the 4-M stage (data not shown). After divisions along the anterior-posterior axis (8-, 16- and 18-M stages), SYS-1::GFP is enriched in the posterior daughter of each cell division, while POP-1::GFP is enriched in the anterior daughter (Figure 3.5A-H). These asymmetries of SYS-1 and POP-1 mirror those seen in anterior-posterior divisions in other *C. elegans* lineages.

Figure 3.5. CEH-34 acts downstream of SYS-1 and POP-1 in the M lineage to specify CC fates.

(A-H) Localization of POP-1::GFP (A) and SYS-1::GFP (E) in the M lineage of wild-type animals. (B and F) M lineage cells marked by anti-FOZI-1 staining; (C and G) the corresponding merged images. POP-1::GFP is enriched in the nuclei of anterior cells (A), while SYS-1::GFP is enriched in the nuclei of posterior cells (E). D and H summarize the asymmetric localization patterns of POP-1::GFP and SYS-1::GFP, respectively, in the M lineage. Black circles represent enriched localization, while grey circles represent lower GFP levels. (I) A *sys-1(q544)* L4 larva with extra M-derived CCs (arrow). (J) The M lineage of the animal shown in I. (K-R) Two *sys-1(RNAi)* larvae with ectopic *ceh-34::gfp* expression. K-M are lateral views while O-Q are dorsal images. (K and O) *ceh-34::gfp* expression; (L and P) anti-FOZI-1 staining (with dorsal M lineage cells labeled); (M and Q) corresponding merged images; (N and R) corresponding lineages for K-M and O-Q, respectively, with green circles representing *ceh-34::gfp*. (S-Z) POPTOP mCherry reporter expression in the M lineage of wild-type (S-V) and *sys-1(RNAi-P)* (W-Z) animals. (S,W) mCherry signal; (T, X) M lineage cells labeled by *hlh-8::gfp*; (U,Y) corresponding merged images; (V, Z) A summary of mCherry expression in the M lineage, with POPTOP expressing cells in red circles. Note the faint mCherry signal in M.dlp and strong mCherry signal in M.vlpa and M.vlpp (U) in the wild-type animal, and the absence of mCherry signal in the M lineage of the *sys-1(RNAi-P)* animal (Y).

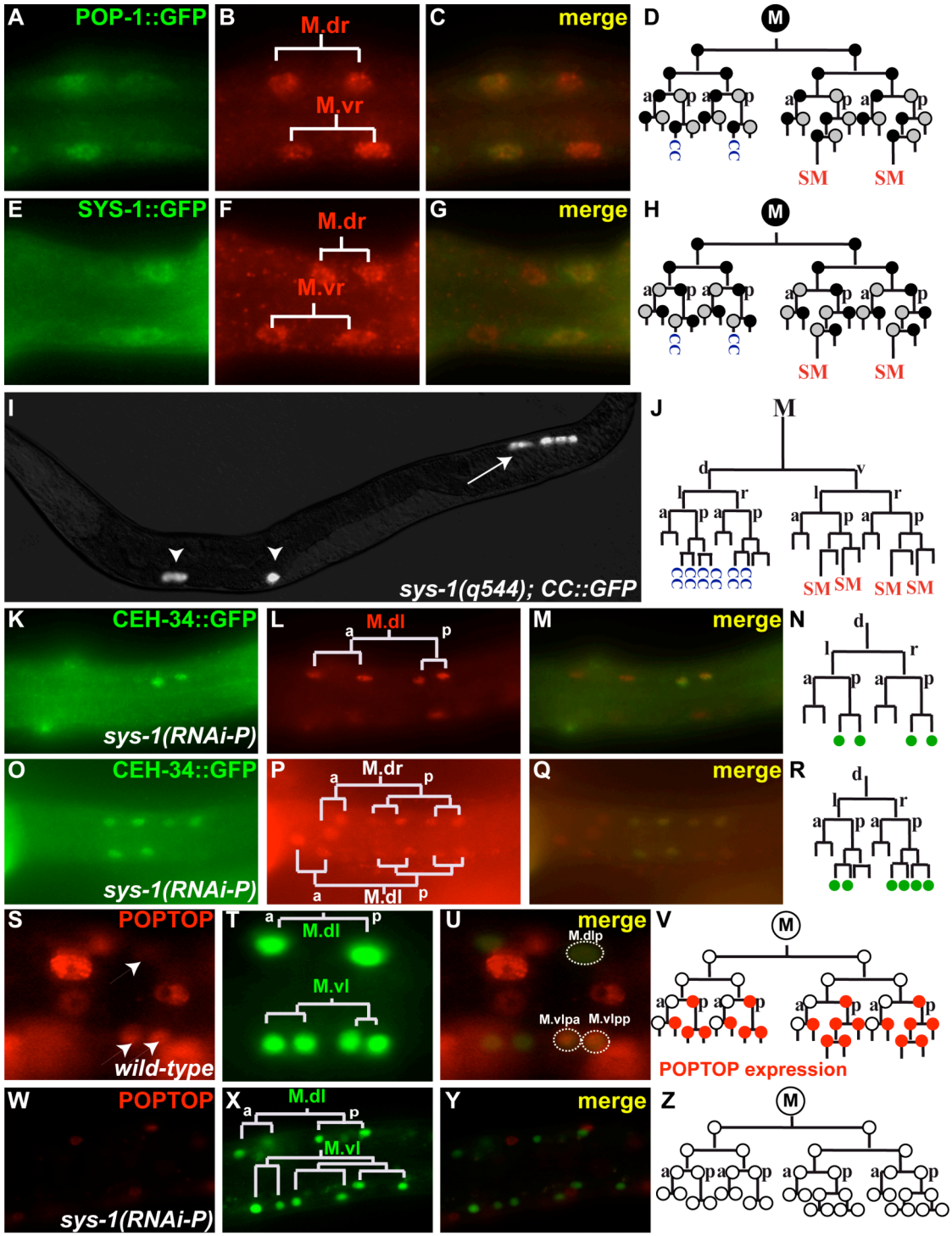
A
POP-1::GFP
B
M.dr
M.vr
C
merge
D
M
SM
SM
E
SYS-1::GFP
F
M.dr
M.vr
G
merge
H
M
SM
SM
I
sys-1(q544); CC::GFP
J
M
SM
SM
SM
SM
K
CEH-34::GFP
sys-1(RNAi-P)
L
M.dl
M
merge
N
O
CEH-34::GFP
sys-1(RNAi-P)
P
M.dr
M.dl
Q
merge
R
S
POPTOP
wild-type
T
M.dl
M.vl
U
merge
M.dlp
M.vlpa
M.vlpp
V
M
POPTOP expression
W
POPTOP
sys-1(RNAi-P)
X
M.dl
M.vl
Y
merge
Z
M

Reduction of SYS-1 levels results in the presence of extra M-derived CCs and SMs

To test whether the asymmetric distribution of SYS-1 reflected a role for *sys-1* in M lineage development, I examined M lineage development in strong loss-of-function mutant *sys-1(q544)* animals and *sys-1(RNAi-P)* animals. In both cases, I observed an increase in the number of dorsal CCs and ventral SMs derived from the M lineage (Figure 3.5I,J, Table 3.2). To determine the underlying cause of this phenotype, I used *hlh-8::gfp* and αFOZI-1 antibody staining to follow the divisions of the M mesoblast in *sys-1(q544 or RNAi-P)* animals.

On the ventral side, in a majority of *sys-1(q544)* animals (67.6%, n=37) M.vlpp and/or M.vrpp underwent an extra division along the anterior-posterior axis, most often producing an SM and a BWM, much like their anterior sister cells, M.vlpa and M.vrpa (Figures 3.5 and 3.6). This behavior was observed in 11 of 12 animals, with some variation in which cells generated the extra SMs (Figure 3.6). This variation may be due to residual activity of SYS-1 in *sys-1(q544)* animals. Similar posterior-to-anterior fate transformations in the ventral M lineage were observed in *sys-1(RNAi-P)* animals (45.8%, n=59). Thus, the extra SMs observed in *sys-1(q544)* animals were most often the result of a posterior-to-anterior fate transformation on the ventral side of the M lineage at the 16-M stage.

Unlike the ventral side, the extra CCs observed in *sys-1(q544 or RNAi-P)* animals on the dorsal side of the M lineage were not simply due to a posterior-to-anterior fate transformation. All 10 *sys-1(q544)* animals and 19 of 24 *sys-1(RNAi-P)* animals had 9 to 12 cells on the dorsal side of the M lineage (rather than the usual 8) due to an extra round of cell division by M.d(l/r)pp or M.d(l/r)pa or both (Figures 3.7 and 3.8). Since M.d(l/r)pp and M.d(l/r)pa do not undergo an extra round of cell division in wild-type animals, our observations suggest that *sys-1* is normally required to suppress further proliferation of the daughters of M.d(l/r)p.

Table 3.2. *ceh-34* functions downstream of POP-1/SYS-1 to specify CC fates

A

Genotype	Number of M-derived CCs (*intrinsic CC:gfp*)				
	n	**0-1**	**2**	**3-4**	**5-7**
wild-type	>200	0%	100%	0%	0%
L4440 RNAi	201	2.5%	97.5%	0%	0%
sys-1(q544)	112	0%	10.7%	58.9%	30.4%
sys-1(RNAi-P)	86	6.9%	41.9%	38.4%	12.8%
sys-1(q544); ceh-34(RNAi-P)	22	100%	0%	0%	0%
pop-1(RNAi-P)	67	65.7%	20.9%	13.4%	0%
pop-1(q624)	68	20.6%	79.4%	0%	0%
pop-1(q645)	49	2.0%	8.2%	59.2%	30.6%
pop-1(q645); ceh-34(RNAi-P)	53	100%	0%	0%	0%
wrm-1(RNAi-P)	96	13.5%	51.0%	33.4%	2.1%
lit-1(RNAi-P)	71	14.1%	45.1%	32.3%	8.5%

B

Genotype	Number of M-derived SMs *(hlh-8::gfp)*			
	n	**0-1**	**2**	**3-4**
wild-type	>200	0%	100%	0%
L4440RNAi	>200	0%	100%	0%
sys-1(q544)	37	0%	32.4%	67.6%
sys-1(RNAi-P)	59	0%	54.2%	45.8%
pop-1(RNAi-P)	99	41.4%	49.5%	9.1%
pop-1(q645)	22	0%	0%	100%
wrm-1(RNAi-P)	45	0%	22.2%	77.8%
lit-1(RNAi-P)	47	8.5%	46.8%	44.7%

Figure 3.6 Ventral M lineage of *sys-1(q544)* animals.

Lineage data of individual *sys-1(q544)* animals scored by following *hlh-8::gfp.* Each row represents an individual animal. Some cells could not be followed due to technical reasons and are thus marked as not determined. B and BWM denote body wall muscle, while S and SM represent sex myoblast. Each division shown here occurs along the anterior-posterior axis.

M.vl	M.vr
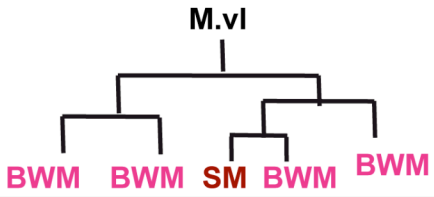	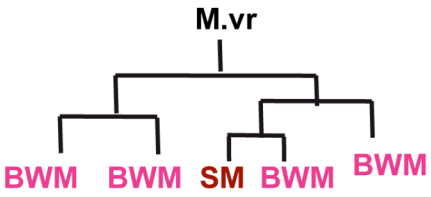
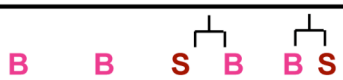	not determined
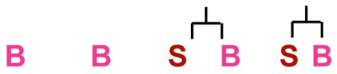	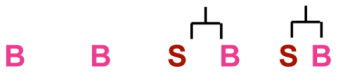
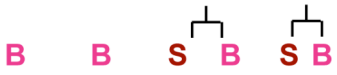	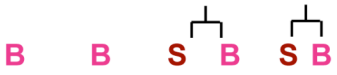
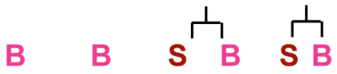	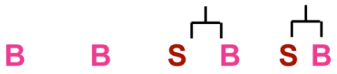
not determined	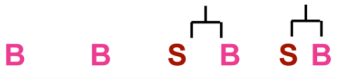
not determined	
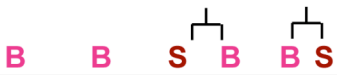	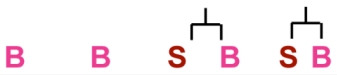
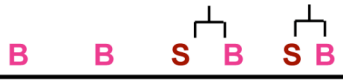	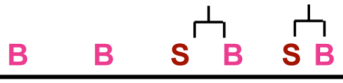
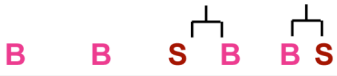	not determined
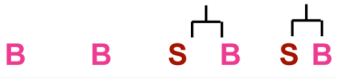	not determined
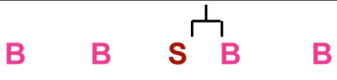	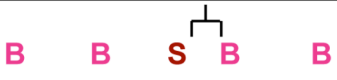
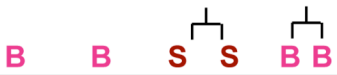	

Figure 3.7. Dorsal M lineage of *sys-1(RNAi-P)* animals.

Lineage data of individual *sys-1(RNAi-P)* animals scored by following *hlh-8::gfp* and *intrinsic CC::gfp*. Each row represents an individual animal. Some cells could not be followed due to technical reasons and are thus marked as not determined. B and BWM denote body wall muscle, while C and CC represent coelomocyte. Question marks (?) denote cells that were still in the process of dividing and not yet differentiated. Each division shown here occurs along the anterior-posterior axis.

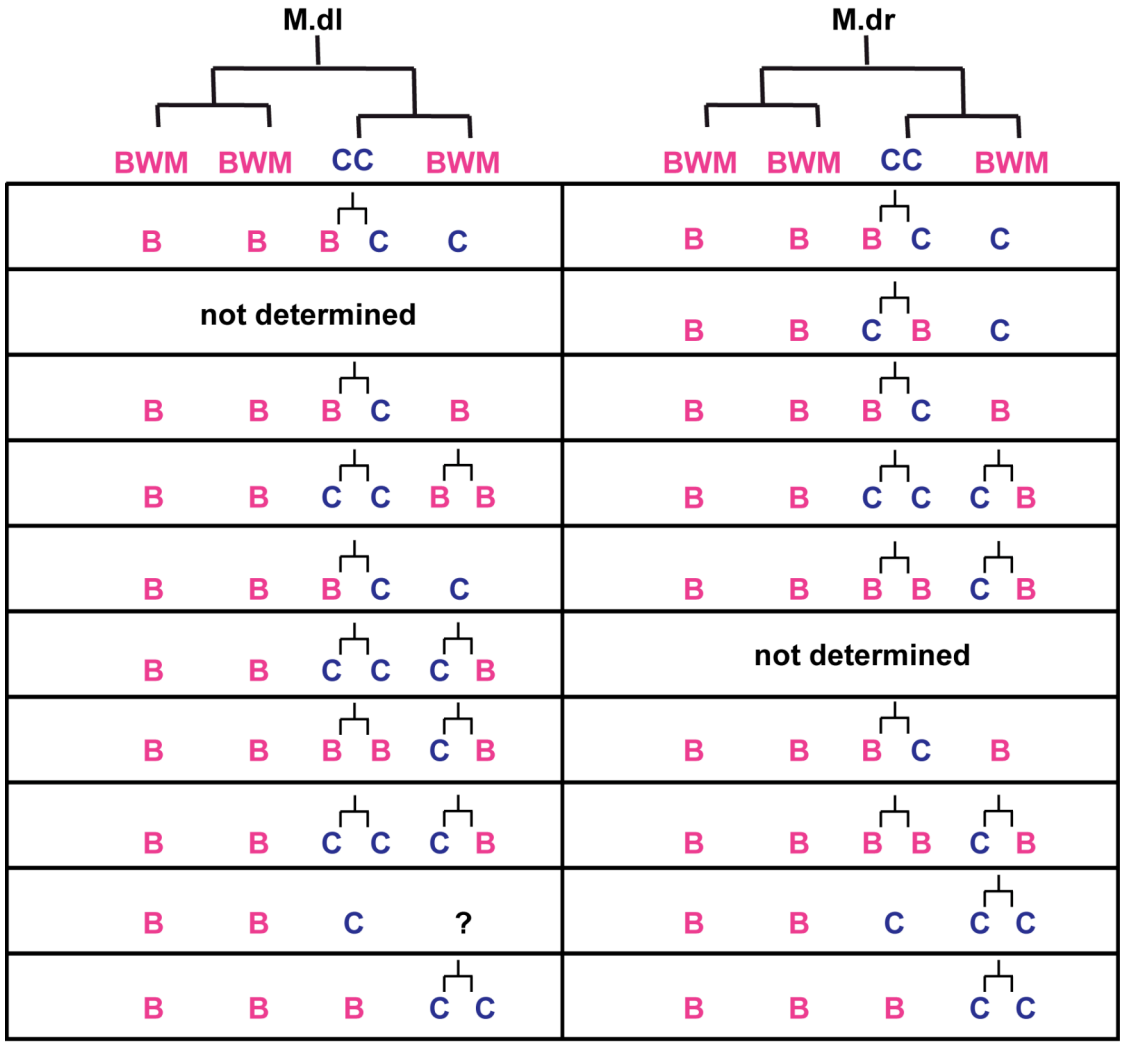
M.dl
BWM BWM CC BWM
M.dr
BWM BWM CC BWM
B B B C C
not determined
B B C B C
B B B C B
B B C C B B
B B B C C B
B B C C C B
B B B B C B
not determined
B B B C B
B B C C C B
B B B B C B
B B C ? B B C C C
B B B C C B B B C C

Figure 3.8. *ceh-34::gfp* M lineage expression in *sys-1(RNAi-P)* animals.

Data of individual *sys-1(RNAi-P)* animals scored for *ceh-34::gfp* expression using anti-GFP antibodies. M lineage cells are marked using anti-FOZI-1 staining. Each row represents an individual animal, with the first row showing a wild-type animal. Some cells could not be followed due to technical reasons and are thus marked as not determined. Filled green circles denote cells expressing *ceh-34::gfp* while open circles are cells not expressing *ceh-34::gfp*. Question marks (?) denote cells that were still in the process of dividing and not yet differentiated. Each division shown here occurs along the anterior-posterior axis.

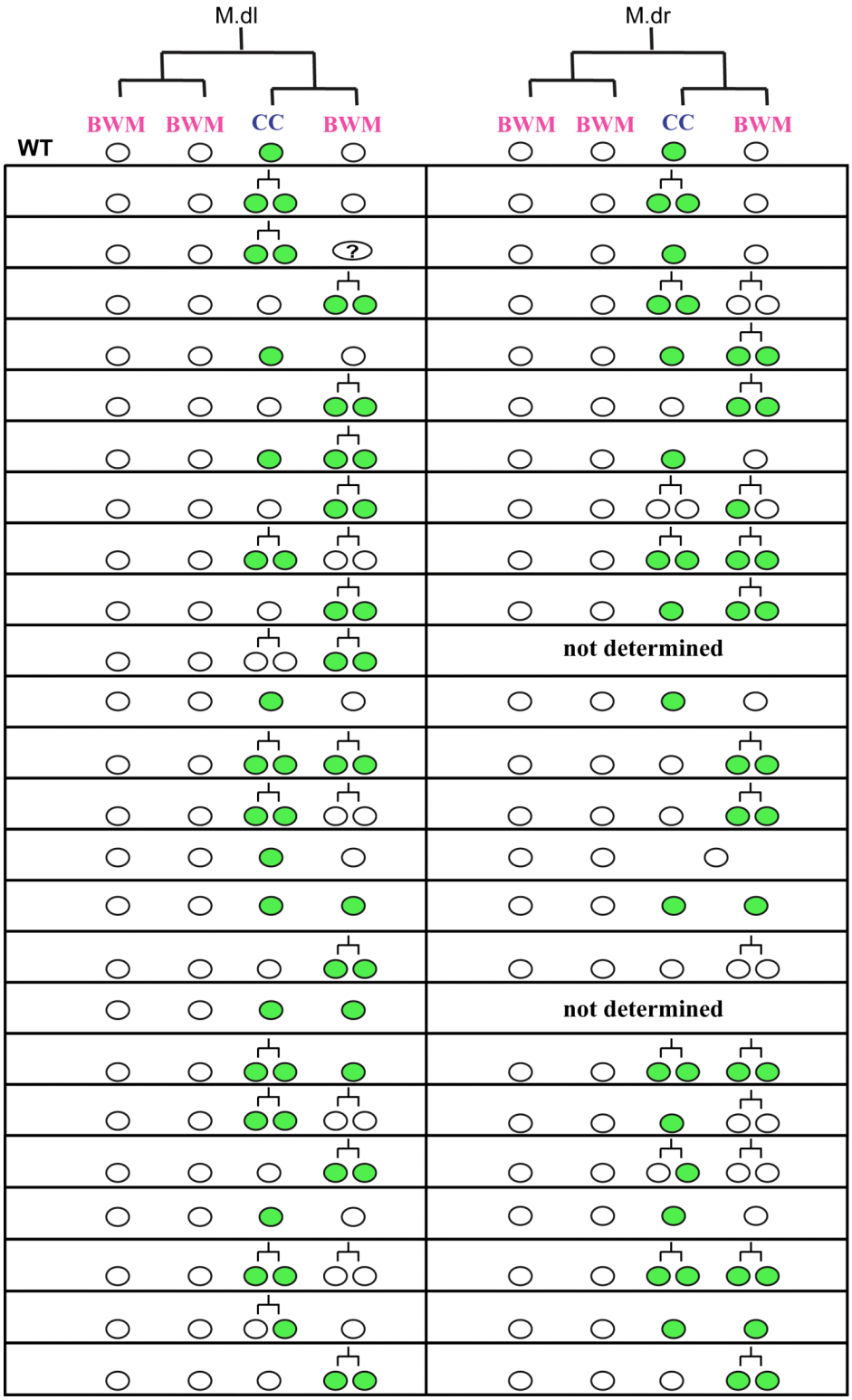
M.dl
M.dr
BWM
BWM
CC
BWM
BWM
BWM
CC
BWM
WT
?
not determined
not determined

Increased cell proliferation alone does not account for all the extra CCs observed in *sys-1(q544)* and *sys-1(RNAi-P)* animals. In instances where M.d(l/r)pa and M.d(l/r)pp did not undergo an extra division, I saw a transformation of the BWM fate of M.d(l/r)pp to the CC fate of its anterior sister M.d(l/r)pa (Figure 3.8). As shown in Figures 3.5 and 3.7, in *sys-1(q544)* and *sys-1(RNAi-P)* animals, descendants of M.d(l/r)pa and M.d(l/r)pp show a strong bias toward the CC fate. These observations suggest that in wild-type animals, *sys-1* is required to suppress the CC fate in M.d(l/r)pp, the posterior sisters of the CC precursor cells M.d(l/r)pa.

sys-1 *represses CC fates in the M lineage by negatively regulating* ceh-34 *and* eya-1 *expression*

Because *ceh-34* and *eya-1* are each necessary and together sufficient for specifying M-derived CCs, I next asked whether the extra M-derived CCs in *sys-1* mutant animals were due to inappropriate *ceh-34* and *eya-1* expression. Indeed, I found that *sys-1(RNAi-P)* resulted in the ectopic expression of *ceh-34::gfp* (Figures 3.5K-R and 3.8) and *eya-1::gfp* (data not shown) within the M lineage in a pattern consistent with the pattern of transformations to the CC fate described above.

To confirm that the extra CCs in *sys-1* mutants are due to the ectopic expression of *ceh-34*, I performed *ceh-34(RNAi-P)* in a *sys-1(q544)* mutant background. As shown in Table 3.2, *ceh-34(RNAi-P)* resulted in a loss of all M lineage-derived CCs in *sys-1(q544)* animals. Thus *sys-1* negatively regulates *ceh-34* and *eya-1* expression in the posterior sister cells of M-derived CCs and prevents those cells from adopting the CC fate.

pop-1 *is required to activate* ceh-34 *expression to properly specify M-derived CCs*

I examined the role of *pop-1* in the M lineage by using two mutant alleles of *pop-1*, *q645* and *q624*, as well as by performing *pop-1(RNAi-P)*. *q624* is a weak loss-of-function allele of *pop-1* which inhibits DNA binding, while *q645* carries a point mutation in the β-catenin interacting domain (Siegfried and Kimble, 2002). I detected a range of M lineage defects in *pop-1(q624), pop-1(q645)* and *pop-1(RNAi-P)* animals. Both *pop-1(q624)* and *pop-1(RNAi-P)* worms exhibit a loss of M-derived CCs (20.6%, n=68 for *pop-1(q624)* and 65.7%, n=67 for *pop-1(RNAi-P*)) and SMs (41.4%, n=99 for *pop-1(RNAi-P)*), an M lineage phenotype opposite to that of *sys-1* mutants (Table 3.2). The loss of SMs was due to a fate transformation of M.v(l/r)pa to the fate of its posterior sister M.v(l/r)pp (Figure 3.9). The loss of CCs was due to a combination of under-proliferation of the dorsal M lineage, as well as to fate transformation of M.d(l/r)pa to the fate of its posterior sister M.d(l/r)pp (normally fated to become BWMs). Furthermore, the loss of M-derived CCs in *pop-1(RNAi-P)* animals was often accompanied by the loss of *ceh-34::gfp* expression in the M lineage (Supplemental Figure 3.10). Intriguingly, 13.4% (n=67) of *pop-1(RNAi-P)* animals (Table 3.2) displayed a phenotype similar to *sys-1* loss of function, in which extra dorsal cells and CCs were produced. This phenotype may reflect a complete knockdown of *pop-1* in M.v(l/r)pa (see Discussion). Despite this complication, the most penetrant phenotypes of *pop-1(q624)* and *pop-1(RNAi-P)* animals indicate that *pop-1* is required for specification of the M-derived CC fate by positively regulating proliferation and *ceh-34* expression in M.dlpa and M.drpa.

Interestingly, *pop-1(q645)* animals displayed an M lineage phenotype that resembled that of *sys-1* mutants. 89.8% (n=49) of *q645* animals had extra M-derived CCs on the dorsal side and 100% of *q645* (n=22) animals had extra SMs on the ventral side (Table 3.2). Like in *sys-1* mutants, the extra SMs in *q645* mutants arise due to a

Figure 3.9. Ventral M lineage of *pop-1(RNAi-P)* animals.

Lineage data of individual *pop-1(RNAi-P)* animals scored by following *hlh-8::gfp*. Each row represents an individual animal. B and BWM denote body wall muscle, while S and SM represent sex myoblast. Each division shown here occurs along the anterior-posterior axis.

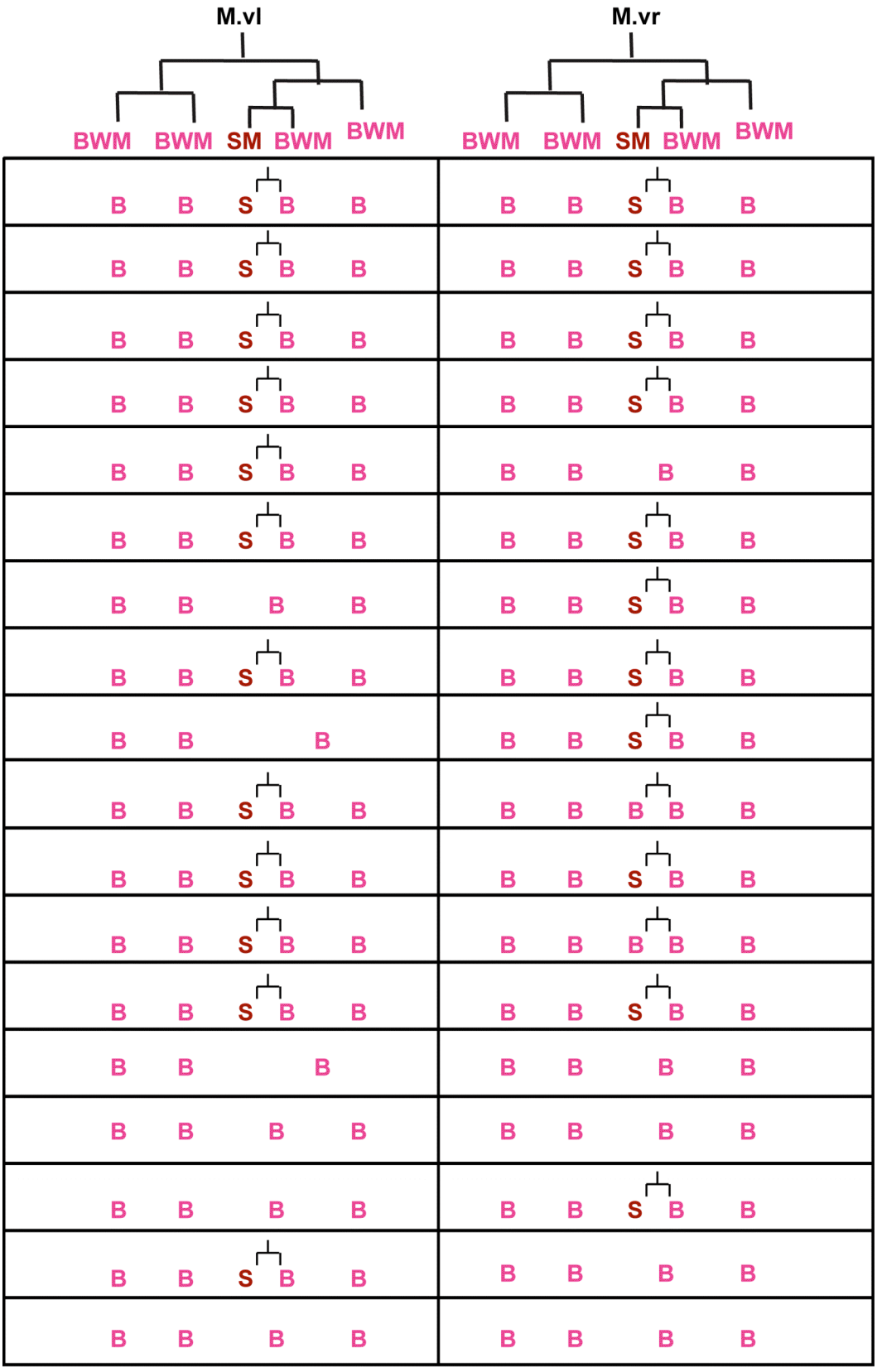
M.vl
BWM BWM SM BWM BWM
M.vr
BWM BWM SM BWM BWM
B B S B B
B B S B B
B B S B B
B B S B B
B B S B B
B B S B B
B B B B
B B S B B
B B B
B B S B B
B B S B B
B B S B B
B B S B B
B B B
B B B B
B B B B
B B S B B
B B S B B
B B B B
B B S B B
B B B B
B B B B
B B S B B
B B B B
B B S B B
B B B B
B B B B
B B S B B
B B B B
B B B B

Figure 3.10. *ceh-34::gfp* M lineage expression in *pop-1(RNAi-P)* animals.

Data of individual *pop-1(RNAi-P)* animals scored for *ceh-34::gfp* expression using anti-GFP antibodies. M lineage cells are marked using anti-FOZI-1 staining. Each row represents an individual animal, with the first row showing a wild-type animal. Some cells could not be followed due to technical reasons and are thus marked as not determined. Asterisks (*) denote animals that displayed seven cells on the left side and only three or one on the right side of the animal. These may be artifacts caused by fixation during staining. Filled green circles denote cells expressing *ceh-34::gfp* while open circles are cells not expressing *ceh-34::gfp*. Some animals displayed very faint *ceh-34::gfp* expression and are marked by fainter green circles. Each division shown here occurs along the anterior-posterior axis.

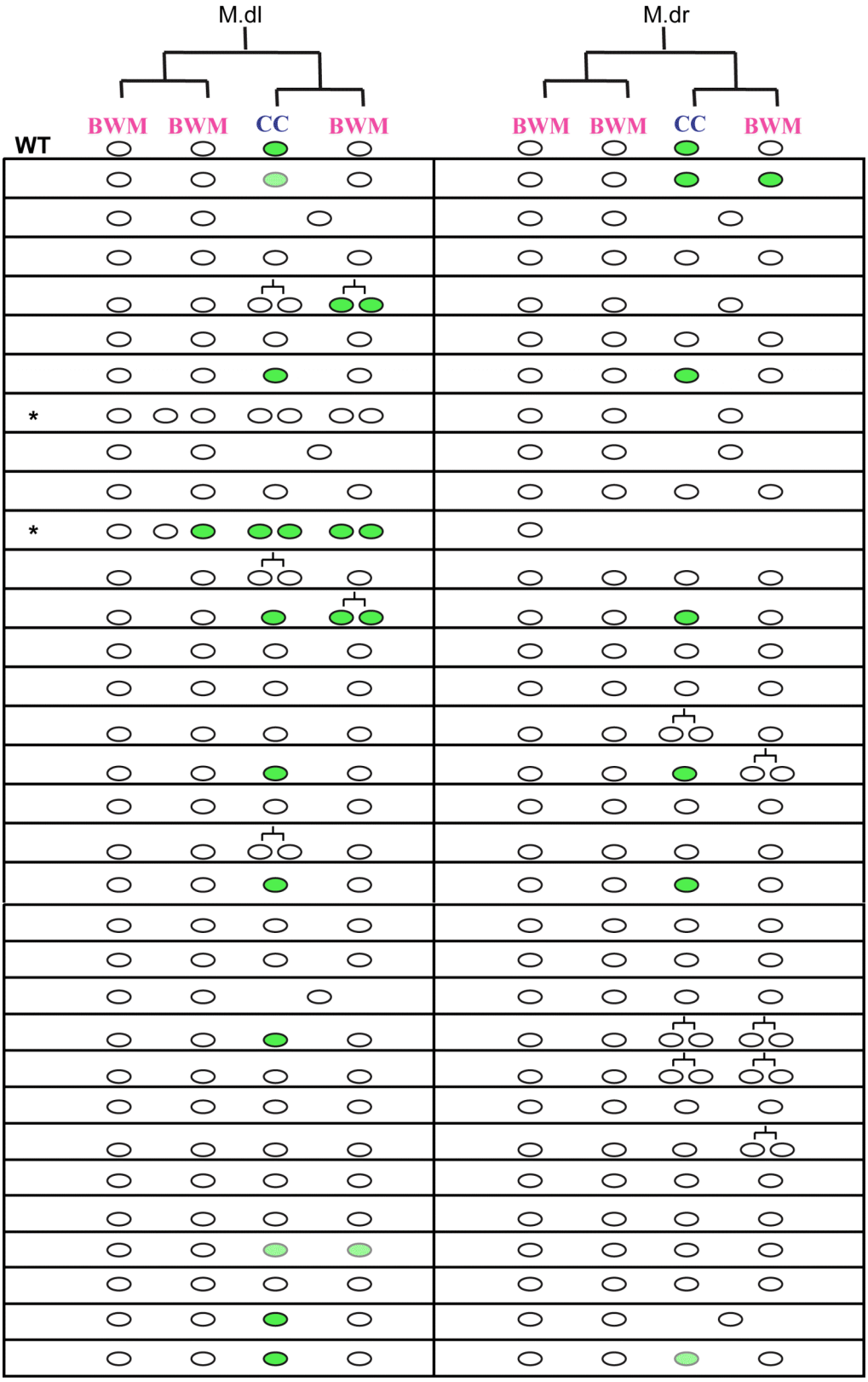
M.dl
M.dr
BWM
BWM
CC
BWM
BWM
BWM
CC
BWM
WT
*
*

fate transformation of M.v(l/r)pp to M.v(l/r)pa (Figure 3.11), and the ectopic CCs arise from the extra divisions of M.d(l/r)pa and M.d(l/r)pp and posterior-to-anterior fate transformations among the descendants of these two cells (data not shown). Furthermore, generation of extra CCs in *q645* animals depends on the presence of *ceh-34*, as *ceh-34(RNAi-P)* in *pop-1(q645)* mutants resulted in the loss of all M-derived CCs (Table 3.2). Since the *q645* mutation is located in a conserved β-catenin binding domain of POP-1 (Siegfried and Kimble, 2002), the similarity in phenotypes of *pop-1(q645)* to *sys-1* loss of function animals suggests that SYS-1 is required for the normal activity of POP-1 in M.d(l/r)pp and M.v(l/r)pp (see Discussion below).

Reduction of wrm-1 *and* lit-1 *results in extra CC and SM fates*

POP-1 nuclear levels have been shown to be regulated by the LIT-1 kinase and another β-catenin, WRM-1. These two factors facilitate the nuclear export of POP-1 in an asymmetric manner to modulate POP-1 activity (Lo et al., 2004; Takeshita and Sawa, 2005). Recently it has been shown that in the M lineage, WRM-1 localizes to the anterior cortex during anterior-posterior cell divisions but to the nuclei of posterior daughters afterwards (Takeshita and Sawa, 2005). The localization of *wrm-1::gfp* and *lit-1::gfp* to the nuclei of each of the posterior daughters of asymmetric divisions in the M lineage was confirmed (data not shown). I also saw an increase in the number of CCs and SMs in *wrm-1(RNAi-P)* and *lit-1(RNAi-P)* animals (Table 3.2). These results are consistent with a role for *wrm-1* and *lit-1* in suppressing the posterior CC and SM fates by exporting POP-1 out of the nucleus.

Figure 3.11. Ventral M lineage of *pop-1(q645)* animals.

Lineage data of individual *pop-1(q645)* animals scored by following *hlh-8::gfp*. Each row represents an individual animal. Some cells could not be followed due to technical reasons and are thus marked as not determined. B and BWM denote body wall muscle, while S and SM represent sex myoblast. Each division shown here occurs along the anterior-posterior axis.

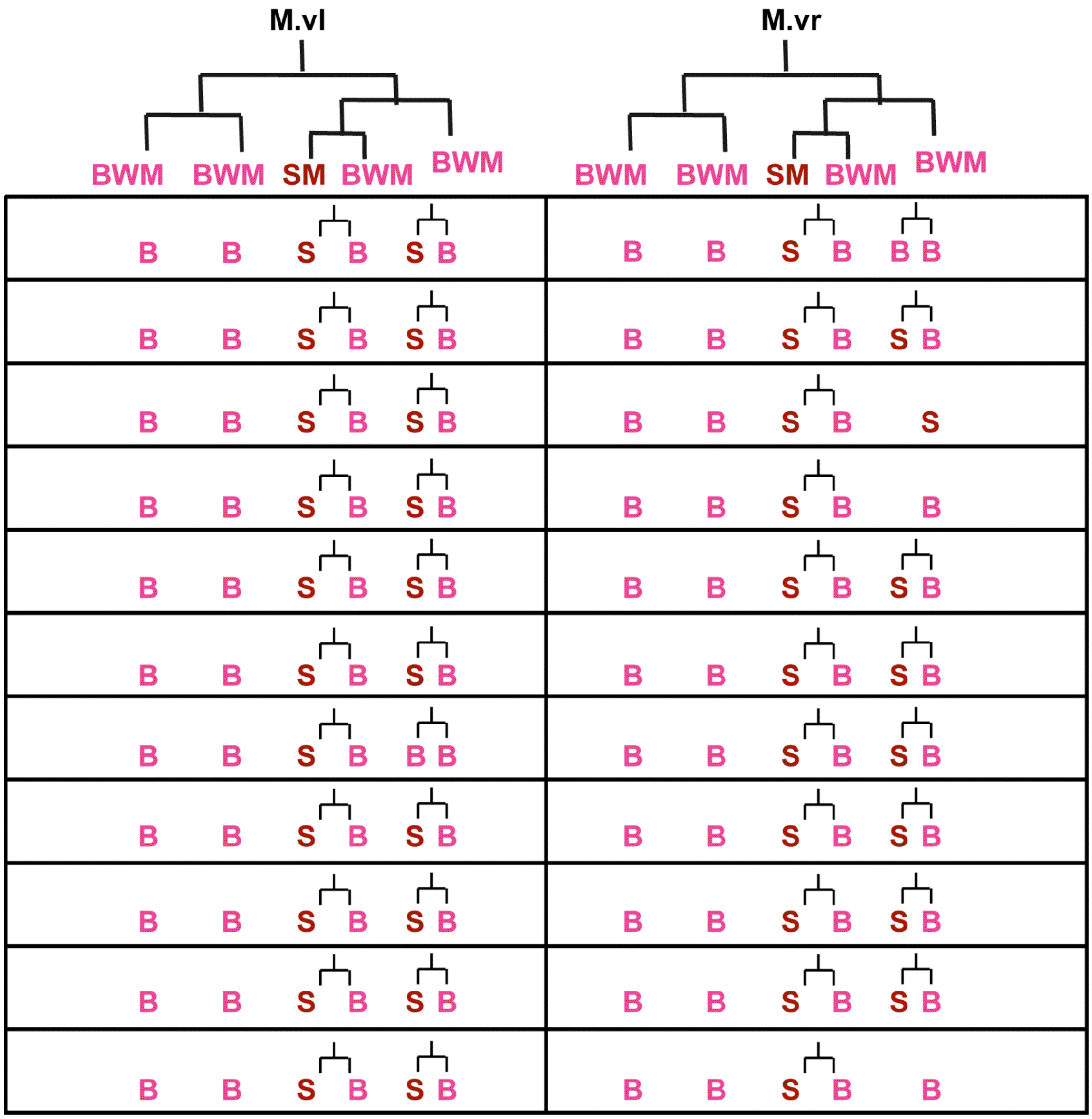
M.vl
M.vr
BWM BWM SM BWM BWM
BWM BWM SM BWM BWM
B B S B S B
B B S B B B
B B S B S B
B B S B S B
B B S B S B
B B S B S
B B S B S B
B B S B B
B B S B S B
B B S B S B
B B S B S B
B B S B S B
B B S B B B
B B S B S B
B B S B S B
B B S B S B
B B S B S B
B B S B S B
B B S B S B
B B S B S B
B B S B S B
B B S B B

POP-1 functions as a transcriptional activator in the posterior daughters of the M lineage

Previous studies have shown that a high SYS-1 to POP-1 ratio makes POP-1 a transcriptional activator (Kidd et al., 2005). To determine if this is the case in the M lineage, I monitored the expression of a recently described reporter of TCF/LEF activity called POPTOP mCherry (Green et al., 2008). Faint mCherry expression was detected in M.d(l/r)p and M.v(l/r)p, but not in their anterior counterparts, just before these cells divide (M.dlp in Figure 3.5S-U). The mCherry signal remains visible in both the anterior and posterior descendants of M.d(l/r)p and M.v(l/r)p (M.vlpa and M.vlpp in Figure 3.5S-U). Faint mCherry expression was again detectable in the posterior descendants of M.d(l/r)a and M.v(l/r)a (data not shown). This pattern of mCherry expression was seen in 15 out of 16 animals examined; the overall expression pattern of mCherry is summarized in Figure 3.5V. Taking into account the slow folding rate of mCherry (Shaner et al., 2005), which could account for the faint signals, and the potential persistence of mCherry in both daughters of a cell expressing the reporter, these results are consistent with activation of the POPTOP reporter in the posterior cells of the M lineage.

Because the posterior cells in the M lineage have a high SYS-1 to POP-1 ratio, I next asked whether the activation of the POPTOP reporter in the posterior cells requires SYS-1 by examining the expression of mCherry in *sys-1(RNAi-P)* animals. *sys-1(RNAi-P)* consistently led to an overall decrease of the mCherry signal in larvae (Figures 3.5W-Y). Furthermore, in 8 out of 10 animals scored, *sys-1(RNAi-P)* led to a loss of mCherry expression in most, if not all, M lineage descendants (Figure 3.5W-Z). Thus I conclude that a high SYS-1 to POP-1 ratio in the posterior daughters of the M lineage leads to the change of POP-1 to a transcriptional activator.

Discussion

The Six homeodomain protein CEH-34 and its cofactor EYA-1 are required for the specification of non-muscle mesodermal fates in *C. elegans*

The mesoderm gives rise to a variety of muscle and non-muscle cell types. Previous studies in both vertebrates and invertebrates have identified a number of factors, including the myogenic regulatory factors (MRFs), that are critical for the specification of myogenic fates (Pownall et al., 2002). Much less is known about the mechanisms involved in the specification of non-myogenic mesodermal cells. I report here the identification and characterization of a Six homeodomain protein CEH-34 and its cofactor EYA-1 in specifying the non-muscle coelomocyte (CC) cells in the *C. elegans* postembryonic mesoderm. *ceh-34* and *eya-1* are both expressed in the CC precursor cells in the M lineage. Furthermore, *ceh-34* and *eya-1* are each necessary and together sufficient for CC fate specification in the M lineage. CEH-34 and EYA-1 are also at least partially required to specify the embryonically-derived CCs.

An evolutionarily conserved Six-Eya cassette in mesodermal development

CEH-34 belongs to a highly conserved family of homeodomain proteins called the Six family. Previous studies have shown the Pax-Six-Eya-Dac network functions in multiple developmental processes, including eye and mesoderm development in Drosophila and vertebrates, and kidney and sensory organ development in mammals (Heanue et al., 1999; Xu et al., 1999; Hanson, 2001; Clark et al., 2006). Mutations in Six1 and Eya1 in humans have also been shown to cause the Brancio-oto-renal (BOR) syndrome (Kochhar et al., 2007). However, the composition of the Pax-Six-Eya-Dac network appears to vary in different developmental contexts. For example, *ey* and *dac* are coexpressed in the developing mushroom bodies of the *Drosophila* central nervous

system, but *eya* and *so* are absent there (Kurusu et al., 2000; Martini et al., 2000; Noveen et al., 2000). Similarly, *eya* and *dac* have been found to function independently in Drosophila neuronal specification, even within single cells (Miguel-Aliaga et al., 2004). In *C. elegans* the Pax6 homolog *vab-3* is required for proper head morphogenesis and directly regulates the expression of the Six gene *ceh-32* (Dozier et al., 2001). *vab-3* also genetically interacts with *eya-1* during embryonic morphogenesis, but mutants in the single Dac homolog *dac-1* do not display any anterior morphogenesis defects (Colosimo et al., 2004). Here I show that proper specification of the non-muscle coelomocytes in the *C. elegans* postembryonic mesoderm requires the functions of both *ceh-34* and *eya-1*, but not *dac-1* or any of the five Pax genes individually. Although I cannot rule out the possibility that some, or all, of the Pax genes may function redundantly in the M lineage, our data are consistent with the notion that not all members of the Pax-Six-Eya-Dac network always function together in different cell and tissue types.

Six and Eya proteins bind to each other and function together in various developmental contexts, including in the mesoderm. In Drosophila, *Six4* and *Eya* function together for the proper patterning of the non-dorsal mesoderm (Clark et al., 2006). Six1 and Eya2 proteins in mouse function together to regulate the expression of myogenic regulatory factors involved in multiple aspects of skeletal myogenesis (Grifone et al., 2005). In this study, I showed that CEH-34 and EYA-1 can physically interact and that each protein is necessary and together they are sufficient to promote the non-muscle coelomocyte fate in the *C. elegans* postembryonic mesoderm. These findings suggest that the Six-Eya protein complex represents an evolutionarily conserved cassette essential for mesodermal development.

The conservation of the Six-Eya protein complex is likely due to the distinct biochemical properties of these two proteins. In general, Six proteins alone can bind to

DNA, but cannot activate transcription of downstream targets, suggesting a general repressive effect of Six proteins on their own (Li et al., 2003). Eya proteins are phosphatases that do not bind DNA directly, but can function as co-activators of Six proteins and recruit additional co-activators (Li et al., 2003). Thus proper activation of downstream target genes requires the function of the Six-Eya protein complex. Even in cases where some Six proteins have intrinsic activation domains, activation of target genes via these proteins is only clearly evident in the presence of Eya (Kawakami et al., 1996; Spitz et al., 1998; Ohto et al., 1999).

CEH-34 and EYA-1 act downstream of the D/V patterning mechanisms as well as mesoderm-intrinsic transcription factors in the M lineage

Both CEH-34 and EYA-1 localize asymmetrically to the dorsal side of the M lineage, in the CC precursor cells. Previous studies have shown that SMA-9, the homolog of the Schnurri protein, antagonizes the Sma/Mab TGFβ signaling pathway and is required for the proper specification of the dorsal CC fates, while the LIN-12/Notch signaling pathway is required for ventral SM fates (Greenwald et al., 1983; Foehr et al., 2006). I found that SMA-9 is required for the expression of *ceh-34* and *eya-1* in the dorsal M lineage, while LIN-12 is required for repressing *ceh-34* on the ventral side of the M lineage. These results place *ceh-34* and *eya-1* downstream of both signaling pathways involved in dorsal-ventral asymmetry in the M lineage.

ceh-34 and *eya-1* expression is also regulated by transcription factors intrinsic to the M lineage. It has been shown previously that the transcription factors *hlh-1*, *fozi-1* and *mab-5* are expressed in all the M-derived BWM and CC precursor cells. While all three factors are required for M-derived CC fate, HLH-1, the *C. elegans* homolog of the myogenic regulatory factor MyoD, functions redundantly with the zinc finger protein FOZI-1 and the Hox factor MAB-5 to specify M-derived BWM fates

(Amin et al., 2007). HLH-1, like the vertebrate myogenic regulatory factors (MRFs), is sufficient to induce BWM fates when ectopically expressed in the *C. elegans* early embryo (Fukushige and Krause, 2005). However, expression of FOZI-1 and MAB-5 are not sufficient to induce BWM fate (Amin et al., 2007). In this study, I found that the expression of *ceh-34* and *eya-1* in M-derived CC precursors is lost in *hlh-1*, *fozi-1* and *mab-5* mutants. Taken together, my data suggests that *hlh-1*, *fozi-1* and *mab-5* encode M lineage intrinsic transcription factors that make a set of cells competent to form BWMs or CCs, and that *ceh-34* and *eya-1* are further required to specify non-muscle CCs from these bipotent precursors.

This is not the first example in which cells expressing a MRF do not necessarily adopt muscle fates. It has recently been shown that cells initially expressing the Myf5 MRF give rise to brown fat cells in addition to muscles (Seale et al., 2008). Once the brown adipose tissue is differentiated, Myf5 expression is no longer detectable. Similarly, HLH-1 is expressed in the CC precursor cells, but not in the differentiated CCs (Harfe et al., 1998a). While HLH-1 is required for the expression of *ceh-34* and *eya-1* to generate non-muscle CC cells, it is not known whether Myf5 is required for the specification of non-muscle brown fat cell fates.

CEH-34 and EYA-1 function downstream of the Wnt/β-catenin asymmetry pathway that regulates anterior-posterior asymmetry in the M lineage

The Wnt/β-catenin asymmetry pathway is involved in many anterior-posterior fate decisions during *C. elegans* development (Mizumoto and Sawa, 2007). Specifically, POP-1, the *C. elegans* TCF/Lef transcription factor, is asymmetrically distributed during anterior-posterior divisions in which the anterior daughter retains a higher concentration of POP-1 in the nucleus compared to the posterior daughter, while the divergent β-catenin SYS-1 is enriched in the nucleus of the posterior

daughter (Lin et al., 1998; Huang et al., 2007; Phillips et al., 2007). This anterior nuclear enrichment of POP-1 is facilitated at least in part by the LIT-1 kinase and a β-catenin homolog WRM-1, which mediate the nuclear export of POP-1 in the posterior cell (Lo et al., 2004; Nakamura et al., 2005; Takeshita and Sawa, 2005). The ratio of high levels of SYS-1 to POP-1 in the posterior cell allows for binding of SYS-1 to the POP-1 transcription factor converting it from a repressor to an activator, while high concentrations of POP-1 in the anterior cell keeps POP-1 as a repressor (Kidd et al., 2005; Liu et al., 2008). SYS-1 nuclear levels have also been shown to be the limiting factor as to whether POP-1 acts as a repressor or activator (Kidd et al., 2005; Liu et al., 2008). The asymmetric distribution of nuclear POP-1 and SYS-1 results in proper specification of cell fates along the anterior-posterior axis in the *C. elegans* early embryo, with a low SYS-1 to POP-1 ratio inhibiting posterior fates, allowing the production of anterior fates (Lin et al., 1995; Lin et al., 1998; Huang et al., 2007).

The reciprocal asymmetric distribution of POP-1 and SYS-1 in sister cells along the anterior-posterior axis is maintained during postembryonic development, but also extends to cells born along the proximal-distal axis in the somatic gonad and the vulval precursor cells (Herman, 2001; Siegfried et al., 2002; Kidd et al., 2005; Phillips et al., 2007; Green et al., 2008). Recently, it has been shown using a reporter of POP-1 transcriptional activity (POPTOP) that high SYS-1 to POP-1 ratios in the daughter cells of P5.p and P7.p lead to transcriptional activation of the POPTOP reporter (Green et al., 2008). Intriguingly, in the postembryonic lineages examined to date, loss of function mutants for both *pop-1* and *sys-1* give identical mutant phenotypes (Siegfried et al., 2004; Huang et al., 2007; Green et al., 2008).

In this chapter, I described that each anterior-posterior division in the M lineage results in POP-1 being enriched in the anterior daughter cell and SYS-1 in the posterior daughter cell. I also found that knocking down the level of SYS-1 (in *sys-*

1(q544) and *sys-1(RNAi-P)* animals) resulted in partially penetrant posterior-to-anterior fate transformations and the ectopic expression of *ceh-34* and *eya-1* in posterior cells. Reduced levels of POP-1 (in *pop-1(q624)* and *pop-1(RNAi-P)* animals) give a reciprocal result: partially penetrant anterior-to-posterior fate transformations and loss of *ceh-34* and *eya-1* expression. In contrast to the phenotype of these *pop-1* loss-of-function mutants, *q645*, a mutation in POP-1 that blocks its ability to bind SYS-1 (Siegfried and Kimble, 2002), display the same phenotype as *sys-1* loss-of-function. Like *sys-1* mutants, RNAi of *lit-1* or *wrm-1*, which presumably leads to the accumulation of POP-1 in the posterior nuclei, resulted in the loss of posterior fates. Finally, I found that the POPTOP reporter is activated in the posterior cells in the M lineage and that its activation requires the function of SYS-1. These results can be reconciled by the model presented in Figure 3.12.

In this model, I propose that cells that express the mesoderm-intrinsic transcription factors MAB-5, FOZI-1 and HLH-1 are fated to become either myogenic BWMs or non-myogenic CCs. Expression of *ceh-34* and *eya-1* promotes the CC fate. POP-1 functions as a repressor in the anterior daughters of each division by repressing an unknown transcriptional repressor of *ceh-34* and *eya-1* so that *ceh-34* and *eya-1* are expressed in the anterior cells to specify CC fate. However, not all cells expressing MAB-5, FOZI-1 and HLH-1 can respond to the POP-1 repressive activity. TCF/LEF proteins often act synergistically with other cell or tissue competence factors to affect gene expression in a cell-type specific manner (Barolo, 2006). I propose that another competence factor (Factor X in Figure 3.12) functions to distinguish the daughters of M.d(l/r)p from the daughters of M.d(l/r)a and acts as an additional activator of *ceh-34* and *eya-1*. Thus, as illustrated in Figure 3.12, the expression of *ceh-34* and *eya-1* and the specification of the CC fate only happen because of a combination of three sets of activities: 1) the mesoderm intrinsic transcription factors that specify CC and BWM

Figure 3.12. A model for non-muscle CC fate specification in the M lineage. (A) *ceh-34* and *eya-1* expression and subsequent specification of M-derived CC fate requires the combinatorial actions of three sets of factors: the M lineage intrinsic transcription factors including MAB-5, FOZI-1 and HLH-1 that are required for CC and BWM fate, the cell competence factor(s) X, and the repressive activity of POP-1 due to a low SYS-1 to POP-1 ratio. This low SYS-1 to POP-1 ratio leads to the repression of a repressor of *ceh-34* and *eya-1*, which in turn results in the expression of *ceh-34* and *eya-1*. (B) Regulatory inputs to *ceh-34* and *eya-1*, including the functions of the dorsal-ventral patterning systems (LIN-12/Notch and SMA9). Solid lines in (A) and (B) do not represent direct regulation.

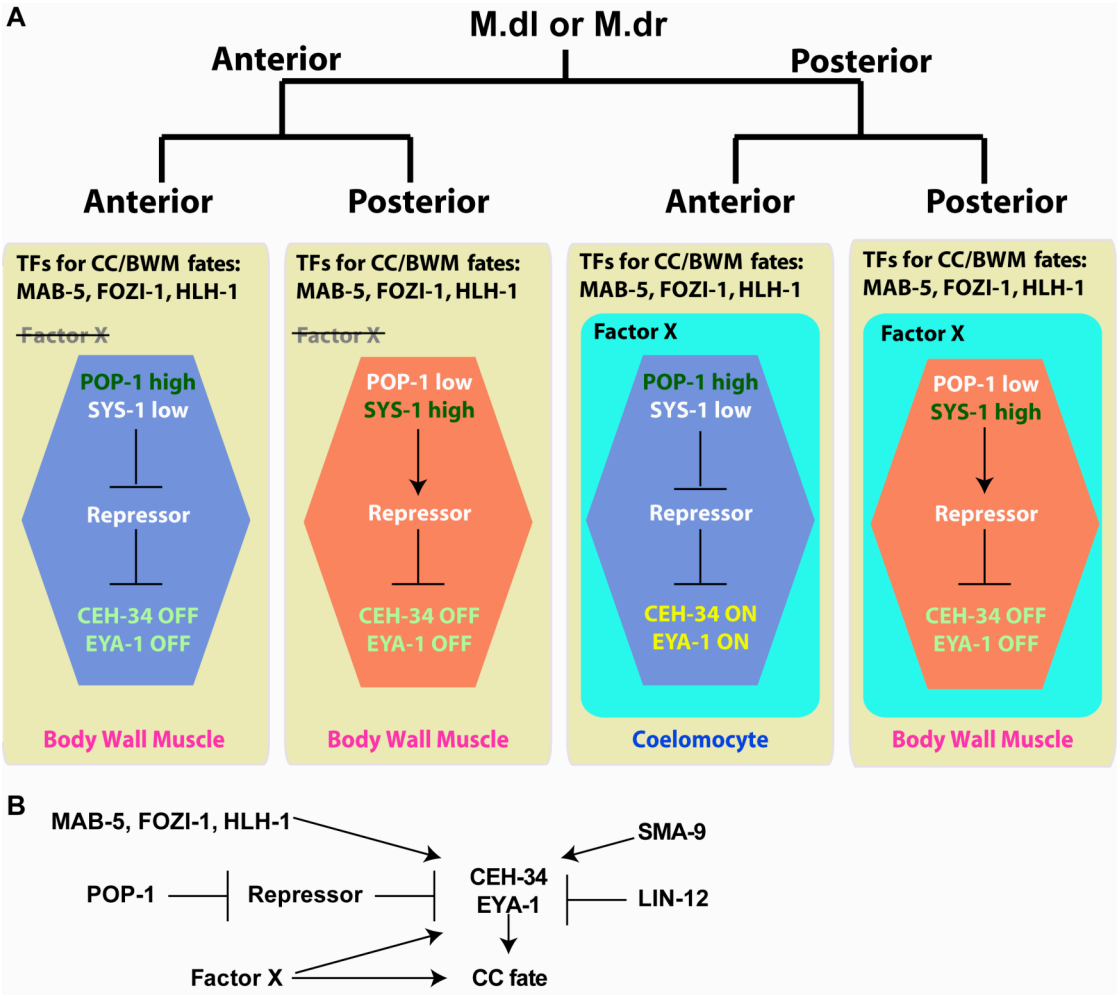
A
M.dl or M.dr
Anterior
Posterior
Anterior
Posterior
Anterior
Posterior
TFs for CC/BWM fates:
MAB-5, FOZI-1, HLH-1
Factor X
POP-1 high
SYS-1 low
Repressor
CEH-34 OFF
EYA-1 OFF
Body Wall Muscle
TFs for CC/BWM fates:
MAB-5, FOZI-1, HLH-1
Factor X
POP-1 low
SYS-1 high
Repressor
CEH-34 OFF
EYA-1 OFF
Body Wall Muscle
TFs for CC/BWM fates:
MAB-5, FOZI-1, HLH-1
Factor X
POP-1 high
SYS-1 low
Repressor
CEH-34 ON
EYA-1 ON
Coelomocyte
TFs for CC/BWM fates:
MAB-5, FOZI-1, HLH-1
Factor X
POP-1 low
SYS-1 high
Repressor
CEH-34 OFF
EYA-1 OFF
Body Wall Muscle
B
MAB-5, FOZI-1, HLH-1
SMA-9
POP-1
Repressor
CEH-34
EYA-1
LIN-12
Factor X
CC fate

fates, 2) the POP-1 repressive activity and 3) the competence Factor X. The absence of either activity 2 or 3 would lead to the ground BWM fate. The existence of Factor X in regulating *ceh-34* and *eya-1* expression and for providing competence for cells to become CCs (Figure 3.12B) is consistent with my observations that a) the defects in *sys-1* or *pop-1* mutants are only restricted to the daughters of M.d(l/r)p and M.v(l/r)p, and b) ectopic expression of *ceh-34* and *eya-1* throughout the M lineage did not convert all BWMs to CCs. Finally, the expression of *ceh-34* and *eya-1* and the specification of CCs on the dorsal side are also under the control of dorsal-ventral patterning mechanisms that involve the LIN-12/Notch and TGFβ (antagonized by SMA-9) signaling pathways (Figure 3.12). I envision that a similar model could be applied to the ventral M lineage for the specification of SMs.

This model states that a complex containing POP-1 and SYS-1 functions as a transcriptional activator, while POP-1 functions as a repressor. Applying this model to my data presented above, POP-1 repressor activity and ectopic CC fates in M.d(l/r)pp were achieved by 1) reducing SYS-1 levels, 2) increasing the nuclear levels of POP-1 by *wrm-1(RNAi)* or *lit-1(RNAi),* and 3) blocking POP-1 binding to SYS-1 as in the *pop-1(q645)* allele. Conversely, lowering the level of POP-1 led to a higher ratio of POP-1-SYS-1 complexes and resulted in the loss of CC fates in M.d(l/r)pa in *pop-1(RNAi)* and *pop-1(q624)* animals.

This model predicts that complete loss of POP-1 function in the M lineage would result in a failure to activate the repressor of *ceh-34* and *eya-1* in the M lineage. Indeed, our data support this conclusion, as a small percentage (Table 3.2, Figure 3.10) of *pop-1(RNAi-P)* animals, but not *q624* animals, displayed an M lineage phenotype resembling that caused by *sys-1* loss-of-function, including the presence of extra CCs and extra cells expressing *ceh-34* and *eya-1*. This phenotype may reflect a complete knockdown of POP-1 in the daughters of M.d(l/r)p and M.v(l/r)p.

Finally, I observed extra proliferation in the M lineage in *sys-1(RNAi-P or q544)* and *pop-1(q645)* mutants and reduced cell proliferation in *pop-1(RNAi-P)* animals. Reduced cell proliferation in the T lineage has also been observed in *pop-1(RNAi)* animals (Herman, 2001). Disruptions of β-catenin and TCF/LEF have been reported in developmental defects and diseases, including cancer (van de Wetering et al., 2002; Mazieres et al., 2005; Firestein et al., 2008; Grigoryan et al., 2008). Given this prior knowledge of a link between Wnt pathway mutations and cancer, it is possible that SYS-1 and POP-1 may have a direct role in regulating cell proliferation.

A conserved paradigm for mesoderm development?

My model for patterning and fate specification in the M lineage shares many similarities with mesodermal patterning and fate specification in the Drosophila embryo. In Drosophila, dorsal-ventral patterning requires *dpp* signaling, which contributes to the restriction of *D-six4* regulation to the ventral mesoderm (Clark et al., 2006). Anterior-posterior patterning of the early mesoderm in Drosophila requires the Wnt signaling pathway. Specifically, the repressive form of the LEF/TCF homolog Pangolin represses the expression of the forkhead genes *sloppy paired 1 and 2 (slp)* in posterior compartments of parasegments, while the active form of Pangolin can activate *slp* expression in the anterior compartments. *slp* functions to repress the transcription of *bagpipe*, a key regulator of visceral mesoderm fates (Lee and Frasch, 2000;Lee and Frasch, 2005). Since Six and Eya proteins also function in the vertebrate mesoderm, including myogenesis and kidney development, I speculate that vertebrates may use similar combinational mechanisms to activate Six and Eya expression in the various mesodermal tissues.

ACKNOWLEDGEMENTS

We thank CGC (the *C. elegans* Genetics Center), David Eisenmann, Judith Kimble, Morris Maduro, Brian Harfe, Yuji Kohara, Shohei Mitani, Paul Sternberg and Asako Sugimoto for strains and plasmids; Marisa Foehr, Ken Kemphues, Diane Morton and Chenxi Tian for helpful discussions and valuable comments on the manuscript. This work was supported by NIH R01 GM066953 (to J.L.). S.-E.L. was a Rawlings Cornell Presidential Research Scholar and T.L.C. was a Howard Hughes Undergraduate Research Scholar at Cornell University.

CHAPTER 4[3]

THE FORKHEAD TRANSCRIPTION FACTOR LET-381 IS REQUIRED FOR DORSAL CELL FATES IN THE C. ELEGANS POSTEMBRYONIC MESODERM

Introduction

The specification of diverse cell types from pluripotent progenitor cells results from the differential instructions that govern these progenitors. These instructions can be in the form of intercellular signaling or in the form of asymmetric distribution of key determinants passed along during cell divisions in which the two daughter cells inherit different determinants and hence adopt different fates. In general, these events converge upon the expression and/or activity of transcription factors that can activate cell-type specific expression of genes required for proper differentiation. For example, in the mesoderm, when the expression of a family of transcription factors known as the myogenic regulatory factors is activated, these transcription factors in turn activate the expression of muscle-specific genes (Pownall et al., 2002). While a number of transcription factors have well established roles in development, there are many transcription factors for which the function has not yet been characterized.

The *C. elegans* postembryonic mesodermal lineage, the M lineage, offers a unique opportunity to study these mechanisms at single cell resolution. The M lineage arises from a single pluripotent cell, the M mesoblast, which is born during embryogenesis and remains dormant until the larva hatches. This blast cell divides

[3] A portion of the RNAi screen described in this chapter was performed by Zach Via, while cloning was performed by Herong Shi.

during early larval growth to give rise to 18 cells. Two of these cells differentiate into coelomocytes (CCs), which are non muscle cells with a scavenger-like function, and 14 become striated body wall muscles (BWMs), which are involved in locomotion. The two remaining cells become sex myoblasts (SMs) which further migrate to the presumptive vulva where they proliferate and give rise to the 16 sex muscles that are used for egg-laying. These include 8 type 1 and type 2 vulval muscles (4 vm1s and 4 vm2s) and 8 type 1 and type 2 uterine muscles (4 um1s and 4 um2s) (Sulston and Horvitz, 1977; Sulston et al., 1983). This lineage and the different cell types are depicted in detail in Figure 4.1.

In recent years, studies have identified a number of transcription factors that function autonomously within the M lineage to regulate proliferation, cleavage orientations and proper specification of these diverse cell types. The Hox genes *mab-5* and *lin-39* function redundantly with their cofactor *ceh-20*, and are required for the proliferation, cleavage orientations and specification of the M mesoblast and its descendents (Liu and Fire, 2000). *hlh-8*, the *C. elegans* homolog of the vertebrate Twist, is regulated by *mab-5, lin-39 and ceh-20* and is required for patterning the mesoderm (Harfe et al., 1998b; Corsi et al., 2000; Liu and Fire, 2000). Another homeobox gene, *mls-2*, functions downstream of *ceh-20* and is also required for proper proliferation and cleavage orientations (Jiang et al., 2005; Jiang et al., 2008). *mls-2* functions upstream of the MyoD homolog HLH-1, which together with the zinc-finger protein FOZI-1 and MAB-5 is required for the proper specification of CC and BWM fates (Harfe et al., 1998a; Jiang et al., 2005; Amin et al., 2007). Meanwhile, the Six2 homolog *ceh-34* and its cofactor *eya-1* are required for the specification of the CC fate (Chapter 3, this dissertation). During the specification of sex muscle fates, the T-box factor *mls-1* acts downstream of *hlh-8* and is required for uterine muscle fates (Kostas and Fire, 2002).

Figure 4.1. The *C. elegans* hermaphrodite postembryonic M lineage.

Times are indicated post-hatching at 25˚C. (A) The M lineage showing all differentiated cell types that arise from M (modified from Sulston and Horvitz, 1977). (B) A schematic lateral view of the M lineage through larval development. D, dorsal; V, ventral; L, left; R, right; A, anterior; P, posterior.

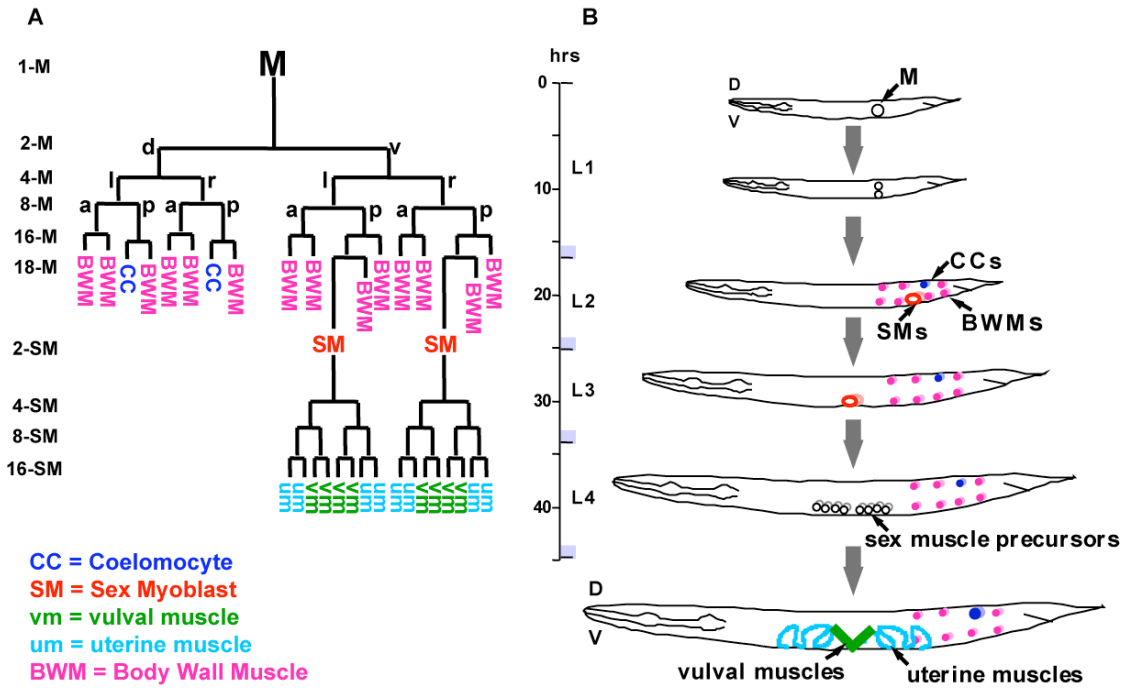
A
1-M
2-M
4-M
8-M
16-M
18-M
2-SM
4-SM
8-SM
16-SM
M
d
v
l
r
a
p
BWM
CC
SM
CC = Coelomocyte
SM = Sex Myoblast
vm = vulval muscle
um = uterine muscle
BWM = Body Wall Muscle
B
hrs
0
10
20
30
40
L1
L2
L3
L4
D
V
M
CCs
SMs
BWMs
sex muscle precursors
vulval muscles
uterine muscles

In addition to these cell-type specific factors, *sma-9* and *lag-1* function in establishing the dorsal-ventral polarity of the M lineage. *sma-9* encodes a homolog of the Drosophila and vertebrate Schnurri homologs and antagonizes the Sma/Mab TGFβ pathway to promote dorsal fates (Foehr et al., 2006). *lag-1* encodes the CBF1/Su(H)/LAG-1 (CSL) DNA binding factor that functions downstream of lin-12/Notch signaling and has been shown to promote ventral fates (Foehr and Liu, 2008). Meanwhile, the Wnt/β-catenin asymmetry pathway regulates anterior-posterior asymmetry within the M lineage (Chapter 3, this dissertation). Though it is known that TGFβ, LIN-12/Notch and the Wnt/β-catenin asymmetry pathways play crucial roles in establishing asymmetry in the *C. elegans* mesoderm, targets of these pathways in the M lineage are still unknown. Thus further screening for factors that function in the M lineage is required.

There are 934 putative transcription factors in the *C. elegans* genome (Reece-Hoyes et al., 2005). In this chapter I describe my efforts to identify additional transcription factors that play a role in the M lineage. I constructed an RNAi feeding library targeting the majority of the genes encoding these transcription factors and performed a high-throughput RNAi screen. This screen revealed a role for transcription factors previously not reported to participate in proper M lineage development. Here I describe my further characterization of one gene, *let-381*, that encodes an essential forkhead transcription factor that is required for proper dorsal-ventral asymmetry in the M lineage. My results indicate that *let-381* acts downstream of or in parallel to the TGFβ and LIN-12/Notch signaling pathways in the M lineage to modulate dorsal-ventral asymmetry.

Materials and Methods

C. elegans strains

Strains were maintained and manipulated using standard conditions (Brenner, 1974). Analyses were performed at 20˚C, unless otherwise noted. The strain LW0683 *[rrf-3(pk1426); ayIs6(hlh-8::gfp); ayIs2(egl-15::gfp); ccIs4438 (intrinsic CC:::gfp)]* (Chapter 3, this dissertation) was used to visualized M lineage cells in RNAi experiments. LW1734 *[rrf-3(pk1426); ayIs6(hlh-8::gfp); ayIs2(egl-15::gfp); ccIs4438(intrinsic CC:::gfp); jjIs1475(myo-3::rfp)]* (Chapter 3, this dissertation) was also used to perform lineage analysis in *let-381(RNAi)* animals. The M lineage was followed in live animals under a fluorescence stereomicroscope and confirmed using a compound microscope. Other strains used in this work are:

LGI: *let-381(gk302)* (gift from Shohei Mitani, Tokyo Women's Medical College, Tokyo, Japan), *let-381(tm288)* (gift from Donald Moerman, C. elegans Reverse Genetics Core Facility, Vancouver, B.C., Canada)

LG II: *rrf-3(pk1426)* (Sijen et al., 2001)

LG III: *sma-3(jj3)* (Foehr et al., 2006), *lin-12(n941)* (Greenwald et al., 1983)

LG V: *him-5(e1467)* (Hodgkin et al., 1979)

The strain LW1569 *[rrf-3(pk1426); sma-3(jj3); ayIs6(hlh-8::gfp); ccI(secreted CC:::gfp); cup-5(ar465)]* was generated to perform *let-381* epistasis experiments.

Plasmid constructs and transgenic lines

The following constructs were used for RNAi experiments:

L4440: control RNAi vector (Timmons and Fire, 1998)

pNMA49 and pNMA50: RNAi constructs for *fozi-1* and *mab-5*, respectively (Chapter 3, this dissertation)

pNMA51: *hlh-1* cDNA cloned into L4440 vector from pVZ1200 (gift from Mike Krause, NIDDK, NIH, U.S.A.)

A fragment spanning the *let-381* promoter (-4971 to 0) and the entire coding region of *let-381* was PCR amplified from N2 genomic DNA using the iProof™ High-Fidelity DNA Polymerase (Bio-Rad). The PCR product was cloned into the vector pPD95.75 (kind gift of Andrew Fire) in frame with *gfp* to generate the following construct:

pNMA99, *let-381p::let-381::gfp::unc-54 3'UTR*

A full-length *let-381* cDNA, *yk679a12*, was obtained from Yuji Kohara (National Institute of Genetics, Japan). This cDNA was used to make the following constructs:

pNMA85, *hsp16p::let-381::let-381 3'UTR*

pNMA86, *hlh-8p::let-381::let-381 3'UTR*

pNMA70, GST-let-381 (amino acids 179-320)

All constructs were confirmed by sequencing. Details on all constructs are available upon request. Transgenic lines were generated using the plasmid pRF4 (Mello et al., 1991) as a marker.

RNAi library construction and screening

934 putative transcription factors were identified on the basis of putative DNA-binding elements by manual curation (Reece-Hoyes et al., 2005). RNAi clones targeting these genes were retrieved from commercially available feeding RNAi libraries and organized into 96-well plates. Clones were retrieved from two RNAi libraries, with preference given to clones from the C. elegans ORF-RNAi library v1.1 (Rual et al., 2004). In total, 630 clones were retrieved from this library, with some overlap of target genes for these clones. For genes not found in the ORF-RNAi library,

clones were retrieved from the *Caenhorbaditis elegans* RNAi feeding library provided by Gene Service Ltd, constructed by Julie Ahringer's group at The Wellcome CRC Institute, University of Cambridge, Cambridge, England (Kamath et al., 2003). Another 267 clones were retrieved from this library. 91 genes had no RNAi clones in either library. To test the accuracy of these clones, a random set of clones retrieved from each library was purified from bacteria and sequenced using primers specific to the L4440 RNAi vector (Timmons and Fire, 1998). 11.1% (n=81) and 12.82% (n=78) of clones tested from the ORF-RNAi library and Ahringer RNAi library, respectively, did not match their predicted sequence.

RNAi screening was performed as previously described (Kamath and Ahringer, 2003), with some minor changes. Briefly, bacteria was grown in LB with 12.5 μg/ml Tetracycline and 75 μg/ml Ampicillin for 12-14 hours at 37˚C with shaking and then seeded onto NGM agar plates (Brenner, 1974) with 25 mg/ml carbenicillin and 4 mM IPTG. dsRNA production was induced at room temperature overnight and these RNAi plates were used within one week of induction.

To observe the effects of RNAi during postembryonic development, we performed RNAi by ingestion using the strain LW0683 in a synchronous population of L1 larvae. L1 animals were synchronized by treating gravid adults with hypochlorite solution (20% Clorox, 5% 10N NaOH) and harvesting embryos in M9 buffer without food source. Larvae were permitted to hatch for at least 24 hours in M9 buffer and 100-200 synchronous L1s were then plated in duplicate on prepared RNAi plates for genes of interest. RNAi was performed at 25˚C and animals were scored for M lineage phenotypes or gene expression via immunostaining 24-48 hours after plating. For each round of screening, L4440 was used as a negative control and pNMA49 (*fozi-1*), pNMA50 (*mab-5*) and pNMA51 (*hlh-1*) were used as positive controls for M lineage phenotypes induced by RNAi. RNAi clones from the newly generated library that

caused M lineage phenotypes were verified via sequencing, re-transformed into HT115: W3110, *rnc14::ΔTn10* (Dasgupta et al., 1998) bacterial cells and re-tested for M lineage phenotypes.

Antibody Production and Immunostaining

Plasmid pNMA70 was used to generate GST-fusion proteins in BL21(DE3) cells for LET-381. GST-fusion proteins were bound to glutathione sepharose 4B beads (Amersham Biosciences) and cleaved from GST by GST-3CPro precision protease (Amersham Biosciences) and soluble LET-381 (amino acids 179-320) was further purified by SDS-PAGE. Gel slices containing purified LET-381 protein were used to immunize two rats R27 and R28 (Cocalico Biologicals, PA). Resulting antiserum was tested by Western blot analysis using bacterially expressed GST-LET-381 fusion proteins. Antibodies were affinity purified against GST-LET-381 bound to a nitrocellulose membrane (Olmsted, 1981;Smith and Fisher, 1984).

Animal fixation and immunostaining were performed following the protocol of Hurd and Kemphues (Hurd and Kemphues, 2003). The following antibodies were used: affinity-purified anti-FOZI-1 (Amin et al., 2007), affinity purified anti-LET-381 (1:30, R27 and R28) and goat anti-GFP (Rockland Immunochemicals; 1:5000). All secondary antibodies were from Jackson ImmunoResearch Laboratories and used in a dilution of 1:50 to 1:200. Differential interference contrast and epifluorescence microscopy were performed using a Leica DMRA2 compound microscope. Images were captured with a Hamamatsu Orca-ER Camera using the Openlab software (Improvision). Subsequent image analysis was performed using Adobe Photoshop 7.0 and Adobe Illustrator CS3.

Results

Identification of transcription factors involved in M lineage development

In an RNAi screen to identify transcription factors important for M lineage development (see Materials and Methods), 37 of the approximately 730 transcription factors screened displayed M lineage phenotypes when knocked down (Table 4.1). Among the 37 genes that displayed an M lineage phenotype when knocked down, seven were previously identified to play a role in the M lineage. These seven genes were *mls-1*, *hlh-1*, *fozi-1*, *mab-5, mls-2, lag-1* and *unc-62* (Harfe et al., 1998a; Liu and Fire, 2000; Kostas and Fire, 2002; Jiang et al., 2005; Amin et al., 2007; Foehr and Liu, 2008). The identification of these genes validated the efficacy of the RNAi screen. However, RNAi against the genes *sma-9* and *hlh-8*, two genes important for proper patterning of the M lineage (Corsi et al., 2000;Foehr et al., 2006), did not result in any M lineage phenotypes in the screen, suggesting that RNAi by feeding is not effective against all genes that function in the M lineage (data not shown). Among the remaining 30 genes, RNAi against most of them resulted in extra type I vulval muscles (observed by *egl-15::gfp*) while only 4 genes when knocked down affected earlier M lineage fates, namely the decisions of cells to become CCs and SMs (observed by using *intrinsic CC::gfp* and *hlh-8::gfp*). I have described my analysis of one of these four genes, *ceh-34*, in Chapter 3. In this chapter, I describe my characterization of another one of these genes, *let-381*, that when knocked down by RNAi results in highly reproducible M lineage phenotypes (Table 4.1).

let-381(RNAi) results in dorsal to ventral transformation in the M lineage

let-381 encodes an essential forkhead-domain containing transcription factor (Hope et al., 2003). RNAi by feeding bypassed the embryonic requirement for *let-381*,

Table 4.1. Transcription factors necessary for M lineage development

Gene name	Transcription factor type	M lineage phenotype	n	RNAi Penetrance
mls-1	Tbox	extra vm1s	135	28.15%
hlh-1	MyoD, bHLH	missing CCs, extra SMs	111	72.19%
fozi-1	C2H2 Zinc Finger	missing CCs, extra SMs	107	83.18%
mab-5	HOX, AbdB Class	missing CCs, extra SMs	97	64.95%
mls-2	HMX homeodomain	missing CCs, extra CCs	70	32.90%
lag-1	CSL	Extra vm1s	53	86.79%
unc-62	Meis, TALE homeodomain	No M lineage descendents present (CCs or SMs)	100	100%
ceh-34	Six2 homeodomain	No CCs, extra BWMs	107	82.20%
let-381	Forkhead	Missing CCs, extra SMs	125	95.20%
dct-13	CCCH tandem zinc finger	Extra vm1s	92	46.74%
nhr-179	Nuclear hormone receptor	Extra vm1s	54	5.88%
T04G9.1	AT Hook	Extra vm1s	58	9.43%
hmg-4	SSRP1 HMG Box	Missing SMs	56	91.07%
ztf-19	C2H2 zinc finger	Multiple patterning defects	81	27.20%
Y74C9A.4	GATA, MYB	Extra vm1s	41	41.50%
pha-4	Forkhead	Extra vm1s	39	30.8%
hlh-10	bHLH	Extra vm1s	42	61.9%

Table 4.1 (continued)

Gene name	Transcription factor type	M lineage phenotype	n	Penetrance
ceh-12	HLXB9 homeodomain	Extra vm1s	43	44.19%
unc-130	Forkhead	Extra vm1s	75	45.33%
syd-9	C2H2 zinc finger	Extra vm1s	18	55.60%
nhr-245	Nuclear hormone receptor	Extra vm1s	110	21.82%
ekl-4	MYB	Extra vm1s	55	12.80%
C08G9.2	C2H2 zinc finger	Extra vm1s	54	24.07%
nhr-140	Nuclear hormone receptor	Extra vm1s	91	5.50%
nhr-199	Nuclear hormone receptor	Extra vm1s	17	58.80%
W08E12.1	bZIP	Extra vm1s	16	87.50%
C07E3.6	Homedomain	Extra vm1s	62	24.19%
mxl-1	Max	Extra vm1s	103	27.18%
nhr-4	Nuclear hormone receptor	Extra vm1s	89	17.98%
ztf-22	C2H2 zinc finger	Extra vm1s	97	13.40%
hlh-27	bHLH	Extra vm1s	63	37.50%
nhr-91	Nuclear hormone receptor	Extra vm1s	65	46.15%
B0336.3	CCCH zinc finger	Extra vm1s	102	16.70%
B0336.7	C2CH zinc finger	Extra vm1s	83	90.36%
Y65B4Br.5	NAC, TS-N	Extra vm1s	101	85.14%
H20J04.3	MADF	Extra vm1s	108	26.90%
ZK686.4	C2H2 zinc finger	Extra vm1s	90	40.00%

and *let-381(RNAi)* animals survived to be viable adults. The majority of these animals lacked M lineage-derived CCs and had extra type I vulval muscles as shown in Figure 4.2 (as observed by intrinsic *CC::gfp* and *egl-15::gfp*, respectively) and Table 4.2. To determine the cause of this phenotype I followed the development of the M lineage in *let-381(RNAi)* animals using a combination of cell-type specific markers. Like wild-type animals, *let-381(RNAi)* animals exhibited normal cleavage orientations and proliferation in the early M lineage to give rise to 16 descendants, observed by expression of the *hlh-8p::gfp* reporter and αFOZI-1 immunostaining (Harfe et al., 1998b; Amin et al., 2007). In wild-type animals, two of these 16 cells, M.vrpa and M.vlpa, divide once more along the anterior-posterior axis and give rise to an SM and a BWM. Meanwhile, their dorsal counterparts, M.drpa and M.dlpa, differentiate into CCs. In *let-381 (RNAi)* animals, these two dorsal cells behaved like their ventral counterparts and divided an extra time and then gave rise to an SM (expressing *hlh-8::gfp*) and a BWM (expressing *myo-3::rfp*). These ectopic SMs behave like bona fide SMs in that they migrate to the presumptive vulva, proliferate and give rise to extra sex muscles as observed using *hlh-8::gfp* and *egl-15::gfp* (Figure 4.2A-D). Thus, *let-381* is required for proper dorsal-ventral asymmetry in the M lineage.

There are two deletion alleles available for *let-381*, *tm288* and *gk302* (see Materials and Methods, Figure 4.3A). Just as is the case with RNAi depletion during embryogenesis, *let-381(tm288 or gk302)* leads to embryonic lethality, with very few escapers that survive to become sterile adults (data not shown). I examined the M lineage phenotype of these escapers using *egl-15::gfp* and a *secreted CC::gfp* markers (see Materials and Methods) to identify vm1s and CCs, respectively. Sterile *let-381(tm288) or let-381(gk302)* animals had extra cells expressing *egl-15::gfp*, much like what was observed in *let-381(RNAi)* animals (Figure 4.2E). Interestingly, *let-381(tm288) or let-381(gk302)* animals carrying the *secreted CC::gfp* did not have any

Figure 4.2. *let-381* is required for dorsal-ventral asymmetry. All images are ventral/lateral views with anterior to the left. (A,B) Early M lineage in wild-type (A) and *let-381(RNAi)* (B) animals. Stages of the early M lineage (1-M to 18-M) are indicated in (A). (C,D) L4440 empty vector RNAi treated contol (C) and *let-381(RNAi)* (D) adults. CCs are visualized using *intrinsic CC::gfp*, with embryonic CCs labeled with arrowheads and M-derived CCs with arrows. Type I vulval muscles are visualized using *egl-15::gfp*, denoted by asterisks. (E) A let-381(gk302) adult with egl-15::gfp to label type I vms. M, M mesoblast; d, dorsal; v, ventral; l, left; r, right; a, anterior; p, posterior; CC, coelomocyte; BWM, body wall muscle; SM, sex myoblast.

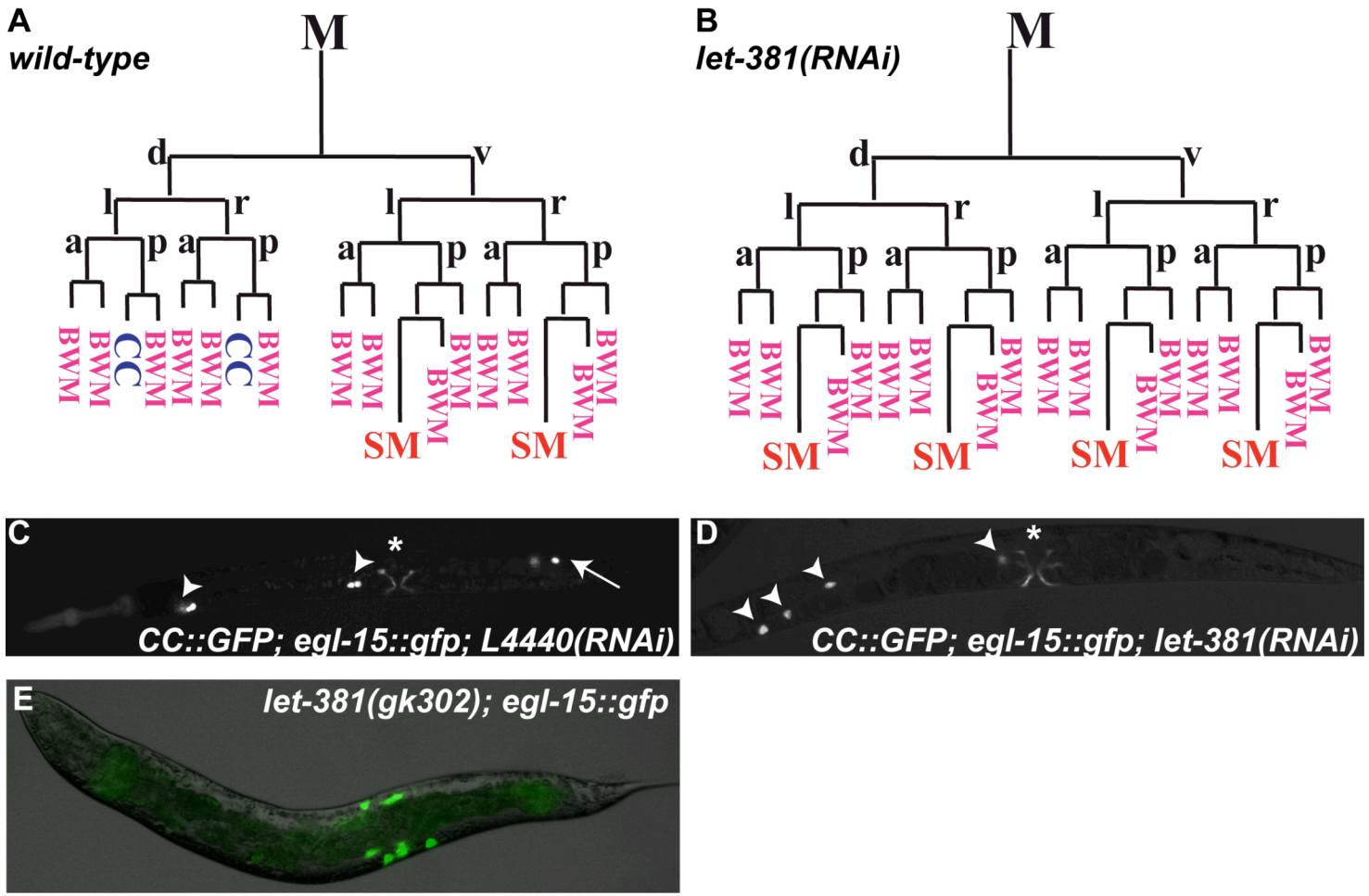
A
wild-type
M
d
v
l
r
a
p
BWM
CC
SM
B
let-381(RNAi)
C
CC::GFP; egl-15::gfp; L4440(RNAi)
D
CC::GFP; egl-15::gfp; let-381(RNAi)
E
let-381(gk302); egl-15::gfp

Figure 4.3. LET-381 is expressed in the dorsal M lineage precursors of CCs and BWMs. Images are lateral views with anterior to the left and dorsal up (unless otherwise noted). (A) Schematic representation of the *let-381* translational reporter. Regions deleted by gk302 and tm288 are shown relative to the *let-381* locus and are drawn to scale. αLET-381 antibodies were generated against antigens containing cDNA shown here (aa179-320). (B-G): Representative images of live animals expressing *let-381::gfp* at different developmental stages. (B) (C)(D)bean stage and (E) three-fold stage embryos. (F) A L1 larva and (G) adult head and (H) adult tail. (I-O) The left side of 2 L1 larvae double labeled with anti-LET-381 (I,M), anti-FOZI-1 antibody (J,N) and DAPI (L) at the 8-M (I-L) and 16-M stage (M-O). (K,O) Merged images of I and J and of M and N, respectively. (P-R) L1 larva double labeled with LET-381::GFP (P) and anti-FOZI-1 antibody (Q) at the 16-M stage. (R) A merged image of P and Q. (S) Summary of LET-381 expression in the M lineage, with LET-381-positive cells in green circles.

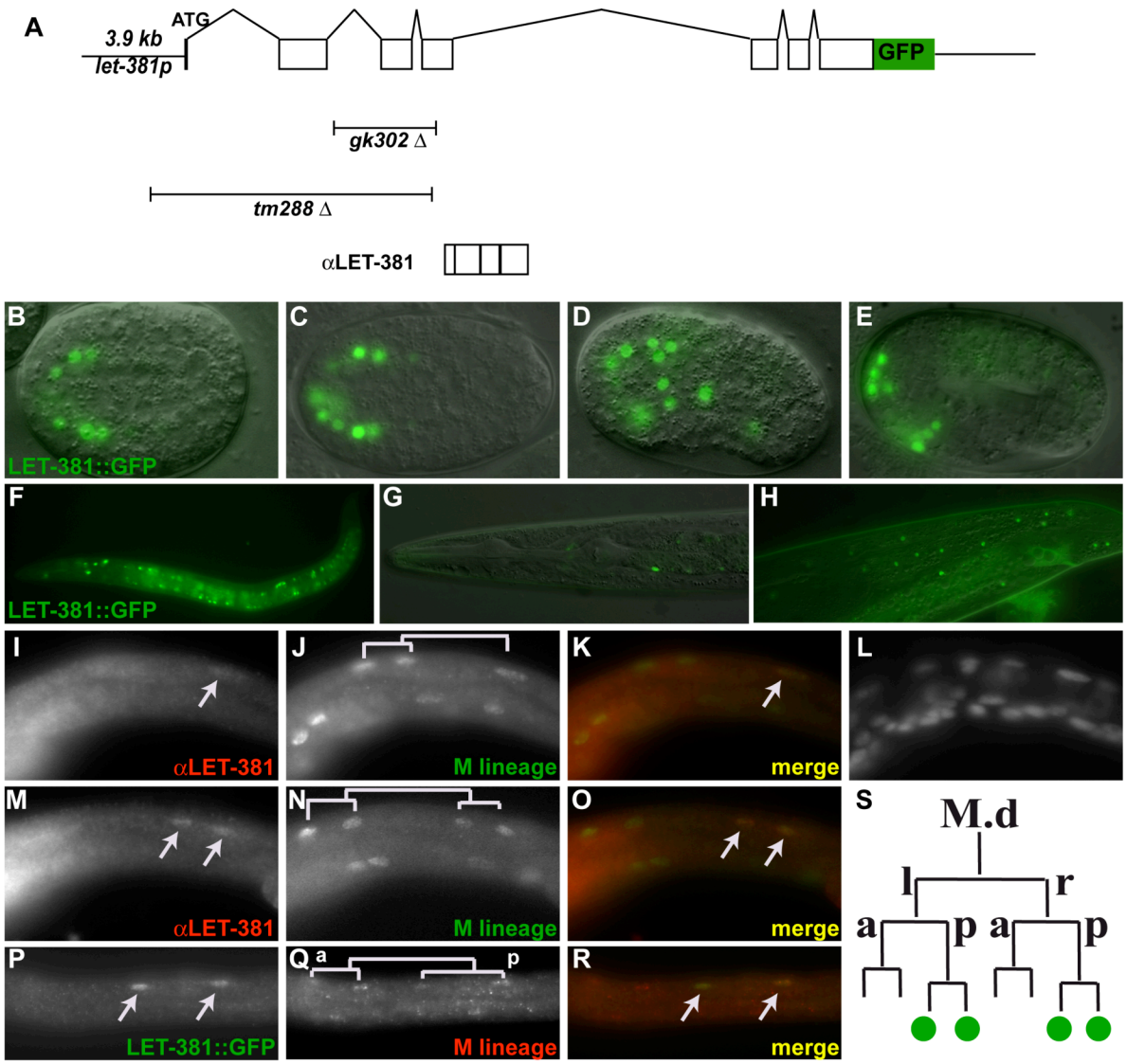
A
3.9 kb
let-381p
ATG
GFP
gk302 Δ
tm288 Δ
αLET-381
B
LET-381::GFP
C
D
E
F
LET-381::GFP
G
H
I
αLET-381
J
M lineage
K
merge
L
M
αLET-381
N
M lineage
O
merge
P
LET-381::GFP
Q a
p
M lineage
R
merge
S
M.d
l
r
a
p
a
p

distinguishable CCs. Instead this secreted GFP was spread throughout the entire animal, indicative of no functional CCs (data not shown). This indicates that *let-381* is not only required for specifying the M lineage-derived CCs, but also required for the specification or differentiation of the four embryonically-derived CCs.

LET-381 is expressed within the dorsal M lineage

To examine the expression pattern of *let-381* and its subcellular localization, I used two complementary approaches. First, I examined the localization of a translational *let-381::gfp* fusion (pNMA99, Figure 4.3A). This fusion was able to rescue the lethal phenotype of *tm288* mutants. It can also restore the embryonic and M-derived CCs (data not shown) as well as to restore the wild-type numbers of *egl-15::gfp* expressing vm1s in *tm288* mutants (data not shown). Thus, the *let-381::gfp* fusion is functional and the expression pattern likely reflects that of the endogenous LET-381 pattern. I also generated antibodies against a recombinant LET-381 protein (see Materials and Methods and Figure 4.3A) and performed immunostaining and observed a similar expression pattern to that of the *let-381::gfp* reporter. As predicted for a forkhead transcription factor, LET-381 was localized to the nucleus throughout development. Both *let-381::gfp* and αLET-381 immunostaining were detected in a small number of cells in wild-type animals during embryogenesis and throughout larval development (Figure 4.3B-H).

To determine the expression pattern of *let-381* in the M lineage, I performed double-labeling experiments using the *let-381::gfp* fusion or αLET-381 with αFOZI-1 immunofluorescence staining to label M lineage cells (Amin et al., 2007). LET-381 is transiently expressed in the M lineage and is first detected in M.dlp and M.drp as they begin to divide (Figure 4.3I-L). Expression continued in the daughters of these divisions (M.dlpa, M.dlpp, M.drpa and M.drpp) until the cells differentiate (Figure

4.3M-S). Thus LET-381 is expressed in the dorsal posterior of the M lineage within cells that give rise to two CCs and two BWMs (Figure 4.3S).

let-381 may function in parallel to or downstream of *sma-9*

let-381(RNAi) results in the same M lineage mutant phenotype to that of *sma-9(cc604)* loss of function animals (Foehr et al., 2006). The transformation of dorsal CC fates into ventral SM fates in *sma-9(cc604)* animals can be suppressed by mutations in the Sma/Mab TGFβ pathway (Foehr et al., 2006). I tested if mutations in this pathway could also suppress the *let-381(RNAi)* phenotype in the M lineage. *let-381(RNAi)* in a *sma-3(jj3)* mutant background resulted in the same M lineage phenotype as seen by *let-381(RNAi)* in a wild-type background (Table 4.2). These results indicate that the *sma-3(jj3)* mutation cannot suppress the *let-381(RNAi)* phenotype. Because of the relationship between SMA-9 and the Sma/Mab TGFß pathway, my results suggest that *let-381* functions either downstream of or in parallel to *sma-9* in regulating dorsal M lineage fates.

let-381 is epistatic to *lin-12*/Notch

The LIN-12/Notch signaling pathway functions in parallel to *sma-9* and the TGFβ pathway in establishing dorsal-ventral polarity in the M lineage (Foehr and Liu, 2008). Loss of function mutations in the Notch receptor, LIN-12, result in a duplication of dorsal CC fates and a loss of ventral SM fates (Greenwald et al., 1983). I performed *let-381(RNAi)* in a *lin-12(n941)* null mutant background to examine the relationship between *lin-12* and *let-381*. While *lin-12(n941)* fed on L4440 control RNAi bacteria (see Materials and Methods) have extra CCs (100%; n=89) and are missing the SM-derived vm1s (70.8%; n=89; as observed by *secreted CC::gfp* and *egl-15::gfp*, respectively), *lin-12(n941)*; *let-381(RNAi)* animals display a complete

Table 4.2. Results of epistasis analysis between *let-381(RNAi)* and mutants in Sma/Mab TGFβ and LIN-12/Notch pathways

Genotype	Number of M-derived CCs (*intrinsic CC:gfp*)	Number of vm1s (*egl-15::gfp*)
wild-type	**2** (100%) n>200	**2** (100%) n>200
let-381(RNAi)	**0** (93.1%); **2** (6.9%) n=144	**>4** (93.1%), **4** (6.9%) n=144
sma-3(jj3)	**0** (2.2%); **2** (97.8%) n>200	n.d.
sma-3(jj3); let-381(RNAi)	**0** (93.1%), **2** (6.9%) n=144	n.d.
lin-12(n941)	**4** (100 %) n=89	**0** (70.8%); **1-2** (29.2%) n=89
lin-12(n941) let-381(RNAi)	**0** (100%) n=113	**0** (10.72%); **>4** (89.38%) n=113

loss of M-derived CCs (100%; n=113) and have extra vm1s (89.38%; n=113; Table 4.2). Thus *let-381* is epistatic to *lin-12* and is required for the specification of ectopic ventral CC fates in a *lin-12(n941)* mutant.

Discussion

Identification of transcription factors required for proper mesodermal development

In this chapter, I describe a large-scale RNAi screen to identify transcription factors involved in proper development of the *C. elegans* postembryonic mesoderm, the M lineage. Seven of the nine transcription factors that were previously known to function in the M lineage were successfully identified in this screen. However, RNAi of *sma-9* and *hlh-8* did not result in M lineage phenotypes, suggesting that there might be false negatives in the RNAi screen. Despite this caveat, I have identified a number of transcription factors that are involved in M lineage development that have not been previously studied/identified. Further characterization of these transcription factors and their specific roles in the M lineage will help elucidate the mechanisms of proper patterning of the mesoderm in *C. elegans* and other metazoans.

When knocked down, all of the genes known to function in the M lineage, with the exception of *lag-1*, displayed similar phenotypes as previously described. Previous studies have shown that the CSL homolog LAG-1 functions as part of the Notch signaling pathway to regulate dorsal-ventral asymmetry (Foehr and Liu, 2008). In particular, knock-down of *lag-1* results in a low penetrance of extra M-derived CCs, most likely at the expense of the ventral SMs (Foehr and Liu, 2008). In this chapter, I have shown that knock-down of *lag-1* using RNAi by ingestion results in the proper number of SMs, but leads to improper numbers of a particular class of SM

descendants, the type I vulval muscles. An intriguing possibility is that in addition to the role of LIN-12/Notch signaling and its downstream target LAG-1 in establishing dorsal-ventral polarity in the early M lineage, these components may also play a role in proper specification of the sex muscles in the SM lineage. Future studies to examine the role of LIN-12/Notch signaling components in the SM lineage will be needed to elucidate the manner in which Notch signaling affects the specification of sex muscles. The results from this RNAi screen provide an excellent starting point to study this. Of the 30 RNAi clones targeting genes not previously identified to affect the M lineage in this screen, 26 display defects in patterning of the SM lineage. It will be interesting to see how many of these genes interact with components in the Notch signaling pathway in regulating sex muscle specification.

Another point of interest is the overall enrichment of factors affecting this later SM lineage, compared to only four genes affecting the specification of the early M lineage-derived BWM, CC and SM fates. I hypothesize that this reflects spatiotemporal issues associated with RNAi by feeding. Since the L1 larvae are fed with bacteria producing dsRNA, and the M lineage occurs in the posterior of the worm, there must be sufficient time allowed in which the worms can ingest the bacteria and pump it to the posterior in order for the dsRNA to induce RNAi in the M lineage. This hypothesis is supported by the observation that though *mab-5* is required for the expression of *hlh-8::gfp* in the M mesoblast and its early descendants, *mab-5(RNAi)* by ingestion does not abolish *hlh-8::gfp* expression in the M mesoblast or its early divisions (data not shown), but does affect CC fate specification at a high penetrance. A low penetrance of defects observed with *mls-2(RNAi)* and lack of SM to CC transformations in *lag-1(RNAi)* animals would also correlate with the late induction of RNAi in the M lineage by feeding. The SMs on the other hand migrate to the vulva, which is more anterior and divide later than the early M lineage. This

spatiotemporal difference may allow the more efficient knock down of targets in the SM lineage compared to the earlier M lineage.

A conserved forkhead domain protein regulates dorsal-ventral asymmetry in the M lineage

Forkhead transcription factors are well conserved and play multiple roles in metazoan development. In Drosophila and vertebrates, forkhead genes are expressed in and required for mesodermal patterning (Lee and Frasch, 2000; Topczewska et al., 2001a; Topczewska et al., 2001b; Zaffran et al., 2001; Yu et al., 2003; Rojas et al., 2005). In zebrafish, the Fast1 forkhead factor is required for dorsal axial mesoderm development (Sirotkin et al., 2000). A set of three Fox genes have been implicated in dorsal-ventral patterning in the Xenopus mesoderm (El-Hodiri et al., 2001). In the RNAi screen described in this chapter, I identified a role of an essential forkhead transcription factor, LET-381, in dorsal-ventral asymmetry in the *C. elegans* postembryonic mesoderm. Specifically, *let-381* is required for the specification of dorsal CC fates in the M lineage. Loss of *let-381* leads to a transformation of these fates to that of their ventral counterparts to give rise to an SM and a BWM. *let-381* is also asymmetrically expressed in the M lineage on the dorsal side. While the phenotype of *let-381* mimics loss of function mutants of *sma-9*, SMA-9 itself is not asymmetrically distributed in the M lineage, as it is found in dorsal and ventral descendants of the M mesoblast (Foehr et al., 2006). Additionally, while SMA-9 antagonizes Sma/Mab TGFβ components in the dorsal M lineage, LET-381 does not, as mutant alleles of core components of this signaling pathway cannot suppress the *let-381(RNAi)* phenotype. These data suggest that LET-381 may function downstream of or in parallel to SMA-9 in regulating dorsal fates, possibly as a cofactor for SMA-9. LET-381 also is required for the extra CC fates in the *lin-12(n941)* null mutant

background. Examining the expression pattern of LET-381 in *sma-9* and *lin-12* mutant backgrounds should help further resolve these relationships between *let-381* and the dorsal-ventral asymmetry pathway.

Because of the requirement of forkhead proteins for proper dorsal-ventral asymmetry in zebrafish and frogs, these studies suggest that the functions of these forkhead transcription factors in mesoderm development may be conserved in metazoan development. Future studies of LET-381 function may serve as a useful model to understand the role of these forkhead proteins in generating proper asymmetry in the mesoderm during animal development.

CHAPTER 5

CONCLUSIONS AND FUTURE PERSPECTIVES

In this dissertation, I have described my studies of a number of transcription factors and some downstream components of signaling pathways that are involved in the specification of different cell fates in the *C. elegans* postembryonic mesoderm, the M lineage. These studies uncovered the role of three transcription factors that function redundantly within the M lineage to specify striated body wall muscle (BWM) fates as well as factors that are involved in specifying nonmuscle coelomocyte (CC) fates. Questions remain concerning these processes and a number of future experiments will help address these questions

Myogenic cell fate specification

Myogenesis in vertebrates is dependent on the family of bHLH transcription factors known as the myogenic regulatory factors, or MRFs (Pownall et al., 2002). These factors are MyoD, Myf5, MRF4 and myogenin. Studies in mouse have shown that these factors are both necessary and sufficient to specify skeletal muscles. Moreover, they function redundantly, as MyoD and Myf5 single mutants still generate muscle, but double mutants lack all skeletal muscles. There is only one MyoD homolog in *C. elegans* (*hlh-1*) and Drosophila (*nautilus*), and MyoD is not absolutely required in these animals to specify striated muscles, as striated muscles are still present in null mutants for *hlh-1* and *nautilus* (Chen et al., 1992; Chen et al., 1994; Balagopalan et al., 2001; Wei et al., 2007). I have shown in this dissertation that two non-bHLH transcription factors, the Hox protein MAB-5 and the zinc-finger protein FOZI-1 function redundantly with HLH-1 to specify BWM fates. *mab-5(e1239)* and

fozi-1(cc609) null mutants and *hlh-1(cc561ts or RNAi)* animals have a transformation of 1-3 BWMs to sex myoblasts (SMs), while most BWMs are specified normally. In *hlh-1(cc561ts or RNAi); fozi-1(cc609)* or *hlh-1(cc561ts or RNAi); mab-5(e1239)* double mutant animals, most, if not all BWMs are transformed to SMs. *fozi-1(cc609) mab-5(RNAi)* does not result in a similar synergistic loss of BWM fates, suggesting these two factors function within the same process to regulate BWM fates. Together, these results suggest that *hlh-1* and *fozi-1*/*mab-5* function redundantly to specify BWM fates. But why in the double and triple mutant animals are some M-derived BWMs still present? I proposed a model in Chapter 2 in which a third myogenic pathway (factor Y) regulates BWM development in parallel to HLH-1 and FOZI-1/MAB-5 (Figure 2.8). A caveat to this hypothesis is that it is possible that there was residual HLH-1 function in the temperature sensitive mutant and RNAi and this led to leaky production of BWM fates in the M lineage. Analysis of *hlh-1(cc450)* null mutants with *fozi-1* or *mab-5* null alleles was not possible since null alleles of *hlh-1* are embryonic lethal and preclude the ability to examine postembryonic phenotypes. Mosaic analysis rescuing the embryonic lethality of the null mutant of *hlh-1*, doubled with a *fozi-1* null mutation could circumvent the requirement of *hlh-1* in the embryo. Analysis in rescued animals with no M lineage expression of *hlh-1* and *fozi-1* would resolve the issue of residual *hlh-1* activity in the temperature-sensitive and RNAi backgrounds.

In Chapter 4, I described an RNAi screen designed to search for additional factors that behave like *hlh-1*, *mab-5* and *fozi-1* when knocked down by RNAi. Since all myogenic factors identified to date are transcription factors, I focused on putative transcription factors. While this screen was successful in identifying factors required for proper M lineage development, no transcription factor when knocked down displayed an identical phenotype to that of mutants in these BWM specification genes.

Moreover, I also performed this screen in *hlh-1(cc561)* and *fozi-1(cc609)* single mutants as a sensitized background and did not find any additional factors that led to a synergistic loss of BWM fates when knocked down (data not shown). The failure to identify another factor involved in BWM fate specification may be due to two main reasons. First, due to the inaccuracy of some RNAi clones used in the library and the lack of RNAi clones available for some factors, only about 730 of the 934 putative transcription factors encoded by the *C. elegans* genome were screened (Chapter 4). Second, RNAi is not 100% effective in knocking down gene function and varies from gene to gene as observed in the M lineage. Since the RNAi screen did not encompass all transcription factors and the variance of RNAi effect, this screen did not effectively show if there is or is not a third myogenic factor Y. Additional RNAi screening or mutagenesis screens may aide in the potential search of this factor. An intriguing mutant isolated by Jun Liu is *cc616*, which results in the absence of CCs and the presence of extra BWMs. Further characterization of the mutant phenotype and identification of the corresponding wild-type gene for *cc616* will be needed in order to understand the function of this candidate factor Y.

The emerging theme from this study and other similar studies on invertebrate myogenesis has been the use of a number of transcription factors that function redundantly with the MyoD homolog. Meanwhile, the MyoD family of bHLH transcription factors is exclusively required and sufficient for striated muscle fate specification in vertebrates. The work I described in Chapter 2 of this dissertation, along with similar studies to determine the factors required for myogenesis during *C. elegans* embryonic development, identified unique sets of transcription factors that are required to specify muscles that appear to be anatomically the same. This adds another layer of complexity in which even simple organisms such as *C. elegans* have evolved multiple mechanisms to specify the same types of cells.

Non-myogenic fate specification from myogenic precursors

The mesoderm gives rise to both myogenic and non-myogenic cell fates. Recently, a paper was published in which brown fat cells arise from a lineage of cells that express the myogenic regulatory factor Myf5 (Seale et al., 2008). However, it remains unclear whether Myf5 is itself required for the brown fat cell fate. Similarly, in the *C. elegans* M lineage, two non-muscle CCs are derived from cells that express the MyoD homolog HLH-1. Moreover, *hlh-1* is required for the specification of the CC fate as mutations or RNAi of *hlh-1* lead to a transformation of these fates to SMs. Therefore, though MyoD is necessary and sufficient to generate striated muscle fates, it appears to at least be required for some non-muscle fates in *C. elegans* as well. The same two factors that function redundantly with *hlh-1* in BWM fate specification in the M lineage, *fozi-1* and *mab-5*, are also required for the CC fate. Unlike the story in BWM fate specification, all three of these genes are individually required for the CC fate. These studies suggest that HLH-1, FOZI-1 and MAB-5 all converge on specific gene(s) required for the CC fate. In Chapter 3, I described my characterization of the Six2 homeodomain protein CEH-34 and its putative cofactor EYA-1. These two proteins are both necessary and sufficient to induce CC fates in the M lineage. Moreover, the expression of *ceh-34* and *eya-1* is dependent on *hlh-1*, *fozi-1* and *mab-5*. *ceh-34* and *eya-1* function and/or expression was also found to be downstream of dorsal-ventral (TGFβ and Notch) and anterior-posterior (Wnt/β-catenin) patterning mechanisms. These results led to the model presented in Figure 3.12 in which a combination of the mesoderm intrinsic factors (HLH-1, MAB-5 and FOZI-1) and the dorsal-ventral and anterior-posterior signaling pathways control the expression of *ceh-34* and *eya-1* to control the CC fate. While these factors are involved in *ceh-34* and *eya-1* regulation, there is at least one other competence factor that is likely required to further regulate *ceh-34* and *eya-1* expression in the daughters of M.d(l/r)p but not

M.d(l/r)a. This factor X may be another factor that is required for the expression of *ceh-34* and *eya-1* in the daughters of M.d(l/r)p, but not M.d(l/r)a as shown in Figure 3.12. An alternative hypothesis would be that this competence factor functions to repress *ceh-34* and *eya-1* expression in the daughters of M.d(l/r)a, but not M.d(l/r)p, thereby giving the same spatial expression pattern of *ceh-34* and *eya-1*.

I also showed that when *ceh-34* and *eya-1* are forced to be expressed throughout the M lineage, there are ectopic CCs produced from the M lineage. Because the efficiency of this ectopic CC production was quite low, I was not able to determine if this was the result of over-proliferation in the M lineage or the direct result of cell fate transformations of SMs or BWMs to CCs. These results also showed that only 1-2 extra cells were able to be directed to the CC fate by *ceh-34* and *eya-1*, suggesting maybe these factors require the presence of factor X to act combinatorially to induce CC fates.

let-381 is an intriguing possibility because it is required for CC fates in the M lineage and expressed in the daughters of M.d(l/r)p, but not M.d(l/r)a. Future work should examine the role of LET-381 in regulating the expression of *ceh-34* and *eya-1*. *let-381* may also restrict the production of ectopic CCs to these cells. Forced expression of *let-381, ceh-34* and *eya-1* within the M lineage or ubiquitously in the worm may help elucidate this question. A major caveat to these experiments is the potential inefficiency of transgenic animals that harbor multiple transgenes to produce sufficient levels of each protein. An important control would be to monitor the expression of each of the transgenes by RT-PCR and/or antibody staining. Further isolation of mutants that affect CC fates in the M lineage or RNAi screens of a similar nature may help to identify other potential competence factors required for the CC fate.

Again, a common theme that has emerged from my work is that the specification of cell fates in the mesoderm is dependent on a number of inductive signaling events and combinatorial actions of transcription factors. With the exception of *fozi-1*, all of the genes I described in this section are conserved throughout metazoan development. In Chapter 1, I described a similar integration of signaling factors and mesoderm-intrinsic factors that pattern the Drosophila embryonic mesoderm to allow for the proper specification of its multiple cell types. My work suggests that many of these networks are at least partially conserved in all animal systems and the *C. elegans* M lineage will continue to serve as a useful model of mesodermal development.

Global identification of M lineage-specific factors

In the previous two sections I have described the potential of additional factors that may be required to specify either the BWM or CC fates. Methods I have suggested or attempted to find such factors include additional mutagenesis screens or large scale RNAi screens. Although these screens have proven quite useful in the lab in identification of many M lineage specific factors, they do have their shortcomings. Mutagenesis screens are powerful, but performing the screens and mapping of the genes is quite time- and labor-intensive. RNAi is relatively quicker but can be inefficient and vary from gene to gene. In both cases, functional redundancy can be problematic. These drawbacks suggest the potential need for another method to find M lineage specific factors. One way is to isolate total RNA from cells of the M lineage in wild-type animals and compare the global gene expression profile to that of the entire worm to see which genes are enriched in the M lineage. I have failed in my attempt to dissociate larval cells and specifically sort for GFP-positive M lineage cells (Appendix 2). Dissociation of larval cells for cell sorting has not been previously reported and is

technically very difficult due to the physical barrier provided by the thick larval cuticle.

Another approach in which to isolate total mRNA from specific cell types uses a FLAG-tagged polyA-binding (PAB-1) protein driven by tissue-specific promoters (Roy et al., 2002; Von Stetina et al., 2007). In this approach, PAB-1 is crosslinked to mRNAs and purified using α-FLAG antibodies. The crosslinks can be reversed and the RNA can be purified away from PAB-1. In the M lineage, the *hlh-8* promoter can be used to drive this FLAG-PAB-1 transgene throughout all the undifferentiated cells of the M lineage. The Liu lab has generated integrated lines that express this transgene in this manner and I have confirmed expression of the FLAG-tagged protein by Western blot analysis. Future work will involve fine tuning the FLAG immunoprecipitation protocol and confirming the presence of M lineage specific transcripts by RT-PCR. Once this is done, microarray analysis comparing M lineage specific RNA to total worm RNA will indicate which genes are specifically enriched within the M lineage. Once this technique is up and running, additional uses for it will be to identify downstream targets of genes that are known to function in the M lineage, such as the mesoderm intrinsic factors *fozi-1*, *hlh-1* and *mab-5*. These types of experiments will help elucidate if these three genes in general share the same or different downstream targets in regulating BWM or CC fates. In the long run, identification of additional genes functioning in the M lineage will expedite our discovery and understanding of genes and gene networks that function in vertebrate mesoderm development.

Identification of direct transcriptional regulators in the M lineage

In this dissertation, I have described experiments that focused mostly on identifying genetic networks involved in specification of CC and BWM fates. These

genetic studies have helped in the understanding of how genes like *fozi-1*, *mab-5*, *hlh-1*, *let-381*, *ceh-34* and *eya-1* function relative to one another and which genes are required for the expression of each. In general, these studies fail to show direct transcriptional regulation of any of these genes or their targets. For example, in the model presented in Figure 3.12, is the expression of *ceh-34* and *eya-1* directly regulated by FOZI-1, HLH-1, MAB-5, Factor X and the repressor? Or are there other intermediate genes that function to mediate this regulation? I think that future work in dissecting these mechanisms will be important to fully understand how mesoderm development in *C. elegans* is regulated. In vitro gel-shift experiments and mutagenesis of predicted protein binding sites on transgenic reporters are often very useful in determining if transcriptional regulation is direct or not. Yeast one-hybrid assays are also commonly used to determine direct binding of a protein to a DNA element, but often lead to false positive results. Chromatin immunoprecipitation assays are also often used to identify protein-DNA interactions in vivo, but use of these assays for M lineage specific factors is likely not feasible due to the low percentage of cells expressing the protein of interest. Therefore, I think that a combination of promoter bashing and mutational analysis of M lineage specific genes like *ceh-34*, *eya-1* and *let-381* as well as comparative analysis of promoters from related genes in closely related *C. elegans* species will be required to narrow down potential transcription factor binding sites. This can be followed by a combination of yeast one-hybrid assays and gel-shift experiments to determine if particular proteins can indeed directly bind these elements in vitro.

In summary, I have identified a number of regulatory interactions of genes involved in mesoderm specification in *C. elegans*. Future studies in this project will be aimed at identifying additional genetic interactions and biochemical interactions of

transcription factors and their target binding sites and genes, providing ideas as to how these interactions may affect vertebrate development as well.

APPENDIX 1[4]

MAPPING TWO SUPPRESSORS OF *sma-9(cc604)*: *jj1* AND *jj3*

Schnurri (Shn) is a multiple zinc finger protein that in Drosophila has been shown to function downstream of the *decapentaplegic (dpp)* signal and its receptor in *dpp* signaling (Arora et al., 1995; Grieder et al., 1995; Dai et al., 2000; Marty et al., 2000; Udagawa et al., 2000). Homologs of Schnurri have since been identified in Xenopus and mouse and appear to have a conserved role in mediating the TGFβ signaling pathway (Yao et al., 2006). Schnurri homologues in mammals appear to play a role in many cell types. For example, Schnurri-2 plays a role in adipogenesis, while Schnurri-3 regulates bone mass and osteoblast function (Jin et al., 2006; Jones et al., 2006; Jones et al., 2007). Therefore, it is important to study the role of Schnurri proteins to further understand their various and distinct cell-type specific functions.

In *C. elegans* there is one Schnurri homolog, *sma-9*. Mutations in the *sma-9* locus result in a small body size, similar to that of mutants in the Sma/Mab TGFβ pathway (Liang et al., 2003). *sma-9* also plays a role in the postembryonic mesoderm, the M lineage. Early during M lineage development, the dorsal M lineage gives rise to six bodywall muscles (BWMs) and two non-muscle coelomocytes (CCs). On the ventral side, there are eight BWMs and two sex myoblasts (SMs). *sma-9* loss-of-function results in a loss of the dorsal M lineage and a duplication of the ventral M lineage, in which there are no CCs, two SMs and 16 BWMs (Foehr et al., 2006). These phenotypes in *C. elegans* provide an avenue in which to study the function of the

[4] This work is summarized in the published work in Development (Foehr M.F., Lindy A.S., Fairbank R.C., Amin N.M., Xu M., Yanowitz J., Fire A.Z. and Liu J., 2006. Development 133: 2887-2896).

Schnurri homolog *sma-9* and a model in which to identify other factors that may interact with Schnurri in different cell types.

To identify genes that interact with *sma-9*, a suppressor screen was carried out by Rachel Fairbank and Jun Liu in which seven potential suppressor alleles were isolated that suppressed the *sma-9* mutant phenotype of missing CCs. This appendix describes my initial characterization of four of these suppressors. Two of these suppressors were single locus mutations that mapped to autosomal positions. To identify the genes affected by these two mutations, I performed snip-SNP mapping. Here I describe my efforts to narrow down the genetic positions of these two suppressors.

Materials and Methods

C. elegans strains

Strains were maintained and manipulated using standard conditions (Brenner, 1974). All analyses were performed at 20˚C. A suppressor screen was carried out by Rachel Fairbank and Jun Liu in *sma-9(cc604); cup-5(ar465); arIs39(secreted CC::gfp)* X animals. *Secreted CC::gfp* is a coelomocyte marker using a *myo-3::secreted GFP* construct (Harfe et al., 1998a). Seven independent suppressor mutations were isolated.

LG X: *sma-9(cc604)* (Foehr et al., 2006)

LG III: *cup-5(ar465)* (Fares and Greenwald, 2001)

LG V: *him-5(e1467)* (Hodgkin et al., 1979)

sma-9(cc604) was crossed into the CB4856 strain (Hodgkin and Doniach, 1997) and out-crossed 9 times to generate an isogenic background of *sma-9(cc604)* that was used for snip-SNP mapping.

snip-SNP mapping

Mapping of *jj1* was performed via snip-SNP mapping as previously described (Wicks et al., 2001). The following primers were used to PCR amplify fragments containing SNPs (single nucleotide polymorphisms) that exist between the reference N2 strain and the CB4856 Hawaiian strain:

NMA-41 5'-AAAATGCGCTTCTCACCAG-3'

NMA-42 3'-TAGCAAACTTCTGATCCAAGC-3'

JKL-491 5'-GTTGTCCCAATCCTCATCATTG-3'

JKL-492 3'-TGAATTTCGAGAATGGAGTACG-3'

NMA-68 5'-TAGGAAAGTTGTGTCCACCTGG-3'

NMA-69 5'-TGATGACTCCTTCTTCAGCTGC-3'

JKL-503 5'-GGTTTTTGGGGTTACGGTAGTC-3'

JKL-504 3'-TCCCAGTTACTGTAGCTCCATG-3'

NMA-41 and NMA-42 were used to amplify a fragment surrounding a SNP on chromosome II at position -14.1595 and digestion with HinfI results in an extra restriction fragment in CB4856 DNA. JKL-491 and JKL-492 were used to amplify a fragment surrounding a SNP on chromosome II at position +0.7867 and digestion with DraI results in an extra restriction fragment in CB4856 DNA. NMA-68 and NMA-69 were used to amplify a fragment surrounding a SNP on chromosome II at position -13.8247 and digestion with HinfI results in an extra restriction fragment in CB4856 DNA. JKL-503 and JKL-504 were used to amplify a fragment surrounding a SNP on chromosome IV at position -0.91 and digestion with ApoI results in an extra restriction fragment in CB4856 DNA.

Results

jji and *jj3* suppressor mutations are not on X chromosome

sma-9 is located on the X chromosome and therefore potential suppressors that mapped to the X chromosome may affect the *sma-9* locus to suppress its phenotype. To determine if the suppressor alleles of the *sma-9(cc604)* M lineage mutant phenotype mapped to the X chromosome I used the cross scheme shown in Figure A1.1. Briefly, I crossed *him-5* males that were wild-type for *sma-9* and the suppressor locus. I allowed the cross-progeny that were now heterozygous for *sma-9* and its suppressor to self-fertilize and scored the following generation. If the suppressor was not linked to *sma-9* and the X chromosome, there would be independent segregation of the suppressor mutation and the *sma-9(cc604)* allele. However, if they were linked these mutations would segregate together and most animals would appear wild-type (2 M-derived CCs; Figure A1.1). Since these mutations do not suppress the *sma-9(cc604)* at 100% penetrance, a small percentage of animals would display a missing CC phenotype. I performed this analysis with four of the seven suppressor alleles of *sma-9*, *jj1, jj2, jj3 and jj5.* Of the four alleles, *jj1* and *jj3* appeared to be single site mutations that mapped to an autosome. Meanwhile, the mapping data for *jj2* and *jj5* is more ambiguous and it seems these mutations may map to more than one locus. The data of this analysis are summarized in Table A1.1.

jj3 maps to chromosome III

To further map *jj1* and *jj3* to their chromosomal locations, I used linkage mapping using the physical marker *cup-5* as well as snip-SNP mapping (see next section). I took advantage of the *cup-5* mutation, *ar465*, which is a recessive mutation

Figure A1.1. Mapping scheme to determine autosome- or X-linkage. *sma-9(cc604)* mutant animals with a suppressor mutation *sup(jj1-7)* were crossed to wild-type males. Heterozygous progeny were allowed to self-fertilize and scored for linkage of suppressor mutation to *sma-9(cc604)* and the X chromosome. Predicted M lineage phenotype frequencies are shown if suppressor is X-linked or if it assorts independently of *sma-9(cc604)*.

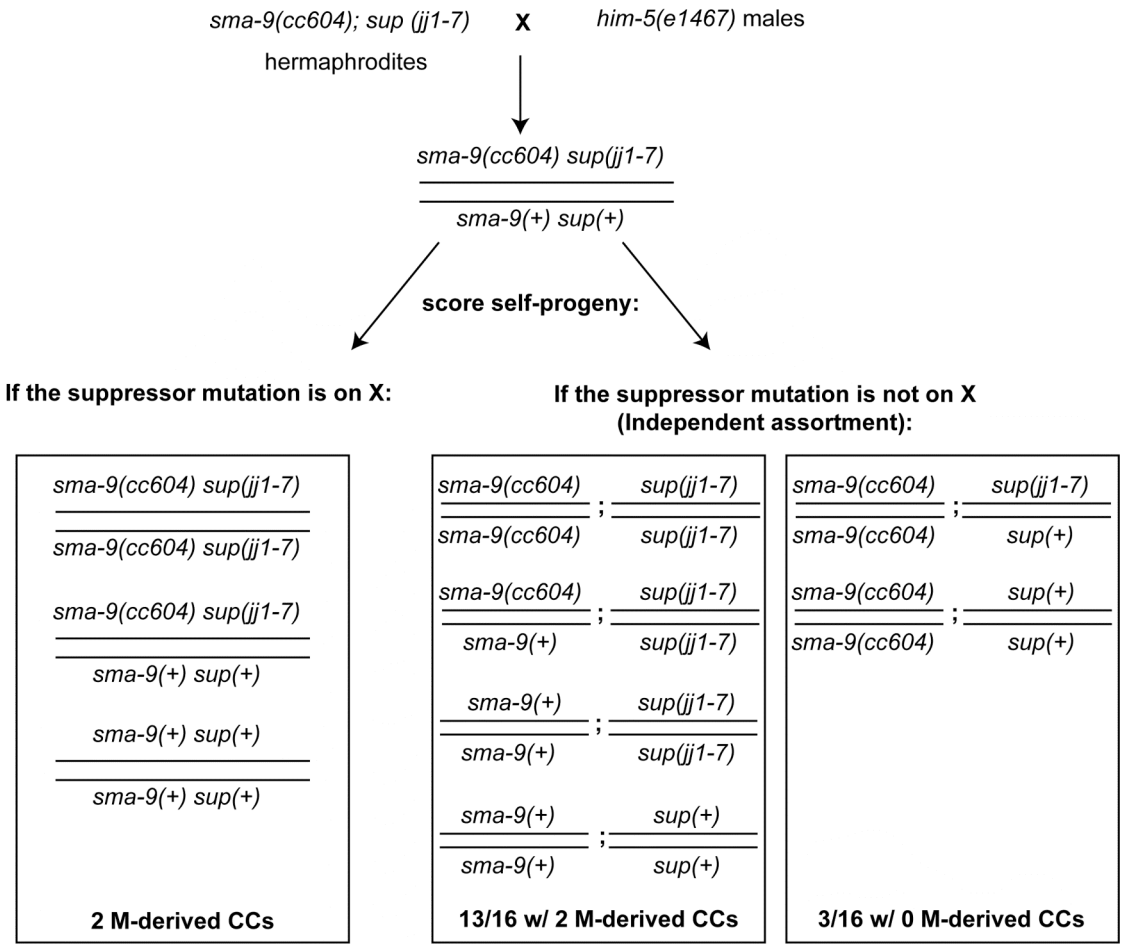
sma-9(cc604); sup (jj1-7) hermaphrodites
X
him-5(e1467) males
sma-9(cc604) sup(jj1-7)
sma-9(+) sup(+)
score self-progeny:
If the suppressor mutation is on X:
If the suppressor mutation is not on X (Independent assortment):
sma-9(cc604) sup(jj1-7) / sma-9(cc604) sup(jj1-7)
sma-9(cc604) sup(jj1-7) / sma-9(+) sup(+)
sma-9(+) sup(+) / sma-9(+) sup(+)
2 M-derived CCs
sma-9(cc604) ; sup(jj1-7) / sma-9(cc604) ; sup(jj1-7)
sma-9(cc604) ; sup(jj1-7) / sma-9(+) ; sup(jj1-7)
sma-9(+) ; sup(jj1-7) / sma-9(+) ; sup(jj1-7)
sma-9(+) ; sup(+) / sma-9(+) ; sup(+)
13/16 w/ 2 M-derived CCs
sma-9(cc604) ; sup(jj1-7) / sma-9(cc604) ; sup(+)
sma-9(cc604) ; sup(+) / sma-9(cc604) ; sup(+)
3/16 w/ 0 M-derived CCs

Table A1.1. *jj1* and *jj3* map to autosomal positions.

Suppressor	Penetrance	F2s observed		F2s expected if on X	F2s expected if not on X
		n	**4 CC (%)**	**4 CC (%)***	**4 CC (%)***
jj1	85%	137	18.98	3.75	19.69
jj2	95%	398	9.30	1.25	19.06
jj3	91%	343	23.03	2.25	19.31
jj5	82%	186	36.56	4.50	19.88

***** Expected frequencies account for penetrance of *cc604* suppression

on chromosome III that allows for more of the *myo3::secreted GFP* to be absorbed by the CCs (Fares and Greenwald, 2001). In this cross scheme, I crossed the suppressor strains harboring *jj1* or *jj3* in the *sma-9(cc604); cup-5(ar465)* mutant background to males from the CB*sma-9(cc604)* strain that have a wild-type allele of *cup-5* and the second-site suppressor. The resulting cross progeny were then allowed to self and the next generation was scored for animals homozygous for the suppressor mutation (2 M-derived CCs). If the suppressor mutation was linked to *cup-5(ar465)*, all animals would display bright CCs, while independent assortment of the two loci would result in which only one-quarter of the homozygotes for the suppressor mutation would also have bright CCs. This cross scheme is summarized in Figure A1.2.

I scored animals in the F2 generation of this cross for both *jj1* and *jj3*. For *jj1*, 26 of 34 animals that were homozygous for *jj1* displayed faint CCs and were therefore considered not to be homozygous for *cup-5*. In the case of *jj3*, 34 of 34 animals homozygous for *jj3* displayed bright CCs and were therefore homozygous for *cup-5*. Thus *jj1* does not map to chromosome III while *jj3* does map to III.

_jj3_ does not appear to have an M lineage phenotype

To determine if *jj3* itself had an M lineage phenotype, I attempted to outcross the *jj3* mutation from the *sma-9(cc604)* mutant background. I used *cup-5(ar465)* to follow the *jj3* mutation as I crossed *sma-9(cc604); cup-5(ar465) jj3* to *him-5* males that are homozygous for these three loci. I then allowed the heterozygous cross progeny to self-fertilize and I scored any animals with bright CC::GFP for an M lineage phenotype. I observed over 200 worms that were homozygous for *cup-5(ar465)* and found no M lineage phenotype. Since these animals are very likely to be homozygous for *jj3* and have a one-fourth chance to carry two mutant *sma-9* alleles, it appears to be unlikely that *jj3* has an M lineage phenotype on its own. Because *sma-*

Figure A1.2. Mapping scheme to determine chromosome location and position. *sma-9(cc604); cup-5(ar465); sup(jj1-7)* in an N2 Bristol background (blue bars) were crossed to *sma-9(cc604)* mutants in the CB4856 Hawaiian reference strain (orange bars). Linkage of suppression to the *cup-5(ar465)* mutation was scored using brightness of *secreted CC::gfp* as a marker for *cup-5(ar465)* and 2 M-derived CCs as a marker for the *sup(jj1-7)* phenotype. Further mapping of recombination was performed using SNP markers to distinguish between the N2 (blue) and CB4856 (orange) chromosome.

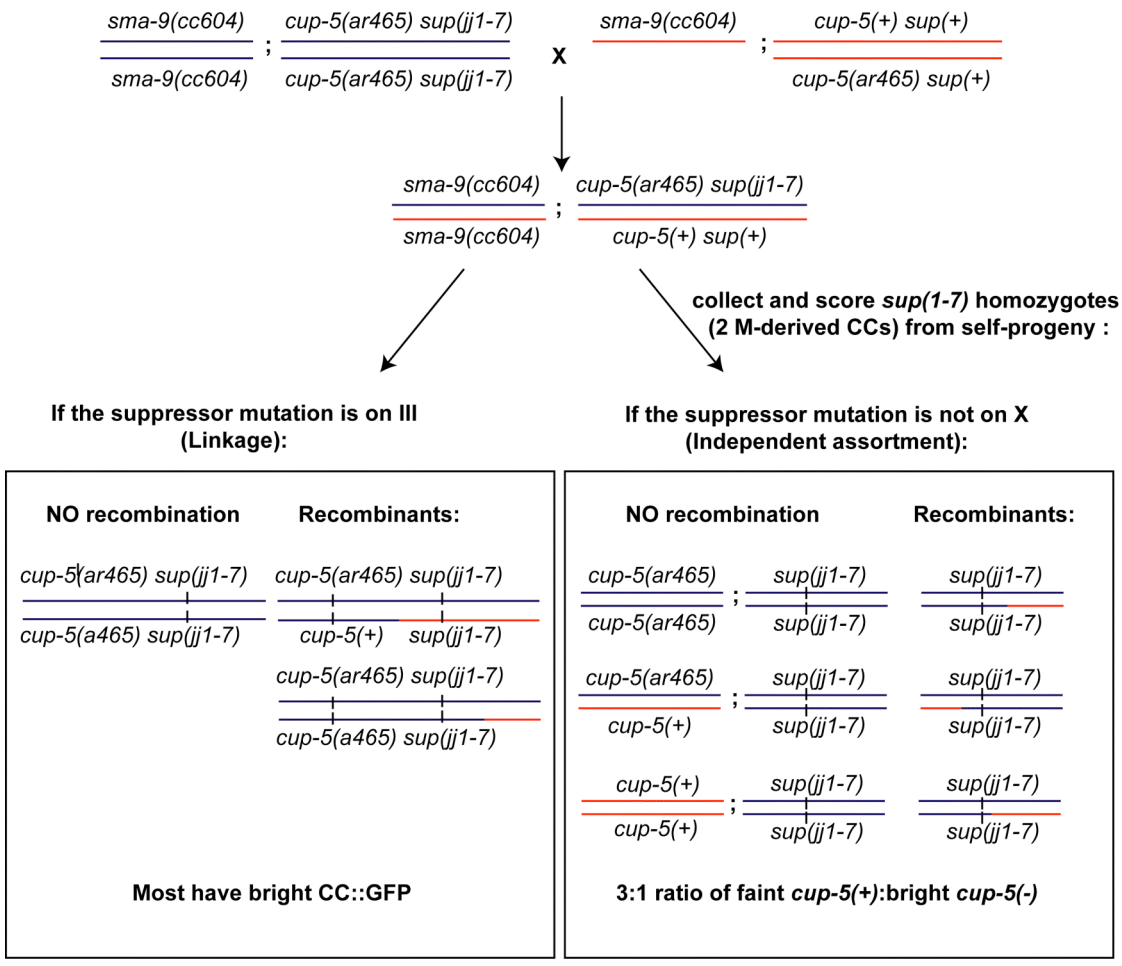
sma-9(cc604) ; cup-5(ar465) sup(jj1-7)
sma-9(cc604) cup-5(ar465) sup(jj1-7)
X
sma-9(cc604) ; cup-5(+) sup(+)
cup-5(ar465) sup(+)
sma-9(cc604) ; cup-5(ar465) sup(jj1-7)
sma-9(cc604) cup-5(+) sup(+)
collect and score sup(1-7) homozygotes
(2 M-derived CCs) from self-progeny :
If the suppressor mutation is on III
(Linkage):
If the suppressor mutation is not on X
(Independent assortment):
NO recombination
Recombinants:
cup-5(ar465) sup(jj1-7)
cup-5(a465) sup(jj1-7)
cup-5(ar465) sup(jj1-7)
cup-5(+) sup(jj1-7)
cup-5(ar465) sup(jj1-7)
cup-5(a465) sup(jj1-7)
Most have bright CC::GFP
NO recombination
Recombinants:
cup-5(ar465) ; sup(jj1-7)
cup-5(ar465) sup(jj1-7)
sup(jj1-7)
sup(jj1-7)
cup-5(ar465) ; sup(jj1-7)
cup-5(+) sup(jj1-7)
sup(jj1-7)
sup(jj1-7)
cup-5(+) ; sup(jj1-7)
cup-5(+) sup(jj1-7)
sup(jj1-7)
sup(jj1-7)
3:1 ratio of faint cup-5(+):bright cup-5(-)

9(cc604) results in a small body size, I attempted to isolate *jj3* animals from these animals based on a wild-type body size. Interestingly, I was unable to detect any *cup-5(ar465)* animals that had a wild-type body size, suggesting that *jj3* may somehow play a role in body size as well as in suppressing the M lineage phenotype of *sma-9(cc604)*.

jj1 maps to chromosome II

To map *jj1* to a chromosome, I performed linkage analysis with the homozygous F2 *jj1* progeny obtained in the cross scheme outlined in Figure A1.2. The suppressor mutation was isolated in the Bristol reference strain N2, while the CB*sma-9(cc604)* males were in the Hawaiian background strain CB4856. To determine which chromosome of the N2 background *jj1* was linked to, I used snip-SNP mapping to examine which SNP from the Hawaiian background were excluded in the majority of the *jj1* progeny (Hodgkin and Doniach, 1997; Wicks et al., 2001). I tested the SNP marker at map position +0.78 on chromosome II and found that none of the 32 *jj1* homozygotes tested had an allele of the Hawaiian SNP at this position. Thus *jj1* maps to chromosome II and is close to the center of the chromosome. This was further supported by testing SNP markers on the center of chromosome IV for exclusion of CB4856-specific SNPs. 25 of 32 *jj1* homozygous animals tested positive for a CB4856-specific SNP at +3.6811 on IV. Additional SNP testing on the ends of chromosome II identified 7 animals of 32 *jj1* homozygotes that had a CB4856-specific SNP at +13.82 and 4 of 32 that had a CB4856-specific SNP at -14.15 of chromosome II. These animals likely represent recombination between the N2 and CB4856 DNA away from the *jj1* locus. Thus *jj1* maps to chromosome II between map positions -14.15 and +13.82.

Discussion

jj1 and *jj3* represent two single-locus *sma-9* suppressors

sma-9 encodes a large multiple zinc finger protein that is homologous to the Schnurri family of proteins. Mutations in *sma-9* result in a small body size and a loss of dorsal M-derived coelomocyte (CC) fates (Liang et al., 2003; Foehr et al., 2006). Schnurri plays a role downstream of the TGFβ ligand/receptor interaction pathway in Drosophila and vertebrate development (Arora et al., 1995; Grieder et al., 1995; Dai et al., 2000; Marty et al., 2000; Udagawa et al., 2000; Yao et al., 2006). In a screen to identify factors that genetically interact with *sma-9*, seven independent suppressors of the *sma-9(cc604)* M lineage mutant phenotype were isolated by Rachel Fairbank and Jun Liu (Foehr et al., 2006). I further characterized four of these suppressor mutations and found that two of them, *jj1* and *jj3*, each mapped to a single autosomal locus. Additionally, *jj3*, when outcrossed from the *sma-9(cc604)* mutant background, does not appear to have an M lineage mutant phenotype on its own. Interestingly, *jj3* mutations may also result in a small body size. Because of the role of *sma-9* and TGFβ signaling in body size regulation in *C. elegans* and Schnurri homologues in modulating TGFβ signaling, an intriguing set of candidates for *jj1* and *jj3* are core members of the Sma/Mab TGFβ signaling pathway in *C. elegans*. The two regulatory Smads, *sma-2* and *sma-3*, along with the co-mediator Smad, *sma-4*, are members of this pathway and map to chromosome III. Meanwhile, the type II receptor for this pathway, *sma-6*, maps to chromosome II. This project was further pursued by Marisa Foehr and Amanda Lindy, who found that *jj3* and *jj1* are mutations in *sma-3* and *sma-6*, respectively (Foehr et al., 2006). Additional analysis determined that mutations in all members of the core Sma/Mab TGFβ pathway, including the ligand DBL-1, the receptors SMA-6 and DAF-4, the regulatory Smads SMA-2 and SMA-3 and the co-

regulatory Smad SMAD-4 can suppress the *sma-9(cc604)* M lineage phenotype, while retaining a small body size (Foehr et al., 2006). This was an unexpected result, as mutations in each of these components in an otherwise wild-type background do not result in any M lineage phenotype (Foehr et al., 2006). These results suggest two modes of SMA-9/Schnurri function in *C. elegans* development. First, SMA-9 functions together with the core Sma/Mab pathway in regulating body size and second, SMA-9 antagonizes the role of the same pathway in the M lineage. Clearly there are well-defined roles of SMA-9 depending on the cellular context. It will be interesting to see what defines these roles in the two developmental stages. One possible method in which *sma-9* can modulate these two different roles is via alternative splicing to produce distinct isoforms of SMA-9/Schnurri that may function in either body size or M lineage development. Alternatively, other factors may exist that interact with SMA-9 to modify its function in either body size or the M lineage. Further characterization of the remaining *sma-9(cc604)* suppressors may help address these possibilities.

jj2 and jj5 are not single locus suppressors of *sma-9(cc604)*

In addition to *jj1* and *jj3*, *jj2* and *jj5* very efficiently suppress the *sma-9* mutant phenotype (Table A1.1). However, based on the preliminary evidence provided in this appendix, mapping of *jj2* and *jj5* may prove to be difficult. It does not appear that either of these two suppressors map to a single locus nor is it clear whether they map to the X chromosome or to an autosome. Future work may involve attempting to identify the mutations associated with these two suppressors. With the successful recovery of informative suppressor mutations (*jj1* and *jj3*), continued screening for factors interacting with *sma-9* via suppressor studies may also prove to be useful in understanding the modulation of SMA-9 function.

APPENDIX 2

ISOLATION OF THE M MESOBLAST USING FLUORESCENCE ACTIVATED CELL SORTING

Introduction

The mesodermal germ layer gives rise to multiple cell types during metazoan development. It arises in the embryo as a multipotent pool of progenitors that in mammals can give rise to cells that comprise muscle, bone, blood and notochord, among other tissues. The diversification of this germ layer must therefore require a dynamic transcriptional profile to ensure the proper differentiation of these tissues. Over the years, work in model organisms such as *C. elegans*, Drosophila, Xenopus, zebrafish and mouse has resulted in a better understanding of important factors involved in mesodermal development. Factors such as the transcription factor Twist have been identified to play a role in establishment and maintenance of mesoderm in many model organisms, while more specialized factors collectively known as myogenic regulatory factors, the MyoD family, are required to specify muscle fates. Many of the studies that have identified these factors are the results of forward genetic screens to identify individual factors required for the specification of various cell types. With the recent advent of microarray technology to study global gene expression changes in mutants of cell-type specific factors, there is a potential to identify many more of the genes important in mesodermal development.

Many transcription factors are expressed in multiple cell types and have cell-type specific activities. For example, in *C. elegans* development, the zinc finger protein FOZI-1 is expressed in mesodermal and neuronal precursor cells and is

required for the specification of their derivatives (Johnston et al., 2006; Amin et al., 2007). To perform its function in these cells, FOZI-1 likely regulates different downstream targets. Because very few cells in *C. elegans* express FOZI-1 (Amin et al., 2007), microarray analysis with mRNA isolated from whole animals that are either wild-type or mutant for *fozi-1* would likely not reveal major differences in expression of FOZI-1 targets nor would it distinguish between its roles in different cell types. I am specifically interested in identification of targets of FOZI-1 and the MyoD homolog, HLH-1, in the postembryonic mesoderm, the M lineage, to specify striated body wall muscle (BWM) and non-muscle coelomocyte (CC) cell fates.

One way to enrich for FOZI-1 expressing cells is to drive expression of *fozi-1* under the control of an inducible promoter such as the heat shock promoter. By inducing this promoter at higher temperatures, expression of *fozi-1* can be forced throughout the animal and downstream targets would in time be activated in all larval cells. The major caveat to this approach is that FOZI-1 expression would be forced in cells that do not normally express it. If FOZI-1 is dependent on the cellular context for its function, gene expression profiling would not accurately depict the endogenous targets of FOZI-1 in specific cell types, but perhaps only general targets. To study the function of FOZI-1 in specific cell types like the mesoderm, it is therefore preferable to isolate mRNA only from these mesodermal cells that express FOZI-1.

An alternative approach is to isolate mRNA specifically from the cells of interest. Recently in *C. elegans*, researchers have been able to dissociate embryonic cells and use fluroscence activated cell sorting (FACS) to isolate cells expressing a cell-type specific GFP reporter (Christensen et al., 2002; Fox et al., 2005; Strange et al., 2007). In this appendix, I describe my attempts to isolate M lineage cells using FACS for further global gene expression analysis.

Materials and Methods

C. elegans strains

In this study, the strain PD4667 which has an integrated *hlh-8::gfp (46T)* transgene, was used for all the analyses described. Worms were cultured on 100 mm NGM plates seeded with NA22 *Escherichia coli* (*Caenhorhabditis* Genetics Center).

Embryonic Dissociation

Dissociation of embryonic cells was mostly performed as previously described by Strange and colleagues (Strange et al., 2007). Briefly, gravid adults were harvested and treated with a 20% hypochlorite solution to release the embryos. Embryos were separated from dead adult carcasses using a 50% sucrose solution and washed with sterile water to remove the debris and sucrose. 500 μl of chitinase solution (using Chitinase C7809 – Sigma, diluted to 1U/ml in ice-cold egg buffer) was added to freshly isolated 100 μl embryo pellets and incubated at room temperature with gentle agitation for 20-80 min until >80% of the eggshells were digested (time varied from experiment to experiment). Eggs were centrifuged to pellet them, supernatant removed and replaced with 800 μl ice-cold L-15 media (Invitrogen) with 10% FBS supplemented with sucrose (0.165 g sucrose/20 ml media). Cells were gently dissociated by repeatedly pipetting up and down with a 100-1000 μl pipettor for approximately 2 minutes. Dissociation was monitored under the microscope by placing 10 μl droplets on a slide and stopped when at least 50-70% of the embryos were dissociated. Cells were passed through a cell strainer (40 mm filter, BD Falcon 352340) placed in a 50 ml centrifuge tube and spun in a clinical centrifuge at the highest setting at 4 degrees Celsius. Suspensions were once again spun down and the supernatant was removed and replaced with fresh ice-cold egg buffer (118 mM NaCl,

48 mM KCl, 2 mM $CaCl_2$, 2 mM $MgCl_2$, 25 mM HEPES, pH 7.3) and collected in a 1.7 ml microcentrifuge tube. Cell concentration was approximated using a hemacytometer kindly provided by the Huffaker lab.

Fluorescence activated cell sorting (FACS)

Dissociated cells were sorted using a hi-speed FACSAria cell sorter via services of the Biomedical Science Flow Cytometry Core Laboratory at Cornell University with the help of James Lee Smith II. Prior to sorting, propidium iodide (PI) was added to the single cell suspension to a concentration of 5 μg/ml. Cells were sorted based on high intensity of GFP fluorescence and lack of PI fluorescence. Live cells (lack PI fluorescence) were harvested in two RNAse-free 1.7 microcentrifuge tubes (GFP positive and GFP negative) in 300 μl RNA Lysis Solution from PureLink Micro-to-Midi Total RNA Purification System (Invitrogen). Cells were vortexed every 15 minutes during sorting to ensure all sorted cells were in lysis buffer. Some cells were sorted onto glass polyL-lysine coated microscope slides to analyze efficiency of sorting.

RNA isolation and cDNA synthesis

Once cells were sorted to GFP positive and negative populations into RNA lysis buffer, 3 μl of 2-mercaptoethanol was added to the 300 ml volume of RNA Lysis Solution. RNA isolation was performed per instructions of PureLink Micro-to-Midi Total RNA Purification System (Invitrogen) kit. RNA quality and quantity was analyzed using the Nanodrop device (ThermoScientific). cDNA synthesis was performed using the Superscript III First-Strand Synthesis Kit (Invitrogen).

Real-time PCR

cDNA generated from mRNA of sorted cell populations was used as template for real-time PCR with SYBRgreen mix (BioRad). PCR was monitored in a BioRad iCycler Thermal cycler using Bio-Rad iQ5 software for data analysis. Levels of *hlh-8* and *mls-2* were quantified and normalized to *act-1* mRNA levels. The following primers were used to amplify *hlh-8*, *mls-2* and *act-1*:

NMA-163: 5'-CCAGGAATTGCTGATCGTATGCAGAA-3'

NMA-164: 5'-TGGAGAGGGAAGCGAGGATAGA-3'

YJ-211: 5'-ACCAATTGCTGGACCTTCAC-3'

YJ-212: 5'-AGTGTGGAGGAATGCTGGAT-3'

YJ-213: 5'-CTTTGGACTTCCGACTGCTC-3'

YJ-214: 5'-TTTCATCCTTCTCTTCTCCATTG-3'

NMA-163 and NMA-164 were used to amplify *act-1*. YJ-211 and YJ-212 were used to amplify *hlh-8*. YJ-213 and YJ-214 were used to amplify *mls-2*.

Microscopy

Differential interference contrast and epifluorescence microscopy were performed using a Leica DMRA2 compound microscope. Images were captured with a Hamamatsu Orca-ER Camera using the Openlab software (Improvision). Subsequent image analysis was performed using Adobe Photoshop 7.0 and Adobe Illustrator CS3.

Results

C. elegans larval cells can not be dissociated by collagenase treatment followed by mechanical agitation

Recent advances have been made in dissociating *C. elegans* embryonic cells in order to culture these cells for physiological studies or sort these cells based on cell-type specific GFP reporters for gene expression studies (Christensen et al., 2002; Fox et al., 2005; Strange et al., 2007). However, studies of this nature have not been reported for dissociation of larval cells. One roadblock to these studies is the physical barrier provided by the complex cuticle of the various larval stages which is composed of many collagen proteins that are encoded by the *C. elegans* genome (Politz and Edgar, 1984; C. elegans Sequencing Consortium, 1998). I treated L1 larvae during the proliferation of the postembryonic mesoderm with various types and concentrations of collagenase to disrupt the cuticle enough to dissociate larval cells and use FACS to sort GFP expressing mesodermal cells. I treated worms with crude collagenase (Sigma, C9722 Type IA-S Collagenase) at concentrations of 100 mg/ml and 1 mg/ml in 25 μM $CaCl_2$ and incubated at 37˚C with shaking. Samples were removed at various time points and mechanically agitated by vortexing and/or pipetting up and down repeatedly, after which they were scored under the microscope for dissociation of cuticles. Animals remained alive for over 24 hours in collagenase and no amount of mechanical agitation afterwards resulted in any obvious disruption of cuticle and dissociation of cells. Thus this avenue of treatments does not appear to be useful to dissociate and isolate specific larval cells.

Isolation of the M mesoblast from dissociated embryonic cells

Although it would be most useful to isolate M lineage cells during larval growth when the postembryonic mesoderm is actively dividing, the M mesoblast is itself born during embryogenesis (Sulston et al., 1983). Isolation of this cell from the embryo could provide some insight into how the M mesoblast is specified and help identify additional genes that have enriched expression in the M mesoblast. I dissociated embryos as described in Materials and Methods and was able to visualize single GFP-positive cells among the dissociated cell population (Figure A2.1). The optimum amount of single GFP-positive cells were obtained by enriching for late stage embryos, likely due to the fact that the M mesoblast is born during late embryogenesis (Sulston et al., 1983). However, many of the embryos that were treated with chitinase to release the eggshell hatched into L1 larvae and were not disrupted. These larvae remained in the dissociated cell culture during FACS (Figure A2.2).

During FACS, single GFP-positive cells were separated from L1 larvae expressing GFP based on size differences (Figure A2.2). Additionally, cells that had taken up propidium iodode (PI) were identified based on fluorescence and not sorted.From the population of single cells that remained alive during sorting, a high proportion did not express *hlh-8::gfp* (Figure A2.2). Roughly 2000 GFP-positive cells were isolated in the time that 96,000 GFP-negative cells were collected. GFP-positive cells were collected on a microscope slide and were confirmed to be GFP-positive that were about the same size of the M mesoblast in a heterogeneous embryonic cell mixture (data not shown). Thus sorting of the M mesoblast using FACS and the *hlh-8::gfp* reporter was successful.

Figure A2.1. Dissociation of embryos prior to FACS analysis. (A) Harvested embryos often express a single GFP expressing cell. Most embryos with *hlh-8::gfp* are at late embryogenesis stage. Disruption of eggshell with chitinase results in hatching of majority of these animals expressing *hlh-8::gfp*. Arrows highlight M mesoblast in embryos that do hatch upon chitinase treatment. (B) Embryo suspension after chitinase treatment and mechanical disruption. Arrows highlight single cells that are GFP-positive.

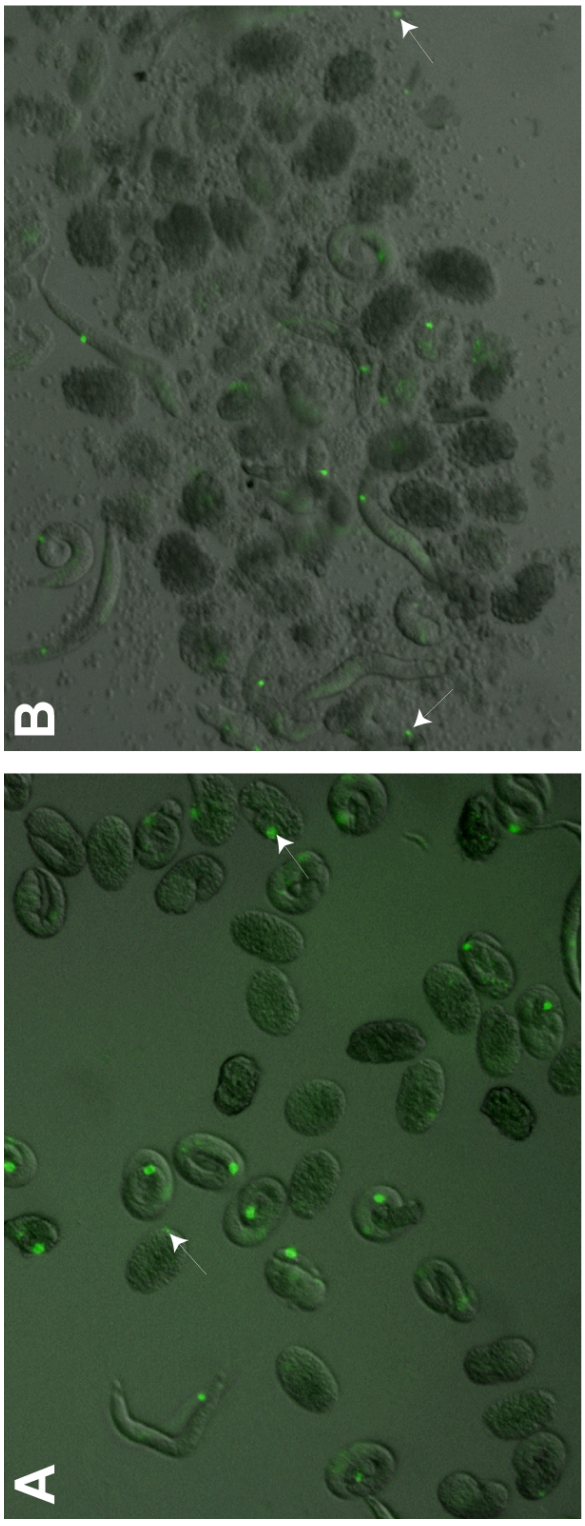
B
A

Sorted M cells have enriched expression of *hlh-8*, but not *mls-2*

To further determine the efficiency of sorting the M mesoblast, I used real-time PCR to examine the relative levels of *hlh-8* and *mls-2* gene expression in GFP-positive versus GFP-negative cells. Previous studies have shown that both of these genes are expressed in the M mesoblast during embryogenesis (Harfe et al., 1998b; Jiang et al., 2005). I found that *hlh-8*, but not *mls-2*, is enriched the GFP-positive cell population at a five-fold increase compared to the levels in the GFP-negative population (Figure A2.3). *mls-2* expression is detected in multiple cells in addition to M in the embryo (Jiang et al., 2005). Therefore it is likely that *mls-2* expression is not enriched in the M mesoblast in relation to the rest of the embryonic cell population. Thus the GFP-positive FACS sorted cells appear to be enriched for a pool of M mesoblast cells.

Discussion

Cell sorting provides useful but limited gene expression profiling tool

Global gene expression profiling would be beneficial in identification of cell type specific genes and the targets of genes known to function in specific cell types. In this appendix, I have described the isolation of the M mesoblast from dissociated embryonic cells to prepare for gene expression profiling. The sorting appears to be successful, as the cells isolated expressed the marker *hlh-8::gfp* and had an enrichment of *hlh-8* mRNA levels. Though these studies suggest that isolation of mRNA from the M mesoblast for global gene expression analysis is possible, caveats to using this approach still remain. First, the M mesoblast is born during embryogenesis, but remains quiescent until hatching of the L1 larva (Sulston and Horvitz, 1977; Sulston et al., 1983). Thus the gene expression profile that exists early during the specification of the M mesoblast will likely be drastically different than the profile as M begins to

Figure A2.2. FACS (Fluorescence activated cell sorting) criteria to isolate the M mesoblast. (A) Overall summary and counts of events during cell sorting. (B) Plot of cell count vs. GFP intensity on X axis. (C) High GFP fluorescence events were further separated based on size. 88.5% of events had a high level of scatter, indicative of hatched L1s with *hlh-8::gfp*. 6.7% of all GFP events had similar scatter and assumed to be single cell population. (D) Plot of fluorescence of single cell population, with PI on Y axis and GFP on X axis. GFP positive and negative cells collected as indicated.

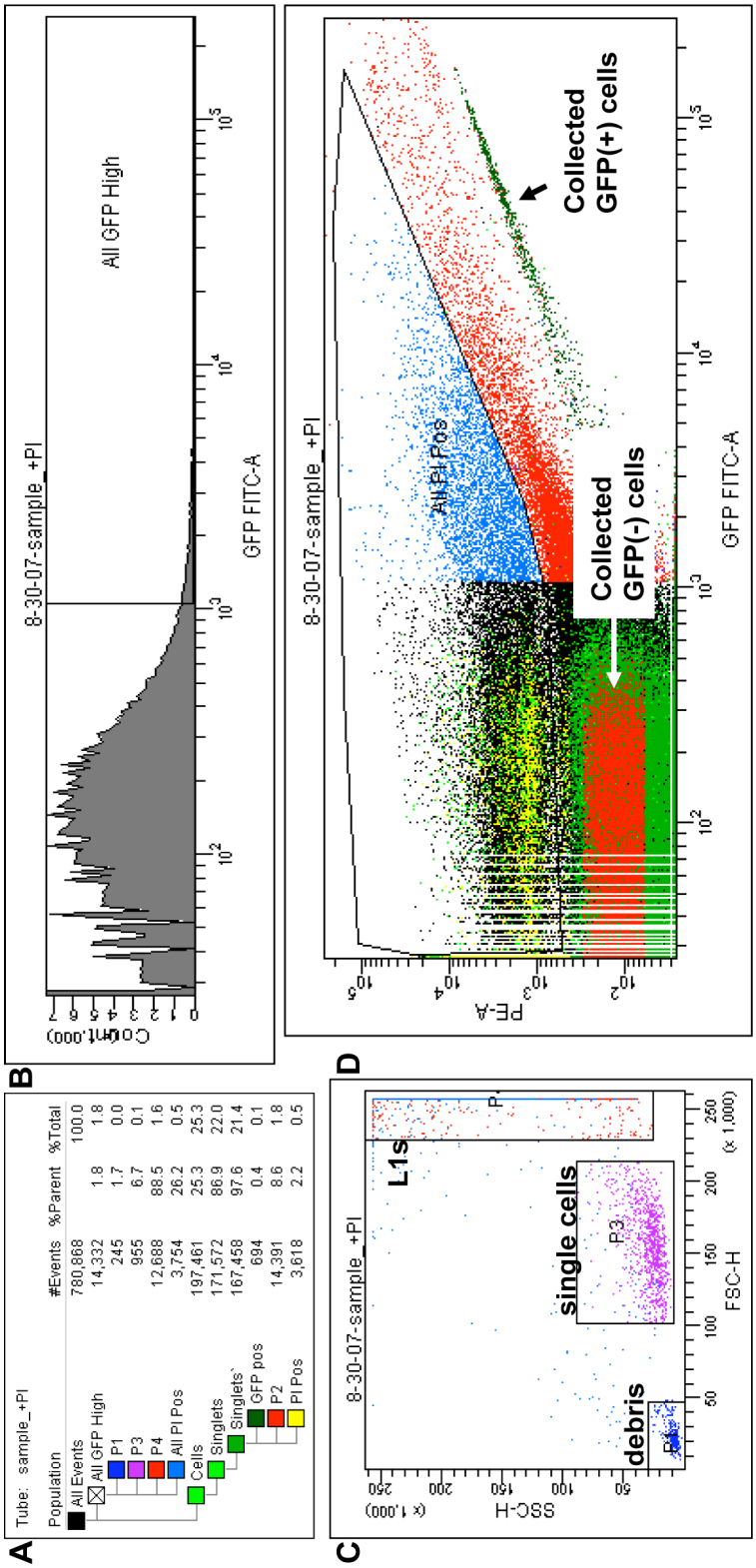
A
Tube: sample_+PI
Population
#Events
%Parent
%Total
All Events
780,868
100.0
All GFP High
14,332
1.8
1.8
P1
245
1.7
0.0
P3
955
6.7
0.1
P4
12,688
88.5
1.6
All PI Pos
3,754
26.2
0.5
Cells
197,461
25.3
25.3
Singlets
171,572
86.9
22.0
Singlets`
167,458
97.6
21.4
GFP pos
694
0.4
0.1
P2
14,391
8.6
1.8
PI Pos
3,618
2.2
0.5
B
8-30-07-sample_+PI
All GFP High
Count (,000)
GFP FITC-A
C
8-30-07-sample_+PI
L1s
single cells
debris
P1
P3
SSC-H
(x 1,000)
FSC-H
(x 1,000)
D
8-30-07-sample_+PI
All PI Pos
Collected GFP(+) cells
Collected GFP(-) cells
PE-A
GFP FITC-A

Figure A2.3 Relative levels of *hlh-8* and *mls-2* mRNA in GFP positive and GFP negative cell sorted populations. RT-PCR was performed on cDNA made from cell sorted population and mRNA levels were normalized to *act-1*. Levels are plotted on Y axis. *hlh-8* mRNA levels are enriched in GFP positive cells while *mls-2* mRNA levels are not.

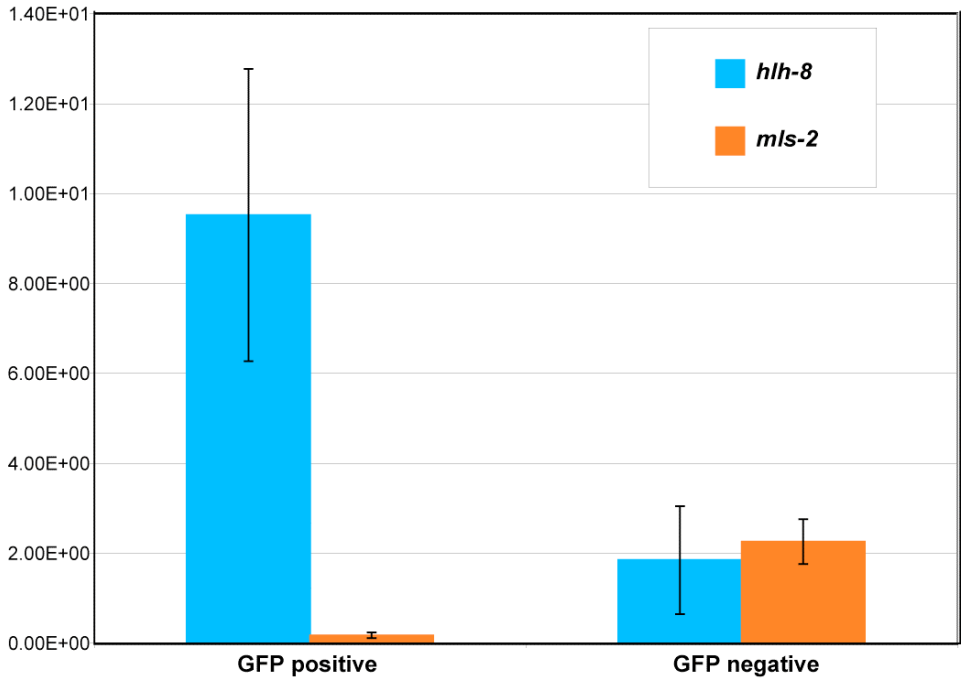
1.40E+01
1.20E+01
1.00E+01
8.00E+00
6.00E+00
4.00E+00
2.00E+00
0.00E+00
hlh-8
mls-2
GFP positive
GFP negative

divide, preventing discovery of new genes whose expression is activated as M lineage patterning occurs. Future studies using this sorted GFP population of M mesoblasts will be limited to the factors that are required to specify the M mesoblast during embryogenesis. The inability to dissociate larval cells described in this appendix prevents the use of FACS in a similar manner as shown here for the M mesoblast.

Another major caveat to using cell sorting of dissociated embryonic or larval cells to examine global gene expression would be the disruption of intercellular signaling networks. For example, the M lineage depends on a number of signaling pathways including components from the Sma/Mab TGFβ, LIN-12/Notch and the Wnt signaling pathways (Greenwald et al., 1983; Foehr et al., 2006; Foehr and Liu, 2008). Dissociation of cell-cell contacts would likely negatively impact the ability of these pathways to regulate proper patterning in the M lineage and thus lead to false positive or negative data in microarray analyses.

Alternative methods to identify targets of mesoderm-specific gene function

I have used one method to attempt to identify mesodermal targets of genes that function in mesodermally and non-mesodermally derived cell types. One reason for enriching for mesodermal cells in this project was to ensure that the cells in which RNA was isolated had expressed high levels of the gene of interest. For example, FOZI-1 is expressed in a small number of cells during larval growth, including the M lineage (Amin et al., 2007). mRNA levels of *fozi-1* targets in wild-type vs. *fozi-1* mutant animals would therefore not show appreciable differences if the entire animals are used for the mRNA preparation. By enriching for the cells that express FOZI-1 and thereby its target genes, I could enrich for differences in target gene expression in wild-type and *fozi-1* mutant animals.

Recently, an mRNA tagging has been developed in *C. elegans* in which an epitope-tagged poly-A binding protein (PAB-1) is driven in a tissue specific manner and used to immunoprecipitate polyA-containing mRNAs (Roy et al., 2002; Von Stetina et al., 2007). This will potentially be a useful tool to isolate mRNA from the M lineage and look at expression profiles in various mutants to identify downstream targets. One major advantage of this technique is that it does not rely on the disruption of cell-cell contacts thus preserving signaling pathways important for development. In addition, this approach has been used successfully in larvae, relieving a need to develop methods to dissociate larval cells for FACS (Von Stetina et al., 2007).

APPENDIX 3

IDENTIFICATION OF CIS-REGULATORY ELEMENTS IN THE *ceh-34* PROMOTER

Introduction

The Six family of homeodomain proteins is important in regulating cell fates of multiple tissue types (Kawakami et al., 2000). The Drosophila *sine oculis* gene is the founding member of this Six family of genes (Cheyette et al., 1994; Serikaku and O'Tousa, 1994). The role of *sine oculis(so)* is best characterized in the Drosophila eye, where it functions downstream of the Pax6 gene *eyeless* (*ey*) and is required for proper eye development (Halder et al., 1998). The role of *so* is mediated by its cofactor *eyes absent* (*eya*) to which it binds and is further mediated downstream by the transcription factor *dachshund (dac)* to regulate eye specification genes (Chen et al., 1997; Pignoni et al., 1997; Shen and Mardon, 1997; Halder et al., 1998). Meanwhile, other Six family members play roles in specification of other cell types. *D-six4* has been shown to be involved in patterning cells in the Drosophila mesoderm (Clark et al., 2006). In mammals, Six2 is required for proper kidney development and functions downstream of Hoxa2 in the formation of the second branchial arch (Self et al., 2006; Kutejova et al., 2008). Six1 and Six4 act upstream of the myogenic regulatory factor Myf5 during skeletal muscle formation in embryo limb buds (Giordani et al., 2007).

In Chapter 3 of this dissertation, I described my characterization of the *C. elegans* Six2 homolog *ceh-34*. CEH-34 functions together with the eyes absent homolog EYA-1 to regulate specification of two non-muscle mesodermally-derived

cells, known as coelomocytes (CCs). *ceh-34* and *eya-1* both function downstream of a number of transcription factors required for both muscle and non-muscle cells derived from the postembryonic mesoderm, *fozi-1*, *mab-5* and *hlh-1*. They are also asymmetrically expressed within the postembryonic mesoderm due to the effects of the TGFβ, Notch and Wnt signaling components (Chapter 3). Understanding the mechanisms by which these components converge on the expression of *ceh-34* and *eya-1* may help elucidate mechanisms by which Six family proteins are regulated during vertebrate development.

In this appendix, I describe my attempts to identify *cis*-regulatory elements of the *ceh-34* promoter. I have shown in Chapter 3 that the 3.9 kb sequence immediately upstream of the start codon of *ceh-34* is required for *ceh-34* expression within the CC precursor cells in the M lineage. In this chapter, I use promoter bashing in an attempt to identify sequences in the promoter that are necessary for proper expression of *ceh-34* in the M lineage.

Materials and Methods

C. elegans strains

Strains were maintained and manipulated using standard conditions at 20˚C (Brenner, 1974). The strain LW1066 (*jjIs1066; hlh-8::rfp*) was used to generate transgenic lines and examine M lineage expression of translational *gfp::ceh-34* fusions.

Plasmid constructs and transgenic lines

The plasmid pNMA94 (Chapter 3) containing 3.9 kb of the *ceh-34* promoter upstream of *gfp::ceh-34 ORF::ceh-34 3' UTR* was used as a template to generate the

following plasmids with respective promoter sequence relative to first coding ATG of *ceh-34* (also depicted in Figure A3.1):

pNMA101 -3890 to -1698, -600 to -1

pNMA102 -1640 to -1

pNMA103 -2685 to -1698, -559 to -1

pNMA104 -3890 to -2685, -1914 to -1698, -559 to -1

pNMA105 -3890 to -2685, -2262 to -1698, -559 to -1

All constructs were confirmed by sequencing. Transgenic lines were generated using the plasmid pRF4 *(rol-6d)* or pJKL815 (*myo-2::rfp*; Chapter 3) as a marker using standard injection techniques (Mello et al., 1991).

Immunostaining

Immunostaining was performed as described by Hurd and Kemphues (Hurd and Kemphues, 2003). Affinity-purified anti-FOZI-1 antibodies (Amin et al., 2007) were used at 1:200 dilution, while anti-GFP antibodies (Rockland Immunochemicals) were used at 1:5000. Secondary antibodies were from Jackson ImmunoResearch Laboratories and used in a dilution of 1:50 to 1:200. Differential interference contrast and epifluorescence microscopy were performed using a Leica DMRA2 compound microscope.

Results

Distinct promoter elements are required for *ceh-34* expression

To determine the *cis*-regulatory regions in the *ceh-34* promoter, I generated deletions in the functional translational *gfp::ceh-34* reporter (see Materials and Methods) driven by a 3.9 kb region upstream of the ATG start codon and tested for the

ability of these modified reporters to direct *gfp::ceh-34* expression in the M lineage. As shown in Figure A3.1, deletion of the region -3900 to -1300 base pairs relative to the *ceh-34* translational start site lead to the loss of M lineage expression. Further deletions in this region identified a 348 base pair sequence (-2262 to -1914) that is required for M lineage expression of *ceh-34*.

In addition to its role in the M lineage, *ceh-34* is required for larval viability and anterior morphogenesis (Chapter 3). The functional *gfp::ceh-34* fusion is also expressed in the head of developing larvae and adults in a number of cells (Chapter 3). I examined the expression of the various promoter bashing constructs (Figure A3.1). Two regions (-2262 to -1914 and -1698 to -559) are required for *gfp::ceh-34* expression in the head. Removal of either region alone resulted in an overall decrease in gfp detectable in the head, while removal of both led to a complete loss of detectable gfp in live animals. Thus there may be multiple *cis*-elements in the *ceh-34* promoter normally required for its anterior expression in the various cells of the head.

A conserved forkhead binding site exists in required promoter sequence

To search for potential binding sites in the required 348 base pairs of the *ceh-34* promoter, I used a comparative genomics approach. I retrieved promoter sequences for the *ceh-34* homologues from the closely related *Caenorhabditis briggsae*, *Caenorhabditis brenneri* and *Caenorhabditis remanei* species. I used the DIALIGN software (Morgenstern, 2004) to perform an alignment of the promoters from these three species with the *C. elegans ceh-34* promoter. The required 348 base pairs of the *ceh-34* promoter required for M lineage expression in *C. elegans* contains blocks of conserved sequences with the other closely related species (Figure A3.2). I used the TESS (Transcription Element Search System) to screen for potential trans-acting factors that could bind to the *ceh-34* promoter in these conserved blocks to activate its

Figure A3.1. *ceh-34* expression constructs and patterns. *pNMA94* is capable of rescuing M lineage phenotypes associated with *ceh-34(n4796)*. Promoter bashing constructs are indicated with relative position to translational start site of *gfp::ceh-34* (0). "+++" indicates wild-type expression pattern of GFP in indicated cell type. "+" describes expression in fewer cells, while "-" describes no detectable expression. Expression in the head was determined at a qualitative level only and was not quantified.

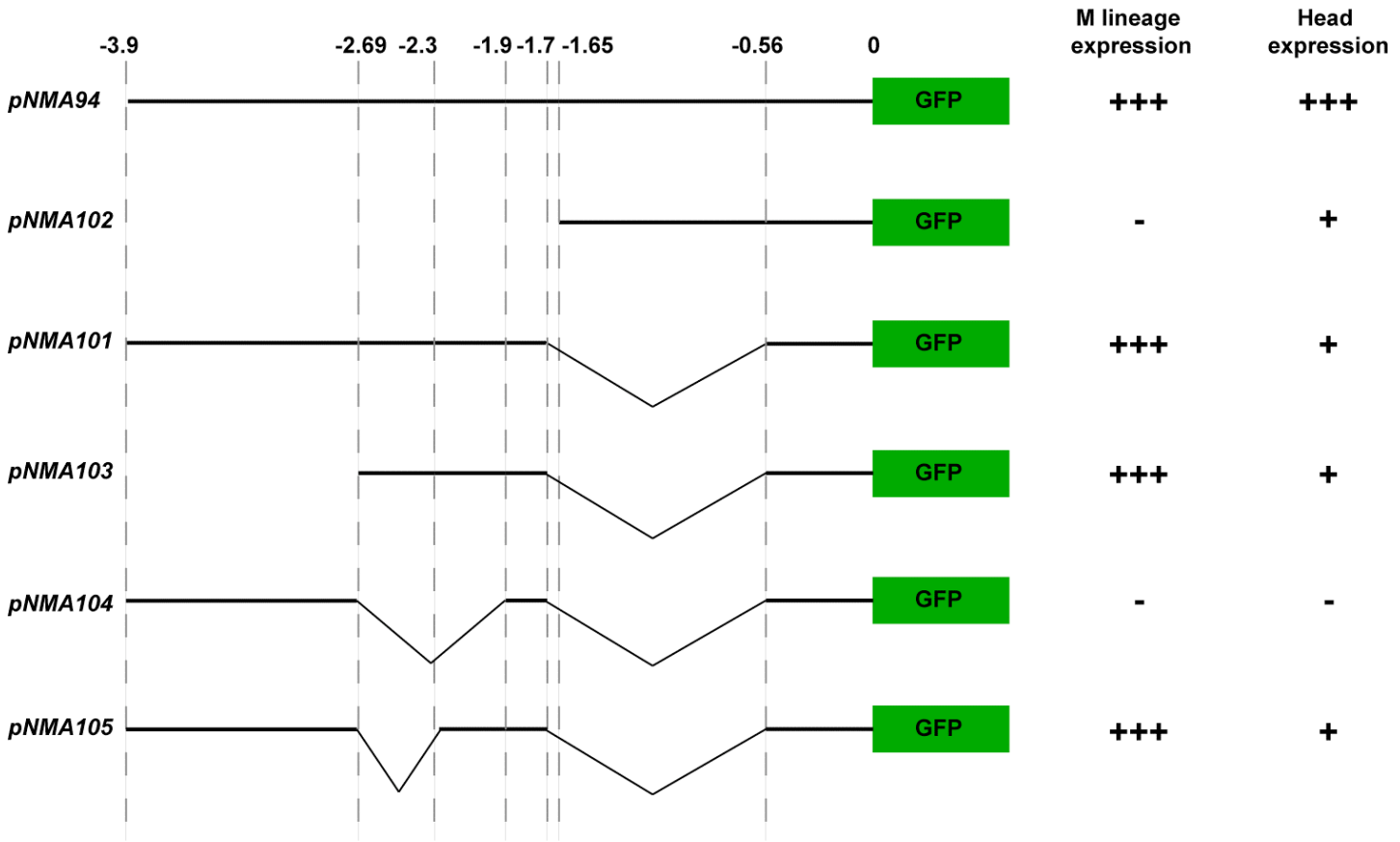
-3.9
-2.69
-2.3
-1.9
-1.7
-1.65
-0.56
0
M lineage expression
Head expression
pNMA94
GFP
+++
+++
pNMA102
GFP
-
+
pNMA101
GFP
+++
+
pNMA103
GFP
+++
+
pNMA104
GFP
-
-
pNMA105
GFP
+++
+

Figure A3.2. Alignment of non-overlapping regions of deletions contained in pNMA104 and pNMA105. *ceh-34* promoter shown are from top to bottom, *C. elegans*, *C. briggsae*, *C. remanei* and *C. brenneri* and aligned using DIALIGN software. Blocks and degree of conservation among the species are denoted below the sequence with asterisks (*). Putative binding sites identified by the Transcription Element Search Software are indicated above the corresponding sequences.

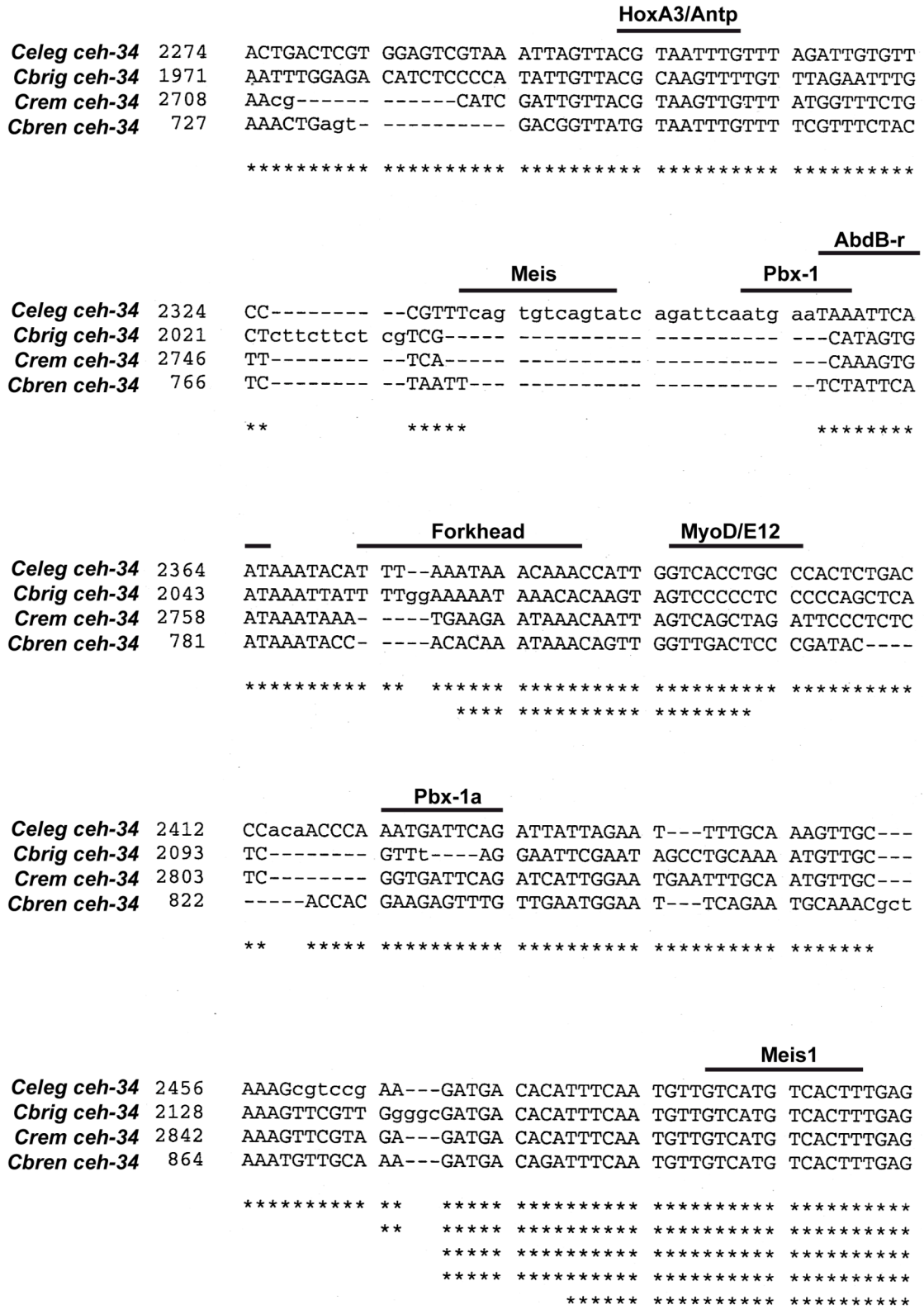
HoxA3/Antp
Celeg ceh-34 2274 ACTGACTCGT GGAGTCGTAA ATTAGTTACG TAATTTGTTT AGATTGTGTT
Cbrig ceh-34 1971 AATTTGGAGA CATCTCCCCA TATTGTTACG CAAGTTTTGT TTAGAATTTG
Crem ceh-34 2708 AAcg------ ------CATC GATTGTTACG TAAGTTGTTT ATGGTTTCTG
Cbren ceh-34 727 AAACTGagt- ---------- GACGGTTATG TAATTTGTTT TCGTTTCTAC
AbdB-r
Meis
Pbx-1
Celeg ceh-34 2324 CC-------- --CGTTTcag tgtcagtatc agattcaatg aaTAAATTCA
Cbrig ceh-34 2021 CTcttcttct cgTCG----- ---------- ---------- ---CATAGTG
Crem ceh-34 2746 TT-------- --TCA----- ---------- ---------- ---CAAAGTG
Cbren ceh-34 766 TC-------- --TAATT--- ---------- ---------- --TCTATTCA
Forkhead
MyoD/E12
Celeg ceh-34 2364 ATAAATACAT TT--AAATAA ACAAACCATT GGTCACCTGC CCACTCTGAC
Cbrig ceh-34 2043 ATAAATTATT TTggAAAAAT AAACACAAGT AGTCCCCCTC CCCCAGCTCA
Crem ceh-34 2758 ATAAATAAA- ----TGAAGA ATAAACAATT AGTCAGCTAG ATTCCCTCTC
Cbren ceh-34 781 ATAAATACC- ----ACACAA ATAAACAGTT GGTTGACTCC CGATAC----
Pbx-1a
Celeg ceh-34 2412 CCacaACCCA AATGATTCAG ATTATTAGAA T---TTTGCA AAGTTGC---
Cbrig ceh-34 2093 TC-------- GTTt----AG GAATTCGAAT AGCCTGCAAA ATGTTGC---
Crem ceh-34 2803 TC-------- GGTGATTCAG ATCATTGGAA TGAATTTGCA ATGTTGC---
Cbren ceh-34 822 -----ACCAC GAAGAGTTTG TTGAATGGAA T---TCAGAA TGCAAACgct
Meis1
Celeg ceh-34 2456 AAAGcgtccg AA---GATGA CACATTTCAA TGTTGTCATG TCACTTTGAG
Cbrig ceh-34 2128 AAAGTTCGTT GgggcGATGA CACATTTCAA TGTTGTCATG TCACTTTGAG
Crem ceh-34 2842 AAAGTTCGTA GA---GATGA CACATTTCAA TGTTGTCATG TCACTTTGAG
Cbren ceh-34 864 AAATGTTGCA AA---GATGA CAGATTTCAA TGTTGTCATG TCACTTTGAG

Figure A3.2 (continued)

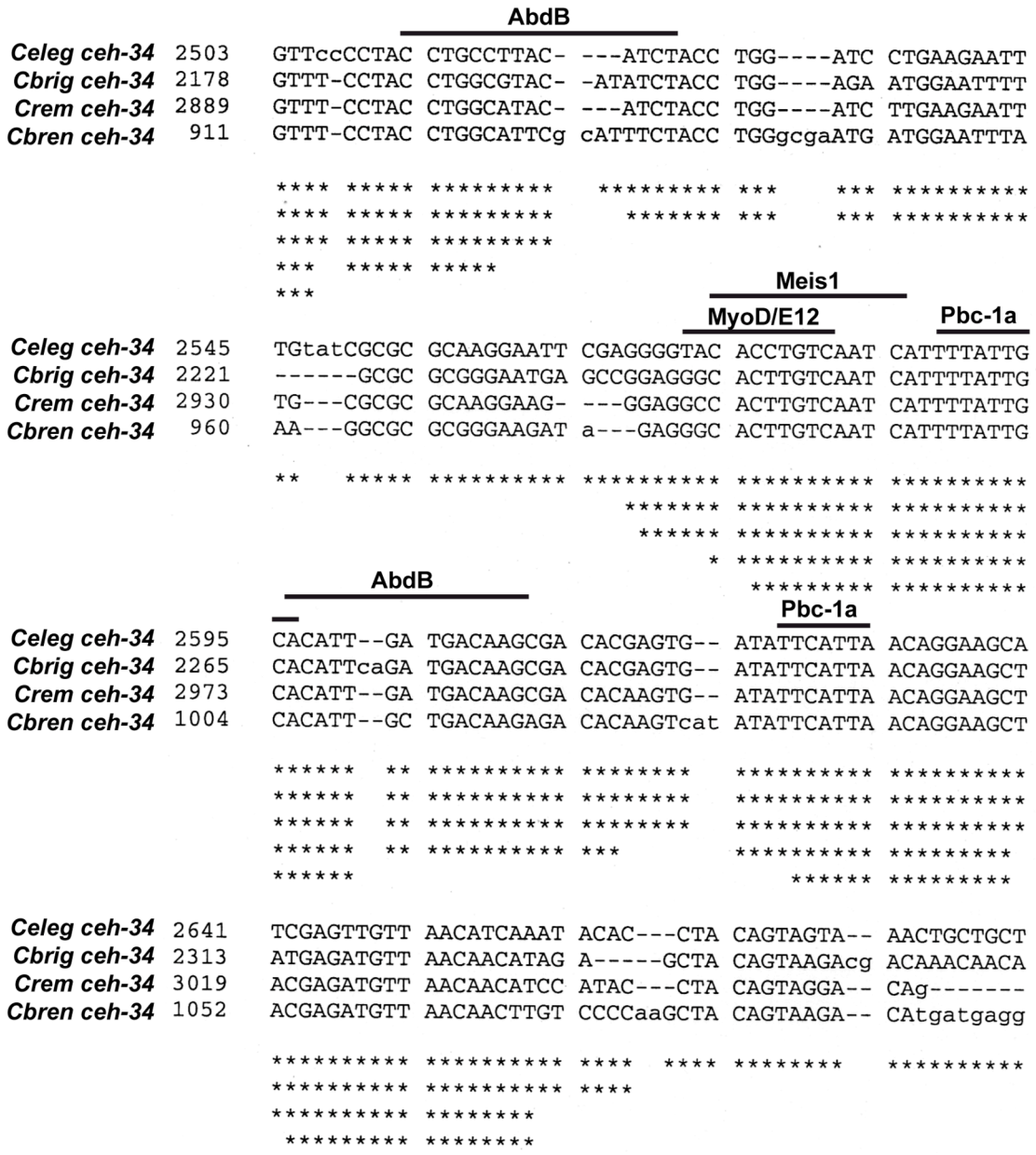

expression. Homologs of known M lineage factors and their putative binding sites identified from this analysis are summarized in Figure A3.2. These include binding sites for MyoD, Pbx-1a, Meis, AbdB transcription factors of which the homologs function upstream of *ceh-34* in the M lineage are *hlh-1*, *ceh-20*, *unc-62* and *mab-5*, respectively (Harfe et al., 1998a; Liu and Fire, 2000). Interestingly, there was also a conserved forkhead binding domain in a conserved region of this promoter element (Figure A3.2). As described in Chapter 4 of this work, I have identified a forkhead transcription factor, *let-381*, which is required for dorsal fates and its expression precedes *ceh-34* expression.

Discussion

ceh-34 promoter bashing identifies potential *cis*-regulatory elements

In this appendix, I have described my preliminary analyses in an effort to identify the cis-regulatory elements in the *ceh-34* promoter. As shown in Figure A3.2, deletion of an approximately 800 base pair region (-2685 to -1914) upstream of the *ceh-34* coding region abolishes expression of a reporter driven by the rest of the *ceh-34* promoter. Deletion of only half of this region (-2685 to -2262), however, does not affect *ceh-34* expression in the M lineage. These data suggest that the remaining ~400 base pairs not deleted in this latter reporter (-2262 to -1914) are required for *ceh-34* expression in the M lineage. Further analysis is required to determine whether this region has any M lineage specific *cis*-regulatory elements. First, the requirement of this 400 base pair region must be tested by specifically deleting this element alone in the *ceh-34* promoter. Second, if this element is required, it can be further narrowed down by deletion analysis and then placed upstream of a basal promoter driving a reporter to determine if this element is sufficient for M lineage expression.

Putative trans-acting factors in *ceh-34* regulation

In Chapter 3, I identified a number of factors that act upstream of the *ceh-34* and *eya-1* genes in specifying muscle vs. non-muscle fates. It remains unclear if these factors are acting directly on the *ceh-34* promoter to regulate its transcription or if potential direct *ceh-34* regulators are not yet identified. In addition to the promoter bashing results outline above to identify *cis*-regulatory elements, I used a comparative and informatics approach to search for potential transcriptional regulators of the *ceh-34* promoter. I compared sequences upstream of the coding region of *ceh-34* from four closely related nematode species and identified blocks of conservation. In the future, these sites should provide insight into the regulation of *ceh-34*, and should be the first to be considered when searching for transcription factor binding sites. Using the TESS program to identify putative binding sites in 400 base pair region of the *ceh-34* promoter, I have found a number of potential binding sites for transcription factors that function upstream of *ceh-34* in the M lineage. If this 400 base pair region is found to be sufficient to drive a gfp reporter in the M lineage, mutations should target these individual binding sites to determine which are required for the proper M lineage expression of *ceh-34*. Because *ceh-34* is required for the specification of a non-muscle cell versus a muscle cell, it will be interesting to see if these various M lineage components act in combination to activate ceh-34 expression, or if some factors activate global expression of *ceh-34* in the M lineage while others repress it in muscle cells.

APPENDIX 4

ANALYSIS OF FOZI-1 GENE FUNCTION IN C. ELEGANS DEVELOPMENT BY TRANSGENIC RESCUE ASSAYS

Introduction

fozi-1 encodes a putative transcription factor that is required for proper cell fate specification in at least two cell types during *C. elegans* development. First, *fozi-1* plays a role in the asymmetric fate decision between two distinct neuronal cells, ASEL and ASER (Johnston et al., 2006). *fozi-1* is also required within the postembryonic mesoderm, the M lineage, to properly specify non-muscle cells known as coelomocytes, CCs, and striated body wall muscles, BWMs (Amin et al., 2007). FOZI-1 is expressed within the precursors of these cells and functions cell autonomously to specify each of these cells (Johnston et al., 2006; Amin et al., 2007). Though FOZI-1 is expressed in ASER and within the CC and BWM precursors, there are likely distinct regulators of its expression based on the cellular context. Identification of regulators of FOZI-1 expression can lead to a better understanding of how this unique transcription factor functions.

The *cis*-regulatory element(s) required for *fozi-1* expression in the ASER neuron are 1 kb within the *fozi-1* promoter (Johnston et al., 2006). In this appendix, I describe my attempts to identify the minimal promoter sequence that is required for *fozi-1* expression in the M lineage. Unlike what was observed in the ASEL and ASER neuron pair, I was unable to identify such a sequence for the M lineage expression within the *fozi-1* promoter.

Materials and Methods

C. elegans strains

Strains were maintained and manipulated using standard conditions at 20°C (Brenner, 1974). The Bristol reference strain N2 was used to generate transgenic lines and examine the expression pattern of *fozi-1* transcriptional reporters.

Plasmid constructs and transgenic lines

Two fragments of the *fozi-1* locus were amplified from the cosmid K01B6 using the following primers:

NMA-79: 5'-CACATCAAACTGAAGCAGCCGCGGTTCACACTGTAAGTATATGG-3'

NMA-80: 5'-GATGATGCAAGCATCATGGCCCCGGGTCTGGAAATATATTTTTTAC-3'

NMA-81: 5'-GAAAAATGTGATTGAAAAATGGCGCGCCTGAGACATCCAGGGATCATCC-3'

NMA-82: GAACGGTGGCTGCTTCAGTTGGATCCGTTTGTTGCAATGGAAAAGG-3'

NMA-79 and NMA-80 were used to amplify the first intron of *fozi-1*, while NMA-81 and NMA-82 were used to amplify approximately 5 kb of the promoter of *fozi-1*. The first intron and promoter are depicted in Figure A4.1. These fragments were cloned into the vector pPD117.01 (kind gift of Andrew Fire) to generate the following plasmids:

pNMA10: 5013 bp fozi-1p::gfp::let-858 3'UTR

pNMA11: *7115 bp fozi-1 intron one::gfp::let-858 3'UTR*

All constructs were confirmed by sequencing. Transgenic lines were generated using the *rol-6* as a marker using standard injection techniques (Mello et al., 1991). Differential interference contrast and epifluorescence microscopy were performed using a Leica DMRA2 compound microscope.

Results

fozi-1 M lineage expression requires additional *cis*-regulatory elements compared to its neuronal expression

FOZI-1 is expressed in the descendents of the M mesoblast starting from the first division of M and continues in the precursors of the CCs and BWMs (Amin et al., 2007). In addition to its M lineage expression, FOZI-1 is also localized to the nuclei of a subset of neuronal cells (Johnston et al., 2006; Amin et al., 2007). *fozi-1* contains a large 7kb first intron upstream of the translational start site. I tested whether this intron or the 5 kb promoter sequence upstream of the first exon were sufficient to drive the expression of a *gfp* reporter in a similar pattern to the endogenous FOZI-1 pattern previously observed. As previously reported, *gfp* driven by the first intron alone was expressed in neuronal cells in the head and along the ventral nerve cord (Johnston et al., 2006). However, no M lineage expression was detected. Transgenic animals that were co-injected with the *5 kb fozi-1 promoter::gfp* and *7 kb fozi-1 intron one::gfp* reporters also failed to produce M lineage expression of GFP (Figure A4.1). Thus the M lineage-specific cis-elements for *fozi-1* expression are lacking from these two regions of the *fozi-1* locus.

Figure A4.1. Promoter dissection of the *fozi-1* promoter. *fozi-1* exon/intron boundaries are depicted. Neuronal expression is defined by expression in the ventral nerve cord and in anterior neurons. "+++" indicates expression was detected in a similar pattern as seen with aFOZI-1 immunostaining. "-" indicates no expression and "n.d." indicates not determined.

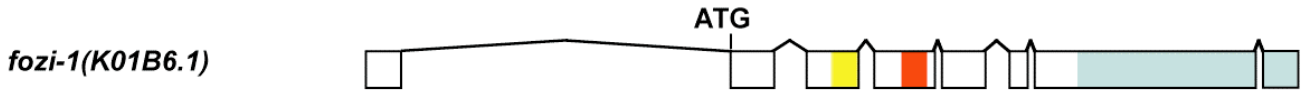

Transcriptional reporters:		Neuronal expression	M lineage expression
pNMA10	*5013 bp fozi-1p* — GFP — *let-858 3'UTR*	n.d.	n.d.
pNMA11	*7115 bp fozi-1 intron one* — GFP — *let-858 3'UTR*	+++	-
pNMA10 + *pNMA11*	*5013 bp fozi-1p* — GFP — *let-858 3'UTR*; *7115 bp fozi-1 intron one* — GFP — *let-858 3'UTR*	+++	-

Discussion

fozi-1 transcription in the M lineage may be regulated by long range *cis*-acting elements

FOZI-1 plays a crucial role in at least two cell lineages in *C. elegans*, including the specification of non-muscle and muscle fates in the postembryonic mesoderm (Johnston et al., 2006; Amin et al., 2007). The regulation of *fozi-1* expression in these two lineages appears to be dependent on two different *cis*-regulatory elements. In this appendix, I show that an element within the large first intron of *fozi-1* is able to drive expression of a *gfp* reporter in the head neurons and the ventral nerve cord, but not in the M lineage. A *gfp* reporter driven by 5 kb of sequence upstream of the first exon of *fozi-1* also does not result in M lineage expression. These results suggest that the M lineage specific *cis*-regulatory element of *fozi-1* may by much further from the transcriptional start site than the neuronal enhancer. This conclusion is supported by the fact that rescue of *fozi-1* mutant M lineage phenotypes was only achieved by two overlapping genomic fragments that span the entire intergenic region of *fozi-1* and M01A8.2, a region that spans over 15 kb (data not shown). The inability to identify *cis*-regulatory element of *fozi-1* prohibits additional testing to identify transcription factors that may regulate *fozi-1* expression. Therefore, other methods must be used to identify mechanisms of how this unique zinc-finger, FH2 formin homology domain containing protein is regulated in order to properly specify muscle and non-muscle fates in the *C. elegans* postembryonic mesoderm.

REFERENCES

Abrell, S. and Jackle, H. (2001). Axon Guidance of Drosophila SNb Motoneurons Depends on the Cooperative Action of Muscular Kruppel and Neuronal Capricious Activities. ***Mech. Dev.*** **109, 3-12.**

Agius, E., Oelgeschlager, M., Wessely, O., Kemp, C. and De Robertis, E. M. (2000). Endodermal Nodal-Related Signals and Mesoderm Induction in Xenopus. ***Development*** **127, 1173-1183.**

Amaya, E., Stein, P. A., Musci, T. J. and Kirschner, M. W. (1993). FGF Signalling in the Early Specification of Mesoderm in Xenopus. ***Development*** **118, 477-487.**

Amin, N. M., Hu, K., Pruyne, D., Terzic, D., Bretscher, A. and Liu, J. (2007). A Zn-finger/FH2-Domain Containing Protein, FOZI-1, Acts Redundantly with CeMyoD to Specify Striated Body Wall Muscle Fates in the Caenorhabditis Elegans Postembryonic Mesoderm. ***Development*** **134, 19-29.**

Araki, I., Saiga, H., Makabe, K. W. and Sato, N. (1994). Expression of AMD1, a Gene for a MyoD1-Related Factor in the Ascidian Halocynthia Roretzi. ***Roux's Arch. Dev. Biol.*** **203, 320-321-327.**

Arnold, H. H. and Braun, T. (2000). Genetics of Muscle Determination and Development. ***Curr. Top. Dev. Biol.*** **48, 129-164.**

Arora, K., Dai, H., Kazuko, S. G., Jamal, J., O'Connor, M. B., Letsou, A. and Warrior, R. (1995). The Drosophila Schnurri Gene Acts in the Dpp/TGF Beta

Signaling Pathway and Encodes a Transcription Factor Homologous to the Human MBP Family. ***Cell*** **81, 781-790.**

Artero, R., Prokop, A., Paricio, N., Begemann, G., Pueyo, I., Mlodzik, M., Perez-Alonso, M. and Baylies, M. K. (1998). The Muscleblind Gene Participates in the Organization of Z-Bands and Epidermal Attachments of Drosophila Muscles and is Regulated by Dmef2. ***Dev. Biol.*** **195, 131-143.**

Azpiazu, N. and Frasch, M. (1993). Tinman and Bagpipe: Two Homeo Box Genes that Determine Cell Fates in the Dorsal Mesoderm of Drosophila. ***Genes Dev.*** **7, 1325-1340.**

Azpiazu, N., Lawrence, P. A., Vincent, J. P. and Frasch, M. (1996). Segmentation and Specification of the Drosophila Mesoderm. ***Genes Dev.*** **10, 3183-3194.**

Baker, R. and Schubiger, G. (1996). Autonomous and Nonautonomous Notch Functions for Embryonic Muscle and Epidermis Development in Drosophila. ***Development*** **122, 617-626.**

Balagopalan, L., Keller, C. A. and Abmayr, S. M. (2001). Loss-of-Function Mutations Reveal that the Drosophila Nautilus Gene is Not Essential for Embryonic Myogenesis Or Viability. ***Dev. Biol.*** **231, 374-382.**

Barolo, S. (2006). Transgenic Wnt/TCF Pathway Reporters: All You Need is Lef? ***Oncogene*** **25, 7505-7511.**

Bate, M. (1990). The Embryonic Development of Larval Muscles in Drosophila. ***Development*** **110, 791-804.**

Baylies, M. K., Bate, M. and Ruiz Gomez, M. (1998). Myogenesis: A View from Drosophila. ***Cell*** **93, 921-927.**

Beiman, M., Shilo, B. Z. and Volk, T. (1996). Heartless, a Drosophila FGF Receptor Homolog, is Essential for Cell Migration and Establishment of several Mesodermal Lineages. ***Genes Dev.*** **10, 2993-3002.**

Ben-Yair, R. and Kalcheim, C. (2005). Lineage Analysis of the Avian Dermomyotome Sheet Reveals the Existence of Single Cells with both Dermal and Muscle Progenitor Fates. ***Development*** **132, 689-701.**

Bodmer, R. (1993). The Gene Tinman is Required for Specification of the Heart and Visceral Muscles in Drosophila. ***Development*** **118, 719-729.**

Bondue, A., Lapouge, G., Paulissen, C., Semeraro, C., Iacovino, M., Kyba, M. and Blanpain, C. (2008). Mesp1 Acts as a Master Regulator of Multipotent Cardiovascular Progenitor Specification. ***Cell. Stem Cell.*** **3, 69-84.**

Bour, B. A., O'Brien, M. A., Lockwood, W. L., Goldstein, E. S., Bodmer, R., Taghert, P. H., Abmayr, S. M. and Nguyen, H. T. (1995). Drosophila MEF2, a Transcription Factor that is Essential for Myogenesis. ***Genes Dev.*** **9, 730-741.**

Bourgouin, C., Lundgren, S. E. and Thomas, J. B. (1992). Apterous is a Drosophila LIM Domain Gene Required for the Development of a Subset of Embryonic Muscles. ***Neuron*** **9, 549-561.**

Bowerman, B., Draper, B. W., Mello, C. C. and Priess, J. R. (1993). The Maternal Gene Skn-1 Encodes a Protein that is Distributed Unequally in Early C. Elegans Embryos. ***Cell*** **74, 443-452.**

Bowerman, B., Eaton, B. A. and Priess, J. R. (1992). Skn-1, a Maternally Expressed Gene Required to Specify the Fate of Ventral Blastomeres in the Early C. Elegans Embryo. ***Cell*** **68, 1061-1075.**

Brand-Saberi, B., Gamel, A. J., Krenn, V., Muller, T. S., Wilting, J. and Christ, B. (1996a). N-Cadherin is Involved in Myoblast Migration and Muscle Differentiation in the Avian Limb Bud. ***Dev. Biol.*** **178, 160-173.**

Brand-Saberi, B., Muller, T. S., Wilting, J., Christ, B. and Birchmeier, C. (1996b). Scatter factor/hepatocyte Growth Factor (SF/HGF) Induces Emigration of Myogenic Cells at Interlimb Level in Vivo. ***Dev. Biol.*** **179, 303-308.**

Braun, T., Rudnicki, M. A., Arnold, H. H. and Jaenisch, R. (1992). Targeted Inactivation of the Muscle Regulatory Gene Myf-5 Results in Abnormal Rib Development and Perinatal Death. ***Cell*** **71, 369-382.**

Brennan, K., Baylies, M. and Arias, A. M. (1999). Repression by Notch is Required before Wingless Signalling during Muscle Progenitor Cell Development in Drosophila. ***Curr. Biol.*** **9, 707-710.**

Brenner, S. (1974). The Genetics of Caenorhabditis Elegans. ***Genetics*** **77, 71-94.**

Bretscher, A. (1981). Fimbrin is a Cytoskeletal Protein that Crosslinks F-Actin in Vitro. ***Proc. Natl. Acad. Sci. U. S. A.*** **78, 6849-6853.**

Bruneau, B. G., Logan, M., Davis, N., Levi, T., Tabin, C. J., Seidman, J. G. and Seidman, C. E. (1999). Chamber-Specific Cardiac Expression of Tbx5 and Heart Defects in Holt-Oram Syndrome. ***Dev. Biol.*** **211, 100-108.**

Bruneau, B. G., Nemer, G., Schmitt, J. P., Charron, F., Robitaille, L., Caron, S., Conner, D. A., Gessler, M., Nemer, M., Seidman, C. E. et al. (2001). A Murine Model of Holt-Oram Syndrome Defines Roles of the T-Box Transcription Factor Tbx5 in Cardiogenesis and Disease. ***Cell*** **106, 709-721.**

Buckingham, M. (2001). Skeletal Muscle Formation in Vertebrates. ***Curr. Opin. Genet. Dev.*** **11, 440-448.**

Buckingham, M., Bajard, L., Chang, T., Daubas, P., Hadchouel, J., Meilhac, S., Montarras, D., Rocancourt, D. and Relaix, F. (2003). The Formation of Skeletal Muscle: From Somite to Limb. ***J. Anat.*** **202, 59-68.**

Buckingham, M., Meilhac, S. and Zaffran, S. (2005). Building the Mammalian Heart from Two Sources of Myocardial Cells. ***Nat. Rev. Genet.*** **6, 826-835.**

C. elegans Sequencing Consortium. (1998). Genome Sequence of the Nematode C. Elegans: A Platform for Investigating Biology. ***Science*** **282, 2012-2018.**

Cai, C. L., Liang, X., Shi, Y., Chu, P. H., Pfaff, S. L., Chen, J. and Evans, S. (2003). Isl1 Identifies a Cardiac Progenitor Population that Proliferates Prior to Differentiation and Contributes a Majority of Cells to the Heart. ***Dev. Cell.*** **5, 877-889.**

Carmena, A., Bate, M. and Jimenez, F. (1995). Lethal of Scute, a Proneural Gene, Participates in the Specification of Muscle Progenitors during Drosophila Embryogenesis. ***Genes Dev.*** **9, 2373-2383.**

Carmena, A., Buff, E., Halfon, M. S., Gisselbrecht, S., Jimenez, F., Baylies, M. K. and Michelson, A. M. (2002). Reciprocal Regulatory Interactions between the

Notch and Ras Signaling Pathways in the Drosophila Embryonic Mesoderm. ***Dev. Biol.*** **244, 226-242.**

Carmena, A., Gisselbrecht, S., Harrison, J., Jimenez, F. and Michelson, A. M. (1998a). Combinatorial Signaling Codes for the Progressive Determination of Cell Fates in the Drosophila Embryonic Mesoderm. ***Genes Dev.*** **12, 3910-3922.**

Carmena, A., Murugasu-Oei, B., Menon, D., Jimenez, F. and Chia, W. (1998b). Inscuteable and Numb Mediate Asymmetric Muscle Progenitor Cell Divisions during Drosophila Myogenesis. ***Genes Dev.*** **12, 304-315.**

Chen, C. Y., Croissant, J., Majesky, M., Topouzis, S., McQuinn, T., Frankovsky, M. J. and Schwartz, R. J. (1996). Activation of the Cardiac Alpha-Actin Promoter Depends upon Serum Response Factor, Tinman Homologue, Nkx-2.5, and Intact Serum Response Elements. ***Dev. Genet.*** **19, 119-130.**

Chen, L., Krause, M., Draper, B., Weintraub, H. and Fire, A. (1992). Body-Wall Muscle Formation in Caenorhabditis Elegans Embryos that Lack the MyoD Homolog Hlh-1. ***Science*** **256, 240-243.**

Chen, L., Krause, M., Sepanski, M. and Fire, A. (1994). The Caenorhabditis Elegans MYOD Homologue HLH-1 is Essential for Proper Muscle Function and Complete Morphogenesis. ***Development*** **120, 1631-1641.**

Chen, R., Amoui, M., Zhang, Z. and Mardon, G. (1997). Dachshund and Eyes Absent Proteins Form a Complex and Function Synergistically to Induce Ectopic Eye Development in Drosophila. ***Cell*** **91, 893-903.**

Cheyette, B. N., Green, P. J., Martin, K., Garren, H., Hartenstein, V. and Zipursky, S. L. (1994). The Drosophila Sine Oculis Locus Encodes a Homeodomain-Containing Protein Required for the Development of the Entire Visual System. ***Neuron*** **12, 977-996.**

Chieffo, C., Garvey, N., Gong, W., Roe, B., Zhang, G., Silver, L., Emanuel, B. S. and Budarf, M. L. (1997). Isolation and Characterization of a Gene from the DiGeorge Chromosomal Region Homologous to the Mouse Tbx1 Gene. ***Genomics*** **43, 267-277.**

Christ, B., Huang, R. and Scaal, M. (2007). Amniote Somite Derivatives. ***Dev. Dyn.*** **236, 2382-2396.**

Christensen, M., Estevez, A., Yin, X., Fox, R., Morrison, R., McDonnell, M., Gleason, C., Miller, D. M.,3rd and Strange, K. (2002). A Primary Culture System for Functional Analysis of C. Elegans Neurons and Muscle Cells. ***Neuron*** **33, 503-514.**

Clark, I. B., Boyd, J., Hamilton, G., Finnegan, D. J. and Jarman, A. P. (2006). D-six4 Plays a Key Role in Patterning Cell Identities Deriving from the Drosophila Mesoderm. ***Dev. Biol.*** **294, 220-231.**

Colosimo, M. E., Brown, A., Mukhopadhyay, S., Gabel, C., Lanjuin, A. E., Samuel, A. D. and Sengupta, P. (2004). Identification of Thermosensory and Olfactory Neuron-Specific Genes Via Expression Profiling of Single Neuron Types. ***Curr. Biol.*** **14, 2245-2251.**

Conlon, F. L., Lyons, K. M., Takaesu, N., Barth, K. S., Kispert, A., Herrmann, B. and Robertson, E. J. (1994). A Primary Requirement for Nodal in the Formation and Maintenance of the Primitive Streak in the Mouse. ***Development*** **120, 1919-1928.**

Corsi, A. K., Kostas, S. A., Fire, A. and Krause, M. (2000). Caenorhabditis Elegans Twist Plays an Essential Role in Non-Striated Muscle Development. ***Development*** **127, 2041-2051.**

Crozatier, M. and Vincent, A. (1999). Requirement for the Drosophila COE Transcription Factor Collier in Formation of an Embryonic Muscle: Transcriptional Response to Notch Signalling. ***Development*** **126, 1495-1504.**

Cunliffe, V. and Smith, J. C. (1992). Ectopic Mesoderm Formation in Xenopus Embryos Caused by Widespread Expression of a Brachyury Homologue. ***Nature*** **358, 427-430.**

Dai, H., Hogan, C., Gopalakrishnan, B., Torres-Vazquez, J., Nguyen, M., Park, S., Raftery, L. A., Warrior, R. and Arora, K. (2000). The Zinc Finger Protein Schnurri Acts as a Smad Partner in Mediating the Transcriptional Response to Decapentaplegic. ***Dev. Biol.*** **227, 373-387.**

Dasgupta, S., Fernandez, L., Kameyama, L., Inada, T., Nakamura, Y., Pappas, A. and Court, D. L. (1998). Genetic Uncoupling of the dsRNA-Binding and RNA Cleavage Activities of the Escherichia Coli Endoribonuclease RNase III--the Effect of dsRNA Binding on Gene Expression. ***Mol. Microbiol.*** **28, 629-640.**

DeVore, D. L., Horvitz, H. R. and Stern, M. J. (1995). An FGF Receptor Signaling Pathway is Required for the Normal Cell Migrations of the Sex Myoblasts in C. Elegans Hermaphrodites. ***Cell*** **83, 611-620.**

Dodou, E., Verzi, M. P., Anderson, J. P., Xu, S. M. and Black, B. L. (2004). Mef2c is a Direct Transcriptional Target of ISL1 and GATA Factors in the Anterior Heart Field during Mouse Embryonic Development. ***Development*** **131, 3931-3942.**

Dozier, C., Kagoshima, H., Niklaus, G., Cassata, G. and Burglin, T. R. (2001). The Caenorhabditis Elegans Six/sine Oculis Class Homeobox Gene Ceh-32 is Required for Head Morphogenesis. ***Dev. Biol.*** **236, 289-303.**

Dressler, G. R. (2006). The Cellular Basis of Kidney Development. ***Annu. Rev. Cell Dev. Biol.*** **22, 509-529.**

Duan, H., Skeath, J. B. and Nguyen, H. T. (2001). Drosophila Lame Duck, a Novel Member of the Gli Superfamily, Acts as a Key Regulator of Myogenesis by Controlling Fusion-Competent Myoblast Development. ***Development*** **128, 4489-4500.**

Duan, H., Zhang, C., Chen, J., Sink, H., Frei, E. and Noll, M. (2007). A Key Role of Pox Meso in Somatic Myogenesis of Drosophila. ***Development*** **134, 3985-3997.**

Dubois, L., Enriquez, J., Daburon, V., Crozet, F., Lebreton, G., Crozatier, M. and Vincent, A. (2007). Collier Transcription in a Single Drosophila Muscle Lineage: The Combinatorial Control of Muscle Identity. ***Development*** **134, 4347-4355.**

Dunin-Borkowski, O. M. and Brown, N. H. (1995). Mammalian CD2 is an Effective Heterologous Marker of the Cell Surface in Drosophila. ***Dev. Biol.*** **168, 689-693.**

Dunwoodie, S. L. (2007). Combinatorial Signaling in the Heart Orchestrates Cardiac Induction, Lineage Specification and Chamber Formation. ***Semin. Cell Dev. Biol.*** **18, 54-66.**

El-Hodiri, H., Bhatia-Dey, N., Kenyon, K., Ault, K., Dirksen, M. and Jamrich, M. (2001). Fox (Forkhead) Genes are Involved in the Dorso-Ventral Patterning of the Xenopus Mesoderm. ***Int. J. Dev. Biol.*** **45, 265-271.**

Fares, H. and Greenwald, I. (2001). Regulation of Endocytosis by CUP-5, the Caenorhabditis Elegans Mucolipin-1 Homolog. ***Nat. Genet.*** **28, 64-68.**

Feldman, B., Gates, M. A., Egan, E. S., Dougan, S. T., Rennebeck, G., Sirotkin, H. I., Schier, A. F. and Talbot, W. S. (1998). Zebrafish Organizer Development and Germ-Layer Formation Require Nodal-Related Signals. ***Nature*** **395, 181-185.**

Fire, A., Xu, S., Montgomery, M. K., Kostas, S. A., Driver, S. E. and Mello, C. C. (1998). Potent and Specific Genetic Interference by Double-Stranded RNA in Caenorhabditis Elegans. ***Nature*** **391, 806-811.**

Firestein, R., Bass, A. J., Kim, S. Y., Dunn, I. F., Silver, S. J., Guney, I., Freed, E., Ligon, A. H., Vena, N., Ogino, S. et al. (2008). CDK8 is a Colorectal Cancer Oncogene that Regulates Beta-Catenin Activity. ***Nature*****.**

Foehr, M. L., Lindy, A. S., Fairbank, R. C., Amin, N. M., Xu, M., Yanowitz, J., Fire, A. Z. and Liu, J. (2006). An Antagonistic Role for the C. Elegans Schnurri

Homolog SMA-9 in Modulating TGFbeta Signaling during Mesodermal Patterning. ***Development*** **133, 2887-2896.**

Foehr, M. L. and Liu, J. (2008). Dorsoventral Patterning of the C. Elegans Postembryonic Mesoderm Requires both LIN-12/Notch and TGFbeta Signaling. ***Dev. Biol.*** **313, 256-266.**

Fortini, M. E., Lai, Z. C. and Rubin, G. M. (1991). The Drosophila Zfh-1 and Zfh-2 Genes Encode Novel Proteins Containing both Zinc-Finger and Homeodomain Motifs. ***Mech. Dev.*** **34, 113-122.**

Fox, R. M., Von Stetina, S. E., Barlow, S. J., Shaffer, C., Olszewski, K. L., Moore, J. H., Dupuy, D., Vidal, M. and Miller, D. M.,3rd. (2005). A Gene Expression Fingerprint of C. Elegans Embryonic Motor Neurons. ***BMC Genomics*** **6, 42.**

Frasch, M. (1995). Induction of Visceral and Cardiac Mesoderm by Ectodermal Dpp in the Early Drosophila Embryo. ***Nature*** **374, 464-467.**

Frasch, M. (1999). Controls in Patterning and Diversification of Somatic Muscles during Drosophila Embryogenesis. ***Curr. Opin. Genet. Dev.*** **9, 522-529.**

Fukushige, T., Brodigan, T. M., Schriefer, L. A., Waterston, R. H. and Krause, M. (2006). Defining the Transcriptional Redundancy of Early Bodywall Muscle Development in C. Elegans: Evidence for a Unified Theory of Animal Muscle Development. ***Genes Dev.*** **20, 3395-3406.**

Fukushige, T. and Krause, M. (2005). The Myogenic Potency of HLH-1 Reveals Wide-Spread Developmental Plasticity in Early C. Elegans Embryos. ***Development*** **132, 1795-1805.**

Furuya, M., Qadota, H., Chisholm, A. D. and Sugimoto, A. (2005). The C. Elegans Eyes Absent Ortholog EYA-1 is Required for Tissue Differentiation and Plays Partially Redundant Roles with PAX-6. ***Dev. Biol.*** **286, 452-463.**

Gaudet, J. and Mango, S. E. (2002). Regulation of Organogenesis by the Caenorhabditis Elegans FoxA Protein PHA-4. ***Science*** **295, 821-825.**

Gilbert, S. F. (2006). ***Developmental Biology*****. Sunderland, MA: Sinauer.**

Giordani, J., Bajard, L., Demignon, J., Daubas, P., Buckingham, M. and Maire, P. (2007). Six Proteins Regulate the Activation of Myf5 Expression in Embryonic Mouse Limbs. ***Proc. Natl. Acad. Sci. U. S. A.*** **104, 11310-11315.**

Gisselbrecht, S., Skeath, J. B., Doe, C. Q. and Michelson, A. M. (1996). Heartless Encodes a Fibroblast Growth Factor Receptor (DFR1/DFGF-R2) Involved in the Directional Migration of Early Mesodermal Cells in the Drosophila Embryo. ***Genes Dev.*** **10, 3003-3017.**

Goldstein, M. A. and Burdette, W. J. (1971). Striated Visceral Muscle of Drosophila Melanogaster. ***J. Morphol.*** **134, 315-334.**

Green, J. L., Inoue, T. and Sternberg, P. W. (2008). Opposing Wnt Pathways Orient Cell Polarity during Organogenesis. ***Cell*** **134, 646-656.**

Greenwald, I. S., Sternberg, P. W. and Horvitz, H. R. (1983). The Lin-12 Locus Specifies Cell Fates in Caenorhabditis Elegans. ***Cell*** **34, 435-444.**

Grieder, N. C., Nellen, D., Burke, R., Basler, K. and Affolter, M. (1995). Schnurri is Required for Drosophila Dpp Signaling and Encodes a Zinc Finger Protein Similar to the Mammalian Transcription Factor PRDII-BF1. *Cell* 81, 791-800.

Grifone, R., Demignon, J., Houbron, C., Souil, E., Niro, C., Seller, M. J., Hamard, G. and Maire, P. (2005). Six1 and Six4 Homeoproteins are Required for Pax3 and Mrf Expression during Myogenesis in the Mouse Embryo. *Development* 132, 2235-2249.

Grigoryan, T., Wend, P., Klaus, A. and Birchmeier, W. (2008). Deciphering the Function of Canonical Wnt Signals in Development and Disease: Conditional Loss- and Gain-of-Function Mutations of Beta-Catenin in Mice. *Genes Dev.* 22, 2308-2341.

Halder, G., Callaerts, P., Flister, S., Walldorf, U., Kloter, U. and Gehring, W. J. (1998). Eyeless Initiates the Expression of both Sine Oculis and Eyes Absent during Drosophila Compound Eye Development. *Development* 125, 2181-2191.

Halfon, M. S., Carmena, A., Gisselbrecht, S., Sackerson, C. M., Jimenez, F., Baylies, M. K. and Michelson, A. M. (2000). Ras Pathway Specificity is Determined by the Integration of Multiple Signal-Activated and Tissue-Restricted Transcription Factors. *Cell* 103, 63-74.

Han, Z. and Olson, E. N. (2005). Hand is a Direct Target of Tinman and GATA Factors during Drosophila Cardiogenesis and Hematopoiesis. *Development* 132, 3525-3536.

Han, Z., Yi, P., Li, X. and Olson, E. N. (2006). Hand, an Evolutionarily Conserved bHLH Transcription Factor Required for Drosophila Cardiogenesis and Hematopoiesis. ***Development*** **133, 1175-1182.**

Hanson, I. M. (2001). Mammalian Homologues of the Drosophila Eye Specification Genes. ***Semin. Cell Dev. Biol.*** **12, 475-484.**

Harfe, B. D., Branda, C. S., Krause, M., Stern, M. J. and Fire, A. (1998a). MyoD and the Specification of Muscle and Non-Muscle Fates during Postembryonic Development of the C. Elegans Mesoderm. ***Development*** **125, 2479-2488.**

Harfe, B. D., Vaz Gomes, A., Kenyon, C., Liu, J., Krause, M. and Fire, A. (1998b). Analysis of a Caenorhabditis Elegans Twist Homolog Identifies Conserved and Divergent Aspects of Mesodermal Patterning. ***Genes Dev.*** **12, 2623-2635.**

Harris, E. S., Li, F. and Higgs, H. N. (2004). The Mouse Formin, FRLalpha, Slows Actin Filament Barbed End Elongation, Competes with Capping Protein, Accelerates Polymerization from Monomers, and Severs Filaments. ***J. Biol. Chem.*** **279, 20076-20087.**

Haun, C., Alexander, J., Stainier, D. Y. and Okkema, P. G. (1998). Rescue of Caenorhabditis Elegans Pharyngeal Development by a Vertebrate Heart Specification Gene. ***Proc. Natl. Acad. Sci. U. S. A.*** **95, 5072-5075.**

Hayes, S. A., Miller, J. M. and Hoshizaki, D. K. (2001). Serpent, a GATA-Like Transcription Factor Gene, Induces Fat-Cell Development in Drosophila Melanogaster. ***Development*** **128, 1193-1200.**

Heanue, T. A., Reshef, R., Davis, R. J., Mardon, G., Oliver, G., Tomarev, S., Lassar, A. B. and Tabin, C. J. (1999). Synergistic Regulation of Vertebrate Muscle Development by Dach2, Eya2, and Six1, Homologs of Genes Required for Drosophila Eye Formation. ***Genes Dev.*** **13, 3231-3243.**

Herman, M. (2001). C. Elegans POP-1/TCF Functions in a Canonical Wnt Pathway that Controls Cell Migration and in a Noncanonical Wnt Pathway that Controls Cell Polarity. ***Development*** **128, 581-590.**

Herrmann, B. G., Labeit, S., Poustka, A., King, T. R. and Lehrach, H. (1990). Cloning of the T Gene Required in Mesoderm Formation in the Mouse. ***Nature*** **343, 617-622.**

Higgs, H. N. and Peterson, K. J. (2005). Phylogenetic Analysis of the Formin Homology 2 Domain. ***Mol. Biol. Cell*** **16, 1-13.**

Hobert, O. and Ruvkun, G. (1999). Pax Genes in Caenorhabditis Elegans: A New Twist. ***Trends Genet.*** **15, 214-216.**

Hodgkin, J. and Doniach, T. (1997). Natural Variation and Copulatory Plug Formation in Caenorhabditis Elegans. ***Genetics*** **146, 149-164.**

Hodgkin, J., Horvitz, H. R. and Brenner, S. (1979). NONDISJUNCTION MUTANTS OF THE NEMATODE CAENORHABDITIS ELEGANS. ***Genetics*** **91, 67-94.**

Hope, I. A., Mounsey, A., Bauer, P. and Aslam, S. (2003). The Forkhead Gene Family of Caenorhabditis Elegans. ***Gene*** **304, 43-55.**

Horner, M. A., Quintin, S., Domeier, M. E., Kimble, J., Labouesse, M. and Mango, S. E. (1998). Pha-4, an HNF-3 Homolog, Specifies Pharyngeal Organ Identity in Caenorhabditis Elegans. ***Genes Dev.*** **12, 1947-1952.**

Hu, P., Geles, K. G., Paik, J. H., DePinho, R. A. and Tjian, R. (2008). Codependent Activators Direct Myoblast-Specific MyoD Transcription. ***Dev. Cell.*** **15, 534-546.**

Hu, T., Yamagishi, H., Maeda, J., McAnally, J., Yamagishi, C. and Srivastava, D. (2004). Tbx1 Regulates Fibroblast Growth Factors in the Anterior Heart Field through a Reinforcing Autoregulatory Loop Involving Forkhead Transcription Factors. ***Development*** **131, 5491-5502.**

Huang, S., Shetty, P., Robertson, S. M. and Lin, R. (2007). Binary Cell Fate Specification during C. Elegans Embryogenesis Driven by Reiterated Reciprocal Asymmetry of TCF POP-1 and its Coactivator Beta-Catenin SYS-1. ***Development*** **134, 2685-2695.**

Hurd, D. D. and Kemphues, K. J. (2003). PAR-1 is Required for Morphogenesis of the Caenorhabditis Elegans Vulva. ***Dev. Biol.*** **253, 54-65.**

Imamura, H., Tanaka, K., Hihara, T., Umikawa, M., Kamei, T., Takahashi, K., Sasaki, T. and Takai, Y. (1997). Bni1p and Bnr1p: Downstream Targets of the Rho Family Small G-Proteins which Interact with Profilin and Regulate Actin Cytoskeleton in Saccharomyces Cerevisiae. ***EMBO J.*** **16, 2745-2755.**

Ip, Y. T., Maggert, K. and Levine, M. (1994). Uncoupling Gastrulation and Mesoderm Differentiation in the Drosophila Embryo. ***EMBO J.*** **13, 5826-5834.**

Ip, Y. T., Park, R. E., Kosman, D., Yazdanbakhsh, K. and Levine, M. (1992). Dorsal-Twist Interactions Establish Snail Expression in the Presumptive Mesoderm of the Drosophila Embryo. ***Genes Dev.*** **6, 1518-1530.**

Iuchi, S. (2001). Three Classes of C2H2 Zinc Finger Proteins. ***Cell Mol. Life Sci.*** **58, 625-635.**

Jagla, T., Bellard, F., Lutz, Y., Dretzen, G., Bellard, M. and Jagla, K. (1998). Ladybird Determines Cell Fate Decisions during Diversification of Drosophila Somatic Muscles. ***Development*** **125, 3699-3708.**

Jakobsen, J. S., Braun, M., Astorga, J., Gustafson, E. H., Sandmann, T., Karzynski, M., Carlsson, P. and Furlong, E. E. (2007). Temporal ChIP-on-Chip Reveals Biniou as a Universal Regulator of the Visceral Muscle Transcriptional Network. ***Genes Dev.*** **21, 2448-2460.**

James, P., Halladay, J. and Craig, E. A. (1996). Genomic Libraries and a Host Strain Designed for Highly Efficient Two-Hybrid Selection in Yeast. ***Genetics*** **144, 1425-1436.**

Jansen, R. P., Dowzer, C., Michaelis, C., Galova, M. and Nasmyth, K. (1996). Mother Cell-Specific HO Expression in Budding Yeast Depends on the Unconventional Myosin myo4p and Other Cytoplasmic Proteins. ***Cell*** **84, 687-697.**

Jiang, J., Kosman, D., Ip, Y. T. and Levine, M. (1991). The Dorsal Morphogen Gradient Regulates the Mesoderm Determinant Twist in Early Drosophila Embryos. ***Genes Dev.*** **5, 1881-1891.**

Jiang, Y., Horner, V. and Liu, J. (2005). The HMX Homeodomain Protein MLS-2 Regulates Cleavage Orientation, Cell Proliferation and Cell Fate Specification in the C. Elegans Postembryonic Mesoderm. ***Development*** **132, 4119-4130.**

Jiang, Y., Shi, H., Amin, N. M., Sultan, I. and Liu, J. (2008). Mesodermal Expression of the C. Elegans HMX Homolog Mls-2 Requires the PBC Homolog CEH-20. ***Mech. Dev.*** **125, 451-461.**

Jin, W., Takagi, T., Kanesashi, S. N., Kurahashi, T., Nomura, T., Harada, J. and Ishii, S. (2006). Schnurri-2 Controls BMP-Dependent Adipogenesis Via Interaction with Smad Proteins. ***Dev. Cell.*** **10, 461-471.**

Johnston, R. J.,Jr, Copeland, J. W., Fasnacht, M., Etchberger, J. F., Liu, J., Honig, B. and Hobert, O. (2006). An Unusual Zn-finger/FH2 Domain Protein Controls a left/right Asymmetric Neuronal Fate Decision in C. Elegans. ***Development*** **133, 3317-3328.**

Jones, D. C., Wein, M. N. and Glimcher, L. H. (2007). Schnurri-3 is an Essential Regulator of Osteoblast Function and Adult Bone Mass. ***Ann. Rheum. Dis.*** **66 Suppl 3, iii49-51.**

Jones, D. C., Wein, M. N., Oukka, M., Hofstaetter, J. G., Glimcher, M. J. and Glimcher, L. H. (2006). Regulation of Adult Bone Mass by the Zinc Finger Adapter Protein Schnurri-3. ***Science*** **312, 1223-1227.**

Kahane, N., Cinnamon, Y. and Kalcheim, C. (1998). The Origin and Fate of Pioneer Myotomal Cells in the Avian Embryo. ***Mech. Dev.*** **74, 59-73.**

Kalb, J. M., Lau, K. K., Goszczynski, B., Fukushige, T., Moons, D., Okkema, P. G. and McGhee, J. D. (1998). Pha-4 is Ce-Fkh-1, a Fork head/HNF-3alpha,Beta,Gamma Homolog that Functions in Organogenesis of the C. Elegans Pharynx. ***Development*** **125, 2171-2180.**

Kamath, R. S. and Ahringer, J. (2003). Genome-Wide RNAi Screening in Caenorhabditis Elegans. ***Methods*** **30, 313-321.**

Kamath, R. S., Fraser, A. G., Dong, Y., Poulin, G., Durbin, R., Gotta, M., Kanapin, A., Le Bot, N., Moreno, S., Sohrmann, M. et al. (2003). Systematic Functional Analysis of the Caenorhabditis Elegans Genome using RNAi. ***Nature*** **421, 231-237.**

Kaul, A., Koster, M., Neuhaus, H. and Braun, T. (2000). Myf-5 Revisited: Loss of Early Myotome Formation does Not Lead to a Rib Phenotype in Homozygous Myf-5 Mutant Mice. ***Cell*** **102, 17-19.**

Kawakami, K., Ohto, H., Takizawa, T. and Saito, T. (1996). Identification and Expression of Six Family Genes in Mouse Retina. ***FEBS Lett.*** **393, 259-263.**

Kawakami, K., Sato, S., Ozaki, H. and Ikeda, K. (2000). Six Family Genes--Structure and Function as Transcription Factors and their Roles in Development. ***Bioessays*** **22, 616-626.**

Keller, C. A., Grill, M. A. and Abmayr, S. M. (1998). A Role for Nautilus in the Differentiation of Muscle Precursors. ***Dev. Biol.*** **202, 157-171.**

Kenyon, C. (1986). A Gene Involved in the Development of the Posterior Body Region of C. Elegans. ***Cell*** **46, 477-487.**

Kidd, A. R.,3rd, Miskowski, J. A., Siegfried, K. R., Sawa, H. and Kimble, J. (2005). A Beta-Catenin Identified by Functional rather than Sequence Criteria and its Role in Wnt/MAPK Signaling. ***Cell*** **121, 761-772.**

Kim, S., Ip, H. S., Lu, M. M., Clendenin, C. and Parmacek, M. S. (1997). A Serum Response Factor-Dependent Transcriptional Regulatory Program Identifies Distinct Smooth Muscle Cell Sublineages. ***Mol. Cell. Biol.*** **17, 2266-2278.**

Knirr, S., Azpiazu, N. and Frasch, M. (1999). The Role of the NK-Homeobox Gene Slouch (S59) in Somatic Muscle Patterning. ***Development*** **126, 4525-4535.**

Knirr, S. and Frasch, M. (2001). Molecular Integration of Inductive and Mesoderm-Intrinsic Inputs Governs Even-Skipped Enhancer Activity in a Subset of Pericardial and Dorsal Muscle Progenitors. ***Dev. Biol.*** **238, 13-26.**

Kochhar, A., Fischer, S. M., Kimberling, W. J. and Smith, R. J. (2007). Branchio-Oto-Renal Syndrome. ***Am. J. Med. Genet. A.*** **143A, 1671-1678.**

Kofron, M., Demel, T., Xanthos, J., Lohr, J., Sun, B., Sive, H., Osada, S., Wright, C., Wylie, C. and Heasman, J. (1999). Mesoderm Induction in Xenopus is a Zygotic Event Regulated by Maternal VegT Via TGFbeta Growth Factors. ***Development*** **126, 5759-5770.**

Kohno, H., Tanaka, K., Mino, A., Umikawa, M., Imamura, H., Fujiwara, T., Fujita, Y., Hotta, K., Qadota, H., Watanabe, T. et al. (1996). Bni1p Implicated in Cytoskeletal Control is a Putative Target of Rho1p Small GTP Binding Protein in Saccharomyces Cerevisiae. ***EMBO J.*** **15, 6060-6068.**

Kolsch, V. and Paululat, A. (2002). The Highly Conserved Cardiogenic bHLH Factor Hand is Specifically Expressed in Circular Visceral Muscle Progenitor Cells and in all Cell Types of the Dorsal Vessel during Drosophila Embryogenesis. ***Dev. Genes Evol.*** **212, 473-485.**

Korswagen, H. C., Coudreuse, D. Y., Betist, M. C., van de Water, S., Zivkovic, D. and Clevers, H. C. (2002). The Axin-Like Protein PRY-1 is a Negative Regulator of a Canonical Wnt Pathway in C. Elegans. ***Genes Dev.*** **16, 1291-1302.**

Koseki, H., Wallin, J., Wilting, J., Mizutani, Y., Kispert, A., Ebensperger, C., Herrmann, B. G., Christ, B. and Balling, R. (1993). A Role for Pax-1 as a Mediator of Notochordal Signals during the Dorsoventral Specification of Vertebrae. ***Development*** **119, 649-660.**

Kostas, S. A. and Fire, A. (2002). The T-Box Factor MLS-1 Acts as a Molecular Switch during Specification of Nonstriated Muscle in C. Elegans. ***Genes Dev.*** **16, 257-269.**

Kovar, D. R., Kuhn, J. R., Tichy, A. L. and Pollard, T. D. (2003). The Fission Yeast Cytokinesis Formin Cdc12p is a Barbed End Actin Filament Capping Protein Gated by Profilin. ***J. Cell Biol.*** **161, 875-887.**

Krause, M., Fire, A., Harrison, S. W., Priess, J. and Weintraub, H. (1990). CeMyoD Accumulation Defines the Body Wall Muscle Cell Fate during C. Elegans Embryogenesis. ***Cell*** **63, 907-919.**

Kuo, C. T., Morrisey, E. E., Anandappa, R., Sigrist, K., Lu, M. M., Parmacek, M. S., Soudais, C. and Leiden, J. M. (1997). GATA4 Transcription Factor is

Required for Ventral Morphogenesis and Heart Tube Formation. ***Genes Dev.*** **11, 1048-1060.**

Kurusu, M., Nagao, T., Walldorf, U., Flister, S., Gehring, W. J. and Furukubo-Tokunaga, K. (2000). Genetic Control of Development of the Mushroom Bodies, the Associative Learning Centers in the Drosophila Brain, by the Eyeless, Twin of Eyeless, and Dachshund Genes. ***Proc. Natl. Acad. Sci. U. S. A.*** **97, 2140-2144.**

Kutejova, E., Engist, B., Self, M., Oliver, G., Kirilenko, P. and Bobola, N. (2008). Six2 Functions Redundantly Immediately Downstream of Hoxa2. ***Development*** **135, 1463-1470.**

Lawrence, P. A. and Sampedro, J. (1993). Drosophila Segmentation: After the First Three Hours. ***Development*** **119, 971-976.**

Lee, H. H. and Frasch, M. (2000). Wingless Effects Mesoderm Patterning and Ectoderm Segmentation Events Via Induction of its Downstream Target Sloppy Paired. ***Development*** **127, 5497-5508.**

Lee, H. H. and Frasch, M. (2005). Nuclear Integration of Positive Dpp Signals, Antagonistic Wg Inputs and Mesodermal Competence Factors during Drosophila Visceral Mesoderm Induction. ***Development*** **132, 1429-1442.**

Leptin, M. (1991). Twist and Snail as Positive and Negative Regulators during Drosophila Mesoderm Development. ***Genes Dev.*** **5, 1568-1576.**

Lettice, L., Hecksher-Sorensen, J. and Hill, R. (2001). The Role of Bapx1 (Nkx3.2) in the Development and Evolution of the Axial Skeleton. ***J. Anat.*** **199, 181-187.**

Li, S., Zhou, D., Lu, M. M. and Morrisey, E. E. (2004). Advanced Cardiac Morphogenesis does Not Require Heart Tube Fusion. ***Science*** **305, 1619-1622.**

Li, X., Oghi, K. A., Zhang, J., Krones, A., Bush, K. T., Glass, C. K., Nigam, S. K., Aggarwal, A. K., Maas, R., Rose, D. W. et al. (2003). Eya Protein Phosphatase Activity Regulates Six1-Dach-Eya Transcriptional Effects in Mammalian Organogenesis. ***Nature*** **426, 247-254.**

Liang, J., Lints, R., Foehr, M. L., Tokarz, R., Yu, L., Emmons, S. W., Liu, J. and Savage-Dunn, C. (2003). The Caenorhabditis Elegans Schnurri Homolog Sma-9 Mediates Stage- and Cell Type-Specific Responses to DBL-1 BMP-Related Signaling. ***Development*** **130, 6453-6464.**

Liberatore, C. M., Searcy-Schrick, R. D., Vincent, E. B. and Yutzey, K. E. (2002). Nkx-2.5 Gene Induction in Mice is Mediated by a Smad Consensus Regulatory Region. ***Dev. Biol.*** **244, 243-256.**

Lien, C. L., McAnally, J., Richardson, J. A. and Olson, E. N. (2002). Cardiac-Specific Activity of an Nkx2-5 Enhancer Requires an Evolutionarily Conserved Smad Binding Site. ***Dev. Biol.*** **244, 257-266.**

Lilly, B., Galewsky, S., Firulli, A. B., Schulz, R. A. and Olson, E. N. (1994). D-MEF2: A MADS Box Transcription Factor Expressed in Differentiating Mesoderm and Muscle Cell Lineages during Drosophila Embryogenesis. ***Proc. Natl. Acad. Sci. U. S. A.*** **91, 5662-5666.**

Lin, R., Hill, R. J. and Priess, J. R. (1998). POP-1 and Anterior-Posterior Fate Decisions in C. Elegans Embryos. ***Cell*** **92, 229-239.**

Lin, R., Thompson, S. and Priess, J. R. (1995). Pop-1 Encodes an HMG Box Protein Required for the Specification of a Mesoderm Precursor in Early C. Elegans Embryos. ***Cell*** **83, 599-609.**

Lindsley, R. C., Gill, J. G., Murphy, T. L., Langer, E. M., Cai, M., Mashayekhi, M., Wang, W., Niwa, N., Nerbonne, J. M., Kyba, M. et al. (2008). Mesp1 Coordinately Regulates Cardiovascular Fate Restriction and Epithelial-Mesenchymal Transition in Differentiating ESCs. ***Cell. Stem Cell.*** **3, 55-68.**

Liu, J. and Fire, A. (2000). Overlapping Roles of Two Hox Genes and the Exd Ortholog Ceh-20 in Diversification of the C. Elegans Postembryonic Mesoderm. ***Development*** **127, 5179-5190.**

Liu, J., Phillips, B. T., Amaya, M. F., Kimble, J. and Xu, W. (2008). The C. Elegans SYS-1 Protein is a Bona Fide Beta-Catenin. ***Dev. Cell.*** **14, 751-761.**

Lo, M. C., Gay, F., Odom, R., Shi, Y. and Lin, R. (2004). Phosphorylation by the Beta-catenin/MAPK Complex Promotes 14-3-3-Mediated Nuclear Export of TCF/POP-1 in Signal-Responsive Cells in C. Elegans. ***Cell*** **117, 95-106.**

Lo, P. C. and Frasch, M. (2001). A Role for the COUP-TF-Related Gene Seven-Up in the Diversification of Cardioblast Identities in the Dorsal Vessel of Drosophila. ***Mech. Dev.*** **104, 49-60.**

Lo, P. C. and Frasch, M. (2003). Establishing A-P Polarity in the Embryonic Heart Tube: A Conserved Function of Hox Genes in Drosophila and Vertebrates? ***Trends Cardiovasc. Med.*** **13, 182-187.**

Maduro, M. F., Broitman-Maduro, G., Mengarelli, I. and Rothman, J. H. (2007). Maternal Deployment of the Embryonic SKN-1-->MED-1,2 Cell Specification Pathway in C. Elegans. ***Dev. Biol.*** **301, 590-601.**

Maduro, M. F., Meneghini, M. D., Bowerman, B., Broitman-Maduro, G. and Rothman, J. H. (2001). Restriction of Mesendoderm to a Single Blastomere by the Combined Action of SKN-1 and a GSK-3beta Homolog is Mediated by MED-1 and -2 in C. Elegans. ***Mol. Cell*** **7, 475-485.**

Maeda, I., Kohara, Y., Yamamoto, M. and Sugimoto, A. (2001). Large-Scale Analysis of Gene Function in Caenorhabditis Elegans by High-Throughput RNAi. ***Curr. Biol.*** **11, 171-176.**

Mango, S. E., Lambie, E. J. and Kimble, J. (1994). The Pha-4 Gene is Required to Generate the Pharyngeal Primordium of Caenorhabditis Elegans. ***Development*** **120, 3019-3031.**

Marcelle, C., Lesbros, C. and Linker, C. (2002). Somite Patterning: A Few More Pieces of the Puzzle. ***Results Probl. Cell Differ.*** **38, 81-108.**

Martini, S. R., Roman, G., Meuser, S., Mardon, G. and Davis, R. L. (2000). The Retinal Determination Gene, Dachshund, is Required for Mushroom Body Cell Differentiation. ***Development*** **127, 2663-2672.**

Marty, T., Muller, B., Basler, K. and Affolter, M. (2000). Schnurri Mediates Dpp-Dependent Repression of Brinker Transcription. ***Nat. Cell Biol.*** **2, 745-749.**

Matsuzaki, Y., Fujisawa, J. and Yoshida, M. (1995). Identification of Transcriptional Activation Domain of TREB5, a CREB/ATF Family Protein that Binds to HTLV-1 Enhancer. ***J. Biochem. (Tokyo)*** **117, 303-308.**

Mazieres, J., He, B., You, L., Xu, Z. and Jablons, D. M. (2005). Wnt Signaling in Lung Cancer. ***Cancer Lett.*** **222, 1-10.**

Meilhac, S. M., Esner, M., Kelly, R. G., Nicolas, J. F. and Buckingham, M. E. (2004). The Clonal Origin of Myocardial Cells in Different Regions of the Embryonic Mouse Heart. ***Dev. Cell.*** **6, 685-698.**

Mello, C. C., Kramer, J. M., Stinchcomb, D. and Ambros, V. (1991). Efficient Gene Transfer in C.Elegans: Extrachromosomal Maintenance and Integration of Transforming Sequences. ***EMBO J.*** **10, 3959-3970.**

Miano, J. M., Ramanan, N., Georger, M. A., de Mesy Bentley, K. L., Emerson, R. L., Balza, R. O.,Jr, Xiao, Q., Weiler, H., Ginty, D. D. and Misra, R. P. (2004). Restricted Inactivation of Serum Response Factor to the Cardiovascular System. ***Proc. Natl. Acad. Sci. U. S. A.*** **101, 17132-17137.**

Michelot, A., Guerin, C., Huang, S., Ingouff, M., Richard, S., Rodiuc, N., Staiger, C. J. and Blanchoin, L. (2005). The Formin Homology 1 Domain Modulates the Actin Nucleation and Bundling Activity of Arabidopsis FORMIN1. ***Plant Cell*** **17, 2296-2313.**

Michelson, A. M., Abmayr, S. M., Bate, M., Arias, A. M. and Maniatis, T. (1990). Expression of a MyoD Family Member Prefigures Muscle Pattern in Drosophila Embryos. ***Genes Dev.*** **4, 2086-2097.**

Michelson, A. M., Gisselbrecht, S., Zhou, Y., Baek, K. H. and Buff, E. M. (1998). Dual Functions of the Heartless Fibroblast Growth Factor Receptor in Development of the Drosophila Embryonic Mesoderm. ***Dev. Genet.*** **22, 212-229.**

Miguel-Aliaga, I., Allan, D. W. and Thor, S. (2004). Independent Roles of the Dachshund and Eyes Absent Genes in BMP Signaling, Axon Pathfinding and Neuronal Specification. ***Development*** **131, 5837-5848.**

Miskowski, J., Li, Y. and Kimble, J. (2001). The Sys-1 Gene and Sexual Dimorphism during Gonadogenesis in Caenorhabditis Elegans. ***Dev. Biol.*** **230, 61-73.**

Miya, T. and Nishida, H. (2003). An Ets Transcription Factor, HrEts, is Target of FGF Signaling and Involved in Induction of Notochord, Mesenchyme, and Brain in Ascidian Embryos. ***Dev. Biol.*** **261, 25-38.**

Mizumoto, K. and Sawa, H. (2007). Two Betas Or Not Two Betas: Regulation of Asymmetric Division by Beta-Catenin. ***Trends Cell Biol.*** **17, 465-473.**

Molkentin, J. D., Lin, Q., Duncan, S. A. and Olson, E. N. (1997). Requirement of the Transcription Factor GATA4 for Heart Tube Formation and Ventral Morphogenesis. ***Genes Dev.*** **11, 1061-1072.**

Morgenstern, B. (2004). DIALIGN: Multiple DNA and Protein Sequence Alignment at BiBiServ. ***Nucleic Acids Res.*** **32, W33-6.**

Moseley, J. B. and Goode, B. L. (2005). Differential Activities and Regulation of Saccharomyces Cerevisiae Formin Proteins Bni1 and Bnr1 by Bud6. ***J. Biol. Chem.*** **280, 28023-28033.**

Nakamura, K., Kim, S., Ishidate, T., Bei, Y., Pang, K., Shirayama, M., Trzepacz, C., Brownell, D. R. and Mello, C. C. (2005). Wnt Signaling Drives WRM-1/beta-Catenin Asymmetries in Early C. Elegans Embryos. ***Genes Dev.*** **19, 1749-1754.**

Nomura, M. and Li, E. (1998). Smad2 Role in Mesoderm Formation, Left-Right Patterning and Craniofacial Development. ***Nature*** **393, 786-790.**

Nose, A., Isshiki, T. and Takeichi, M. (1998). Regional Specification of Muscle Progenitors in Drosophila: The Role of the Msh Homeobox Gene. ***Development*** **125, 215-223.**

Noveen, A., Daniel, A. and Hartenstein, V. (2000). Early Development of the Drosophila Mushroom Body: The Roles of Eyeless and Dachshund. ***Development*** **127, 3475-3488.**

Ohto, H., Kamada, S., Tago, K., Tominaga, S. I., Ozaki, H., Sato, S. and Kawakami, K. (1999). Cooperation of Six and Eya in Activation of their Target Genes through Nuclear Translocation of Eya. ***Mol. Cell. Biol.*** **19, 6815-6824.**

Okkema, P. G. and Fire, A. (1994). The Caenorhabditis Elegans NK-2 Class Homeoprotein CEH-22 is Involved in Combinatorial Activation of Gene Expression in Pharyngeal Muscle. ***Development*** **120, 2175-2186.**

Okkema, P. G., Ha, E., Haun, C., Chen, W. and Fire, A. (1997). The Caenorhabditis Elegans NK-2 Homeobox Gene Ceh-22 Activates Pharyngeal Muscle Gene Expression in Combination with Pha-1 and is Required for Normal Pharyngeal Development. ***Development*** **124, 3965-3973.**

Olmsted, J. B. (1981). Affinity Purification of Antibodies from Diazotized Paper Blots of Heterogeneous Protein Samples. *J. Biol. Chem.* 256, 11955-11957.

O'Rourke, M. P. and Tam, P. P. (2002). Twist Functions in Mouse Development. *Int. J. Dev. Biol.* 46, 401-413.

Otomo, T., Tomchick, D. R., Otomo, C., Panchal, S. C., Machius, M. and Rosen, M. K. (2005). Structural Basis of Actin Filament Nucleation and Processive Capping by a Formin Homology 2 Domain. *Nature* 433, 488-494.

Paterson, B. M., Walldorf, U., Eldridge, J., Dubendorfer, A., Frasch, M. and Gehring, W. J. (1991). The Drosophila Homologue of Vertebrate Myogenic-Determination Genes Encodes a Transiently Expressed Nuclear Protein Marking Primary Myogenic Cells. *Proc. Natl. Acad. Sci. U. S. A.* 88, 3782-3786.

Peters, H., Doll, U. and Niessing, J. (1995). Differential Expression of the Chicken Pax-1 and Pax-9 Gene: In Situ Hybridization and Immunohistochemical Analysis. *Dev. Dyn.* 203, 1-16.

Phillips, B. T., Kidd, A. R.,3rd, King, R., Hardin, J. and Kimble, J. (2007). Reciprocal Asymmetry of SYS-1/beta-Catenin and POP-1/TCF Controls Asymmetric Divisions in Caenorhabditis Elegans. *Proc. Natl. Acad. Sci. U. S. A.* 104, 3231-3236.

Pignoni, F., Hu, B., Zavitz, K. H., Xiao, J., Garrity, P. A. and Zipursky, S. L. (1997). The Eye-Specification Proteins so and Eya Form a Complex and Regulate Multiple Steps in Drosophila Eye Development. *Cell* 91, 881-891.

Politz, J. C. and Edgar, R. S. (1984). Overlapping Stage-Specific Sets of Numerous Small Collagenous Polypeptides are Translated in Vitro from Caenorhabditis Elegans RNA. *Cell* 37, 853-860.

Pollard, T. D. (1983). Measurement of Rate Constants for Actin Filament Elongation in Solution. *Anal. Biochem.* 134, 406-412.

Popichenko, D., Sellin, J., Bartkuhn, M. and Paululat, A. (2007). Hand is a Direct Target of the Forkhead Transcription Factor Biniou during Drosophila Visceral Mesoderm Differentiation. *BMC Dev. Biol.* 7, 49.

Pourquie, O., Fan, C. M., Coltey, M., Hirsinger, E., Watanabe, Y., Breant, C., Francis-West, P., Brickell, P., Tessier-Lavigne, M. and Le Douarin, N. M. (1996). Lateral and Axial Signals Involved in Avian Somite Patterning: A Role for BMP4. *Cell* 84, 461-471.

Pownall, M. E., Gustafsson, M. K. and Emerson, C. P.,Jr. (2002). Myogenic Regulatory Factors and the Specification of Muscle Progenitors in Vertebrate Embryos. *Annu. Rev. Cell Dev. Biol.* 18, 747-783.

Prall, O. W., Menon, M. K., Solloway, M. J., Watanabe, Y., Zaffran, S., Bajolle, F., Biben, C., McBride, J. J., Robertson, B. R., Chaulet, H. et al. (2007). An Nkx2-5/Bmp2/Smad1 Negative Feedback Loop Controls Heart Progenitor Specification and Proliferation. *Cell* 128, 947-959.

Pruyne, D., Evangelista, M., Yang, C., Bi, E., Zigmond, S., Bretscher, A. and Boone, C. (2002). Role of Formins in Actin Assembly: Nucleation and Barbed-End Association. *Science* 297, 612-615.

Rebagliati, M. R., Toyama, R., Fricke, C., Haffter, P. and Dawid, I. B. (1998). Zebrafish Nodal-Related Genes are Implicated in Axial Patterning and Establishing Left-Right Asymmetry. ***Dev. Biol.*** **199, 261-272.**

Reece-Hoyes, J. S., Deplancke, B., Shingles, J., Grove, C. A., Hope, I. A. and Walhout, A. J. (2005). A Compendium of Caenorhabditis Elegans Regulatory Transcription Factors: A Resource for Mapping Transcription Regulatory Networks. ***Genome Biol.*** **6, R110.**

Reshef, R., Maroto, M. and Lassar, A. B. (1998). Regulation of Dorsal Somitic Cell Fates: BMPs and Noggin Control the Timing and Pattern of Myogenic Regulator Expression. ***Genes Dev.*** **12, 290-303.**

Riechmann, V., Irion, U., Wilson, R., Grosskortenhaus, R. and Leptin, M. (1997). Control of Cell Fates and Segmentation in the Drosophila Mesoderm. ***Development*** **124, 2915-2922.**

Rocheleau, C. E., Downs, W. D., Lin, R., Wittmann, C., Bei, Y., Cha, Y. H., Ali, M., Priess, J. R. and Mello, C. C. (1997). Wnt Signaling and an APC-Related Gene Specify Endoderm in Early C. Elegans Embryos. ***Cell*** **90, 707-716.**

Rojas, A., De Val, S., Heidt, A. B., Xu, S. M., Bristow, J. and Black, B. L. (2005). Gata4 Expression in Lateral Mesoderm is Downstream of BMP4 and is Activated Directly by Forkhead and GATA Transcription Factors through a Distal Enhancer Element. ***Development*** **132, 3405-3417.**

Roth, S., Stein, D. and Nusslein-Volhard, C. (1989). A Gradient of Nuclear Localization of the Dorsal Protein Determines Dorsoventral Pattern in the Drosophila Embryo. *Cell* 59, 1189-1202.

Roy, P. J., Stuart, J. M., Lund, J. and Kim, S. K. (2002). Chromosomal Clustering of Muscle-Expressed Genes in Caenorhabditis Elegans. *Nature* 418, 975-979.

Rual, J. F., Ceron, J., Koreth, J., Hao, T., Nicot, A. S., Hirozane-Kishikawa, T., Vandenhaute, J., Orkin, S. H., Hill, D. E., van den Heuvel, S. et al. (2004). Toward Improving Caenorhabditis Elegans Phenome Mapping with an ORFeome-Based RNAi Library. *Genome Res.* 14, 2162-2168.

Rudnicki, M. A., Braun, T., Hinuma, S. and Jaenisch, R. (1992). Inactivation of MyoD in Mice Leads to Up-Regulation of the Myogenic HLH Gene Myf-5 and Results in Apparently Normal Muscle Development. *Cell* 71, 383-390.

Rudnicki, M. A., Schnegelsberg, P. N., Stead, R. H., Braun, T., Arnold, H. H. and Jaenisch, R. (1993). MyoD Or Myf-5 is Required for the Formation of Skeletal Muscle. *Cell* 75, 1351-1359.

Ruiz-Gomez, M., Romani, S., Hartmann, C., Jackle, H. and Bate, M. (1997). Specific Muscle Identities are Regulated by Kruppel during Drosophila Embryogenesis. *Development* 124, 3407-3414.

Rushlow, C. A., Han, K., Manley, J. L. and Levine, M. (1989). The Graded Distribution of the Dorsal Morphogen is Initiated by Selective Nuclear Transport in Drosophila. *Cell* 59, 1165-1177.

Rushton, E., Drysdale, R., Abmayr, S. M., Michelson, A. M. and Bate, M. (1995). Mutations in a Novel Gene, Myoblast City, Provide Evidence in Support of the Founder Cell Hypothesis for Drosophila Muscle Development. ***Development*** **121, 1979-1988.**

Ryckebusch, L., Wang, Z., Bertrand, N., Lin, S. C., Chi, X., Schwartz, R., Zaffran, S. and Niederreither, K. (2008). Retinoic Acid Deficiency Alters Second Heart Field Formation. ***Proc. Natl. Acad. Sci. U. S. A.*** **105, 2913-2918.**

Saga, Y., Miyagawa-Tomita, S., Takagi, A., Kitajima, S., Miyazaki, J. and Inoue, T. (1999). MesP1 is Expressed in the Heart Precursor Cells and Required for the Formation of a Single Heart Tube. ***Development*** **126, 3437-3447.**

Sagot, I., Rodal, A. A., Moseley, J., Goode, B. L. and Pellman, D. (2002). An Actin Nucleation Mechanism Mediated by Bni1 and Profilin. ***Nat. Cell Biol.*** **4, 626-631.**

Salser, S. J. (1995). Role of Hox Gene Expression in Patterning Cell Fates and Migrations Along the ***Caenorhabditis Elegans*** **Anteroposterior Body Axis.**

Sandmann, T., Girardot, C., Brehme, M., Tongprasit, W., Stolc, V. and Furlong, E. E. (2007). A Core Transcriptional Network for Early Mesoderm Development in Drosophila Melanogaster. ***Genes Dev.*** **21, 436-449.**

Sasai, Y., Lu, B., Steinbeisser, H., Geissert, D., Gont, L. K. and De Robertis, E. M. (1994). Xenopus Chordin: A Novel Dorsalizing Factor Activated by Organizer-Specific Homeobox Genes. ***Cell*** **79, 779-790.**

Schweitzer, R., Howes, R., Smith, R., Shilo, B. Z. and Freeman, M. (1995a). Inhibition of Drosophila EGF Receptor Activation by the Secreted Protein Argos. ***Nature*** **376, 699-702.**

Schweitzer, R., Shaharabany, M., Seger, R. and Shilo, B. Z. (1995b). Secreted Spitz Triggers the DER Signaling Pathway and is a Limiting Component in Embryonic Ventral Ectoderm Determination. ***Genes Dev.*** **9, 1518-1529.**

Seale, P., Bjork, B., Yang, W., Kajimura, S., Chin, S., Kuang, S., Scime, A., Devarakonda, S., Conroe, H. M., Erdjument-Bromage, H. et al. (2008). PRDM16 Controls a Brown fat/skeletal Muscle Switch. ***Nature*** **454, 961-967.**

Self, M., Lagutin, O. V., Bowling, B., Hendrix, J., Cai, Y., Dressler, G. R. and Oliver, G. (2006). Six2 is Required for Suppression of Nephrogenesis and Progenitor Renewal in the Developing Kidney. ***EMBO J.*** **25, 5214-5228.**

Serikaku, M. A. and O'Tousa, J. E. (1994). Sine Oculis is a Homeobox Gene Required for Drosophila Visual System Development. ***Genetics*** **138, 1137-1150.**

Shaner, N. C., Steinbach, P. A. and Tsien, R. Y. (2005). A Guide to Choosing Fluorescent Proteins. ***Nat. Methods*** **2, 905-909.**

Shen, W. and Mardon, G. (1997). Ectopic Eye Development in Drosophila Induced by Directed Dachshund Expression. ***Development*** **124, 45-52.**

Shimada, A., Nyitrai, M., Vetter, I. R., Kuhlmann, D., Bugyi, B., Narumiya, S., Geeves, M. A. and Wittinghofer, A. (2004). The Core FH2 Domain of Diaphanous-Related Formins is an Elongated Actin Binding Protein that Inhibits Polymerization. ***Mol. Cell*** **13, 511-522.**

Shishido, E., Ono, N., Kojima, T. and Saigo, K. (1997). Requirements of DFR1/Heartless, a Mesoderm-Specific Drosophila FGF-Receptor, for the Formation of Heart, Visceral and Somatic Muscles, and Ensheathing of Longitudinal Axon Tracts in CNS. ***Development*** **124, 2119-2128.**

Siegfried, K. R., Kidd, A. R.,3rd, Chesney, M. A. and Kimble, J. (2004). The Sys-1 and Sys-3 Genes Cooperate with Wnt Signaling to Establish the Proximal-Distal Axis of the Caenorhabditis Elegans Gonad. ***Genetics*** **166, 171-186.**

Siegfried, K. R. and Kimble, J. (2002). POP-1 Controls Axis Formation during Early Gonadogenesis in C. Elegans. ***Development*** **129, 443-453.**

Sijen, T., Fleenor, J., Simmer, F., Thijssen, K. L., Parrish, S., Timmons, L., Plasterk, R. H. and Fire, A. (2001). On the Role of RNA Amplification in dsRNA-Triggered Gene Silencing. ***Cell*** **107, 465-476.**

Sirotkin, H. I., Gates, M. A., Kelly, P. D., Schier, A. F. and Talbot, W. S. (2000). Fast1 is Required for the Development of Dorsal Axial Structures in Zebrafish. ***Curr. Biol.*** **10, 1051-1054.**

Slack, J. M., Darlington, B. G., Heath, J. K. and Godsave, S. F. (1987). Mesoderm Induction in Early Xenopus Embryos by Heparin-Binding Growth Factors. ***Nature*** **326, 197-200.**

Slack, J. M., Isaacs, H. V. and Darlington, B. G. (1988). Inductive Effects of Fibroblast Growth Factor and Lithium Ion on Xenopus Blastula Ectoderm. ***Development*** **103, 581-590.**

Smith, D. B. and Johnson, K. S. (1988). Single-Step Purification of Polypeptides Expressed in Escherichia Coli as Fusions with Glutathione S-Transferase. *Gene* 67, 31-40.

Smith, D. E. and Fisher, P. A. (1984). Identification, Developmental Regulation, and Response to Heat Shock of Two Antigenically Related Forms of a Major Nuclear Envelope Protein in Drosophila Embryos: Application of an Improved Method for Affinity Purification of Antibodies using Polypeptides Immobilized on Nitrocellulose Blots. *J. Cell Biol.* 99, 20-28.

Smith, J. C., Price, B. M., Green, J. B., Weigel, D. and Herrmann, B. G. (1991). Expression of a Xenopus Homolog of Brachyury (T) is an Immediate-Early Response to Mesoderm Induction. *Cell* 67, 79-87.

Smith, P. A. and Mango, S. E. (2007). Role of T-Box Gene Tbx-2 for Anterior Foregut Muscle Development in C. Elegans. *Dev. Biol.* 302, 25-39.

Smith, W. C., Knecht, A. K., Wu, M. and Harland, R. M. (1993). Secreted Noggin Protein Mimics the Spemann Organizer in Dorsalizing Xenopus Mesoderm. *Nature* 361, 547-549.

Song, J., Oh, S. P., Schrewe, H., Nomura, M., Lei, H., Okano, M., Gridley, T. and Li, E. (1999). The Type II Activin Receptors are Essential for Egg Cylinder Growth, Gastrulation, and Rostral Head Development in Mice. *Dev. Biol.* 213, 157-169.

Spitz, F., Demignon, J., Porteu, A., Kahn, A., Concordet, J. P., Daegelen, D. and Maire, P. (1998). Expression of Myogenin during Embryogenesis is Controlled by

Six/sine Oculis Homeoproteins through a Conserved MEF3 Binding Site. ***Proc. Natl. Acad. Sci. U. S. A.*** **95, 14220-14225.**

Srivastava, D., Cserjesi, P. and Olson, E. N. (1995). A Subclass of bHLH Proteins Required for Cardiac Morphogenesis. ***Science*** **270, 1995-1999.**

Srivastava, D., Thomas, T., Lin, Q., Kirby, M. L., Brown, D. and Olson, E. N. (1997). Regulation of Cardiac Mesodermal and Neural Crest Development by the bHLH Transcription Factor, dHAND. ***Nat. Genet.*** **16, 154-160.**

Staehling-Hampton, K., Hoffmann, F. M., Baylies, M. K., Rushton, E. and Bate, M. (1994). Dpp Induces Mesodermal Gene Expression in Drosophila. ***Nature*** **372, 783-786.**

Stathopoulos, A., Tam, B., Ronshaugen, M., Frasch, M. and Levine, M. (2004). Pyramus and Thisbe: FGF Genes that Pattern the Mesoderm of Drosophila Embryos. ***Genes Dev.*** **18, 687-699.**

Stepchenko, A. and Nirenberg, M. (2004). Mapping Activation and Repression Domains of the vnd/NK-2 Homeodomain Protein. ***Proc. Natl. Acad. Sci. U. S. A.*** **101, 13180-13185.**

Steward, R. (1989). Relocalization of the Dorsal Protein from the Cytoplasm to the Nucleus Correlates with its Function. ***Cell*** **59, 1179-1188.**

Stockdale, F. E., Nikovits, W.,Jr and Christ, B. (2000). Molecular and Cellular Biology of Avian Somite Development. ***Dev. Dyn.*** **219, 304-321.**

Strange, K., Christensen, M. and Morrison, R. (2007). Primary Culture of Caenorhabditis Elegans Developing Embryo Cells for Electrophysiological, Cell Biological and Molecular Studies. ***Nat. Protoc.*** **2, 1003-1012.**

Su, M. T., Fujioka, M., Goto, T. and Bodmer, R. (1999). The Drosophila Homeobox Genes Zfh-1 and Even-Skipped are Required for Cardiac-Specific Differentiation of a Numb-Dependent Lineage Decision. ***Development*** **126, 3241-3251.**

Sulston, J. E. and Horvitz, H. R. (1977). Post-Embryonic Cell Lineages of the Nematode, Caenorhabditis Elegans. ***Dev. Biol.*** **56, 110-156.**

Sulston, J. E., Schierenberg, E., White, J. G. and Thomson, J. N. (1983). The Embryonic Cell Lineage of the Nematode Caenorhabditis Elegans. ***Dev. Biol.*** **100, 64-119.**

Sundaram, M. and Greenwald, I. (1993). Genetic and Phenotypic Studies of Hypomorphic Lin-12 Mutants in Caenorhabditis Elegans. ***Genetics*** **135, 755-763.**

Swan, K. A., Severson, A. F., Carter, J. C., Martin, P. R., Schnabel, H., Schnabel, R. and Bowerman, B. (1998). Cyk-1: A C. Elegans FH Gene Required for a Late Step in Embryonic Cytokinesis. ***J. Cell. Sci.*** **111 (Pt 14), 2017-2027.**

Takeshita, H. and Sawa, H. (2005). Asymmetric Cortical and Nuclear Localizations of WRM-1/beta-Catenin during Asymmetric Cell Division in C. Elegans. ***Genes Dev.*** **19, 1743-1748.**

Takeuchi, J. K., Mileikovskaia, M., Koshiba-Takeuchi, K., Heidt, A. B., Mori, A. D., Arruda, E. P., Gertsenstein, M., Georges, R., Davidson, L., Mo, R. et al.

(2005). Tbx20 Dose-Dependently Regulates Transcription Factor Networks Required for Mouse Heart and Motoneuron Development. ***Development*** **132, 2463-2474.**

Tao, Y. and Schulz, R. A. (2007). Heart Development in Drosophila. ***Semin. Cell Dev. Biol.*** **18, 3-15.**

Tao, Y., Wang, J., Tokusumi, T., Gajewski, K. and Schulz, R. A. (2007). Requirement of the LIM Homeodomain Transcription Factor Tailup for Normal Heart and Hematopoietic Organ Formation in Drosophila Melanogaster. ***Mol. Cell. Biol.*** **27, 3962-3969.**

Tapanes-Castillo, A. and Baylies, M. K. (2004). Notch Signaling Patterns Drosophila Mesodermal Segments by Regulating the bHLH Transcription Factor Twist. ***Development*** **131, 2359-2372.**

Thisse, C., Perrin-Schmitt, F., Stoetzel, C. and Thisse, B. (1991). Sequence-Specific Transactivation of the Drosophila Twist Gene by the Dorsal Gene Product. ***Cell*** **65, 1191-1201.**

Timmons, L., Court, D. L. and Fire, A. (2001). Ingestion of Bacterially Expressed dsRNAs can Produce Specific and Potent Genetic Interference in Caenorhabditis Elegans. ***Gene*** **263, 103-112.**

Timmons, L. and Fire, A. (1998). Specific Interference by Ingested dsRNA. ***Nature*** **395, 854.**

Tonegawa, A., Funayama, N., Ueno, N. and Takahashi, Y. (1997). Mesodermal Subdivision Along the Mediolateral Axis in Chicken Controlled by Different Concentrations of BMP-4. ***Development*** **124, 1975-1984.**

Tonegawa, A. and Takahashi, Y. (1998). Somitogenesis Controlled by Noggin. ***Dev. Biol.*** **202, 172-182.**

Topczewska, J. M., Topczewski, J., Shostak, A., Kume, T., Solnica-Krezel, L. and Hogan, B. L. (2001a). The Winged Helix Transcription Factor Foxc1a is Essential for Somitogenesis in Zebrafish. ***Genes Dev.*** **15, 2483-2493.**

Topczewska, J. M., Topczewski, J., Solnica-Krezel, L. and Hogan, B. L. (2001b). Sequence and Expression of Zebrafish foxc1a and foxc1b, Encoding Conserved forkhead/winged Helix Transcription Factors. ***Mech. Dev.*** **100, 343-347.**

Udagawa, Y., Hanai, J., Tada, K., Grieder, N. C., Momoeda, M., Taketani, Y., Affolter, M., Kawabata, M. and Miyazono, K. (2000). Schnurri Interacts with Mad in a Dpp-Dependent Manner. ***Genes Cells*** **5, 359-369.**

Umbhauer, M., Marshall, C. J., Mason, C. S., Old, R. W. and Smith, J. C. (1995). Mesoderm Induction in Xenopus Caused by Activation of MAP Kinase. ***Nature*** **376, 58-62.**

van de Wetering, M., Sancho, E., Verweij, C., de Lau, W., Oving, I., Hurlstone, A., van der Horn, K., Batlle, E., Coudreuse, D., Haramis, A. P. et al. (2002). The Beta-catenin/TCF-4 Complex Imposes a Crypt Progenitor Phenotype on Colorectal Cancer Cells. ***Cell*** **111, 241-250.**

Venters, S. J. and Ordahl, C. P. (2005). Asymmetric Cell Divisions are Concentrated in the Dermomyotome Dorsomedial Lip during Epaxial Primary Myotome Morphogenesis. ***Anat. Embryol. (Berl)*** **209, 449-460.**

Venuti, J. M., Goldberg, L., Chakraborty, T., Olson, E. N. and Klein, W. H. (1991). A Myogenic Factor from Sea Urchin Embryos Capable of Programming Muscle Differentiation in Mammalian Cells. ***Proc. Natl. Acad. Sci. U. S. A.*** **88, 6219-6223.**

von Both, I., Silvestri, C., Erdemir, T., Lickert, H., Walls, J. R., Henkelman, R. M., Rossant, J., Harvey, R. P., Attisano, L. and Wrana, J. L. (2004). Foxh1 is Essential for Development of the Anterior Heart Field. ***Dev. Cell.*** **7, 331-345.**

Von Stetina, S. E., Watson, J. D., Fox, R. M., Olszewski, K. L., Spencer, W. C., Roy, P. J. and Miller, D. M.,3rd. (2007). Cell-Specific Microarray Profiling Experiments Reveal a Comprehensive Picture of Gene Expression in the C. Elegans Nervous System. ***Genome Biol.*** **8, R135.**

Wang, B., Weidenfeld, J., Lu, M. M., Maika, S., Kuziel, W. A., Morrisey, E. E. and Tucker, P. W. (2004). Foxp1 Regulates Cardiac Outflow Tract, Endocardial Cushion Morphogenesis and Myocyte Proliferation and Maturation. ***Development*** **131, 4477-4487.**

Wang, D., Chang, P. S., Wang, Z., Sutherland, L., Richardson, J. A., Small, E., Krieg, P. A. and Olson, E. N. (2001). Activation of Cardiac Gene Expression by Myocardin, a Transcriptional Cofactor for Serum Response Factor. ***Cell*** **105, 851-862.**

Wang, D. Z., Li, S., Hockemeyer, D., Sutherland, L., Wang, Z., Schratt, G., Richardson, J. A., Nordheim, A. and Olson, E. N. (2002). Potentiation of Serum Response Factor Activity by a Family of Myocardin-Related Transcription Factors. ***Proc. Natl. Acad. Sci. U. S. A.*** **99, 14855-14860.**

Wang, P., Zhao, J. and Corsi, A. K. (2006). Identification of Novel Target Genes of CeTwist and CeE/DA. ***Dev. Biol.*** **293, 486-498.**

Wang, Z., Wang, D. Z., Hockemeyer, D., McAnally, J., Nordheim, A. and Olson, E. N. (2004). Myocardin and Ternary Complex Factors Compete for SRF to Control Smooth Muscle Gene Expression. ***Nature*** **428, 185-189.**

Wang, Z., Wang, D. Z., Pipes, G. C. and Olson, E. N. (2003). Myocardin is a Master Regulator of Smooth Muscle Gene Expression. ***Proc. Natl. Acad. Sci. U. S. A.*** **100, 7129-7134.**

Watanabe, N., Madaule, P., Reid, T., Ishizaki, T., Watanabe, G., Kakizuka, A., Saito, Y., Nakao, K., Jockusch, B. M. and Narumiya, S. (1997). P140mDia, a Mammalian Homolog of Drosophila Diaphanous, is a Target Protein for Rho Small GTPase and is a Ligand for Profilin. ***EMBO J.*** **16, 3044-3056.**

Wei, Q., Rong, Y. and Paterson, B. M. (2007). Stereotypic Founder Cell Patterning and Embryonic Muscle Formation in Drosophila Require Nautilus (MyoD) Gene Function. ***Proc. Natl. Acad. Sci. U. S. A.*** **104, 5461-5466.**

Wicks, S. R., Yeh, R. T., Gish, W. R., Waterston, R. H. and Plasterk, R. H. (2001). Rapid Gene Mapping in Caenorhabditis Elegans using a High Density Polymorphism Map. ***Nat. Genet.*** **28, 160-164.**

Wilkinson, D. G., Bhatt, S. and Herrmann, B. G. (1990). Expression Pattern of the Mouse T Gene and its Role in Mesoderm Formation. ***Nature*** **343, 657-659.**

Wilm, B., James, R. G., Schultheiss, T. M. and Hogan, B. L. (2004). The Forkhead Genes, Foxc1 and Foxc2, Regulate Paraxial Versus Intermediate Mesoderm Cell Fate. ***Dev. Biol.*** **271, 176-189.**

Xu, P. X., Adams, J., Peters, H., Brown, M. C., Heaney, S. and Maas, R. (1999). Eya1-Deficient Mice Lack Ears and Kidneys and show Abnormal Apoptosis of Organ Primordia. ***Nat. Genet.*** **23, 113-117.**

Xu, Y., Moseley, J. B., Sagot, I., Poy, F., Pellman, D., Goode, B. L. and Eck, M. J. (2004). Crystal Structures of a Formin Homology-2 Domain Reveal a Tethered Dimer Architecture. ***Cell*** **116, 711-723.**

Yamagishi, H., Yamagishi, C., Nakagawa, O., Harvey, R. P., Olson, E. N. and Srivastava, D. (2001). The Combinatorial Activities of Nkx2.5 and dHAND are Essential for Cardiac Ventricle Formation. ***Dev. Biol.*** **239, 190-203.**

Yang, L., Sym, M. and Kenyon, C. (2005). The Roles of Two C. Elegans HOX Co-Factor Orthologs in Cell Migration and Vulva Development. ***Development*** **132, 1413-1428.**

Yao, L. C., Blitz, I. L., Peiffer, D. A., Phin, S., Wang, Y., Ogata, S., Cho, K. W., Arora, K. and Warrior, R. (2006). Schnurri Transcription Factors from Drosophila and Vertebrates can Mediate Bmp Signaling through a Phylogenetically Conserved Mechanism. ***Development*** **133, 4025-4034.**

Yin, Z., Xu, X. L. and Frasch, M. (1997). Regulation of the Twist Target Gene Tinman by Modular Cis-Regulatory Elements during Early Mesoderm Development. ***Development*** **124, 4971-4982.**

Yu, J. K., Holland, N. D. and Holland, L. Z. (2003). AmphiFoxQ2, a Novel Winged helix/forkhead Gene, Exclusively Marks the Anterior End of the Amphioxus Embryo. ***Dev. Genes Evol.*** **213, 102-105.**

Yusuf, F. and Brand-Saberi, B. (2006). The Eventful Somite: Patterning, Fate Determination and Cell Division in the Somite. ***Anat. Embryol. (Berl)*** **211 Suppl 1, 21-30.**

Zaffran, S. and Frasch, M. (2002). The Beta 3 Tubulin Gene is a Direct Target of Bagpipe and Biniou in the Visceral Mesoderm of Drosophila. ***Mech. Dev.*** **114, 85-93.**

Zaffran, S., Kuchler, A., Lee, H. H. and Frasch, M. (2001). Biniou (FoxF), a Central Component in a Regulatory Network Controlling Visceral Mesoderm Development and Midgut Morphogenesis in Drosophila. ***Genes Dev.*** **15, 2900-2915.**

Zaffran, S., Reim, I., Qian, L., Lo, P. C., Bodmer, R. and Frasch, M. (2006). Cardioblast-Intrinsic Tinman Activity Controls Proper Diversification and Differentiation of Myocardial Cells in Drosophila. ***Development*** **133, 4073-4083.**

Zhou, X., Sasaki, H., Lowe, L., Hogan, B. L. and Kuehn, M. R. (1993). Nodal is a Novel TGF-Beta-Like Gene Expressed in the Mouse Node during Gastrulation. ***Nature*** **361, 543-547.**

Zigmond, S. H., Evangelista, M., Boone, C., Yang, C., Dar, A. C., Sicheri, F., Forkey, J. and Pring, M. (2003). Formin Leaky Cap Allows Elongation in the Presence of Tight Capping Proteins. ***Curr. Biol.*** **13, 1820-1823.**